Leibniz-Institut
für Festkörper- und
Werkstoffforschung
Dresden

Annual Report 2015

Contents

Flashback to 2015

The IFW Dresden looks back at an exciting and successful year 2015. With the results of the evaluation, published in March, the IFW was ranked as one of the worldwide leading research institutes in the field of Solid States and Materials Research and was recommended for seven more years of funding through the Federal State of Germany and the Free State of Saxony. In addition to that, the scientific advisory board certified that research at the IFW Dresden is internationally on an outstanding level. The participation in special research fields, the successful fundraising of ERC-Grants and numerous often-quoted publications prove this assessment right.

All Leibniz Institutes are institutionally funded by the federal government and by the German Länder in equal shares. The justification of this funding has to be affirmed for each institute in intervals of seven years by an evaluation panel set up by the senate commission of the Leibniz Association. The prerequisite of confirmed funding is high quality scientific work and its high relevance for the whole society. In spring 2015, the Leibniz Association Senate has published the final report on the evaluation of the IFW in July 2014. The panel of renowned, international scientists confirmed the high quality of research at IFW. The evaluation report states that the IFW fulfils its "mission extremely successfully and has gained a place as one of the world's leading research institutes in this field". Most subdivisions have been rated as "very good to excellent". Thus, for the next seven years we can move forward with our scientific work and strategic measures according to the research program, which is organized into four large research areas

- Research Area 1: Functional quantum materials
- Research Area 2: Function through size
- Research Area 3: Quantum effects at the nanoscale
- Research Area 4: Towards products

The range of materials that are investigated is broad but well-defined. It contains Quantum Materials, a highly topical class of materials in condensed matter physics as well as Functional Materials, representing an important part of modern materials

Prof. Dr. Manfred Hennecke and Dr. Doreen Kirmse,
the Executive Board of the IFW Dresden

engineering. In the last years Nanoscale Materials became a strong focus of present day materials science and a crucial material class for cutting-edge developments in electrical engineering. These three classes, Quantum Materials, Functional Materials and Nanoscale Materials, provide the three materials-oriented pillars of the IFW. The research area "Towards products" binds together materials science and engineering that is at the borderline to prototypes or products. Establishing, fostering and promoting the contact to industry partners is the main aspect within this activity. While being distinctly multidisciplinary, there is a clear common aspect to all activities of the IFW Dresden: all researchers at the IFW Dresden investigate yet unexplored properties of novel materials with the aim to establish new functionalities and applications. In this respect, 2015 was a very productive year for IFW. The appendix gives a complete record of the publications, invited talks, patent applications, completed graduations and theses, academic events, and guest stays. In the main part of this Annual Report outstanding scientific results are presented for each Research Topic of the IFW's research program.

In 2015, there have been several personnel changes in IFW's management positions. In April 2015, Dr. Doreen Kirmse became the new Administrative Director of IFW. Together with the Scientific Director, Professor Dr. Manfred Hennecke, she belongs to the Executive Board the IFW Dresden. Further personnel changes in management positions concern the directorship of two of the five IFW's institutes: (1) In April 2015, Professor Dr. Kornelius Nielsch jointed the IFW as new Director of the Institute for Metallic Materials providing new input into the IFW's Research Program. Together with some new co-workers, he introduced thermoelectric materials as a new research topic. Thermoelectric materials enable direct conversion between thermal and electrical energy. New materials, e.g. special alloys, and the various capabilities of nanostructuring show enhanced efficiency and promise new applications. (2) Professor Dr. Jürgen Eckert has accepted a call to the Montanuniversität Leoben (Austria) and left the IFW in August 2015. A successor for the Institute for Complex Materials will be appointed in a joint procedure together with the Technische Universität Dresden. In the meantime, Dr. Thomas Gemming heads this IFW Institute.

Prof. Dr. Kornelius Nielsch, the new Director of the Institute for Metallic Materials at IFW

Leibniz President Prof. Dr. Matthias Kleiner visiting IFW

Work on materials for energy storage on progress

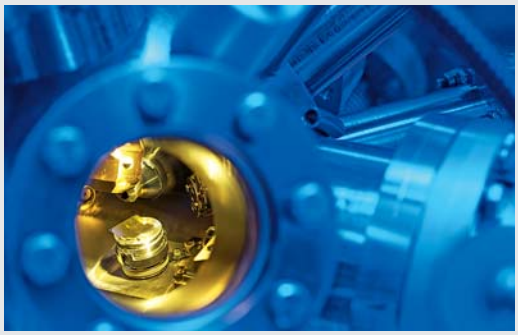

As a Leibniz Institute the IFW is budgeted by the federal government and the German federal states in equal parts. However, a considerable extension of capability is the amount of third party project funding which is also an important index of quality. The level of third party funding in 2015 amounts to 10 Mio. Euro – a level at the forefront of the Leibniz Association. Most of this project funding was acquired in a highly competitive mode from the DFG and the EU. In particular the grant of the new Collaborative Research Centre 1143 on "Correlated magnetism: From frustration to topology" where the IFW is collaborating with the Technische Universität Dresden shows the competitive capability of the IFW. Among the large number of third party funded projects are three DFG-Priority Programs that are coordinated by the IFW. Additionally, IFW scientists participate in seven DFG-Priority Programs and three DFG Research Groups. As in the previous years the IFW has been very successful in initiating EU projects and participating in them. After having been awarded two ERC Starting Grants in 2012 and one ERC Advanced Grant in 2013, IFW researchers could continue their success with this highly prestigious European funding program in 2015 with two ERC Consolidator Grants in 2015. Dr. Christian Hess received an ERC Consolidator Grant for his research on "Electronic order, magnetism, and unconventional superconductivity in real-space". Dr. Alexej Popov received an ERC Consolidator Grant for his project titled "Surface-grafted metallofullerene molecular magnets with controllable alignment of magnetic moments".

Essentially publicly funded, the IFW is obliged to make its research results public. Almost 400 publications in scientific journals and conference proceedings report on the IFW's research results on the year 2015. In 270 invited talks the Institute's scientists presented their work at other places around the world. In 2015, twelve patents were issued for the IFW, and applications for 17 more patents have been made. Apart from these scientific communications the IFW continued its large efforts to make scientific work accessible for the general public and to inspire young people to study science or engineering. The IFW took part in many joint actions like the lecture series "Physics on Saturday", "Junior Doctor" or the "Dresden Long Night of Sciences". Besides these big

Photoelectron spectroscopy

Dr. Julia Hufenbach (middle) receiving the DGM Junior Award 2015

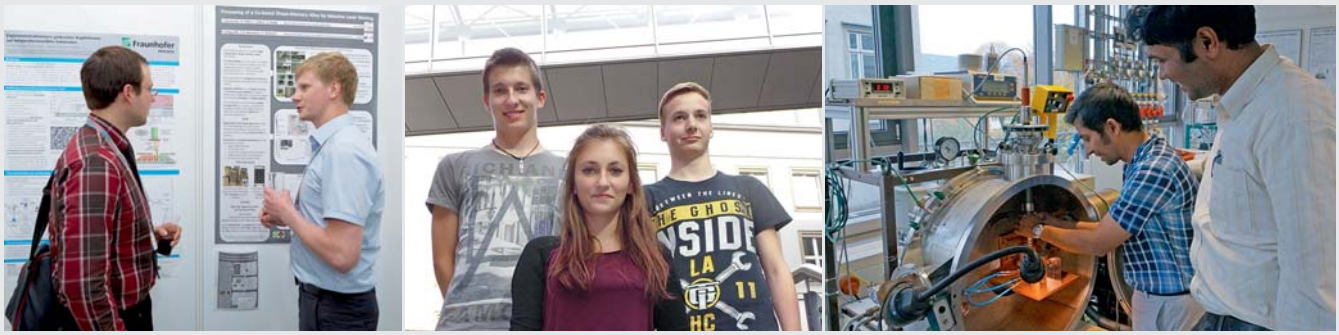

events we organize almost weekly lab-tours for various visitor groups, from school classes through official representatives to guests from foreign organizations. Especially the IFW's superconducting test facility SpuraTrans in Dresden-Niedersedlitz has proved very popular among visitors, be it representatives from companies, students groups or politicians. Furthermore, the facility has been used for an advertising video clip where a prominent skater surfed on a levitating board. The huge publicity of the video on youtube and other channels brought some benefit also to the public outreach of IFW.

A crucial part of the IFW's identity is its vivid life including the cultivation of the scientific dialogue, family-friendly working conditions, intercultural diversity and the support of sportive and cultural activities. In 2015 the IFW organized a series of workshops, colloquia and talks to foster the scientific dialogue and, along the way, allow for social and communication aspects of cooperation. Social events like the annual IFW Summer Day, the Christmas party and vernissages to our art exhibitions also contribute to a good working atmosphere among all IFW groups.

The positive development of the IFW is being fostered continuously by the engagement of colleagues and partners from universities, research institutes and industry, our Scientific Advisory Board and the Board of Trustees as well as the funding organizations. We would like to thank all our partners and friends for their support and cooperation.

Dresden, February 2016

Prof. Dr. Manfred Hennecke
Scientific Director

Dr. Doreen Kirmse
Administrative Director

Postersession at the Werkstoffwoche in Dresden

New apprentices starting their professional training at IFW in 2015

Fellowship holders at research work in the framework of an EU project on metallic glasses

Facts & Figures

Organization

The Leibniz Institute for Solid State and Material Research Dresden (IFW) is one of currently 89 institutes of the Leibniz Association in Germany. It is a legally independent association, headed by the Scientific Director, Prof. Dr. Manfred Hennecke, and the Administrative Director, Dr. Doreen Kirmse.

The scientific body of the IFW Dresden is structured into five institutes, the directors of which are simultaneously full professors at Dresden, respectively Chemnitz Universities of Technology:

- Institute for Solid State Research, Prof. Dr. Bernd Büchner
- Institute for Metallic Materials, Prof. Dr. Kornelius Nielsch
- Institute for Complex Materials, Dr. Thomas Gemming (temp.)
- Institute for Integrative Nanosciences, Prof. Dr. Oliver G. Schmidt
- Institute for Theoretical Solid State Physics, Prof. Dr. Jeroen van den Brink

Further divisions are the Research Technology Division and the Administrative Division.

Financing

The institutional funding of IFW is supplied by the Federal government and by the German states (Länder) in equal parts. In 2015, this funding was about 33.422 million euros in total.

In addition, the IFW receives project funding from external sources of about 9.95 million euros. Thereof, about 43 % came from German Research Foundation (DFG), 25 % from European Union programs, 13 % from Federal Government projects, 13 % from industry and 6 % from other donors including the Free State of Saxony.

"JuniorDoctor" – one of the offers of the Dresden science network. Magnetic levitation attracts the youngsters.

View of the IFW building

IFW Summer day: award ceremony for the best paper airplanes



Personnel

On 31 December 2015, 498 staff members were employed at the IFW, including 108 doctorate students as well as 19 apprentices in seven different vocational trainings and two business students of a vocational academy.

Gender equality, as well as work life balance, are defined goals of the IFW Dresden. In 2015, the percentage of women in scientific positions was 25 % and the percentage of women in scientific leading positions was 21 %. In 2007, the IFW qualified for the certificate “audit berufundfamilie” (a strategic management tool for a better compatibility of family and career) and was already re-audited two more times.

Number of publications and patents

In terms of publications, the qualitative and quantitative level remains high at the IFW. In 2015, IFW scientists have published 397 refereed journal articles, a considerable number of them in high impact journals. Furthermore, IFW members held 270 invited talks at conferences and colloquia.

By 31 December 2015, the IFW holds 120 patents in Germany and 98 international patents.

Research topic 1.1

Exotic ground states and low-energy excitations in bulk systems

People: A. Alfonsov, G. Aslan-Cansever, D. Baumann, N. Bogdanov, L. T. Corredor Bohórquez, D.-N. Cho, S.-L. Drechsler, D. Efremov, S. Fuchs, S. Gass, M. Geyer, H.-J. Grafe, F. Hammerath, R. Hentrich, C. Hess, L. Hozoi, M. Iakovleva, V. Kataev, V. Katukuri, A. Maljuk, K. Manna, S. Nishimoto, K. D. Swamy Reddy, J. Schoop, F. Steckel, H. Stummer, M. Sturza, Z. Sun, S. Sykora, S. Reja, Y. Utz, M. Vogl, A. Wolter-Giraud, S. Wurmehl, L. Xu, R. Yadav, J. Zeisner, A. Zimmermann, S. Zimmermann
Responsible Directors: B. Büchner, J. van den Brink

Abstract: The focus of this research topic is on experimental and theoretical investigations of novel quantum magnets on the basis of complex transition metal (TM) oxides where the coupling of different degrees of freedom (spin, charge, orbital etc.) can give rise to unconventional ground states and novel spin excitations. In our research we extensively exploit a unique combination of relevant mutually complementary methods and expertise available at the IFW Dresden, ranging from material synthesis and crystal growth, transport, magnetic and thermodynamic characterization to various spectroscopic (ARPES, RIXS, spin-polarized STM/STS) and dynamic local spin probe (ESR, NMR) techniques supported by numerical or analytical treatment of many-body models and quantum chemistry calculations.

In 2015, besides continuing investigations of 3*d* TM oxides that since decades provide a rich playground for exploring intriguing Mott-Hubbard physics, we dedicated a **substantial attention to the 5*d* materials, mainly to iridium oxides**. The 5*d* iridates have attracted an enormous recent interest as they enter one more ingredient to the TM-oxide 'Mottness' paradigm — large spin-orbit couplings (SOC's). SOC in 5*d* oxides modifies the very nature of the correlation hole of an electron, changes the conditions for localization, the criteria of Mottness, and further gives rise to new types of magnetic ground states and excitations.

The layered perovskite Sr_2IrO_4 has been recently put forward as a prototype 2D spin-orbital Mott insulator. Using electron spin resonance (ESR) measurements at sub-THz frequencies in strong magnetic fields we were able to untangle the 5d-shell electronic structure of Sr_2IrO_4, in particular, the exact order of the Ir t_{2g} levels [1]. To do that, we have experimentally determined the spectroscopic *g*-tensor which appears inverted as

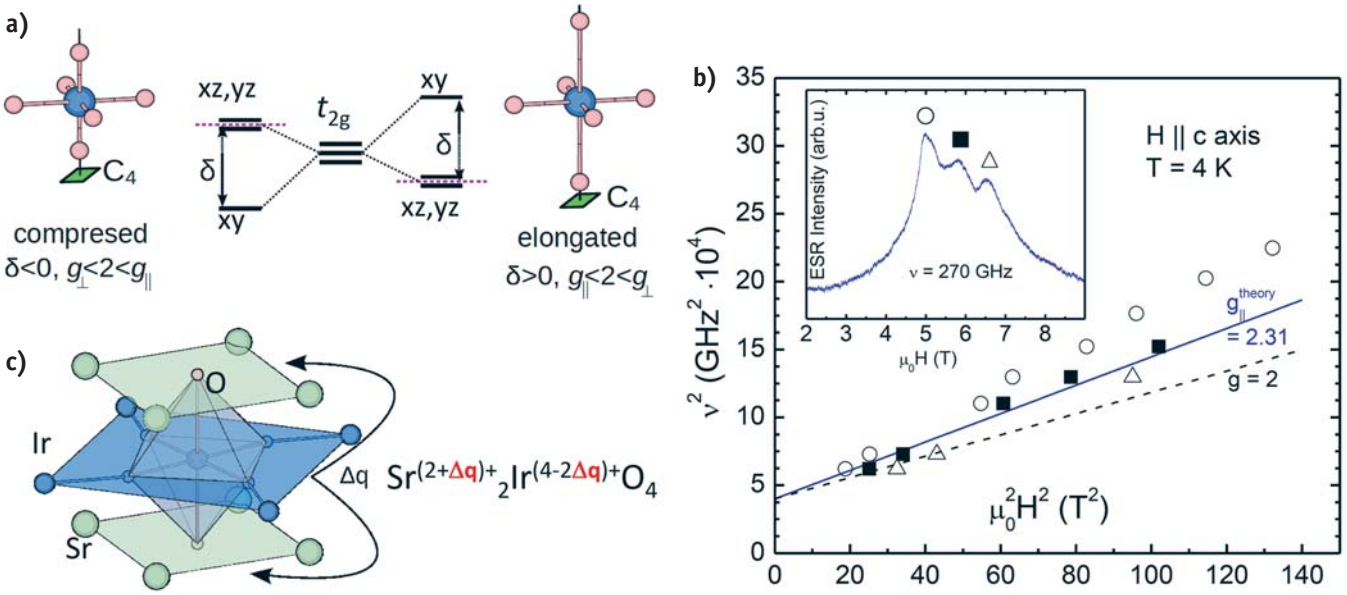

Fig. 1: (a) Canonical theories predict for the elongated IrO_6 octahedra in $SrIr_2O_4$ a positive tetragonal splitting of the Ir 5*d*-orbital states $\delta > 0$ and the $g_{||}$-factor less than 2; **(b)** Frequency vs. magnetic field dependence of the ESR modes (inset) evidence $g_{||} > 2$ implying that the ordering of the orbital states is inverted, as it would be the case for $\delta < 0$ shown in the top panel; **(c)** quantum chemistry calculations show that a specific distribution of ionic charges between the IrO_2 and SrO layers yields an inversion of the Ir 5*d*-levels and predict $g_{||} = 2.31 > 2$ in good agreement with experiment [1].

compared to predictions of canonical ligand-field theory. The inversion of the *g*-tensor implies an inversion of the ordering of the t_{2g} orbital states (Fig. 1). That has been quantitatively confirmed by ab-initio quantum chemistry calculations and we have further shown that the driving force behind this energy-level switching is the interlayer positive-ion charge imbalance [1]. This latter effect we identify in layered 214 iridates opens new perspectives on orbital engineering in both intrinsically-stacked bulk oxides and multilayered heterostructures.

While the antisymmetric Dzyaloshinskii-Moriya coupling reaches impressively large values of more than 10 meV in Sr_2IrO_4 [1], for edge-sharing octahedra in honeycomb iridates it is one of the diagonal components of the symmetric anisotropy that dominates, the recently discovered Kitaev interaction. For Na_2IrO_3 and Li_2IrO_3, two proposed realizations of the Kitaev honeycomb model, we have nailed down the crucial differences with respect to the strengths of the Heisenberg and Kitaev couplings and further provided guidelines for fine tuning of these interactions by varying the Ir-O-Ir bond angles, either via pressure or strain [2]. The promise for exciting Kitaev-Heisenberg physics [3] has been also evaluated in 4*d*-electron honeycomb compounds such as Li_2RhO_3 [4].

Measurements of the heat transport of single crystals of Sr_2IrO_4 [5] have revealed clear-cut evidence for magnetic heat transport within the IrO_2 planes which provides the unique possibility to analyze the thermal occupation and scattering of $j_{eff} = 1/2$ pseudospin excitations. The analysis of the magnetic heat conductivity yields a low-temperature ($T \lesssim 75$ K) magnetic mean free path $l_{mag} \sim 32$ nm, consistent with boundary scattering. Upon heating towards room temperature, the mean free path strongly decreases by one order of magnitude due to thermally activated scattering of the pseudospin excitations. This reveals that the coupling of these excitations to the lattice is radically different from that of $S = 1/2$-excitations in cuprate analogs: while magneto-elastic coupling has only a weak effect on the magnon heat transport of the latter, it is the prevailing scattering mechanism for pseudospin excitations in Sr_2IrO_4.

Iridates such as Sr_2IrO_4 and Na_2IrO_3 also provide striking exemplifications of the power of modern resonant inelastic x-ray scattering (RIXS) spectroscopy. High-resolution RIXS measurements of spin-orbital dynamics in Sr_2IrO_4 sustain the analogy of Sr_2IrO_4 to the cuprate superconductors and have motivated intense efforts towards doping the '214' iridates. We have shown that single-magnon (SM) scattering at the O *K*-edge is allowed when the TM SOC is sizable *and* inversion symmetry at the O site is broken. In

particular, it is allowed for small momentum losses and forbidden for momenta close to the magnetic ordering vector, a situation opposite to magnetic TM *L*-edge RIXS [6]. As the 5*d* SOC is large and inversion symmetry at the O sites is often distinctly broken in iridates — e.g., in Sr_2IrO_4, $CaIrO_3$, and '227' pyrochlores — we predict pronounced SM scattering at the O *K* edge of these magnetic Ir oxides.

Further, we have investigated the magnetic properties of a series of sodium ternary iridates $Na_{1-x}M_{1/3}Ir_{2/3}O_2$ (M = Ni, Cu, and Zn) by local spin probe techniques, muon spin rotation (μSR) and nuclear magnetic resonance (NMR). Similar to the honeycomb iridate Na_2IrO_3, the studied compounds feature hexagonal layers where the M ions were expected to substitute Na ions in the center of each honeycomb. However, the average structure of the layers appears to have disordered M and Ir ions. Our results together with our earlier magnetization measurements give evidence that the doping of the Ir 2D honeycomb lattice has a remarkable impact on the magnetic properties. In contrast to a well-defined antiferromagnetic order in Na_2IrO_3, our data reveal two competing regimes at low temperatures in these frustrated materials: a long range AF ordering and a cluster spin glass behavior with short range spin correlations. The interplay of these regimes depends on the sort of the transition metal ion M.

Materials with $5d^4$ electronic configuration of a TM ion are generally considered to have a non-magnetic ground state with the total angular momentum J = 0. But recently it was argued that the interplay of superexchange energy and spin-orbit coupling may lead to an excitonic type of magnetism. Moreover, Sr_2YIrO_6 (Ir^{5+} having $5d^4$ electronic configuration) was reported to exibit magnetic order at low temperature. However, it was claimed that the distorted IrO_6 octahedra cause the magnetism in this material. To overcome this structural contribution towards finding a better material to study this excitonic mechanism, we have grown Ba_2YIrO_6 single crystals which crystallize in a cubic structure. Interestingly, our study suggests the presence of small magnetic moments in Ba_2YIrO_6, however, their origin is presently unclear. In particular, we find no hints on magnetic order above 0.3 K.

As to the 3*d* TM compounds, the impact of strong electronic correlations, disorder and magnetic frustration on the spin ground state and spin dynamics has been studied in detail in a number of new interesting materials.

We studied the phase diagram of copper nitrate $Cu(NO_3)_2{*}2.5D_2O$ in the context of quantum phase transitions and novel states of matter. We established this compound as an ideal candidate to study quasi-1D Luttinger liquids, 3D Bose-Einstein-condensation of triplons and the crossover between 1D and 3D physics [7]. Magnetocaloric effect, magnetization and neutron scattering data provide clear evidence for transitions into a Luttinger liquid regime and a 3D long-range ordered phase as function of field and temperature. Theoretical simulations of this model material allow us to fully establish the phase diagram and to discuss it in the context of dimerized spin systems.

Magnetic properties of the $CoAl_2O_4$ single crystal where the Co spins form a frustrated spin lattice with the diamond structure (Fig. 2) we addressed in detail with three local spin probe techniques, NMR, μSR and ESR [8]. We found that in the studied single crystal the degree of structural disorder due to the Al-Co site inversion is optimally tuned to obtain insights onto its influence on the ground state and on the low energy magnetic dynamics of the frustrated diamond spin lattice. We observed a critical slowing down of spin fluctuations by approaching a characteristic temperature $T^* = 8$ K which suggests the onset of quasi-static short-range unconventional order at this temperature (Fig. 2). Since in the phase diagram of the diamond spin lattice $CoAl_2O_4$ is located close to the

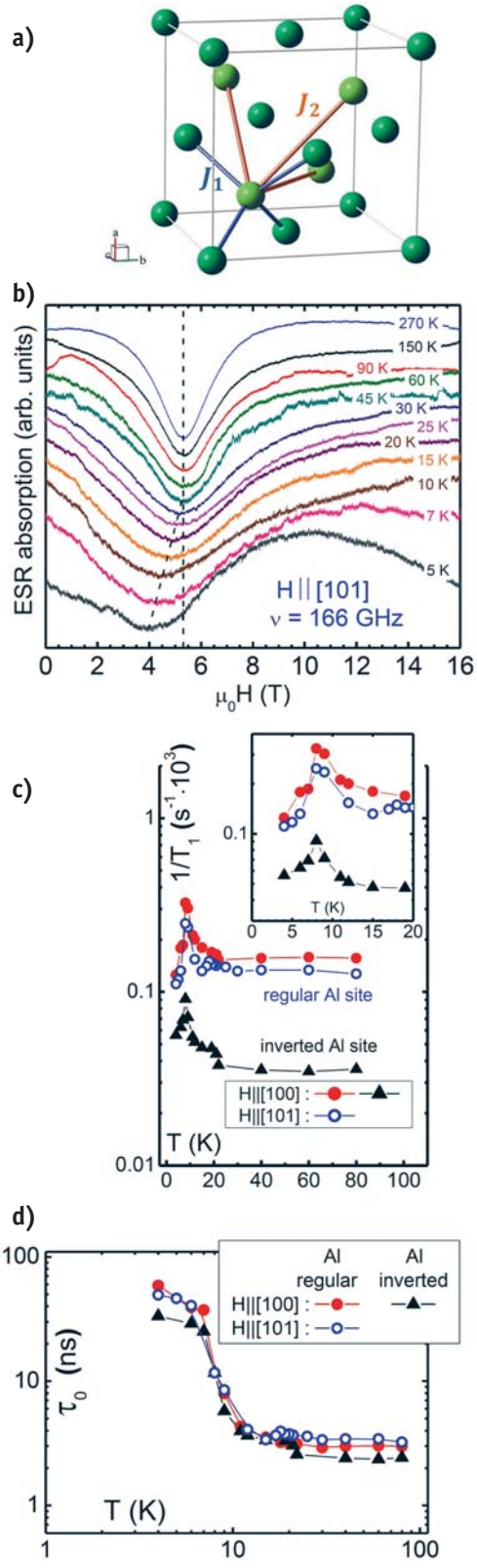

Fig. 2: (a) Co^{3+} (S =3/2) ions in $CoAl_2O_4$ form a frustrated diamond spin lattice with competing antiferromagnetic interactions J_1 and J_2; **(b)** High magnetic field ESR spectroscopy reveals a broadening and shift of the Co^{3+} ESR signal below T ~ 100 K indicating a continuous enhancement of the correlations far above the ordering temperature T* = 8 K; **(c)** Temperature dependence of the ^{27}Al NMR relaxation rate $1/T_1$ exhibits a broad peak at T* = 8 K both for regular and inverted Al sites giving evidence for a crossover to a quasi-static regime of correlated Co electron spins; **(d)** Temperature dependence of the correlation time τ_0 of electron spins extracted from the analysis of ^{27}Al rates $1/T_1$ shows a continuous growth down to the lowest temperature implying a progressive slowing down of the electron spin dynamics across the T* [8].

special critical point which separates collinear and noncollinear spin phases, it appears from our results that Al atoms at the Co sites acting as quenched impurities smear the phase boundary between the two phases. This can yield a competition between the two ground states and give rise to an inhomogeneous magnetic dynamics. We argue that our experimental findings may have important implications for recent theories of an „order by disorder" mechanism in the frustrated diamond spin lattice.

Finally, we investigated the S = 1/2 antiferromagnetic Heisenberg spin chain compound Sr_2CuO_3 doped with 1% and 2% of Ni impurities by means of ^{63}Cu nuclear magnetic resonance [9]. A strong decrease of the spin-lattice relaxation rate T_1^{-1} at low temperatures points toward a spin gap, while a stretching exponent $\lambda < 1$ and a frequency dependence of T_1^{-1} indicate that this spin gap varies spatially and should rather be characterized as a spin pseudogap. The magnitude of the spin pseudogap scales with doping level. Our results therefore evidence the finite-size character of this phenomenon. Moreover, an unusual narrowing of the low-temperature NMR lines reveals the suppression of the impurity-induced staggered paramagnetic response with increasing doping level which is most probably a consequence of the spin pseudogap, which reduces low-energy antiferromagnetic fluctuations.

[1] N. A. Bogdanov et al., Nature Commun. **6**, 7306 (2015).
[2] S. Nishimoto et al., Nature Commun. **7**, 10273 (2016).
[3] Z. Nussinov and J. van den Brink, Rev. Mod. Phys. **87**, 1 (2015).
[4] V. Katukuri et al., Sci. Rep. **5**, 14718 (2015).
[5] F. Steckel et al., arXiv:1507.04252.
[6] B. H. Kim and J. van den Brink, Phys. Rev. B **92**, 081105(R) (2015).
[7] B. Willenberg et al., Phys. Rev. B **91**, 060407(R) (2015).
[8] M. Iakovleva et al., Phys. Rev. B **91**, 144419 (2015)
[9] Y. Utz et al., Phys. Rev. B **92**, 060405(R) (2015)

Large Third Party Projects: DFG-Collaborative Research Center SFB 1143 "Correlated Magnetism: From Frustration to Topology", located at TU Dresden, TU Bergakademie Freiberg, HZDR, MPI Physik komplexer Systeme Dresden, MPI für Chemische Physik fester Stoffe, and IFW Dresden.

Organization of workshops: Xenophon Zotos, C. Hess, P. van Loosdrecht, Workshop "Quantum Magnets 2015", 13.09.2015 - 18.09.2015, Kolymbari, Crete, Greece

Cooperation: Technical University Dresden, Max Planck Institute for Solid State Research Stuttgart, Technical University of Braunschweig, Helmholtz-Zentrum Berlin, Paul Scherrer Institute Villigen, Zavoisky Physical Technical Institute Kazan, Ohio State University

Research topic 1.2

Unconventional superconductivity: Mechanisms, materials & applications

People: S.-H. Baek, A. Bauernfeind, D. Baumann, S. Borisenko, P. Chekhonin, S. Ludwig Drechsler, D. Efremov, M. Enayat, A. Fedorov, G. Fuchs, M. Gillig, U. Gräfe, H. Grafe, V. Grinenko, F. Hammerath, E. Haubold, C. Hess, R. Hühne, R. Kappenberger, S. Khim, K. Koepernik, T. Kühne, M. Kühnel, Y. Kushnirenko, S. Luther, S. Müller-Litvanyi, P. Kumar Nag, G. Prando, S. Richter, T. Schorr, W. Schottenhamel, F. Steckel, M. Sturza, Z. Sun, S. Sykora, Y. Utz, R. Wachtel, A. Wolter-Giraud, S. Wurmehl, C. Wuttke, F. Yuan
Responsible Directors: B. Büchner, K. Nielsch, J. van den Brink

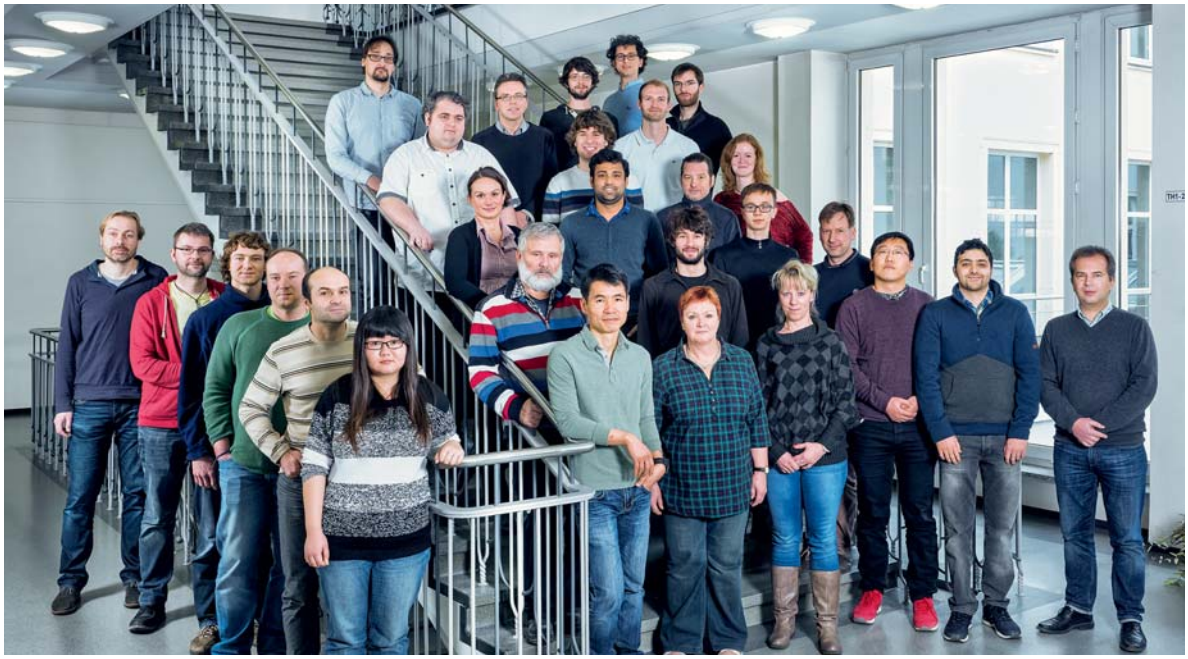

Abstract: The quest to rationalize unconventional superconductivity has been addressed by many research teams from IFF, ITF, and IMW, focusing on synthesis and crystal growth, transport, scanning probe microscopy, nuclear magnetic resonance spectroscopy, thermodynamics, angle-resolved photoemission, theory and functional thin films. The main target was the iron-based superconductors (IBS), but other superconducting and related materials have been investigated as well. In these studies, the rich spectrum of experimental techniques has been applied to various superconductors, many of which have been grown in IFW and in many cases a successful collaboration with theorists led the collection of contributions given below.

Unusual spin fluctuations in the charge and spin stripe ordered lanthanum cuprates: ^{139}La nuclear magnetic resonance studies [1] performed on $La_{1.875}Ba_{0.125}CuO_4$ show that the structural phase transitions in this compound are of displacive type. Our data indicate that charge order triggers the slowing down of spin fluctuations. Below the spin-ordering temperature $T_{SO} = 40$ K, $1/T_1$ reveals the development of enhanced spin fluctuations in the spin-ordered state for H||[001], which are completely suppressed for large fields H||[100]. Therefore, the spin order is stabilized at large fields only for H||[100] involving the spin-flop transition at ~7 T||[100], whereas fields perpendicular to the CuO_2 planes do not suppress the spin fluctuations completely.

Crystal growth and the electronic phase diagram of the 4d doped $Na_{1-\delta}Fe_{1-x}Rh_xAs$: Single crystals of $Na_{1-\delta}Fe_{1-x}Rh_xAs$ have been grown and thoroughly characterized by powder X-ray diffraction, magnetic susceptibility, electronic transport, specific heat, and ARPES

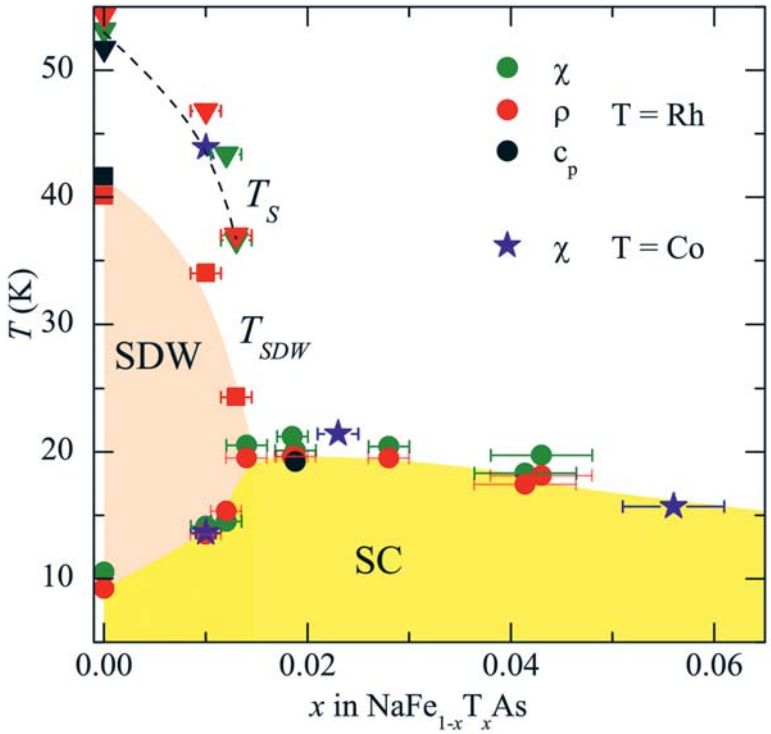

Fig. 1: Electronic phase diagram of $Na_{1-\delta}Fe_{1-x}Rh_xAs$ inferred from magnetization, resistivity, and specific heat measurements. Critical temperatures of $Na_{1-\delta}Fe_{1-x}Co_xAs$ are added to show the generic behavior upon electron doping in $Na_{1-\delta}FeAs$.

[2]. We observe a typical dome-like shape for the superconducting part of the electronic phase diagram which is very similar to that of Co-doped NaFeAs (Fig. 1).

Role of orbital degrees of freedom: We have grown single crystals of $Ba_{1-x}Na_xFe_2As_2$ with $0.25 \leq x \leq 0.4$. Neutron diffraction [3] reveals two successive magnetic transitions: Besides the well-established magnetic transition where the in-plane magnetic moments are arranged in a similar fashion as in other Fe-pnictides, while a spin-reorientation occurs at lower T. This spin reorientation towards alignment of the magnetic moments parallel to the c direction qualitatively agrees with the anisotropies observed in pure and in doped $BaFe_2As_2$, and implies a nearly degenerate orbital configuration.

Breakdown of superconductivity upon Mn doping in $La_{1-y}Y_yFeAsO_{0.89}F_{0.11}$: Combined thermodynamic and NMR studies have shown that the increase in the chemical pressure driven by Y for La substitution in $La_{1-y}Y_yFe_{1-x}Mn_xAsO_{0.89}F_{0.11}$ [4] leads to a less effective suppression of the superconducting ground state by Mn doping. ^{19}F NMR $1/T_1$ measurements exhibit a low-T peak which indicates the onset of very low-frequency dynamics with an amplitude directly related to the proximity of the compound to the QCP between superconducting and magnetic phases. This behavior suggests that T_c is depressed by the decrease in the spin fluctuations around $(\pi/a,0)$, which are widely believed to mediate the pairing, or by the localization effect in the region close to the metal-insulator boundary.

Significant increase of superfluid density [5]: Applied pressure on $LaFeAsO_{0.89}F_{0.11}$ leads to a significant increase of superfluid density over effective band mass of Cooper pairs by ~30% while conserving the high T_c. This can be explained within a multiband model and taking non-magnetic impurities into account. It is assumed that pressure modifies the ratio between intraband and interband impurity scattering rates by only acting on structural parameters while keeping the amount of chemical quenched disorder constant.

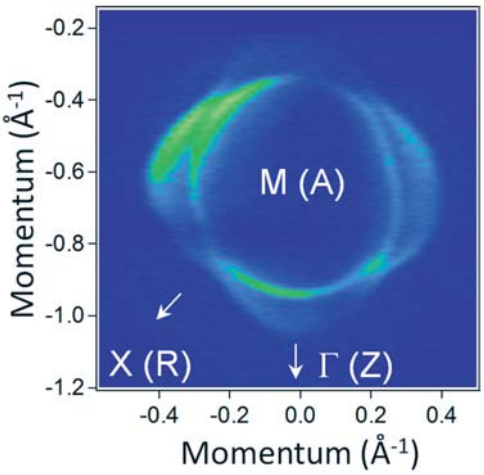

Fig. 2: Fermi surface of LiFeAs split by spin-orbit coupling along high symmetry directions.

Direct observation of spin-orbit coupling in iron-based superconductors [6]: Spin-orbit coupling is a fundamental interaction in solids that can induce a broad range of unusual physical properties. In IBS its role has, so far, not been considered of primary importance. Using angle-resolved photoemission spectroscopy, we directly observed a sizeable spin-orbit splitting in all the main members of the IBS (cf. Fig. 2). We demonstrated that its impact on the low-energy electronic structure and details of the Fermi surface topology is decisive and the largest pairing gap is supported exactly by spin-orbit coupling-induced Fermi surfaces, implying a direct relation between this interaction and mechanism of high-temperature superconductivity.

Interaction-induced singular Fermi surface in a high-temperature oxypnictide superconductor [7]: In the family of IBS, LaFeAsO-type materials possess the simplest electronic structure and host superconductivity with the highest transition temperature $T_c \approx 55$ K. Early theoretical predictions of their electronic structure revealed multiple large circular portions of the Fermi surface with a very good nesting. We showed that a prototypical compound of the 1111-type, $SmFe_{0.92}Co_{0.08}AsO$ possesses a distinctly different Fermi surface, which consists of two singular constructs in the center and corners of the Brillouin zone. Such singularities dramatically affect the low-energy electronic properties of the material, including superconductivity. Occurrence of these singularities correlates with the maximum superconducting transition temperature attainable in each material class over the entire family of IBS.

Tracing the s+– symmetry in iron pnictides by controlled disorder [8]: Consecutive proton irradiation of IBS reduces the superconducting transition temperature monotonically. Our systematic optical THz investigations of $Ba(Fe_{0.9}Co_{0.1})_2As_2$ thin films reveal, however, that the low-energy superconducting gap is first suppressed, but recovers for higher irradiation doses. At the same time the decrease of the superfluid density with disorder comes to a halt. These observations agree with theoretical calculations, which predict a disorder-induced transition of the order parameter from s+– to s++ symmetry. Thereby, we solve the longstanding puzzle of the IBS gap symmetry in favor of s+– symmetry and demonstrate THz spectroscopy as a tool to determine the symmetry of the superconducting order parameter.

Magnetic moment formation due to arsenic vacancies in LaFeAsO-derived superconductors [9]: Arsenic vacancies in LaFeAsO-derived superconductors are nominally non-magnetic defects. However, we find from a microscopic theory that in their vicinity local magnetic moments form due to the bond breaking to neighboring iron atoms. The moments emerging around an arsenic vacancy orient ferromagnetically and cause a substantial enhancement of the paramagnetic susceptibility in both the normal and superconducting state. DFT calculations show that an As vacancy gives rise to a doublet of impurity resonances of Fe $3d_{yz,xz}$ character at the Fermi level.

Strain and doping effects in Fe-based superconducting thin films: We systematically investigated the electronic and magnetic properties of $Ba(Fe_{1-x}Co_x)_2As_2$, $BaFe_2(As_{1-x}P_x)_2$, and $FeSe_{1-x}Te_x$ thin films in different tensile and compressive in-plane strain states. We found that the strain can shift the whole phase diagram including antiferromagnetic regions and the superconducting dome in the direction of higher or lower substitution levels depending on compressive or tensile strain, respectively. A particular emphasis was laid on the preparation of high-quality $FeSe_{1-x}Te_x$ films. The transport properties of the films on different substrates are mainly influenced by the crystalline quality arising from the lattice misfit towards the template [10]. However, we were able to control the interface on selected substrates by using an isostructural seed layer resulting in improved superconducting properties. [11]

Anisotropy of critical currents and upper critical fields: High field studies on $Ba(Fe_{1-x}Co_x)_2As_2$ thin films revealed that the temperature and angular dependence of the upper critical field is best explained by a two-band model in the clean limit (Fig. 3). The anisotropy of the critical current J_c is influenced by the H_{c2} anisotropy (and therefore by multi-band effects) in the broad range of the field angles. However, the extended planar and columnar defects usually present in the samples mask the effect of the intrinsic H_{c2} anisotropy in the vicinity to $H||c$ and $H||ab$. [12] Furthermore, we found that optimally doped $BaFe_2(As_{1-x}P_x)_2$ films show the highest J_c among IBS with a J_c of 6.3 MA/cm^2 at 4.2 K even though no structural defects were observed in TEM and XRD [13]. This suggests that rather weak structural inhomogeneities result in strong pinning centers due to a sharp maximum in vortex core energy near the quantum critical point. Finally, the upper critical field H_{c2} anisotropy γ of $Ca_{10}(Pt_nAs_8)(Fe_{2-x}Pt_xAs_2)_5$ (n = 3, 4) single crystals with long FeAs interlayer distances was studied by angular dependent resistivity measurements. The γ values are much larger than those of other IBS. Remarkably, the values of γ^2 show an almost linear increase with the FeAs/FeSe interlayer distance for IBS. [14]

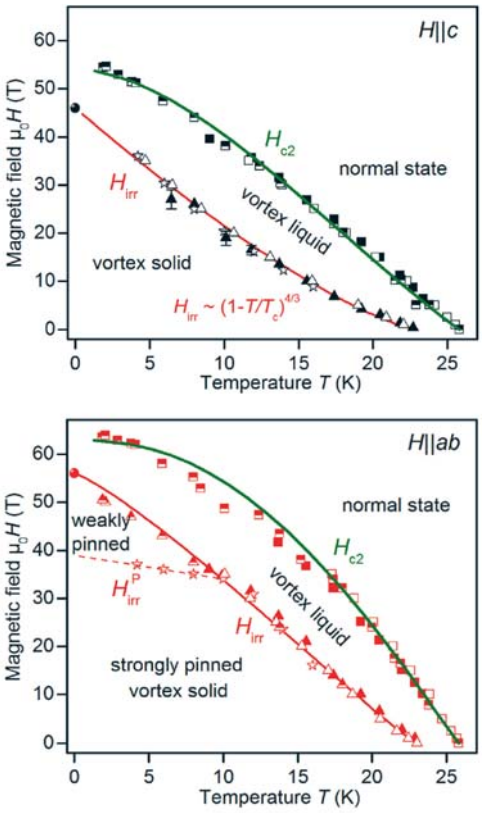

Fig. 3: Magnetic field-temperature phase diagram of a Co-doped Ba-122 thin film with extended defects for H c and H ab [12].

[1] S.-H. Baek et al., Phys. Rev. B **92**, 155144 (2015)
[2] F. Steckel et al., Phys. Rev. B **91**, 184516 (2015)
[3] F. Wasser et al., Phys. Rev. B **91**, 060505(R)
[4] F. Hammerath et al., Phys. Rev. B **92,** 20505 (2015)
[5] G. Prando et al., Phys. Rev. Lett. **114**, 247004 (2015)
[6] S. Borisenko et al., Nature Physics (in press)
[7] A. Charnukha et al., Scientific Reports **5**, 10392 (2015)
[8] M. B. Schilling, arxiv:1511.05017v1 (2015)
[9] K. Kikoin, Scientific Reports **5**, 11280 (2015)
[10] F. Yuan et al., Supercond. Sci. Technol. **28**, 065005 (2015)
[11] S. Molatta et al., Scientific Reports **5**, 16334 (2015)
[12] J. Hänisch et al., Scientific Reports **5**, 17363 (2015)
[13] F. Kurth et al., Appl. Phys. Lett. **106**, 072602 (2015)
[14] F. F. Yuan et al., Appl. Phys. Lett. **107**, 012602 (2015)

A habilitation thesis with the title „Quasiparticle interference: an approach to the pairing mechanism in iron-based superconductors" has been successfully defended by Steffen Sykora.

Large third party projects:

- DFG SPP1458 "High Temperature Superconductivity in Iron Pnictides", coordinated by IFW. Principal investigators of sub-projects: S. Borisenko, J. van den Brink, B. Büchner, S. Drechsler, D. Efremov, J. Fink, H. Grafe, C. Hess, S. Wurmehl
- DFG GRK1621 "Itinerant magnetism and superconductivity in intermetallic systems", Spokesperson: H. H. Klauss (TU Dresden), IFW groups involved: Synthesis and crystal growth, Transport and scanning probe microscopy, Theory, Functional thin films
- ERC Consolidator Grant „Electronic Order, Magnetism, and Unconventional Superconductivity probed in Real-Space", Principal Investigator: C. Hess

Cooperations: Diamond Ltd., Karlsruhe Institute of Technology (KIT), ETH Zurich, Helmholtz-Zentrum Berlin, University of Cologne, Nagoya University, Southeast University Nanjing, NHMFL Tallahasee, HZDR Dresden, P. N. Lebedev Physical Institute Moscow, University Genova

Organization of workshops: Christian Hess, Sergey Borisenko, Ilya Eremin, Workshop "The two-dimensional chalcogenides: exotic electronic orders, superconductivity and magnetism" 31.08. – 03.09.2015, IFW Dresden

Research topic 1.3

Magnetic materials for energy

People: A. Alfonsov, M. Belesi, F. Bittner, C. G. F. Blum, A. Diestel, J. Eckert[1], S. Fähler, A. Funk, M. Gellesch, L. Giebeler, O. Gutfleisch[2], F. Hammerath, M. Herklotz, M. Hinterstein[5], M. Hoffmann, R. Hühne, B. Johansson[3], K. Koepernik, M. Kopte, M. Krautz, X.-Q. Li[3], D. Lindackers, W. Löser, O. Mityashkin, T. Mix, J. D. Moore, K.-H. Müller, V. Neu, R. Niemann, U. Nitzsche, A. Omar, S. Oswald, B. Peters[4], D. Pohl, L. Reichel, M. Richter, J. Romberg, U.K. Rößler, B. Schleicher, S. Schönecker[3], L. Schultz, F. Seifert, S. Selter, K. Skokov, L. Vitos[3], A. Waske, B. Weise, T. G. Woodcock, S. Wurmehl, F. Y. Yang[4]
Responsible Directors: B. Büchner, K. Nielsch, T. Gemming, J. van den Brink

Abstract: Magnetic intermetallic alloys and compounds exhibit diverse physical states which are characterized, e.g., by the size and direction of the atomic moments, their correlation in space and time, their mutual and spin-lattice interaction energies. The related properties and phenomena (spontaneous magnetization and order, magnetic anisotropy, spin polarization at the Fermi energy, phase transitions, magneto-caloric, magneto-electric and magneto-transport effects) enable these materials to be used in energy-efficient applications. Relevant materials comprise permanent magnets for electric motors or generators, magnetic information-storage films and magneto-resistive sensors. Emerging applications include magneto-caloric cooling, direct actuation with magnetic shape-memory alloys and spin-based electronic devices. In the following, we highlight significant publications.

(i) Materials for spintronic applications

We studied the local structural and magnetic properties of $Co_2FeAl_{0.5}Si_{0.5}$ Heusler films with varying thickness by nuclear magnetic resonance (NMR) [1]. A detailed analysis of the NMR spectra showed, that the formation of certain types of order depends not only on the thermodynamic phase diagrams as in bulk samples, but that also kinetic control may contribute to the phase formation in thin films. The very good quality of the films as demonstrated by our NMR study suggests that the technique of off-axis sputtering used to grow the films sets the stage for the optimized performance of $Co_2FeAl_{0.5}Si_{0.5}$ in spintronic devices.

(ii) Multi-caloric effects

In-situ synchrotron XRD measurements of magneto-caloric $LaFe_{11.8}Si_{1.2}$ are used to understand virgin effects and asymmetry of the magnetovolume transition. A remarkable change of the transition kinetics occurs after the first cycle, which we attribute to the formation of cracks originating from the volume change. Tomographic imaging reveals that the bulk material disintegrates via an interlocked state where fragments are loosely connected. Though cracks have opened between the fragments, the transition is sharp due to magnetostatic interactions (cf. Fig.). In the cycled sample we find a strong asymmetry between the transition interval upon heating and cooling originating in isostatic pressure acting on parts of the sample during the cooling transition [2].

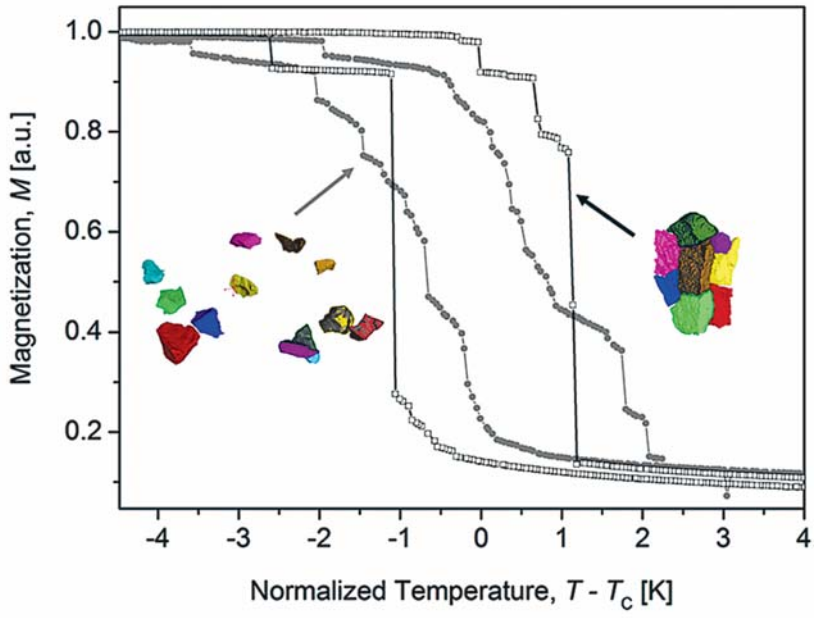

Fig.: The magnetic transition of an interlocked particle ensemble (open squares) is very sharp even though most particles are separated by cracks. For a well separated particle ensemble (solid circles), the transition broadens significantly.

Multi-caloric stacks consisting of a magnetocaloric film on a piezoelectric substrate promise improved caloric properties as the transition temperature can be controlled by both, magnetic and electric fields [3]. We present epitaxially grown magneto-caloric Ni-Mn-Ga-Co thin films on ferroelectric $Pb(Mg_{1/3}Nb_{2/3})_{0.72}Ti_{0.28}O_3$ (PMN-PT) substrates. Structure and microstructure of two samples, being in the austenitic and martensitic state at room temperature, are investigated by X-ray diffraction in two- and four-circle geometry, by atomic force microscopy and by high temperature magnetometry. The combination of these methods allowed separating the influence of epitaxial growth and martensitic transformation. A preferential alignment of twin boundaries is observed already in the as-deposited state, which indicates the presence of pre-stress, without applying an electric field to the substrate. By temperature-magnetic field phase diagram the inverse magnetocaloric effect of the epitaxial Ni-Mn-Ga-Co film is demonstrated.

Zero-field static and dynamic ^{55}Mn NMR experiments of bulk and powder samples of the ferromagnetic Heusler shape-memory alloy Ni_2MnGa give direct access to the sequence of structural phase transitions in this compound, from the high–T austenitic phase down to the low–T martensitic phase. In addition, a detailed investigation of the so-called rf–enhancement factor delivers the local magnetic stiffness and restoring fields for each separate structural environment, thus, differentiating signals coming from austenitic and martensitic components. In this way we can also resolve differences in the local spin moments of the two phases of the order of 0.08 Bohr magnetons, and reveal precursor phenomena of the martensitic transformation well inside the parent austenitic phase [4].

(iii) Magneto-caloric composites

Magneto-caloric $La(Fe,Si)_{13}$ is usually very brittle and requires the combination with another material to form a regenerator that will survive millions of cycles in a device. A novel magneto-caloric composite based on $La(Fe,Si)_{13}$ particles in an amorphous metallic matrix has been studied [5]. Magneto-caloric particles and a powderized Pd-based glass were hot-compacted at the glass transition temperature of the metallic matrix. At this temperature, the viscous matrix can easily fill the pores between the $La(Fe,Si)_{13}$ particles, thereby creating a dense composite. Furthermore, the matrix acts as a buffer during the hot-compaction and prevents crack formation in the particles, which is otherwise known to reduce their performance. Tuning our processing route, the magneto-caloric properties of the composites are almost independent of the compaction pressure.

Alternatively, we have combined $La(Fe,Si)_{13}$-based particles of varying size with a polymer matrix [6]. Such composites were pressed into thin plates. We found that a higher filling factor can be achieved by using a mixture of several particle size fractions. This has beneficial influence both on the magneto-caloric properties and on the thermal conductivity. Tests in an active magnetic regenerator revealed that a maximum temperature span of approximately $\Delta T = 10$ K under a magnetic field change of $\mu_0 H = 1.15$ T can be obtained without cooling load. The stability of the measured ΔT values and the mechanical integrity of the sample after cyclic application of a magnetic field have been monitored for 90,000 cycles and showed very good stability of the magneto-caloric performance.

(iv) Validation of the innovation potential of room-temperature magnetic cooling effect (MCE)

We developed new approaches for MCE materials for room-temperature applications, performing thermal analysis of active magnetic refrigeration cycles, as well as of novel demonstrators for cooling devices. Two test benches for durability lifetime tests as well as a thermal testbench was designed. Recently, we commissioned a novel magnetocaloric demonstrator.

(v) Metamagnetic transitions in FeRh magnetocaloric materials

The fundamental mechanisms governing the metamagnetic transition in FeRh alloys are still poorly understood. The electronic and lattice contributions to the transition are being studied as are the effect of ternary alloying elements on the physical properties and the role of the microstructure on the metamagnetic transition.

(vi) Permanent magnets

The recovery of rare earths (critical materials) from magnet materials is a key demand of modern technologies. We developed a new route for recycling of Nd from Nd-Fe-B magnets by exploiting large scale phase separation phenomena upon melt metallurgical processing with defined Cu fractions [7].

(vii) Rare earth free permanent magnets

The $L1_0$ phases in the binary systems Mn-Al and Mn-Ga have magnetic properties which make them potential candidates to replace certain types of rare earth containing magnets. Phase stability, intrinsic and extrinsic magnetic properties have been studied as a function of composition in Mn-Ga [8]. In the Mn-Al system, the crystalline defects in the material have been studied for the first time using electron backscatter diffraction, which allowed large areas to be analysed. Three different types of twin-like defects have been identified whose relative proportions change after various processing steps [9].

(viii) Metastable phases with novel functionalities

To identify unknown metastable phases with related unexpected properties, we systematically investigated 24 transition metal elements in body-centered tetragonal (bct) geometries by means of density-functional (DF) calculations. We found that the fcc structures of Sc, Ti, Co, Y, Zr, Tc, Ru, Hf, Re, and Os, and bct Zr with c/a = 0.82 are metastable according to their computed phonon spectra. Eight of these predicted phases are so far not known from the respective pressure-temperature phase diagram. Possible ways to stabilize these phases include epitaxial growth, rapid quenching, precipitation, or severe deformation [10].

Epitaxial growth allows us even to produce strained films with structures that are unstable in the bulk. Thereby, the overlayer lattice parameters in the interface plane determine the out-of-plane lattice parameter. We show by DF calculations that this dependence can be discontinuous and predict related first order phase transitions in strained tetragonal films of the elements V, Nb, Ru, La, Os, and Ir. At such a phase transition, properties of the overlayer material are switched. This was demonstrated for the example of the superconducting critical temperature of a vanadium film which we predict to jump by 20% [11].

[1] A. Alfonsov, et al., Phys. Rev. B **91**, 064421 (2015)
[2] B. Schleicher, et al., J. Appl. Phys. **118,** 023908 (2015)
[3] A. Waske et al., Phys. Status Solidi RRL **9**, 136 (2015)
[4] M. Belesi, et al., Phys. Rev. B **91**, 134415 (2015)
[5] M. Krautz, et al., Scripta Materialia **95**, 50 (2015)
[6] A. Waske, et al., Phys. Stat. Sol. RRL **9**, 136 (2015)
[7] M. Moore, et al., J. Alloys Compd. **647**, 997 (2015)
[8] T. Mix, et al., J. Magn. Magn. Mater. **391**, 89 (2015)
[9] F. Bittner, et al., Acta Materialia **101**, 48 (2015)
[10] S. Schönecker, et al., RSC Adv. **5**, 69680 (2015)
[11] S. Schönecker, et al., New J. Phys. **17**, 023005 (2015)

Funding: DFG, Audi AG, BASF, EU

Cooperations: KIT Karlsruhe; MPI CPfS; [1]Montanuniversität Leoben, Austria; Uni Bielefeld; Uni Duisburg-Essen, MPIE Düsseldorf; [2]TU Darmstadt; TU Dresden; TU München; Academy of Science Prague, Czech Republik; Institute Néel / CNRS, France; [3]KTH Stockholm; KITECH, Korea; NCSR Demokritos, Greece; [4]Ohio State University, USA; Uni Exeter (UK);TU Eindhoven, Netherlands; U. Uppsala, Sweden; Audi AG, BASF; Vakuumschmelze Hanau; [5]DESY-PETRA III

Research topic 1.4

Engineering magnetic microtextures

People: A. N. Bogdanov, P. Bonfa[1], R. DeRenzi[1], M. Deutsch[2], M. Doerr[3], T. Goltz[3], H. H. Klauss[3], C. Koz[4], K. Koepernik, A. O. Leonov, E. Lopatina, D. Makarov, N. Martin[2], Ph. Materne, I. Mirebeau[2], Th. Mühl, V. Neu, Ch. F. Reiche, S. Rößler[4], U. K. Rößler, R. Schäfer, L. Schultz, U. Schwarz[4], I. Soldatov, T. Sturm, S. Vock, S. Wirth[4], U. Wolff,
Responsible Directors: B. Büchner, K. Nielsch, O. G. Schmidt, J. van den Brink

Abstract: Existence of specific microtextures, in particular chiral skyrmions, in condensed matter systems relies on particular couplings which are known in the phenomenological Landau theory as Lifshitz invariants in the free energy for an order parameter. Chiral skyrmions in ferromagnetically ordered acentric magnets is now a well-established example of such states [1], but similar textures also exist in chiral nematic liquid crystals [2] with a very similar type of orientational order. Investigations currently are focused on the chiral helimagnet MnGe because of its particularly anomalous properties within the class of ferromagnetic non-centrosymmetric cubic compounds. High-pressure, high-temperature investigations now confirm an invar-like behavior with a change of spin-state and a crucial role of magneto-elastic couplings. New μSR investigations also confirm an anomalous fluctuating magnetic state in this material. Progress in the crucial magnetic imaging and detection is illustrated by two examples: (i) Tips of hard magnetic materials have been proved to allow us quantitative magnetic-force microscopy of inhomogeneous states down to very small scales. (ii) A stroboscopic illumination with polarized light and alternating angle of incidence allows vectorial magneto-optical microscopy of dynamical processes. Finally, theoretical insight into the mechanism for such twisted *Dzyaloshinskii textures* of an orientational order has been instrumental to propose the existence of new types of twisted skyrmionic phases in other materials. Prompted by a theoretical analysis, an experimental search now reveals that a liquid-like intermediate state exists in $Fe_{1+y}Te$, as a twisted or short-range-ordered precursor to an incommensurate antiferromagnetic spin-density wave. This finding of an anomalous precursor in this centrosymmetric magnetic system suggests that *Dzyaloshinskii textures* similar to skyrmionic phases can exist in vast classes of materials.

Chiral helimagnetism in cubic intermetallic compounds

In our continuing cooperation with external experimental groups, new results on the cubic transition metal germanide MnGe with the acentric B20-structure now confirms that an invar-like cross-over or transition between a high-spin and an intermediate low-spin state is crucial to understand the anomalous behaviour of this compound in contrast to the better investigated MnSi and FeGe, where skyrmionic phases and skyrmions have been found earlier. This transition had been predicted earlier from electronic structure calculations within the density-functional theory. New experiments using X-ray diffraction (XRD) and X-ray emission spectroscopy, undertaken by the group at the Laboratoire Leon Brillouin (LLB), show that pressure drives the transition between these two spin-states at room temperature in the paramagnetic state far above the magnetic ordering transition at about 170 K. The suppression of the local magnetic moment on Mn takes place in two steps, first into the intermediate spin-state at about 7 GPa but with a huge hysteresis under cyclical application of pressure. Then, at 23 GPa the local spin-polarization collapses. Calculated behaviour and experiment, thus, are in very good agreement and confirm an invar-like behaviour of MnGe with many anomalies that are rooted in coupling between magnetic spin-polarization and the lattice. The observation of a macroscopic hysteresis in the lattice-parameter versus pressure in a paramagnet can be explained by the long-range elastic couplings that accompanies the cross-over of the high-spin to the low-spin-state. This finding in the chiral helimagnet MnGe, therefore, yields an important insight into the still incompletely understood but technologically important class of intermetallic invar-like compounds: The long-range elastic interactions via the lattice are a crucial ingredient for anomalous behaviour in metallic systems with spin-state transition. The effects complicate, however, the understanding of the chiral helimagnetism and the anomalous fluctuating states near magnetic ordering in MnGe, in contrast to the helimagnets FeGe and MnSi which are basically more conventional ferromagnetic metals. Cooperation with the LLB-group currently is extended in cooperation with P. Bonfa and R. DeRenzi (U Parma) in a study on μ-spin-rotation (μSR) experiments. The experiments confirm anomalous fluctuations of two different types in the ambient pressure state of MnGe in a large temperature interval around the magnetic ordering, in accordance with the expected invar-like spin-state transitions. Supported by ab initio calculations the trapping site of the muonium in MnGe could be identified. This holds promise for further detailed identification of helimagnetic or skyrmionic states in the magnetic-field-temperature phase-diagram of MnGe.

New hard magnetic sensors for quantitative MFM of inhomogeneous magnetization structures

For the highly resolved investigation of magnetic microtextures, pure qualitative magnetic force microscopy (MFM) reveals too little information to reconstruct the three-dimensional inhomogeneous magnetization structures. The advancement of quantitative MFM (qMFM) at the IFW has been extended to the development of ultimate hard magnetic tips based on epitaxial $SmCo_5$ films. The rigidity of the tip against large external fields, but also against the stray field of the sample is a precondition to apply the tip transfer function (TTF) of a calibrated tip for correctly deconvolving measured MFM data. While typical commercial tips (CoCr based) with coercivities of only a few 10 mT fail in that respect, the new SmCo-based nanofabricated MFM sensors do not compromise on the hard magnetic performance. The epitaxial $SmCo_5$ films grow on MgO (110) single crystal substrates with a uniaxial anisotropy of more than 20 T along one well defined in-plane substrate direction and develop coercivities above 2 T (Fig. 1a). A triangular tip is separated from the film and attached to a cantilever in a dual beam (SEM + FIB) nanomanipulation tool (see inset). The TTF (Fig. 1 b) is sharply peaked and compares well in resolution with commercial MFM tips. The superiority of the new sensor is demonstrated by imaging the domain structure of a Sm_2Co_{17} bulk sample with large stray

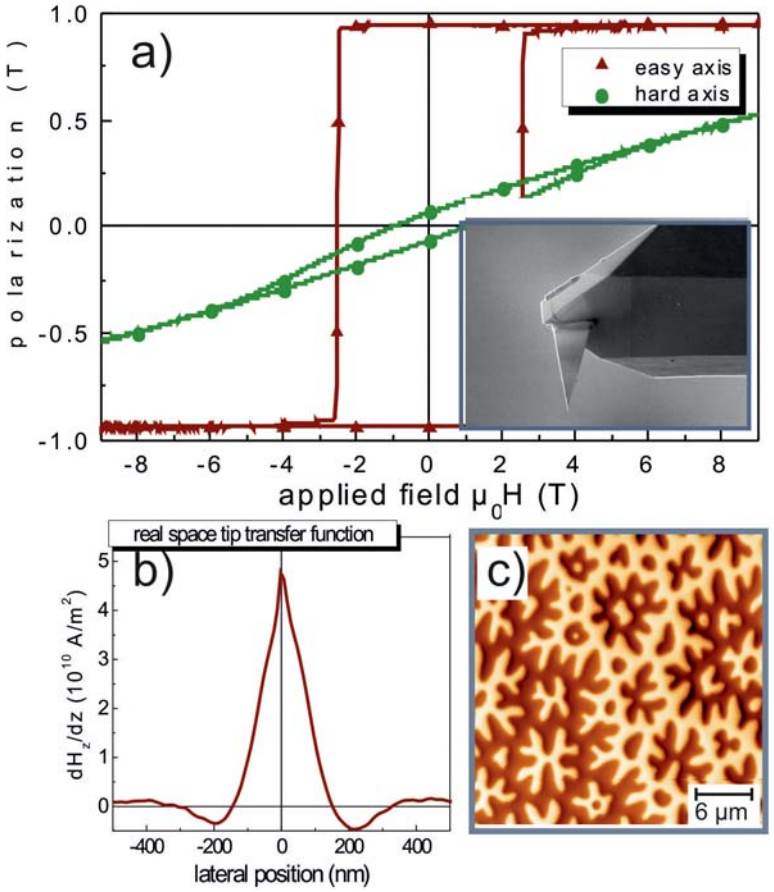

Fig. 1: New hard magnetic sensors for quantitative MFM of inhomogeneous magnetization structures; **a)** hysteresis curves of epitaxial $SmCo_5$ films (inset: MFM tip of $SmCo_5$ material); **b)** tip transfer function of the $SmCo_5$ tip; **c)** domain structure of a Sm_2Co_{17} bulk sample imaged with a hard magnetic $SmCo_5$ tip.

fields. While the magnetization state of commercial tips rotates uncontrollable in the stray field of the sample the new sensors produce a well-defined branched domain pattern (Fig. 1 c), only resolvable with a magnetically rigid tip.

Vectorial Kerr microscopy

A new Kerr-LED lamp was developed for wide-field Kerr Microscopy. Eight monochromatic LEDs are placed in an external controller box that includes electronics. The light of the diodes is guided to the lamp house of the microscope by glass fibers. Their ends are arranged in a cross way and are imaged to the diffraction plane of the microscope. Various Kerr-sensitivity options (longitudinal, transverse and polar Kerr sensitivities) can be chosen by activating different LEDs of the array. The selection is made conveniently by computer control. The following sensitivity choices are available: (i) longitudinal sensitivity with superimposed polar sensitivity, (ii) transverse sensitivity with superimposed polar sensitivity, (iii) pure polar sensitivity. A single domain image is displayed on the screen in each case and the LEDs are activated continuously. Further options are possible by running the LEDs in a pulsed mode in accordance with the camera: (iv) simultaneous display of longitudinal and transverse contrast, i.e. vectorial Kerr microscopy in two separate frames on the screen, (v) display of pure longitudinal contrast in a single frame, and (vi) display of pure transverse contrast in a single frame on the screen. Alternatively, the LED lamp can also be run in a dichromatic mode: Here the controller box contains 4 red and 4 blue LEDs with specific arrangement in the glass fiber cross. Two images of different color and Kerr sensitivity are generated at the same time, which are separated by a color-sensitive image splitting device between microscope and camera. Both images are displayed simultaneously within the same frame on the screen. The dichromatic version adds the simultaneous display of pure longitudinal and transverse images. The vectorial option allows for quantitative Kerr microscopy of magnetization processes that was not possible by using conventional microscopy lamps.

Dzyaloshinskii textures of incommensurate spin-density wave

Within the framework of Landau-theory for general inhomogeneous ordering modes, modulated states with certain general wave-vectors allow for the existence of several twisting terms, known as Lifshitz invariants, as pioneered by Dzyaloshinskii more than 50 years ago. This implies that ordinary ordering continuous phase-transitions are impossible. In the intermediate range before the fully ordered state sets in, there is a gap allowing the existence of textures like skyrmions or similar states. Spin-density waves with rotatable polarization direction are primary candidates for such precursor states that bear similarity with other intermediate states like chiral skyrmions in acentric magnets or blue phases in chiral nematic liquid crystals. Guided by this idea, we identified the incommensurate antiferromagnetic helix-state in the centrosymmetric tetragonal compound $Fe_{1+y}Te$ as a candidate material to display such *Dzyaloshinskii textures* (Fig. 2). This material is well known as the magnetic parent material isostructural with the family of Fe-based '11'-superconductors, FeSe and Fe(Se,Te) which makes it a topical material to understand its magnetism in its own right. In cooperation with the MPI-CPFS and TU-Dresden, a detailed investigation of magnetic order has been performed by using Mössbauer spectroscopy [3]. This local probe is an ideal tool to identify inhomogeneous magnetic textures, and the experiments provided clear evidence from internal magnetic hyperfine fields stemming for a magnetic precursor state with a quasi-static magnetic order in absence of true long-range order above the Neel temperature, where the transition into the antiferromagnetic helix-state sets in. The results are in qualitative agreement with the expected unconventional phase-transition and existence of intermediate meso-phases in this material. This first investigation into with the possibility of twisted modulated states shows that localized or skyrmionic texture on a mesoscopic scale should exist in a much wider range of materials including many different magnetic materials where the basic ordering is incommensurate. It also can be envisaged that similar textures can exist beyond magnetism, e.g. for soft-modes in crystalline materials undergoing driving structural phase-transitions similar texture may eventually exist.

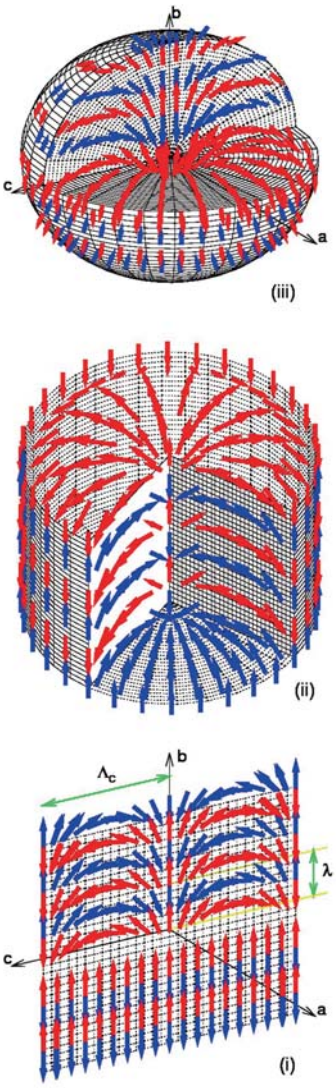

Fig. 2: Dzyaloshinskii textures: twisted modulated antiferromagnetic states from one-dimensional to three-dimensional (i)-(iii).

[1] U. K. Rößler et al., Nature **442** (2006) 797
[2] A. O. Leonov et al., Phys. Rev. E **90** (2013) 042502
[3] Ph. Materne et al., Phys. Rev. Lett. **115** (2015) 177203

Funding: DFG, ERC

Cooperations: [1]CEA Saclay, Laboratoire Leon Brillouin, France; [2]University Parma, Italy; [3]Max Planck Institute, CPFS Dresden, Germany; [4]TU Dresden, Germany

Research topic 1.5

Topological states of matter

People: J. H. Bardarson,[1] M. Capone,[2] S.-W. Cheong,[3] R. Citro,[4] M. Cuoco,[4] B. Dassonneville, H. Ding,[5] J. Dufouleur, O. Eibl,[6] B. Eichler, M. Eschbach,[7] W. Escoffier,[8] S. F. Fischer,[9] H. Funke, P. Gentile,[4] M. P. Ghimire, G. Giovannetti, R. Giraud, J. G. Gluschke,[10] M. Goiran,[8] J. Gooth,[11] S. Gorantla, S. Gutsch,[12] S. Hampel, Z. Han,[13] M. W. Haverkort,[14] J. Henk,[15] N. F. Hinsche,[15] F. Iacovella,[8] W. Jin,[16] D. Kasinathan,[14] B. Kaufmann,[17] J. Kellner,[17] K. Koepernik, D. Kojda,[9] M. Kroener,[12] Y. Kushnirenko, A. Lau, M. Leijnse,[10] M. Liebmann,[17] H. Linke,[10] K. Liu,[13] Z. Liu, R. Lou,[13] P. Marra,[4] I. Mertig,[15] R. Mitdank,[9] M. Morgenstern,[17] C. Nowka, C. Ortix, R. M. Osgood, Jr.,[16] C. Pauly,[17] N. Peranio,[6] L. Plucinski,[7] M. Pratzer,[17] L. Pudewill,[11] T. Qian,[5] B. Rasche,[18] T. Rauch,[15] M. Richter, F. Rittweger,[19] M. Ruck,[18] C. M. Schneider,[7] U. Steiner,[20] L. H. Tjeng,[14] W. Toellner,[11] L. Veyrat, H. Wang,[13] S. Wang,[13] X. Wang,[3] Z. Wang,[12] P. Woias,[12] E. Xypakis,[1] M. Yang, M. Zacharias,[12] S. Zastrow,[11] and R. Zierold[11]

Responsible Directors: B. Büchner, K. Nielsch, O. G. Schmidt, J. van den Brink

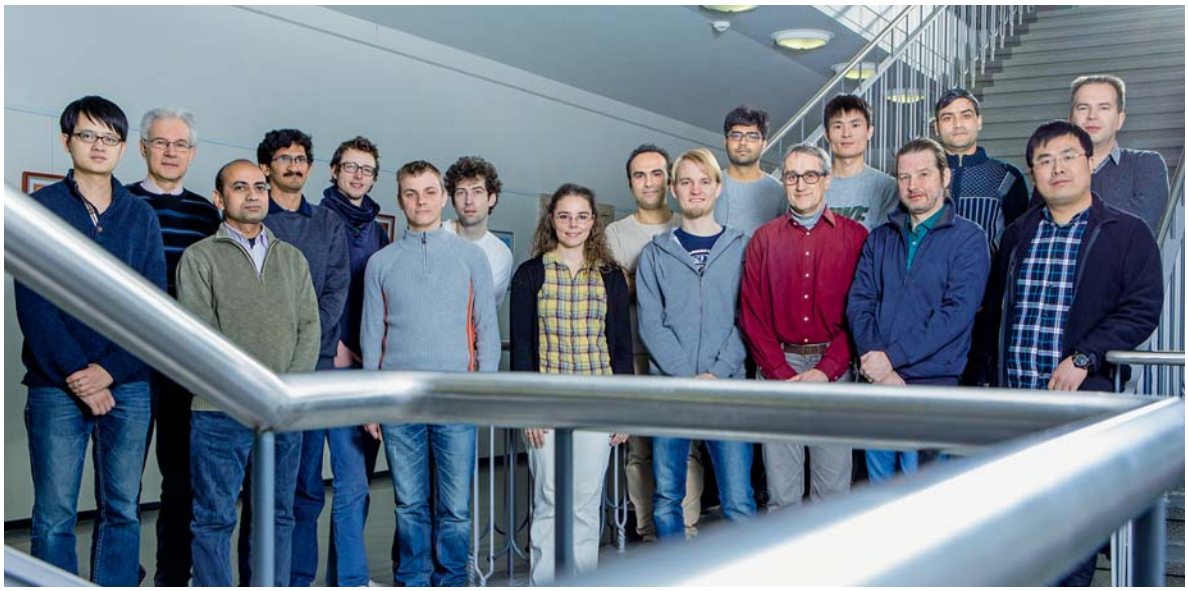

Abstract: Topology is a powerful paradigm behind new developments in quantum condensed matter. The consideration of Berry phase effects led to a novel classification of insulators. Of particular interest, Z_2 topological insulators (TIs) offer the possibility to use the topological protection of states for potential applications in spintronics or quantum computation. Given the diversity and richness of topological states and phases in condensed matter, this research is a source of inspiration for new developments in theory, materials research and cutting-edge experiments. At IFW, topological states of electrons or photons are investigated by combining skillful preparation with experimental and theoretical expertise. Thus, our research on TIs considers different aspects: fundamental theory, identification of new materials, growth or preparation of bulk or nanoscale materials, their characterization as well as study of their electronic structure, spectroscopic and transport properties.

It is fair to say that the principles of non-interacting topological insulating phases are presently well understood. For this reason, the attention in fundamental research has gradually shifted to **interaction-driven topological insulating phases**. Electronic correlations can indeed give rise to insulating topological phases without non-interacting analogs, such as the fractional topological insulators (TIs). They can also spontaneously generate spin (in)dependent chiral orbital currents leading to the quantum anomalous Hall effect or the quantum spin Hall effect. For the case of a honeycomb lattice, we have shown that specific substrate-induced electrostatic potentials can trigger the onset of an interaction-driven topological phase. This is due to substate-induced non-Abelian

gauge fields that reshape the Dirac cones into a quadratic band crossing point. As demonstrated by density functional (DF) calculations, this scenario can realistically occur in graphene placed on top of hexagonal In_2Te_2 monolayers [1]. The mixed-valent compound SmO was found to be a three-dimensional (3D) strongly topological semimetal due to a *4f-5d* band inversion at the X point. We also showed by DF calculations that the topological non-triviality of SmO prevails for a wide range of lattice parameters, making SmO an ideal candidate to investigate topological nontrivial correlated flat bands in thin films. SmO/EuO thin film interfaces are suggested for realizing the quantum anomalous Hall effect [2].

A layered bismuth compound, $Bi_{14}Rh_3I_9$ (Fig. 1), was recently synthesized at TU Dresden and identified as the first ever prepared **weak 3D topological insulator** by a combination of angle-resolved photoemission spectroscopy (ARPES) experiments and DF calculations at IFW. A weak 3D TI has protected edge states on some, but not on all facets of its surface. In particular, it may have such states on surface step edges. Scanning tunneling spectroscopy measurements performed at RWTH Aachen indeed disclosed conducting channels at step edges on a cleavage surface of $Bi_{14}Rh_3I_9$. These channels are less than 1 nm broad, backscatter-free, as well as continuous in space and energy. Dedicated DF calculations confirmed the topography and the position of the gap at the investigated polar surface. The surface of $Bi_{14}Rh_3I_9$ can be engraved using an atomic force microscope, allowing networks of protected channels to be patterned with nanometer precision [3]. We have furthermore shown that a class of weak 3D TIs can feature one-dimensional Dirac electrons on their surface. The occurrence of these line degeneracies is protected by a symmetry that we dubbed as in-plane time-reversal invariance [4].

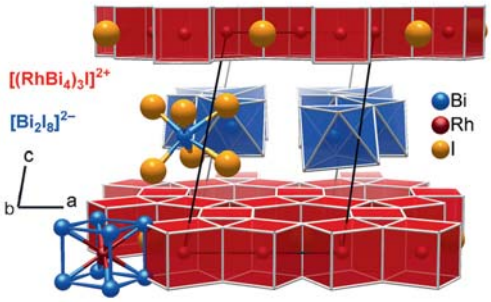

Fig. 1: Atomic polyhedron model of the layered compound $Bi_{14}Rh_3I_9$. Two ionic layer types are repeated in the stack: a cationic 2D TI layer (red) and an anionic spacer layer (blue) [3].

The phase transition from a topological insulator to a trivial band insulator was studied using **angle-resolved photoemission spectroscopy** on $Bi_{2-x}In_xSe_3$ single crystals [5]. We traced the complete evolution of the bulk band structures throughout the transition, Fig. 2. The robust surface state and the bulk-gap size (≈ 0.50 eV) show no significant change upon doping for x = 0.05, 0.10, and 0.175. At $x \geq 0.225$, the surface state completely disappears and the bulk-gap size increases, suggesting a sudden gap closure and topological phase transition around $x \approx 0.175 \ldots 0.225$. We propose that the phase transition is governed by the combined effect of spin-orbit coupling and band hybridization. Our study provided a venue to investigate topological phase transitions induced by nonmagnetic impurities.

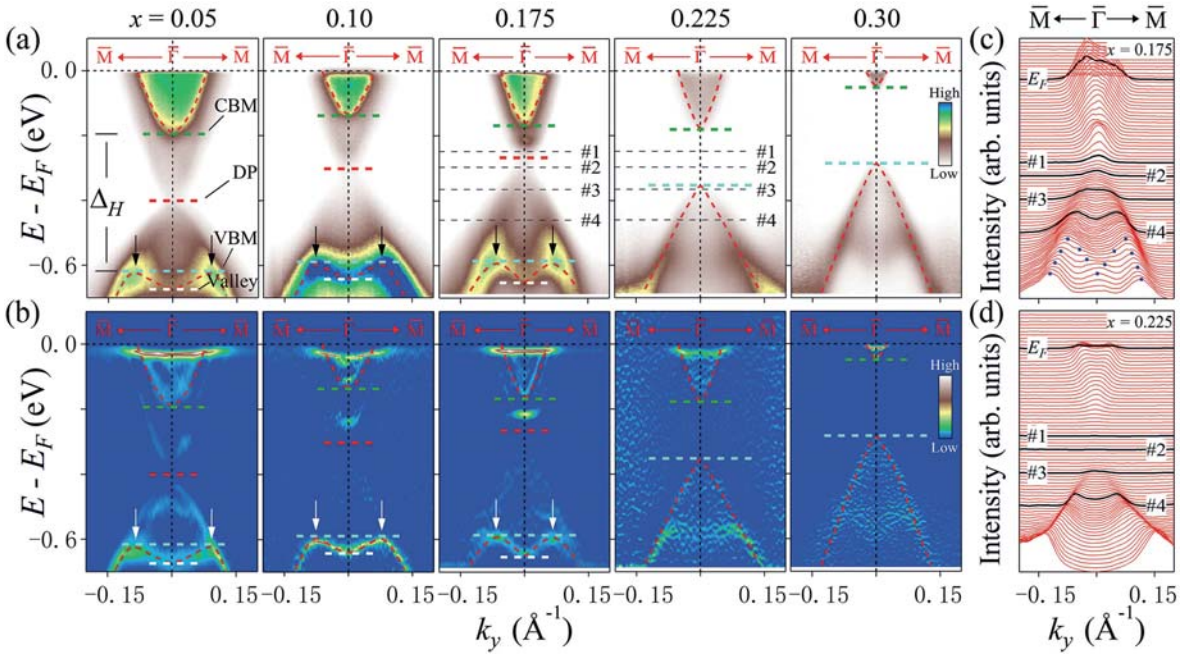

Fig. 2: (a) ARPES intensity plots and **(b)** the corresponding second-derivative plots of $Bi_{2-x}In_xSe_3$ along the Γ-M direction (h = 20 eV) [5].

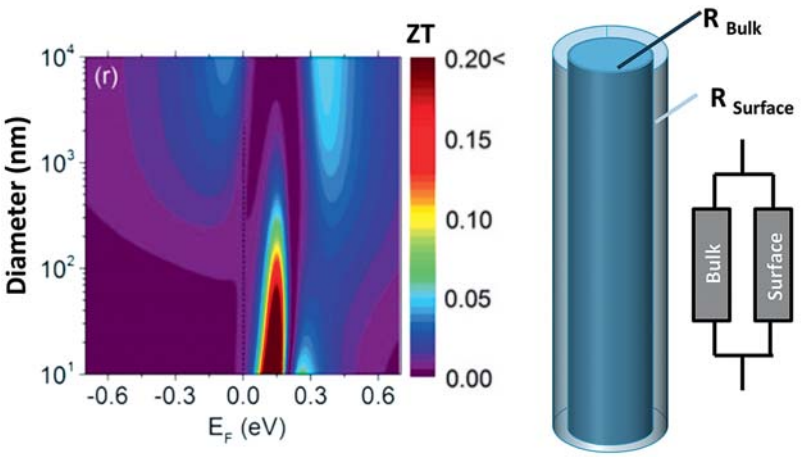

Fig. 3: The thermoelectric figure of merit ZT is plotted as function of diameter and Fermi level E_F of a Bi_2Se_3 nanowire. When the wire diameter is reduced, the surface to volume ratio increases and the thermoelectric transport is increasingly dominated by the surface states calculated by a two-channel model [10].

To obtain a deeper understanding of the established 3D TIs, we performed **transport experiments on nanostructures**. The investigation of surface-states transport on Bi_2Se_3 or Bi_2Te_3 is particularly challenging as intrinsic doping causes a bulk contribution to the conductance. To separate the surface-states contribution from the bulk contribution, we carried out quantum transport experiments on nanostructures of Bi_2Se_3 and Bi_2Te_3. Quantum interferences were measured by sweeping the magnetic field along directions parallel and perpendicular to the nanowire axis. The amplitude of the conductance fluctuation along the perpendicular direction was found to be modulated by an Aharonov-Bohm flux. Numerical simulations performed at MPI PKS Dresden revealed that this modulation is related to the opening of well-defined 1D transverse channels due to the confinement of the TIs surface states [6]. Much effort has been spent to improve the reproducibility and the quality of the nanostructures grown by vapor transport and to understand their electronic properties [7, 8].

We were also able to establish a micro fabricated thermoelectric characterization platform for measuring the thermoelectric and structural properties of single nanowires, produced by dielectrophoresis. The chemical composition of the nanowires was checked and their single-crystalline quality was confirmed by transmission electron microscopy [9]. On this basis, thermoelectric properties of nanowires were studied on Bi_2Te_3, Sb_2Te_3 and Bi_2Se_3. We calculated the thermoelectric performance of TI nanowires, Fig. 3, and showed that it does not derive from the properties of the bulk material in a straightforward way. The competition between surface states and bulk channel causes a significant modification of the thermoelectric transport coefficients if the diameter is reduced into the sub 10 µm range. This limits the maximum thermoelectric performance of TI nanowires and thus their application in devices [10]. The thickness-dependent electrical conductivity and the thermopower were computed in quantum well structures of Sb_2Te_3. Contributions of the bulk and the surface were separated, which allowed to identify a clear impact of the topological surface state on the thermoelectric properties. When the charge carrier concentration is tuned, a crossover between a surface-state-dominated and a Fuchs-Sondheimer transport regime is achieved. These calculations were corroborated by thermoelectric transport measurements on Sb_2Te_3 films, grown by atomic layer deposition, Fig. 4 [11].

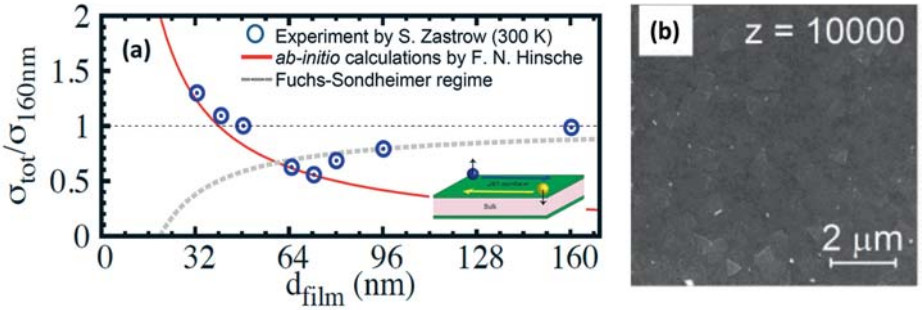

Fig. 4: Thickness dependent transport properties of Sb_2Te_3 films at room temperature. The blue dots show the normalized electrical conductivity **(a)**. A Fuchs-Sondheimer transport and a surface state dominated transport regime has been detected. **(b)** Sb_2Te_3 thin film after 10000 atomic layer deposition cycles which corresponds to approximately 160 nm thickness [11].

Topological insulating phases in superlattices constitute another interesting branch of current research. The experimental realization of one-dimensional Aubry-Andrè-Harper (AAH) systems in optical lattices and photonic waveguide arrays has triggered the interest in this theoretical model. Intriguingly, it can be exactly mapped to the two-dimensional (2D) Hofstadter model (HM) describing topologically non-trivial 2D quantum Hall systems. We have shown that in diagonal AAH models the topological charge pumping is fractionally quantized at well-defined fractions of the pumping period as a result of additional symmetries in parameter space. This phenomenon can possibly be observed in cold atomic gases as a fractional quantization of the center of mass motion of the atomic cloud [12]. In generalized AAH models with diagonal and off-diagonal components we have also shown the occurrence of in-gap end modes topologically protected by inversion symmetry. Using the mapping between the AAH model and the HM, we have discovered that lattice dimerization leads to the appearance of an insulating phase with zero Hall conductivity and concomitant presence of a protected doublet of edge states pinned at specific momenta [13]. In spin-dependent off-diagonal AAH models, which can be obtained for instance by curving nanowires with a conventional Rashba spin-orbit coupling, we have shown the appearance of a novel butterfly spectrum, Fig. 5, characterized by finite-measure complex regions of forbidden energies [14]. If the Fermi energy lies in a gap, the system displays localized end modes protected by topology. This novel butterfly spectrum also posses topologically non-trivial insulating phases at half filling.

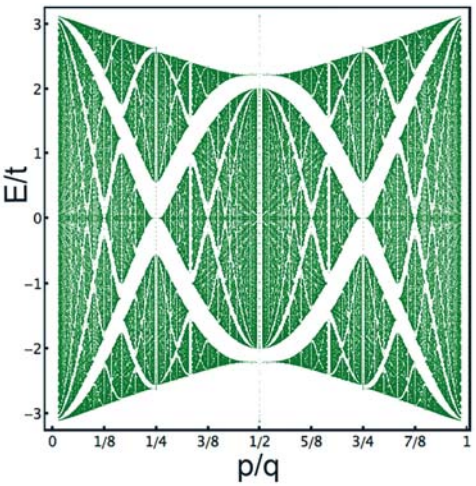

Fig. 5: Butterfly spectrum of a superlattice system obtained by curving a nanowire with Rashba spin-orbit coupling. The spectrum clearly exhibits a self-similar structure [14]

[1] G. Giovannetti *et al.*, Phys. Rev. B **91** (2015) 121417(R).
[2] D. Kasinathan *et al.*, Phys. Rev. B **91** (2015) 195127.
[3] C. Pauly *et al.*, Nature Physics **11** (2015) 338.
[4] A. Lau *et al.*, Phys. Rev. B **91** (2015) 085106.
[5] R. Lou *et al.*, Phys. Rev. B **92** (2015) 115150.
[6] J. Dufouleur *et al.*, arXiv:1504.08030.
[7] C. Nowka *et al.*, Crystal Growth & Design **15** (2015) 4272.
[8] L. Veyrat *et al.*, Nano Letters **15** (2015) 7503.
[9] Z. Wang *et al.*, Nanotech. **26** (2015) 125707.
[10] J. Gooth *et al.*, Semicond. Sci. Tech. **30** (2015) 015015.
[11] N. F. Hinsche *et al.*, ACS Nano **9** (2015) 4406.
[12] P. Marra *et al.*, Phys. Rev. B **91** (2015) 125411.
[13] A. Lau *et al.*, Phys. Rev. Lett. **115** (2015) 216805.
[14] P. Gentile *et al.*, Phys. Rev. Lett. **115** (2015) 256801.

Funding: DFG SPP 1666; DFG SFB 1143; Fellowships funded by the Humboldt Foundation: B. Dassonneville; M. P. Ghimire; *Curved nanomembranes for topological quantum computation*, EU FP7-ICT-FET Young Explorers collaborative project; *Artificial crystals: triggering topological order on demand*, DFG research fellowship

Cooperations: [1]MPI-PKS Dresden, Germany; [2]SISSA Trieste, Italy; [3]Rutgers University New Brunswick, USA; [4]CNR-SPIN Salerno, Italy; [5]Inst. Of Phys. Beijing, China; [6]University Tübingen, Germany; [7]FZ Jülich, Germany; [8]LNCMI-EMFL Toulose, France; [9]Humboldt University Berlin, Germany; [10]Lund University, Sweden; [11]University Hamburg, Germany; [12]University Freiburg, Germany; [13]Renmin University Beijing, China; [14]MPI-CPfS Dresden, Germany; [15]MLU Halle-Wittenberg, Germany; [16]Columbia University New York, USA; [17]RWTH Aachen, Germany; [18]TU Dresden, Germany; [19]MPI Halle, Germany; [20]HTW Dresden, Germany

Research Topic 2.1

Non-equilibrium phases and materials

People: B. Bartusch, S. Donath, J. Eckert, B. Escher, J. Freudenberger, M. Frey, D. Geißler, N. Geißler, T. Gustmann, J.Han, R. Keller, H. Klauß, K. Kosiba, U. Kühn, H. Merker, C. Mix, R. Nawaz Shidad, S. Neumann, S. Pauly, U. Rößler, O. O. Salman, K. Schröder, S. Scudino, F. Silze, D. Seifert, P. Thirathipviwat, H.-P. Trinks, P. Wang, H. Wendrock, T. Wolf, L. Zhang
Responsible Directors: K. Nielsch, T. Gemming, J. van den Brink

Abstract: The most prominent characteristic of non-equilibrium materials is the energetically unfavourable state they have adopted during their synthesis. The entire microstructure or parts of these materials are in structural, compositional or morphological metastability, which defines their unusual and interesting mechanical, chemical and physical properties.
A variety of non-equilibrium materials are the objects of the research conducted in this research area. The present report shall highlight two prominent representatives of non-equilibrium materials, i.e. bulk metallic glasses as well as high entropy alloys.

Two-phase quasi-equilibrium in Ti-based alloys with outstanding glass-forming ability

Bulk metallic glass (BMG) matrix composites have been developed to overcome the detrimental intrinsic brittleness of monolithic amorphous alloys [1]. Very prominent examples are BMG matrix composites containing soft β-type dendrites [2,3]. Several alloys are known to date, in which the supercooled liquid partially decomposes into a β-type phase during solidification. Yet, it is still difficult to tailor and impossible to predict the microstructural evolution on cooling in terms of the crystalline volume fractions and the size of the dendritic precipitates.
The work introduced in the following paragraphs shows that in a Ti-based multicomponent alloy systems a quasi-equilibrium establishes between a supercooled liquid and a β-Ti solid solution during cooling. The unexpected large stability of both metastable phases enables the supercooled liquid to congeal into a glass and, in addition, allows the prediction of crystalline and glassy volume fractions [4]. Within a certain cooling rate regime this quasi-equilibrium is independent of the cooling rate and can be treated analogously to stable equilibria.

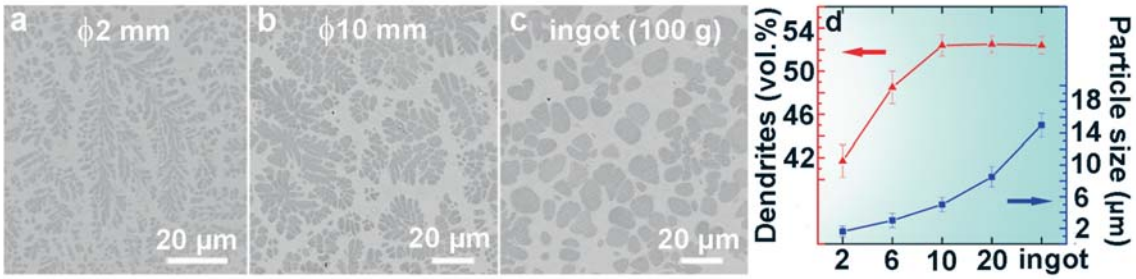

Fig. 1: The β-type dendrites are embedded in a glassy, featureless matrix. If the sample diameter is increased from 2 mm **(a)** to 10 mm **(b)** the crystalline volume fraction increases and the secondary arms become bigger. The same crystalline volume fraction is found in the ingot **(c)** and only coarsening occurs. The crystalline volume fraction and the particle size (for definition see text) are summarised in **(d)**. The x-axis indicates the sample diameter in mm. For sample dimensions above 10 mm the systems attains a quasi-equilibrium.

Fig. 1 a - c depicts the microstructures of $Ti_{45.7}Zr_{33.0}Cu_{5.8}Co_{3.0}Be_{12.5}$ solidified into a rod with a diameter of 2 mm, of 10 mm and into an ingot with a weight of a 100 g, respectively. From these images the secondary dendrite arms ("particle size") as well as the crystalline volume fraction were extracted as a function of the cooling rate (Fig. 1d). Devitrification involves nucleation and growth and hence is time dependent, which generally reflects in the particle sizes and volume fractions [5]. For casting diameters above 10 mm (cooling rate about 40 K/s), however, the volume fraction remains and the dendrites only coarsen in order to reduce the overall interface energy. In other words, the present micrographs represent snapshots of the different stages of the crystallisation process. It seems to be completed in the case of the rod with a diameter of 10 mm. This suggests that the system has attained a state of metastability, in which a further reduction of free energy is kinetically impeded. The supercooled liquid is so resistant against crystallisation in this quasi-equilibrium that the β-Ti dendrites cannot act as heterogeneous nucleation sites. Simultaneously, the glass seems to prevent the transformation of β-Ti to α-Ti. The constant volume fractions are accompanied by a constant composition of both the glass and the dendrites. Conservation of mass dictates the following condition to be obeyed:

$$C_{\beta}^{i} \cdot x + C_{M'}^{i} \cdot (1 - 0.125 - x) = C^{i},$$

where C_{β}^{i}, $C_{M'}^{i}$, and C^{i} are the concentrations of each element i (i: Ti, Zr, Cu, Co) in β-Ti, in the glassy matrix and in the nominal composition, respectively. 0.125 and x are the Be content in the overall composition and the mole fraction of β-Ti, respectively, which has been measured from the micrographs. For any of the four elements Ti, Zr, Cu or Co a crystalline volume fraction near 48 % is predicted, which is in good agreement with the experimental value (52 %). These results can now be translated into a pseudo-binary phase diagram as shown in Fig. 2. The solid green lines represent the equilibrium phases, which comprise the liquid, a β-Ti solid solution (the transformation to α-Ti is ignored here for better clarity) and Be_2Zr and $Cu_{10}Zr_7$. Ti-Zr-Cu-Co-Be is a eutectic system, which is typical of Ti/Zr-rich glass formers [6,7]. The left two red dashed lines describe the temperatures at which nucleation of β-Ti or the other crystalline phases (Be_2Zr and $Cu_{10}Zr_7$) sets in. The degree of undercooling for a given composition is then determined by the temperature difference between the equilibrium liquidus line and the metastable liquidus line. The red dotted line at high Ti concentrations reflects the solubility of Cu, Co and Be in β-Ti during fast cooling. Quenching of metallic melts generally results in supersaturation by solute trapping at the early stages of crystallization [8] and therefore the red dotted line is placed left of the equilibrium solidus line. β-Ti begins to precipitate in the supercooled $Ti_{45.7}Zr_{33.0}Cu_{5.8}Co_{3.0}Be_{12.5}$ liquid when the red dotted line at T_n is crossed. The composition of the liquid is C_L^{Tn} and that of β-Ti is C_{β}^{Tn}. When the temperature falls below T_n, the volume fraction of β-Ti increases quickly due to the fast growth in the

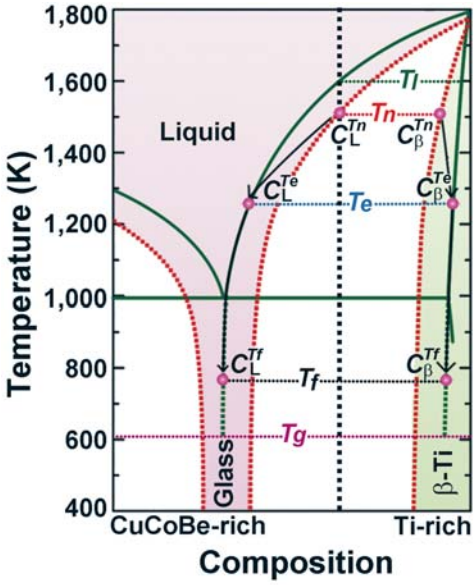

Fig. 2: Pseudo-binary phase diagram indicating the stable (green solid line) and metastable (red and green dashed lines). The vertical black dashed line represents the composition $Ti_{45.7}Zr_{33.0}Cu_{5.8}Co_{3.0}Be_{12.5}$.

moderately undercooled liquid. This is accompanied by a relatively fast composition change of the supercooled liquid from C_L^{Tn} to the equilibrium value, C_L^{Te}. Simultaneously, the dendrites alter the composition from C_β^{Tn} to their equilibrium composition, C_β^{Te}. Below the eutectic temperature, the glass should decompose into various crystalline phases (e.g. Be_2Zr and $Cu_{10}Zr_7$) if the system is given sufficient time. Due to the relatively fast cooling and the outstanding stability of the supercooled liquid this process is suppressed, as is the transformation of β-Ti to α-Ti. These two metastable phases are retained and the green dotted lines describe their compositional changes on further cooling. Since diffusion is restrained at such relatively low temperatures, these lines are rather steep. This is also a result of the negligible changes in the Gibbs free energy differences of both phases at very low temperatures. Once a certain temperature, T_f, is crossed, the compositions of the constituent phases can be assumed constant and temperature-independent. As a final step, the supercooled liquid vitrifies at the glass transition temperature, T_g [4].

To test the hypothesis of a quasi-equilibrium in the present alloy system, various rods (diameter: 10 mm) with differing (Ti,Zr)-to-(Cu,Co,Be) ratios were cast. If the pseudo-binary phase diagram applied, then the respective mole fractions of an alloy with composition $C(x)$ should be given by the lever rule:

$$C(x) = (1-x)\,C_{glass} + x\,C_{dendr},$$

where C_{glass} and C_{dendr} are the compositions of the glassy matrix and the dendrites, respectively. The expected volume fractions, x', can be calculated from the mole fractions, x, by [4]:

$$x' = \frac{x}{x + 0.834 \cdot (1-x)}.$$

The predictions for crystalline volume fractions exceeding 20 % are very reliable [4]. For (Cu,Co,Be)-rich alloys it seems that the outstanding glass-forming ability of the eutectic composition ($Ti_{32.02}Zr_{30.13}Cu_{9.01}Co_{4.84}Be_{24.00}$) slightly extends to the right in Fig. 2 [4].

The present investigations provide a better understanding of how the microstructure in Ti-based BMG matrix composites evolves. The concept of a quasi-equilibrium can account for the observed volume fractions and more importantly is the basis for a successful prediction of the respective volume fractions in this Ti-based BMG matrix composite.

Effect of Cooling Rate on Microstructures and Mechanical Properties of AlCoCrFeNi2.1 Eutectic High Entropy Alloy

A new alloy design strategy for achieving superior mechanical and functional properties has recently been proposed by two independent investigations by Yeh et al. [9] and Cantor et al. [10] in 2004. This so-called high-entropy alloy (HEA) has been originally defined as homogeneous solid solution alloys composed of five or more constituent elements in equal or near equal atomic proportions with simple crystal structures such as *fcc* and *bcc*. However, the single-phased HEAs have been found difficult to reach a reasonable balance between strength and ductility. It is generally known that the *fcc* phases behave ductile but not strong enough whereas *bcc* phases are relatively stronger but with the price of brittleness. In order to address to this important technical issue, Lu *et al*. proposed a strategy to design a composite HEA using the eutectic alloy concept in 2014 [11]. The AlCoFeCrNi2.1 alloy composed of soft-*fcc* and hard-*bcc* phases has been introduced. The alloy showed a balanced combination of high fracture strength (1186 MPa) and high tensile ductility (22.8 %) at room temperature.

In this study, the influence of the cooling rate on microstructural characteristics and consequential mechanical properties of the AlCoFeCrNi2.1 eutectic HEA were investigated in order to archive further strengthening of the alloy by microstructure refinement i.e. refined lamellar spacing λ in this work for example (see Fig. 3). The cooling rate was controlled as a parameter and it was manipulated by changing the sizes of cast samples

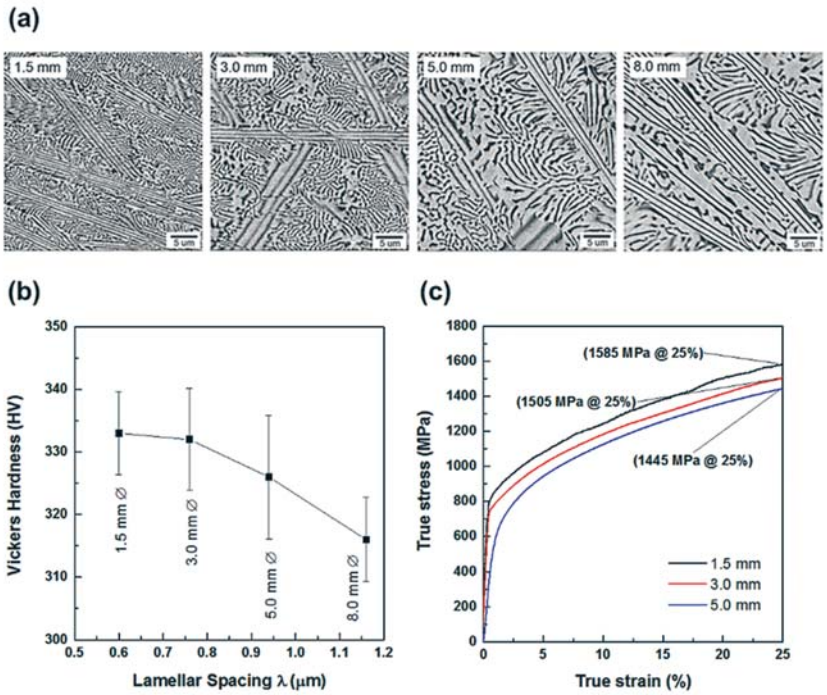

Fig. 3: (a) Backscattered electron SEM images showing the microstructure of AlCoFeCrNi2.1 alloy depending on cooling rate, **(b)** Relationship between cooling rate, lamellar spacing and Vickers hardness, **(c)** Compressive stress-strain curves for AlCoFeCrNi2.1 rods of 1.5, 3.0 and 5.0 mm in diameter.

(Cylindrical rods of 1.5, 3.0, 5.0 and 8.0 mm in diameter). It is well known that strength of eutectic alloys improve as the lamellar spacing refined. We found that the microstructural features i.e. lamellar spacing and volume fraction of constituent phases are changed by different cooling rate during solidification. The increase of cooling rate leads to a formation of relatively finer lamellar spacing and greater volume fraction of the *bcc* phase. For the alloy rod of 1.5 mm in diameter a lamellar spacing of $\lambda = 0.60$ μm and volume fraction of the *bcc* phase of 33 % are estimated whereas the alloy rod of 8.0 mm in diameter shows coarsened lamellar spacing $\lambda = 1.16$ μm and reduced bcc phase fraction (23 %). The refined microstructure with higher volume fraction of the bcc phase cooperatively leads to the enhanced hardness and compressive strength. The alloy with the smallest diameter (1.5 mm) exhibits about 2198 MPa in compressive strength (at 25 % elongation) and 333 HV in micro hardness whilst retaining the high ductility. This new alloy design strategy and process can be readily adapted to large-scale industrial production.

[1] J. Eckert et al., J. Mater. Res. 22 (2007) 285–301.
[2] C.C. Hays et al., Phys. Rev. Lett. 84 (2000) 2901–2904.
[3] D.C. Hofmann et al., Nature 451 (2008) 1085-1089.
[4] L. Zhang et al., Sci. Rep., DOI: 10.1038/srep19235.
[5] D. Turnbull, Contemp. Phys. 10 (1969) 473–488.
[6] D.C. Hofmann et al., PNAS 105 (2008) 20136-20140.
[7] S.Y. Lee et al., J. Mater. Res. 22 (2007) 538-543.
[8] J.C. Baker et al., Acta Metall. 17 (1969) 575-578.
[9] B. Cantor et al., Mat. Sci. Eng. A 375-377 (2004) 213-218.
[10] J.W. Yeh et al., Adv. Eng. Mater. 6 (2004) 299-303.
[11] Y. Lu et al., Sci. Rep. 4 (2014) 6200.

Funding: Iraq Ministry of Higher Education & Scientific Research; China Scholarship Council; German Academic Exchange Service (DAAD), Germany; DFG (PA 2275/2-1 and EC 111/28-1); DFG (EC 111/26-1); ERC Advanced Grant: INTELHYB (ERC-2013-ADG-340025)
Cooperations: TU Dresden; TU Bergakademie Freiberg; Univ. Federal de São Carlos, Brazil; Shenyang Nat. Lab for Materials Science, Institute of Metal Research, China; Univ. of Vienna, Austria; Udmurt State Univ. Russia, Univ. of Cambridge, UK; ESRF Grenoble, France; Tohoku Univ., Japan; Oregon State Univ., USA; Harbin Institute of Technology, China; Institute of Minerals and Materials Technology, India; Univ. of Bremen

Research Topic 2.2

Solidification and Structures

People: J. Eckert, D. Ehinger, J. Freudenberger, D. Geißler, J. Han, I. Kaban, M. Li, B. Opitz, E. Park, P. Ramasamy, O. O. Salman, B. Sarac, S. Scudino, R. N. Shahid, O. Shuleshova, A. Strehle, M. Stoica, D. Sopu, D. Taudien, P. Thirathipviwat, P. Wang, J. Wang, H. Weber, L. Winkelmann, L. Xi
Responsible Directors: K. Nielsch, T. Gemming

Abstract: The main goal of *Solidification and Structures* is to understand and control the phase-formation, microstructure and functional properties in multicomponent metallic alloys. The research is carried out on nanocrystalline and amorphous materials, including multicomponent systems with miscibility gap in liquid and/or solid state. The structure of metallic alloys is in-depth explored using state-of-the-art experimental techniques such as X-ray diffraction, neutron diffraction, and extended X-ray absorption spectroscopy, as well as simulated by molecular dynamics, reverse Monte Carlo and density functional theory calculations.

Structure evolution of soft magnetic bulk metallic glasses (BMGs)

Ferromagnetic metallic glasses and the resulting nanocrystalline alloys, produced through crystallization of the corresponding glassy precursors, are the softest magnetic materials known so far. Based on their unique magnetic properties, many products consisting of ferromagnetic metallic glasses such as for example highly efficient magnetic transformers or high security labels are widely used. Within several new BMG families developed in the last decade, (Fe–Co)–Si–B–Nb glassy alloys play an important role due to combination of high glass-forming ability (GFA) with good magnetic and

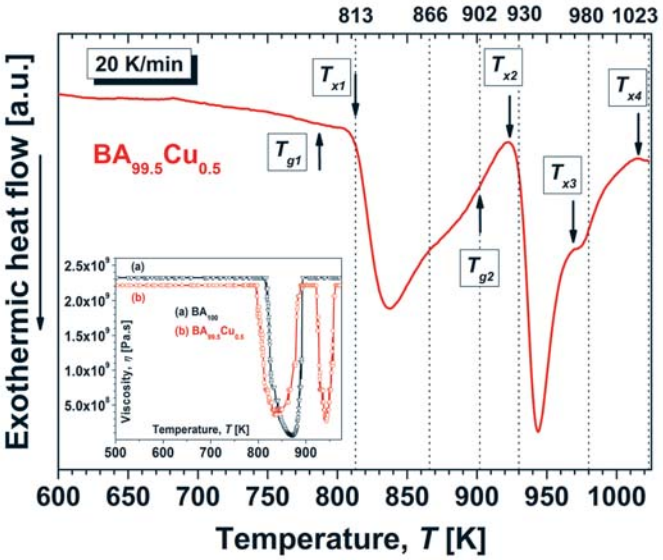

Fig. 1: Differential Scanning Calorimetry (DSC) traces of the $BA_{99.5}Cu_{0.5}$ amorphous rod samples with 2 mm diameter. The characteristic temperatures (T_g: glass-transition, T_x: crystallization) are illustrated with bold characters. The inset displays the variation of the viscosity as a function of temperature, clearly proving that the Cu-added sample shows two supercooled liquid regions.

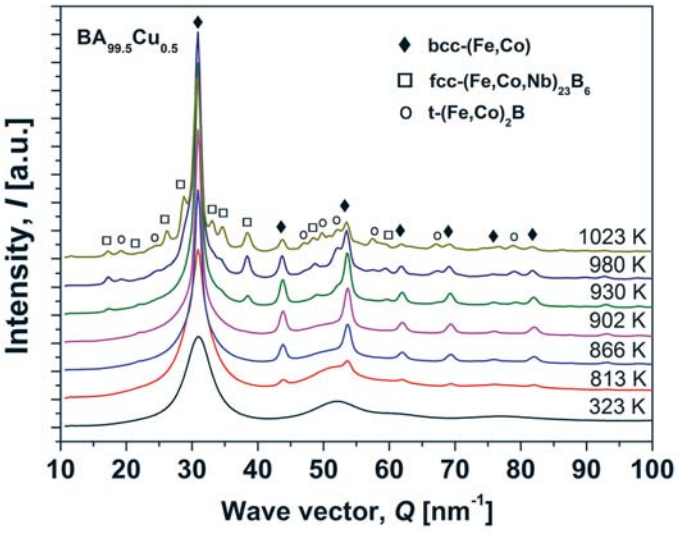

Fig. 2: XRD patterns for $BA_{99.5}Cu_{0.5}$ amorphous rod samples with 2 mm diameter at different temperatures. The corresponding temperatures are marked with dotted lines in Fig. 1. The patterns were measured in transmission configuration using synchrotron radiation upon in situ continuous heating.

mechanical properties. Therefore, several groups have tried to elucidate the influence of a minor addition of Cu on GFA, mechanical and magnetic properties of the resulting alloys. We added 0.5 at.% Cu to the $Fe_{36}Co_{36}B_{19.2}S_{i4.8}Nb_4$ base alloy (hereafter named BA_{100}) and studied the changes induced by mechanical loading [1] as well as the in situ structural relaxation brought by the Cu addition to the base composition [2] through in situ X-ray diffraction (XRD) using synchrotron radiation. Interestingly, the crystallization behavior is drastically changed. In case of the Cu-containing alloy, two glass-transition events are observed (see Fig. 1). Compared to the base alloy, the first glass-transition is slightly shifted towards a lower temperature and is followed by a large exothermic transformation centered at 838 K. Another glass transition-like event and subsequently a pronounced crystallization peak can be observed. Immediately above, a last small exothermic event, most probably indicating complete crystallization of the remaining amorphous matrix, can be detected. Selected XRD patterns revealing the crystallization sequence in detail are plotted in Fig. 2. To correlate the diffraction data with the DSC thermograms, the temperatures corresponding to each pattern are marked with dotted vertical lines in Fig. 1. The inset in Fig. 1 displays the variation of the viscosity as a function of temperature, additionally and clearly proving that the Cu-added sample shows two supercooled liquid regions.

Structural features of plastically deformed BMGs

Although significant progress has been made recently to describe the structural variations characterizing the elastic deformation of BMGs, the atomic rearrangements occurring upon plastic deformation are rather undefined, limiting the understanding of the atomic-scale mechanism responsible for their plastic deformation. This is related to the lack of a periodic arrangement of atoms, which renders the detailed understanding of their deformation mechanisms a very challenging task because structural studies cannot rely on a regular crystal structure and on the dynamics of related defects, such as dislocations. The latest developments of high-energy synchrotron XRD, consisting of focused hard X-ray beam, large range of the diffraction vector Q and high resolution X-ray detectors, permit to overcome this limitation and allow to investigate the atomic rearrangements occurring in bulk metallic glasses upon elasto-plastic deformation. In our work, by means of high-energy XRD, we have created spatially resolved strain maps

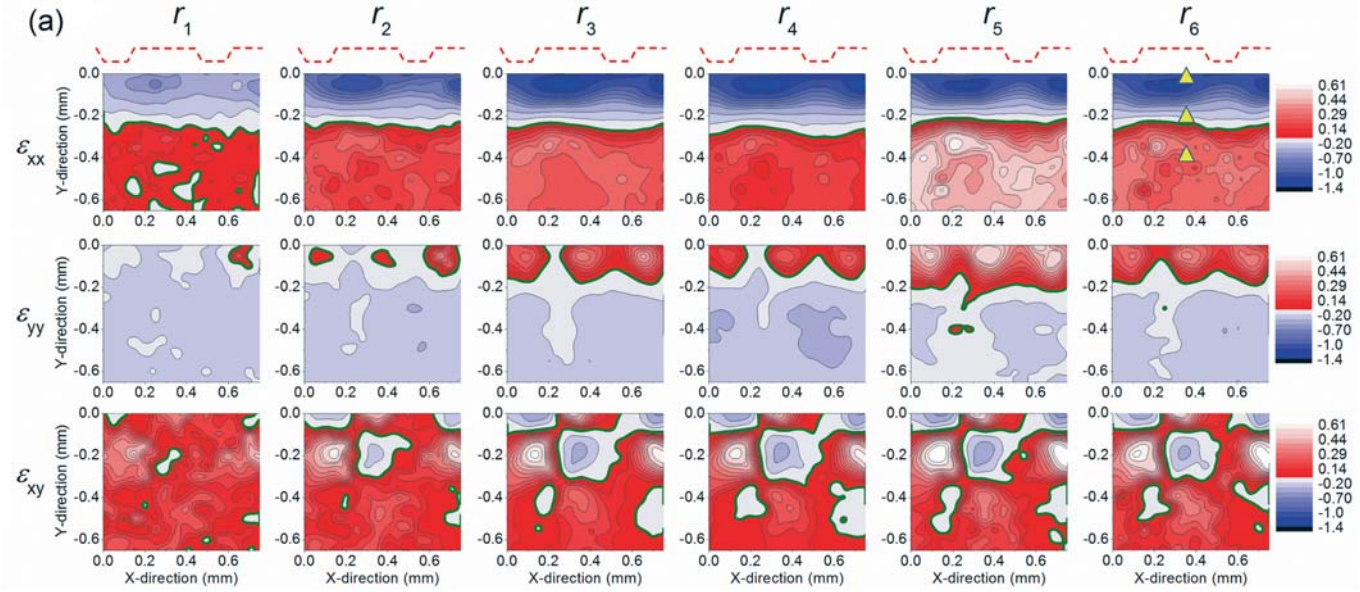

Fig. 3: (a) Strain maps of the ε_{xx}, ε_{yy}, and ε_{xy} components evaluated from the different r_i atomic shells. **(b)** Variation of the shear strain ε_{xy} and of the angle α_1 formed by the principal eigenvector with the X-axis as a function of r for the plastically-deformed BMG along with data for the BMG deformed within the elastic regime (data points marked as 1300 MPa).

of a plastically-deformed $Zr_{52.5}Ti_5Cu_{18}Ni_{14.5}Al_{10}$ (at.%) BMG [3,4] and analyzed the structural changes occurring in the short- (SRO) and medium-range order (MRO). Metallic glasses, ideally isotropic, become anisotropic even in the elastic regime: the strain increases with increasing distance from the nearest-neighbor shell. Such a length-scale dependence of the strain is retained in plastically-deformed glasses, as shown in Fig. 3a, where the components of the strain tensor (ε_{xx}, ε_{yy}, and ε_{xy}) are plotted for the different atomic shells (r_i). Additionally, we have experimentally identified an overall structural signature of plastic deformation in metallic glasses, namely a strong shear strain ε_{xy} and a considerable directional anisotropy (Fig. 3b). These findings are in contrast to the behavior observed for elastically-deformed BMGs (data points marked 1300 MPa in Fig. 3b), which instead display no significant shear component and directional anisotropy, marking a clear difference between elastic and plastic deformation of metallic glasses. These observations not only provide a direct experimental evidence of the effects of plastic deformation on the atomic structure of metallic glasses, but also contribute to the understanding of how one can positively influence the formation and propagation of detrimental shear bands in order to mitigate the room temperature brittleness of bulk metallic glasses.

Deformation behavior of BMGs and composites via molecular dynamics (MD) simulations

A way to improve the plasticity of BMGs is to synthesize BMG matrix composites, which are heterogeneous microstructures combining a glassy matrix with crystalline secondary phases. The interactions between the reinforcing second phase and shear bands (SBs) significantly retard fracture. A detailed atomistic understanding of the underlying mechanism can be provided by MD simulations, showing that multiple SBs are nucleated at the amorphous-crystalline interface and are blocked by crystalline particles. In our study [5] two 3D-periodic $Cu_{64}Zr_{36}$ BMG composites were constructed by inserting 15 B2 CuZr nanowires in the monolithic BMG. [001] nanowires of cross-sectional dimensions of 3.22 x 3.22 nm^2 and an initial length of 19.4 nm are considered. The volume fraction of the crystalline phase was set to 14.1%. Then the deformation mechanisms of BMG composites have been studied under uniaxial tension parallel to the Z-direction (i.e.

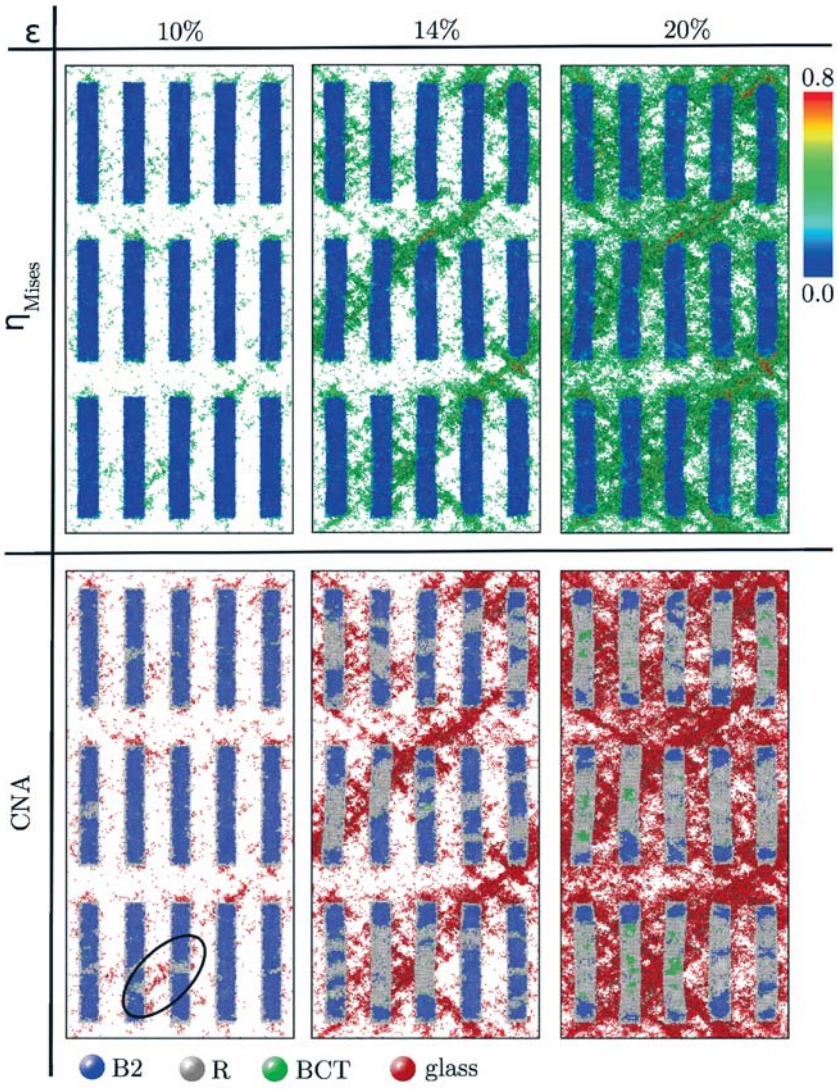

Fig. 4: Local atomic shear strain and CNA for a $Cu_{64}Zr_{36}$ BMG composite containing 15 CuZr B2 nanowires distributed along the deformation direction. In order to capture the stress-induced martensitic transformation in the B2 crystalline phase, only half of the structure and those atoms with an atomic strain higher than 0.3 are shown.

vertically). Figure 4 shows the local atomic shear strain together with the common neighbor analysis (CNA). At a strain of 10%, shear transformation zones (STZs) form around the amorphous-crystalline interface. Also part of the nanowires shows a stress-induced martensitic transformation from the B2 phase to an intermediated R-phase. Increasing the strain up to 14%, small embryonic SBs nucleate at the interface and propagate through the glass, but they are immediately blocked by the next nanowires. Moreover, the strain is distributed mostly around those nanowires which suffer severe martensitic transformation (red atoms in Fig. 4). Once the B2 nanowires undergo transformation to the R-phase, the volume increase associated with this transformation will perturb the strain field around the nanowires, so that the glassy phase will display a compressive strain field next to the R-phase region (gray atoms) and, in return, a tensile strain filed along the undeformed B2 nanowire. The tensile residual strain assists local dilatation and creation of free volume. As a result, the STZs are readily activated in these soft regions characterized by an increased free volume, as can be seen in the area marked with an ellipse in Fig. 4. Even at a strain of 20%, none of these embryonic SBs become critical being confined between the crystalline nanowires, ensuring a homogeneous deformation of the BMG composite. In addition, all nanowires show martensitic transformation under uniaxial tension.

In-situ studies of solidification from undercooled metallic melts

Solidification of deeply undercooled metallic liquids with help of the electromagnetic levitation (EML) method (see Fig. 5) is a traditional research subject at IFW Dresden. Currently, in the frame of the ELIPS program of the European Space Agency (ESA), our

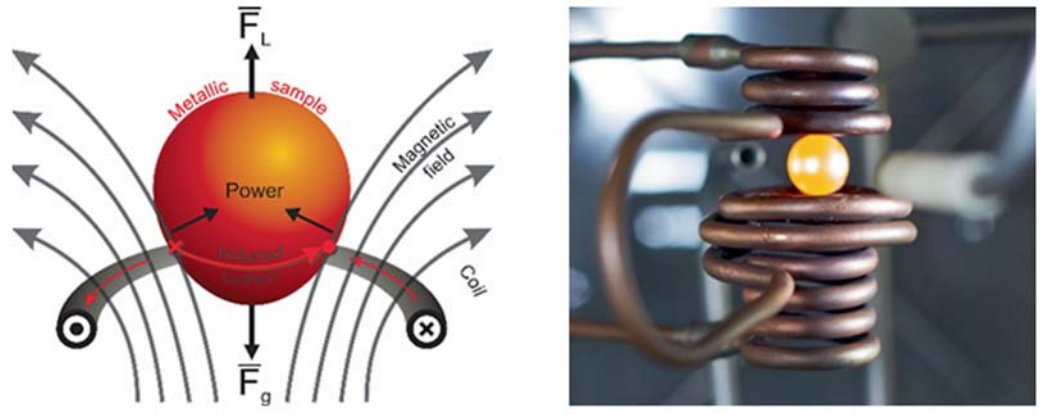

Fig. 5: In electromagnetic levitation the gravity is compensated due to repulsive Lorenz force arising in conductive sample placed in an alternating magnetic field of RF coil. Simultaneously, eddy currents heat up the sample so that it can be completely melted while levitating. By blowing the helium gas over the sample surface the melt can be undercooled well below its liquidus temperature to the amount of several hundred degrees prior nucleation and growth of the solid phase.

institute participates in the international EML microgravity experiments, comprising parabolic flight campaigns and experiments on board of the International Space Station. Aiming to answer the fundamental question about an influence of melt convection on solidification process, several industrially relevant materials, such as soft-magnetic Fe-Co and Fe-Ni alloys, as well as light-weight Ti-Al based materials, are studied [6]. To proceed with these and other activities, a new mobile electromagnetic levitator has been developed by joint efforts of the Department of Research Technology and our group. Inheriting the functionality of the old version, the new facility has received advanced features, which substantially extend the non-contact diagnostics of solidification process from undercooled melts. Of genuine importance is an installation of the high-speed video camera with an acquisition rate up to 180.000 frames per second. This allows direct observation of the advancing solidification front, analysis of its velocity, and detection of rapid transformation events, as illustrated in Fig. 6.

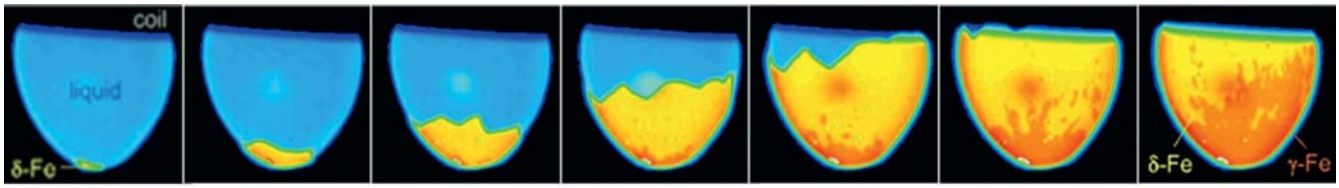

Fig. 6: Solidification of an $Fe_{60}Co_{40}$ alloy undercooled with 255 K, acquired at 30.000 fps with a high-speed video camera. Advanced solidification front, hot due to release of the latent heat, is contrasted with a relatively cold liquid. After a short delay, a second front is sweeping through the sample indicating the transformation of the primary metastable δ-Fe phase with bcc structure into (more) stable fcc γ-Fe.

The foremost distinction of the new EML lies in its mobility. In collaboration with Photon Science group at Deutsches Elektronen-Synchrotron (DESY) in Hamburg, the IFW Dresden mobile EML is designed for in-situ X-ray diffraction experiments at synchrotron facilities. This provides a unique possibility for direct identification of the structure of the crystalline phase growing from an undercooled melt, its relation to the structure of the parent liquid, as well as observation of further solid state transformations. The first in-situ XRD experiments at PETRA III synchrotron at DESY using mobile EML is planned for spring 2016.

[1] M. Stoica et al., J. Appl. Phys. 115 (2014) 053520.
[2] M. Stoica et al., Acta Materialia 95 (2015) 335.
[3] S. Scudino et al., Appl. Phys. Lett. 106 (2015) 031903.
[4] S. Scudino et al., Scr. Mater. 65 (2011) 815.
[5] D. Sopu et al., Appl. Phys. Lett. 106 (2015) 211902.
[6] O. Shuleshova, et al. J. Mater. Sci. 47 (2012) 4497.

Funding: ERC Advanced Grant "INTELHYB" (Grant No. ERC-2013-ADG-340025); EU ITN "VitriMetTech" (FP7-PEOPLE-2013-ITN-607080); DFG (Ka-3209/6-1); DLR Space Administration, BMWi (50WM1546); Ministry of Higher Education & Scientific Research (MoHESR), Iraq; China Scholarship Council (CSC), China; German Academic Exchange Service (DAAD), Germany

Cooperations: University of Torino, Italy; National Polytechnic Institute Grenoble, France; University of Cambridge, UK; University of Göttingen, Germany; ETH Zürich, Switzerland; Warsaw University of Technology, Poland; University of Ioannina, Greece; University of Ulm, Germany; National Institute of Research and Development for Technical Physics, Iasi, Romania; European Synchrotron Radiation Facility Grenoble, France; Breuckmann GmbH & Co. KG, Germany; Aalto University, Finland; Politehnica University Timisoara, Romania; Politehnica University Bucharest, Romania; Institute of Metallurgy and Materials Science, Polish Academy of Sciences, Krakow, Poland; The Institute of Advanced Manufacturing Technology, Krakow, Poland; University of Balearic Islands, Mallorca, Spain; University of Bremen, Germany; Research Foundry Institute, Cracow, Poland; Stockholm University, Sweden; TU Dresden, Germany; RWTH Aachen University, Germany; Institute of Materials Physics in Space, German Aerospace Center (DLR), Germany; Wigner Research Centre for Physics, Budapest, Hungary; Institute of Metal Research, Chinese Academy of Sciences, Shenyang, China; Shandong University, Weihai, China; Swatch group, Switzerland; Tohoku University, Japan; Oregon State University, USA; Harbin Institute of Technology, China; Institute of Minerals and Materials Technology, India; TU Hamburg-Harburg; Udmurt State University, Russian Federation; Tufts University, USA

Research Topic 2.3

Shapeable microelectronics

People: S. Baunack, D. Karnaushenko, D. D. Karnaushenko, B. Koch, D. Makarov[4], A. K. Meyer[3], N. Münzenrieder[1,2], L. Petti[1], R. Schäfer, G. Tröster[1],
Responsible Directors: B. Büchner, K. Nielsch, T. Gemming, O. G. Schmidt, J. van den Brink

Abstract: Mechanical adaptivity of soft polymeric actuators in combination with the imperceptibility of microelectronics paves the way towards an entirely new class of devices – shapeable microelectronics. Being able to self-assemble, mechanically adapt to and deterministically influence the environment electrically or mechanically, the shapeable microelectronics will assess the physiological and electrophysiological activity of living species. Here we demonstrate shapeable microelectronic devices fabricated on a novel, ultrathin (<1 µm) and mechanically active polymeric platform to interface peripheral and central nervous system. The development of a cost-efficient, high-performance and portable magneto-encephalography equipment applying arrays of self-assembled ultrasensitive giant magneto-impedance sensors or gently self-attached to nerves electronic cuff-implants would bring these unique devices to regular medical institutions, offering early stage disease diagnostics with a great spatial resolution hence helping to minimize impact upon a medical treatment.

Living species are able to adapt their shape during the life cycle. Imitating this behavior, synthetic systems adapt to environmental changes as well as interact with the environment mechanically [1], electrically or chemically [2]. Mimicking the mechanics of living organisms, the shape of soft objects can be tailored by using stimuli-responsive polymers [3]. In hydrogel composites [4], a reversible shape transformation including elongation, twisting, or folding [5] is achieved upon external chemical or thermal stimulation rendering these shapeable devices to be mechanically active. Although mechanically adaptive to the environment, these soft actuators do not carry active electronics to assess and communicate the environmental changes. Otherwise, there are ultra-thin and light weight mechanically flexible and even imperceptible electronics [6, 7], which are electrically active but lack reversible self-actuation.

A new class of electronic devices, namely shapeable microelectronics can be deterministically assembled tailoring stress induced physical properties in ultrasensitive magnetic sensors, to access processes happening distantly in the brain (Fig. 1a) via

magneto-encephalography (MEG) techniques. Shapeable devices can be gently attached to the biological tissue enabling enclosure and monitoring (Fig. 1b) of, e.g. nerves and nervous fibers via electro-encephalography (EEG) techniques, supporting regeneration of neuronal cells and guiding their growth.

Encephalography techniques that are based on the detection of electrical potentials, are commonly applied in medical institutions worldwide for health monitoring and are now entering the new field of interfacing the nervous system with the smart implant solutions [8, 9]. The integrated electronics of these devices enables monitoring [10] and stimulation of the biological tissue [11]. Upon an external trigger, the mechanically active cuff implants can be gently attached, applying a precise amount of force to the neural tissue, thus opening and releasing the nervous tissue with a minimal impact.

The magnetic counterpart of EEG, namely MEG, relies on the detection of tiny magnetic fields generated by the electrical currents in the nervous system [12]. Being able to provide the same physiological information as the conventional EEG [13], MEG offers strong advantages in terms of sensitivity and the opportunity to identify diseases, e.g. epilepsy at early stages with a great spatial localization [14]. The development of a cheap and even portable MEG equipment would bring these unique devices to regular medical institutions. Furthermore, if achieved, light-weight MEG devices bear a great potential to revolutionize the field of smart prosthetics, brain-machine and brain-brain interfaces due to a precise volumetric localization and characterization of current sources that corresponds to particular mental activity and that are not accessible directly by EEG techniques.

We aim at the realization of these ambitious goals by offering electronic nervous cuff-implants [9] to interface the peripheral nervous system and cost-efficient giant magneto-impedance (GMI) [15] sensors operating at room temperature to access [16] tiny magnetic fields [17] stemming from the brain activity. Development of these complex shapeable electronic components containing thin-film transistors and sensors, requires multiple fabrication steps to be carried out in a way compatible with microelectronic technology. Here we put forth a platform relying on photopatternable, thermally and chemically stable imide- and acrylic-based polymers. To allow for the self-assembly we use stimuli-responsive hydrogel polymers [2, 3, 18], which develop a differential strain

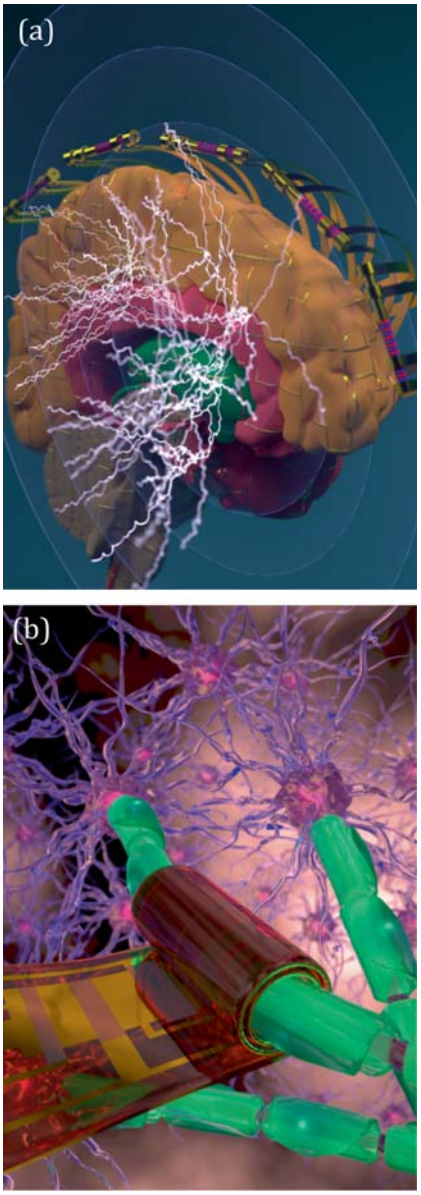

Fig.1: Artistic vision of shapeable microelectronic neuronal interfaces. **(a)** Detection of magnetic field generated by an epileptic seizure happening inside the brain using an array of giant magnetoimpedance sensors; **(b)** Shapeable microelectronics bear great potential to offer neuronal cuff-type implants with unmatched mechanical and electrical functionalities.

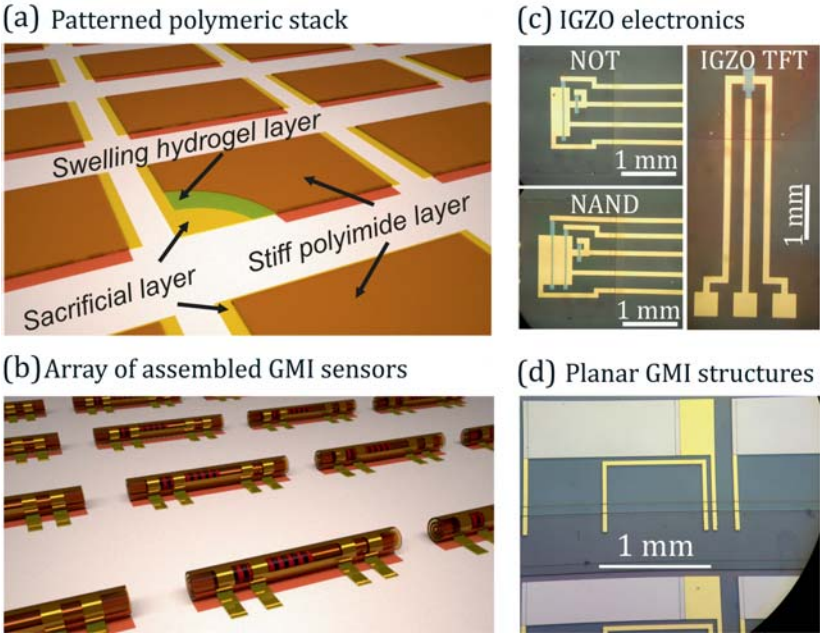

Fig. 2: Shapeable microelectronic technological platform: **(a)** The planar tree-layer polymeric stack of the sacrificial layer, the swelling hydrogel layer and the rigid polyimide layer; **(b)** The array of self-assembled microelectronic devices (GMI sensors); **(c)** Planar IGZO electronic devices fabricated on top of polymeric stack; **(d)** Planar GMI structures fabricated on polymeric three-layer stack.

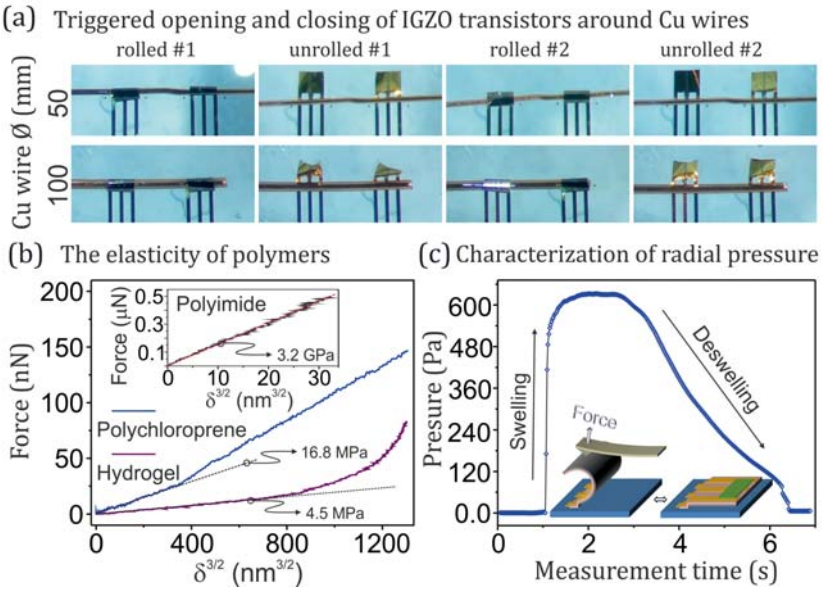

Fig. 3: Mechanical properties of the shapeable microelectronic platform: **(a)** Hooking up several devices to Cu wires with a diameter of 50 µm (top row) and 100 µm (bottom row); The rolled/unrolled state of the devices can be controlled by adjusting the content of isopropanol in the water solution; **(b)** Force-distance curve measured for different polymeric layers using AFM; **(c)** Change of the pressure measured using AFM upon self-assembly of the devices.

during water uptake relying on reinforcement layers. Using optical lithography, we first define sites for the electronic devices by patterning the functional stack (Fig. 2a). The technology allows to process 100's of devices over the entire substrate in a single fabrication run. The swelling state of the hydrogel can be affected by tailoring environmental conditions. This provides a full control over the shape of the device, which can be deterministically set in a planar or bent state, as well as self-assembled into a Swiss roll-like microtube (Fig. 2b) with tunable diameters down to 50 micrometers. By varying the 2D layout, different geometries of the electrodes, semiconductors and magnetic layers can be realized (Fig. 2c,d) on top of the stack. Furthermore, the developed technological platform supports the integration of multiple functional elements forming complex circuits into a single tubular architecture.

Applying the polymeric platform, mechanically adaptive microchannels of cuff-type were realized integrating high-performance Indium Gallium Zinc Oxide (IGZO) [7] microelectronics. The possibility to open/close the architecture repeatedly upon external stimulation allows an automatic attachment and release of a device to/from an object of interest in a biomimetic fashion (Fig. 3a). The mechanical functionality is appealing for neuronal cuff implant applications to enclose and guide the growth of nerves [11]. The achieved device diameters of 50 micrometers are at least two orders of magnitude smaller compared to the state-of-the-art neuronal cuff implants [19]. At the same time, the elasticity of the polymeric layer forming the interior of the channel is about 17 MPa (Fig. 3b), which matches the elasticity of the protective tissues of the central nervous system, as required for in vivo implants [1, 19]. The total radial pressure imposed by the device upon the self-assembly process is about 600 Pa (Fig. 3c), which is well below the harm limit of 1300 Pa characteristic for nerves and axons [20]. The small thickness of the polymers of less than 1 micrometer prevents the IGZO electronics from degradation upon severe mechanical deformations. Even in the most bent state, the signal amplifiers and the advanced logic gates remain intact and maintain their functionality. The integrated electronics could detect ionic signals (mV range) which is sufficient for monitoring the action potential of neuronal axons.

Using the same technology, we developed self-assembled GMI sensors (Fig. 4a) as an alternative to superconducting quantum interference devices (SQUID) [12] for MEG equipment, which would be in the spirit of the conventional EEG devices. Although SQUID-based devices have proven their relevance in neurological disease treatment [11], rather high fabrication and maintenance costs limit their wide spread applicability. In

this respect the GMI devices operate at room temperatures [21] and reveal remarkable sensitivity to small magnetic fields down to the pico-Tesla regime [22]. Self-assembly of initially planar GMI heterostructures could be achieved into an array of three-dimensional tubular architectures (Fig. 4b) possessing enhancement of GMI response in comparison to planar structures. Fabricated GMI systems reveal a stable effect with an amplitude in the range of 50%/Oe [16] below 100 MHz (Fig. 4c) and characteristics comparable to state-of the art GMI devices.

In conclusion, we put forth a novel method relying on strain engineering [9, 16, 18] to realize on-chip integrated GMI sensors as well as nervous cuff-type implants with integrated microelectronics, including signal amplifiers and logics based on high-performance IGZO transistors. The shapeable microelectronics constitutes a major step towards three-dimensionally assembled microelectronics for direct or distant neural network monitoring via encephalography techniques, stimulation and regeneration of neural tissue. Fabrication of complex logic circuits in combination with sensors on mechanically active polymers is attractive for channel multiplexing on the micro scale to reduce the number of interconnect applied at self-confined neural cuff implants. Matched mechanical properties should be of great value, reducing the injury of biological tissue and promoting the biocompatibility.

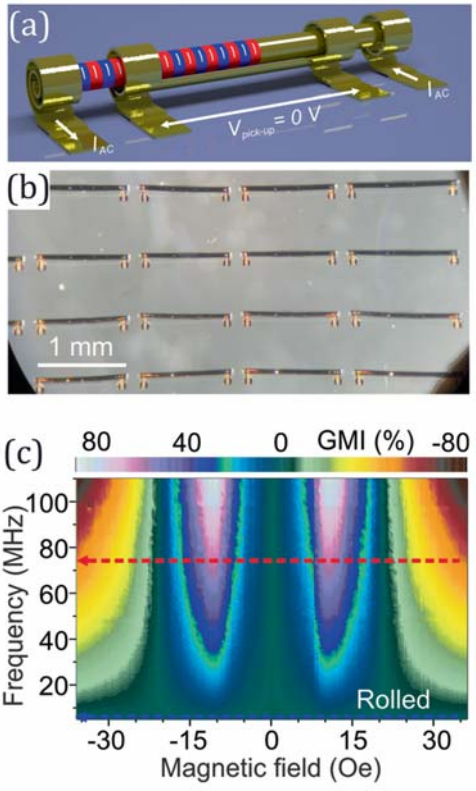

Fig. 4: Giant magnetoimpedance sensors: **(a)** Sketch of an integrated self-assembled GMI sensor with a pick-up coil; **(b)** An array of self-assembled GMI sensors on a glass substrate; **(c)** The response of a self-assembled GMI sensor demonstrating a characteristic double peak profile.

[1] J. Reeder et al., *Adv. Mater.* **2014**, *26*, 4967.
[2] R. Fernandes, D. H. Gracias, *Adv. Drug Deliv. Rev.* **2012**, *64*, 1579.
[3] L. Ionov, *Mater. Today* **2014**, *17*, 494.
[4] R. M. Erb et al., *Nat. Commun.* **2013**, *4*, 1712.
[5] K. Malachowski et al., *Nano Lett.* **2014**, *14*, 4164.
[6] M. Melzer et al., *Nat. Commun.* **2015**, *6*, 6080.
[7] G. A. Salvatore et al., *Nat. Commun.* **2014**, *5*, 2982.
[8] T. Stieglitz et al., *IEEE Eng. Med. Biol. Mag.* **2005**, *24*, 58.
[9] D. Karnaushenko et al., *Adv. Mater.* **2015**, *27*, 6797.
[10] D. Borton et al., *Neurosci. Res.* **2014**, *78*, 21.
[11] X. Navarro et al., *J. Peripher. Nerv. Syst.* **2005**, *10*, 229.
[12] R. Hari, R. Salmelin, *Neuroimage* **2012**, *61*, 386.
[13] M. A. Lebedev, M. A. L. Nicolelis, *Trends Neurosci.* **2006**, *29*, 536.
[14] M. E. Funke et al., *Epilepsia* **2011**, *52*, 10.
[15] L. V Panina et al., *J. Appl. Phys.* **1994**, *76*, 6198.
[16] D. Karnaushenko et al., *Adv. Mater.* **2015**, *27*, 6582.
[17] T. H. Sander et al., *Biomed. Opt. Express* **2012**, *3*, 981.
[18] D. D. Karnaushenko et al., *NPG Asia Mater.* **2015**, *7*, e188.
[19] J. J. FitzGerald et al., *J. Neural Eng.* **2012**, *9*, 16010.
[20] H. C. Powell, R. R. Myers, *Lab. Invest.* **1986**, *55*, 91.
[21] B. Dufay et al., *IEEE Trans. Magn.* **2013**, *49*, 85.
[22] T. Uchiyama et al., *IEEE Trans. Magn.* **2011**, *47*, 3070.

Funding: This work was funded in part by the Nanett project of the German Federal Ministry of Education and Research (BMBF), European Research Council under the European Union's Seventh Framework Programme (FP7/2007-2013)/ERC grant agreement Nr. 306277, European Commission within the European Union s seventh framework program FLEXIBILITY / grant number 287568, German Science Foundation (DFG) grant MA 5144/2-1 and DFG Research Group FOR1713.

Cooperations: [1]Electronics Laboratory, Zürich, Switzerland; [2]Sensor Technology Research Center, University of Sussex, Falmer, Brighton, United Kingdom; [3]Division of Neurodegenerative Diseases, Department of Neurology, Technische Universität Dresden, Dresden, Germany; [4] Intelligente Werkstoffe und Funktionselemente, Helmholtz-Zentrum Dresden-Rossendorf, Dresden.

Research topic 2.4

Nanoscale magnets

IFW People: A. Aliabadi, M. E. Belesi, C. Damm, S. Fähler, M. Gellesch, P. Gerhard, R. Ghunaim, V. Haehnel, M. Haft, F. Hammerath, S. Hampel, C. Hengst, K. Junghans, V. Kataev, C. Konczak, J. Körner, D. Krylov, X. Ma, I. Mönch, T. Mühl, V. Neu, D. Pohl, D. Pohl, A. Popov, C.F. Reiche, B. Rellinghaus, M. Richter, C. Schlesier, H. Schlörb, M. Scholz, F. Schmidt, S. Schneider, L. Schultz, A. Svitova, K. Tschulik, M. Uhlemann, S. Vock, S. Wicht, S. Wurmehl, Y. Zhang
Other involved people: T. Greber, R. Westerstrom (Uni Zurich/PSI), J. Rusz (U Uppsala), P. Schattschneider (TU Wien), O. Hellwig, S. H. Wee (HGST, San Jose, CA, USA), P. Tiemeijer (FEI, Eindhoven), D. Kasinathan (MPI CPfS, Dresden)
Responsible Directors: B. Büchner, K. Nielsch, J. van den Brink

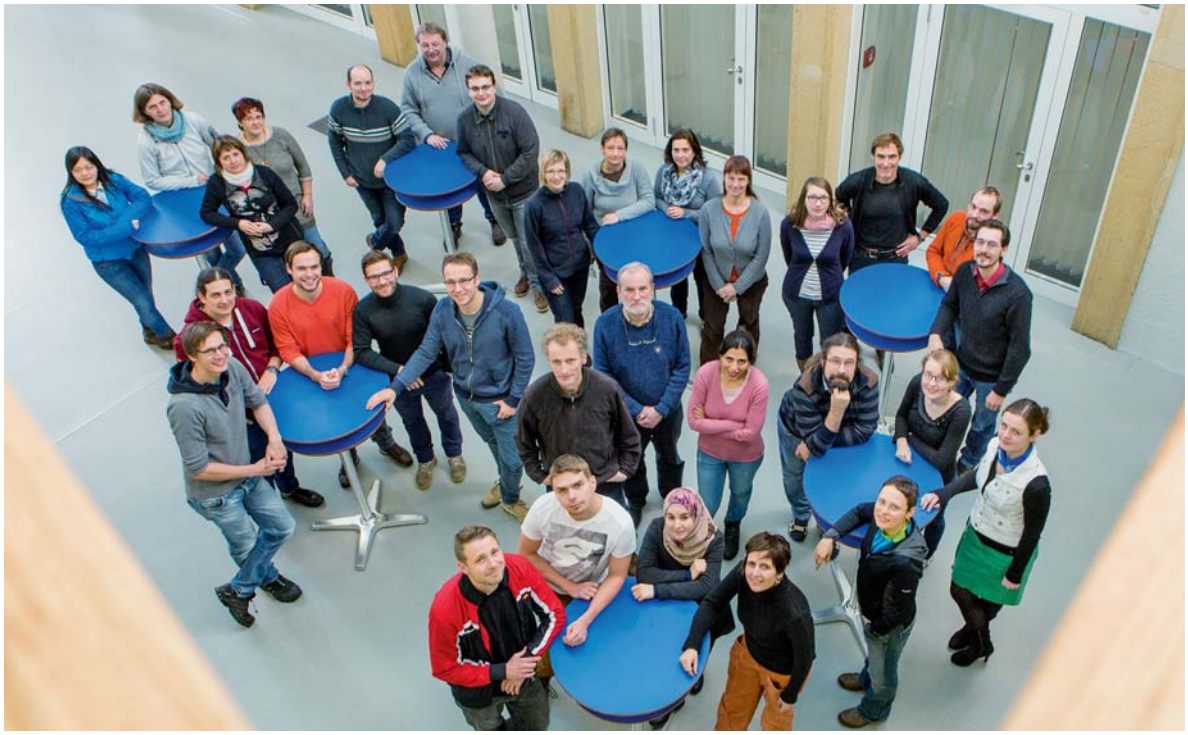

Abstract: Nanoscale magnets range from single molecules to entities of a few million atoms. Due to their inherently small size and their large surface-to-volume ratio, the coupling of magnetic cores to the local chemical environment significantly affects their magnetic moments and anisotropies. Understanding and controlling the properties of such nanomagnets at different length scales is thus the heart of this research topic. The report reviews our work on nanoscale magnets in 2015. The materials related research on molecular magnets, magnetic nanoparticles and nanowires is complemented by efforts to develop novel methods and techniques which are particularly suited for characterizing magnetic materials at smallest possible length scales and with ultimate resolution.

Endohedral metallofullerenes as single molecular magnets

Endohedral metallofullerenes (EMFs) encapsulating lanthanide ions (Ln) are of particular interest because of the specific magnetic properties resulting from the combination of the partially filled 4f shell of metal ions, their exchange interactions in endohedral clusters, and the shielding role of the carbon cage, which protects endohedral spin states from the outer environment. The inhomogeneous environment of Ln ions inside the clusterfullerenes induces a magnetic anisotropy and results in a number of magnetic phenomena. In particular, Dy-based nitride clusterfullerenes, $DySc_2N@C_{80}$ and $Dy_2ScN@C_{80}$, were the first EMFs to exhibit single molecular magnet (SMM) behaviour [1]. Recently we found that in the presence of Ti, the central nitride ion can be replaced by carbon,

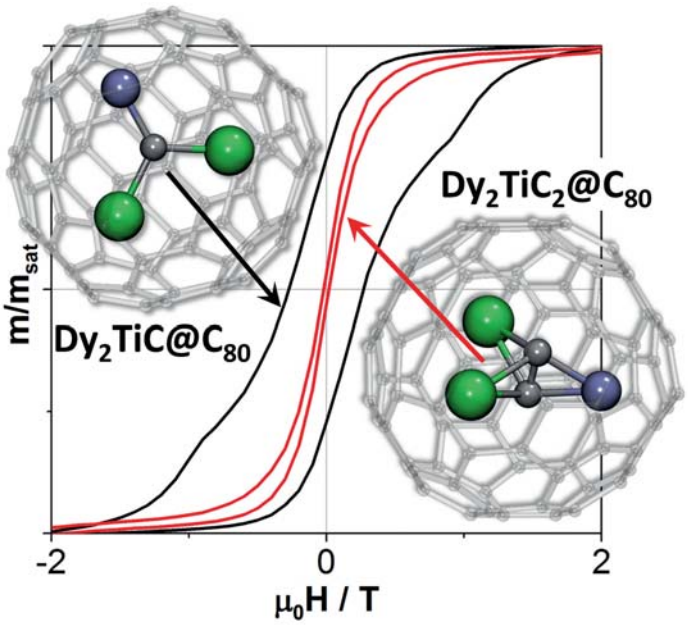

Fig. 1: Molecular structures and SQUID magnetization curves of $Dy_2TiC@C_{80}$ T = 1.8 K (black) and $Dy_2TiC_2@C_{80}$ (red).

yielding $M_2TiC@C_{80}$ with a double Ti = C bond [2]. The Dy analogue, $Dy_2TiC@C_{80}$, exhibits single molecule magnetism, but is softer than the isostructural $Dy_2ScN@C_{80}$ [3]. At the same time, an analogous EMF with two carbon atoms in the endohedral cluster, $Dy_2TiC_2@C_{80}$, was also discovered and found to have poorer SMM properties than $Dy_2TiC@C_{80}$ (Fig. 1).

An important advantage of the EMF-SMMs is their high thermal and chemical stability, which enables sublimation without decomposition. Monolayers of $Dy_2ScN@C_{80}$ on a Rh(111) surface were obtained by vacuum sublimation. X-ray magnetic circular dichroism (XMCD) showed that the first monolayer of $Dy_2ScN@C_{80}$ strongly interacts with the metal surface resulting in alignment of the endohedral clusters parallel to the substrate. Importantly, the EMF retains its SMM behaviour on the metal even in submonolayers [4].

Whereas SQUID and XMCD are of particular use for the study of the low-temperature effects, magnetic properties of EMFs at room-temperature are conveniently addressed by paramagnetic NMR spectroscopy, since paramagnetic chemical shift is proportional to the anisotropy of magnetic susceptibility. Systematic ^{45}Sc and ^{13}C NMR studies of the series of $LnSc_2N@C_{80}$ molecules (Ln runs through the whole 4f row) allowed us to analyze the magnetic anisotropy of the lanthanide ions in nitride clusterfullerenes [5]. We showed that the crystal field is quasi-uniaxial with very large splitting of m_J levels.

Determination of the electron spin density on the N-donor atoms of Cu(II)-(bis)oxamidato complexes by a pulse ELDOR detected NMR

Transition metal-(bis)oxamidato complexes can be utilized as suitable building blocks for the synthesis of the respective polymetallic complexes which are considered as possible candidates for the use in molecular electronic devices. Understanding of exchange pathways in such complexes is therefore important for a rational design of new materials with improved intramolecular magnetic interactions between the metal ions. The spin density distribution in Cu(II) containing (bis)oxamidato type mononuclear complexes $[^nBu_4N]_2[Cu(opboR_2)]$ (R = C_2H_5 **1**, C_3H_7 **2**) studied in the present work [6] (Fig. 2) can be an indicator of the strength of the magnetic superexchange interaction in corresponding trinuclear complexes and thus provide a clue to the control of the interaction pathways. The spin density distribution can be inferred from the analysis of a tensor of the transferred hyperfine (HF) interaction between the electron spin of Cu and the nuclear spins of the nitrogen ligands. To determine the HF tensor we have employed the

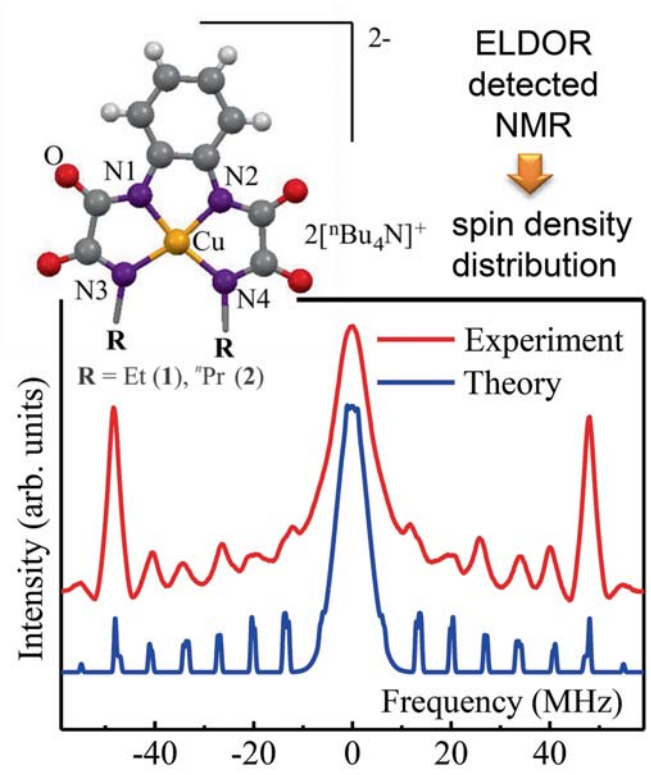

Fig. 2: (top) Structure of the (bis)oxamidato type mononuclear complexes $[^nBu_4N]_2[Cu(opboR_2)]$ (R = C_2H_5 1, C_3H_7 2). Due to covalency of the chemical bonds the Cu(II) electron spin density is distributed towards the nitrogen ligands; **(bottom)** Experimental and theoretical ELDOR detected NMR spectrum. The intensity of the free induction decay signal after application of the detection pulse at $\omega_{mw}^{(2)}$ is plotted as a function of the frequency difference $[\omega_{mw}^{(1)} - \omega_{mw}^{(2)}]/2\pi$, where $\omega_{mw}^{(1)}$ is the frequency of the first exciting pulse.

method of pulse electron double resonance (ELDOR) spectroscopy, which can detect the nuclear magnetic resonance (NMR) transitions with a much better sensitivity than the traditional NMR spectroscopy [6].

We used a microwave (mw) pulse of frequency $\omega_{mw}^{(1)}$ to excite a forbidden electron-nuclear level transition ($\Delta m_s = \pm 1$ and $\Delta m_I = \pm 1$) and to "burn holes" in the electron spin resonance line. The free induction decay signal after a second mw pulse of frequency $\omega_{mw}^{(2)}$ is recorded as a function of the frequency difference $\omega_{mw}^{(1)} - \omega_{mw}^{(2)}$ (Fig. 1). Theoretical modeling of such ELDOR spectrum (Fig. 1) yields the HF tensors. From them, the Cu(II) spin density ρ on nitrogens can be estimated. The value of ρ appears to be smaller on N_{ethyl} (ρ ~ 9.4 %) and N_{prop} atoms (ρ ~ 7.1 %) for **1** and **2**, respectively, as compared to N_{phen} atoms (ρ ~ 12 % for **1** and ρ ~ 9.9 % for **2**). This finding has enabled us to identify the relevant superexchange paths in the respective tri-metallic complexes and in particular to conclude that the Cu-N_{phen}-O-Cu exchange path is stronger than the Cu-N_{ethyl}-O-Cu and Cu-N_{prop}-O-Cu paths.

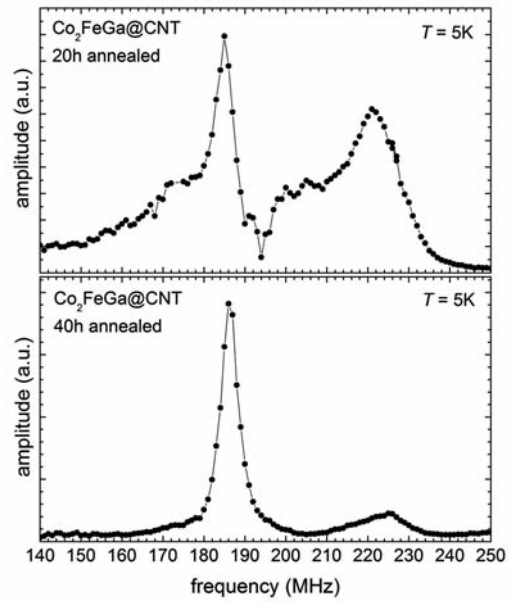

Fig. 3: ^{59}Co NMR spectrum of Co_2FeGa@CNT measured at 5 K, after 20 h (upper part) and 40 h (lower part) of annealing.

Growth model for ternary intermetallic nanoparticles probed with ^{59}Co-NMR

We studied the formation and growth of assemblies of ternary intermetallic magnetic Co_2FeGa nanoparticles as model systems inside Carbon nanotubes (CNT's). The CNTs were used as containers for the nanoparticles since they provide a template for the formation of intermetallic nanoparticles with well-define sizes and protective carbon shells hindering oxidation.

The evolution of particle size and compositions as well as of magnetic properties was studied as a function of progressing annealing time. The challenging observation of the chemical compositions and local structural properties of the nanoparticles was realized by means of ^{59}Co-NMR. Here, it was clearly shown - in agreement with results from TEM and magnetization data - that short and intermediate annealing times (e.g. 20 h, see upper part in Fig. 3) result in particle assemblies with heterogeneous particle compositions reflected in broad NMR spectra with contributions stemming not only from Co_2FeGa (186 MHz) but also from various other byproducts. In contrast, a sufficiently long annealing treatment of 40 h yields homogeneous Co_2FeGa nanoparticles. This

finding is highlighted by the significant reduction of additional contributions in the NMR spectra (see lower figure part). As a consequence of the annealing treatment, initially small particles (~ 10-12 nm) with heterogeneous compositions have evolved to chemically homogeneous particles in the size range of ~ 35 nm, where a further increase of the mean particle diameter is limited by the confining geometry of the inner cavity of the carbon nanotubes.

Quantifying the ratio of orbital to spin magnetic moments on individual FePt nanomagnets

Electron energy loss magnetic chiral dichroism (EMCD) is the electron wave analogon of X-ray magnetic circular dichroism (XMCD). It allows to study magnetic properties quantitatively and with element specificity at the nanoscale in a transmission electron microscope (TEM). We have used a classical EMCD setup, where the sample is illuminated with an electron plane wave thereby acting as a beam splitter. Although this approach is meanwhile established to an extend that it reliably reveals dichroic signals, quantitative results on the orbital and spin magnetic moments obtained from EMCD measurements are only scarcely reported, if at all. We have used a close to parallel electron beam with a diameter of 20 nm to measure EMCD on individual FePt nano islands with a thickness of roughly 10 nm and lateral extensions of some 30 – 50 nm. From the resulting experimental EMCD spectra (cf. Fig. 4), the ratio between the angular magnetic moment and the spin magnetic moment was determined to be $m_l/m_s = 0.084 \pm 0.076$. This value is in agreement with m_l/m_S data obtained from XMCD measurements on ensembles of solution-chemically prepared FePt nanoparticles thereby highlighting the potential of EMCD for quantitative magnetic investigations with highest lateral resolution.

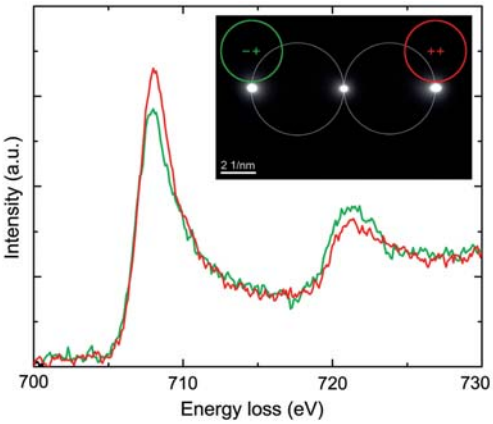

Fig. 4: Electron energy loss spectra (EELS) in the vicinity of the $L_{3,2}$-Fe absorption edge as obtained under three-beam conditions from an individual FePt nano island. The EMCD signal is determined from the intensity difference of the two spectra acquired with the spectrometer entrance apertures placed off-axially at position labelled with a red and green circle in the diffraction plane, respectively.

TEM investigation on the local microstructure of Fe-Ga nanowires

One-dimensional, high aspect ratio nanoscaled magnets are prepared by electrodeposition within nanoporous templates. In recent years the focus was on iron-based alloys with specific magnetic properties such as $Fe_{80}Ga_{20}$ showing high magnetostriction or $Fe_{70}Pd_{30}$ exhibiting a shape memory effect. Stable electrolytic baths have been achieved by complexing the metallic components and the deposition mechanisms were investigated in detail in order to identify deposition conditions for the reproducible preparation of homogeneous, defect free nanowires.

The local microstructure of Fe–Ga nanowires is investigated by TEM considering the dependence on the deposition technique. Using a complexed electrolyte, smooth and homogeneous $Fe_{80}Ga_{20}$ nanowires are electrodeposited into anodic aluminum oxide templates by either applying pulse potential or potentiostatic deposition technique. At optimized deposition conditions the wires show the desired composition of $Fe_{80\pm2}Ga_{20\pm2}$ without a gradient along the growth direction. Composition distribution, structure and microstructure are examined in detail and found to be almost independent of the deposition method. Line EELS and crystal lattice measurements reveal a negligible oxygen content for both preparation routines. Neither Fe/Ga oxides nor hydroxides were found. Both potentiostatically deposited as well as pulse deposited nanowires exhibit a preferred (110) orientation, the latter with slightly larger crystallites. Different contrast patterns were found by TEM that appear more pronounced in the case of pulse deposited wires. High resolution transmission electron microscopy analysis and comparison of differently prepared focused ion beam lamellas reveal that these contrasts are caused by the alternating potential mode and are not induced during the TEM preparation process (Fig. 5). The alternating potential mode causes periodic growth thereby inducing different layers with reduced wire thickness/defects at the layer interfaces [7].

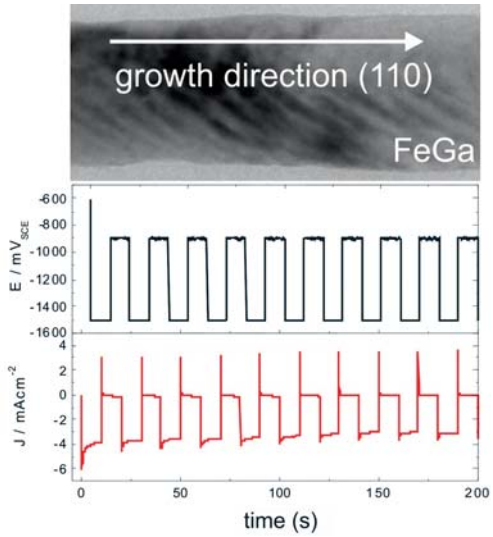

Fig. 5: TEM image **(top)** of a FeGa nanowire showing exemplarily the periodic layer growth caused by the pulsed deposition regime **(bottom)**.

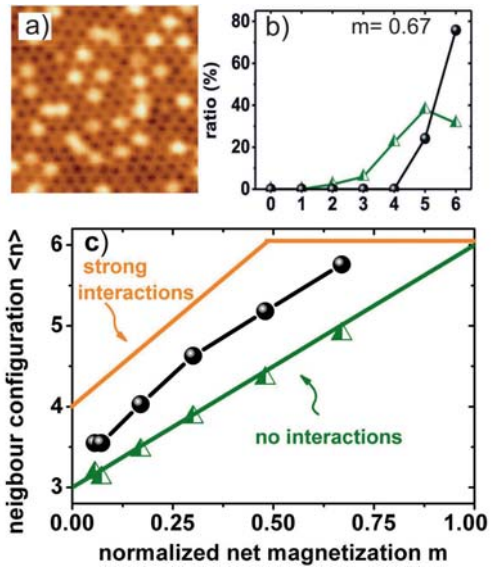

Fig. 6: (a) MFM measurement (1.5 µm x 1.5 µm) of a CoFe nanowire array with normalized net magnetization m = 0.67, **(b)** nearest neighbour distribution function normalized to 100% for the experimental case (black) and a simulated, non-interacting wire ensemble (green), **(c)** average nearest neighbour number <n> as a function of the normalized net magnetization m.

Quantifying magnetostatic nearest neighbor interactions in nanowire arrays by MFM

The magnetostatic interactions in a nanowire array complicate the reconstruction of the ensemble averaged behaviour of the individual nanowires, such as the intrinsic switching field distribution. Simply correcting the shearing of the hysteresis in a mean-field approach does not account for the locally fluctuating demagnetizing field which originates from the individual magnetization configuration in the close surrounding of each nanowire. We proposed a statistical evaluation method of nearest neighbour histograms, which potentially allows judging the strength of the local magnetostatic interactions against the magnitude of the intrinsic switching field distribution.

To this end an in-field Magnetic Force Microscopy (MFM) study of electrochemically produced $Co_{48}Fe_{52}$ nanowires is performed, in which the influence of the magnetic nearest neighbour configuration on the switching behaviour of the individual embedded nanowires is clearly detected. The as-prepared demagnetized nanowire array is magnetized in successively larger magnetic fields and the nearest neighbour configuration around each non-switched (bright) wire is evaluated by counting all neighbouring switched (dark) wires. By considering all non-switched wires in a given MFM measurement, a distribution function is constructed and evaluated for its mean value <n> (see Fig. 6a and b). The deviation of this average nearest neighbour number <n> from the statistical expectation value is a measure of the strength of the local magnetostatic interactions. Fig. 6c shows the results for 6 µm long $Co_{48}Fe_{52}$ nanowires with 70 nm diameter arranged on a hexagonal grid with 100 nm centre-to–centre distance in comparison with the expectation values for non-interacting and strongly interacting wires [8].

High sensitivity cantilever magnetometry based on a co-resonantly coupled sensor

Studying magnetic properties of materials is an important task in the development of new applications for example in spintronics [9]. One method to do this is cantilever magnetometry which allows for the investigation of small magnetic particles and thin films. Therefore, a magnetic sample is placed onto the cantilever which is driven to resonant oscillations and the interaction between an external magnetic field and the sample changes the cantilever's oscillation properties. The oscillation is usually detected with laser deflection or laser interferometry. With decreasing sample size, the signal strength is reduced as well, requiring the development of more sensitive cantilevers. This can be met by the use of nanocantilevers but they lead to an increased complexity of the detection methods.

We are presenting a novel approach based on the coupling of a micro- and a nanocantilever with matched resonance frequencies which induces a strong interplay between the two cantilevers [10]. This leads to the possibility of detecting very small magnetic interactions between a sample attached to the highly sensitive nanocantilever and an external magnetic field. These interactions change the oscillatory state of the coupled system which can easily be detected at the micorcantilever.

We validated the concept by using a commercially available silicon cantilever as micrometer sized oscillator and an iron filled carbon nanotube as nanocantilever (Fig. 7).

The magnetic properties of such FeCNTs have already been investigated [11, 12], making the sample suitable to demonstrate the applicability of the coupled sensor for obtaining magnetic information.

Fig. 7: SEM image of a co-resonantly coupled sensor.

Our measurements show an increase in signal strength by several orders of magnitude compared to cantilever magnetometry experiments with similar nanomagnets and at the same time could be used to determine the expected magnetic properties of the iron nanowire.
With this experiment we do not only demonstrate the functionality of our sensor design but also its potential for very sensitive magnetometry measurements while maintaining a facile oscillation detection with a conventional microcantilever setup [13].

Tailored manipulation of fluids in magnetic gradient fields by electrodeposited magnetic structures

Downscaling and miniaturization of conventional fluidic systems approach their physical limitations. The classical fluid mechanical approaches have to be combined with interfacial interactions. Studying the interactions of different driving forces to manipulate fluids or particles is a challenging task. One of the main issues is to realize the transport of fluids and particles in small gaps by magnetic and electric fields and their gradients using defined arrangements of electrodes and magnets on the microscale. A microchannel test system has been simulated and prepared using electrodeposited CoFe soft micromagnets arranged underneath Au electrodes (Fig. 8). The potential change caused by the expected enrichment of paramagnetic ions in regions of high magnetic field gradients [14, 15] is measured and used to move the fluid frictionless along the designed structures.

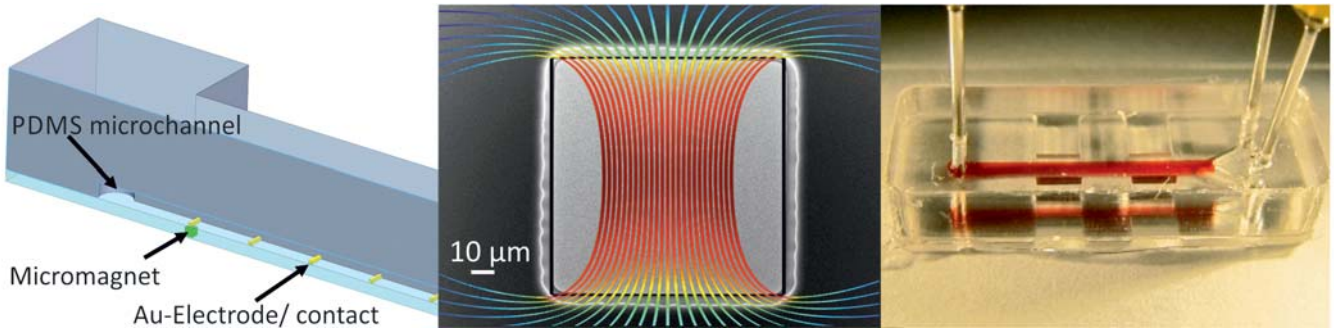

Fig. 8: Schematic image of magnet and electrode arrangement **(left)**, electrodeposited CoFe structure and simulated strayfield **(middle)**, cell design **(right)**.

[1] Westerström et al., Phys. Rev. B **89** (2014) 060406.
[2] Svitova et al., Nat. Commun. **5** (2014) 3568.
[3] Junghans et al., Angew. Chem.-Int. Edit. Engl. **54** (2015) 13411.
[4] Westerström et al., Phys. Rev. Lett. **114** (2015) 087201.
[5] Zhang et al., Chem. Sci. **6** (2015) 2328.
[6] A. Aliabadi et al., J. Phys. Chem. B **119** (2015) 13762.
[7] Pohl et al., Nanotechnology **27** (2016) 035705.
[8] Vock et al., J. Appl. Phys. **118** (2015) 233901.
[9] Chappert et al., Nature Materials **6** (2007) 813.
[10] Reiche et al., Nanotechnology **26** (2015) 335501.
[11] Philippi et al., J. Appl. Phys. **110** (2011) 084319.
[12] Banerjee et al., Appl. Phys. Lett. **96** (2010) 252505.
[13] Koerner et al., submitted to Nanotechnology
[14] Yang et al., J. Phys. Chem. Lett. **3** (2013) 3559.
[15] Pulko et al., Appl. Phys. Lett. **105** (2014) 232407.

Funding: DFG Research Unit FOR1154 “Towards Molecular Spintronics”; WGL - Pakt für Forschung und Innovation 2014; DFG, ERC grant “Gram3”; Joint study agreement, HGST – A Western Digital Company, San Jose, CA, USA

Cooperations: TU Chemnitz; Zavosiky Physical Technical Institute Kazan; TU Dresden; TU Wien; Univ. Arizona; Univ. of Uppsala; Univ. Zürich; Paul Scherrer Institute; MPI CPfS Dresden

Research topic 2.5

Materials for Energy Efficiency, Storage & Conversion

People: J. Balach, J. Eckert, A. Gebert, L. Giebeler, H.-J. Grafe, T. Jaumann, F. Karnbach, M. Klose, S. Oswald, B. Rellinghaus, L. Schultz, U. Stoeck, A. Surrey, M. Uhlemann, M. Antonietti[4], D. Baczyzmalski[3], C. Bonatto Minella[5], C. Cierpka[3], K. Eckert[1], N. Fechler[4], G. Mutschke[2], X. Yang[1]
Responsible Directors: B. Büchner, K. Nielsch, T. Gemming

Abstract: 2015th research brought highlights in stabilizing the performance of lithium-sulfur batteries by a mesoporous carbon-modified separator, giving new detailed insights into the formation of hydrogen bubbles on electrodes during water-splitting in a magnetic field and how a mesoporous nitrogen-doped carbon can influence the dehydrogenation and hydrogenation mechanism in the view of thermodynamics of nanoconfined lithium borohydride.

Functional Hybrid Separators for Advanced Lithium-Sulfur Batteries

Due to the exceptional high theoretical specific energy density of 2.6 kWh kg^{-1}, the lithium–sulfur (Li-S) battery has emerged as the promising candidate for next-generation rechargeable batteries skilled to meet forthcoming energy storage targets set for battery-electric vehicles and smart grids connected with solar/wind power systems.[1] However, two of the main causes of the poor cycling life of the Li-S batteries are due to the insulating nature of sulfur and the so-called shuttle effect of lithium polysulfide intermediates, which decrease the active material utilization [1]. In order to solve these issues, we proposed the modification of the cell configuration by integrating functional carbon interlayers [2] or hybrid separators [3-5] with large electrochemically active surface between the anode and the cathode.

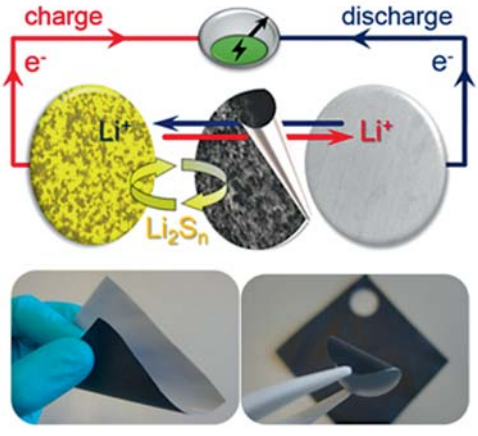

Fig. 1: Functionalized separator [3]

We focus our research work on the development of functional hybrid separators by a straightforward coating modification of a commercial Celgard polypropylene separator with mesoporous carbon materials. The Li-S cells with a mesoporous carbon-coated separator retain capacities of the order of 700 mAh g^{-1} after 500 cycles at 1 C, despite the use of a simple cathode mixture containing a high sulfur/non-porous carbon (Super P) ratio of 7:2 [3]. The enhanced electrochemical performance of the Li-S batteries is attributed to the unique features of the mesoporous carbon-coating, which effectively reduces the resistance of the sulfur cathode, prompts fast electron/lithium ion transport through the carbon network, successfully sequestrates, stores and maintains available the sulfur active material for further reutilization and buffers the large volume change

during sulfur/Li_2S conversion reaction. In addition, the cyclic stability of the Li–S cells were improved by using a polypropylene-supported N-doped MPC hybrid separator as polysulfide adsorbent [4, 5]. The N-doping of the carbon-coating allows to chemically adsorb and reinforce the confinement of lithium polysulfide intermediates through coupling interactions between charged lithium polysulfide and the polarized nitrogen-neighboring carbon surface that restrains active sulfur material loss.
Our work highlights the importance of the rational design of modified separators with mesoporous carbon structures and this proof of concept may bring reliability for advanced high-performance Li-S batteries.

Hydrogen bubbles generated at a Pt-microelectrode – Dynamics of evolution and dissolution

Novel and efficient energy storage solutions stay in the focus of energy research. One challenge is making water electrolysis economically competitive due to fast H_2 detachment and transport away from the electrode to minimize overpotentials. Studies of H_2 bubble nucleation, growth, detachment, dissolution and single bubble behavior in external magnetic fields at a Pt microelectrode are key issues for a detailed understanding of the underlying mechanisms and further increase of efficiency. The combination of electrochemical measurements, extensive image processing by high speed microscopy and particle as well as astigmatism tracking velocimetry allows evaluating the dynamics of bubble evolution and detachment process with respect to bubble radius, contact angle and complex velocity field around the bubble in particular, and due to the impact of superimposed magnetic fields [6]. For the first time it was figured out that single bubble dissolution proceeds over a three step mechanism. The experimental results are supported by numerical analysis.

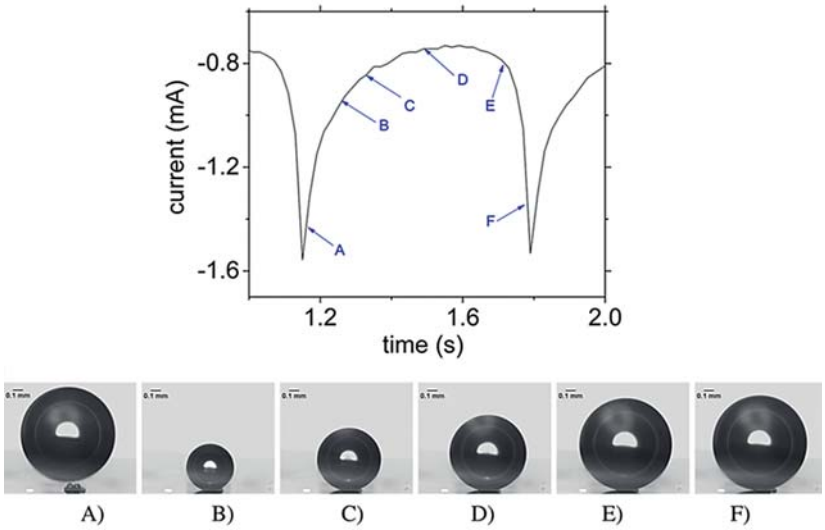

Fig. 2: Current-time behavior of one bubble period generated potentiostatically at $E_{MSE} = -1.5$ V in 1 M H_2SO_4 at a Pt microelectrode (Ø 100 µm) and characteristic stages of bubble evolution [6].

Improving the hydrogen storage properties of $LiBH_4$ through nanoconfinement

$LiBH_4$, a complex hydride, contains the highest amount of hydrogen among the solid hydrogen storage materials and is thus a promising material for mobile applications. Unfortunately, the hydrogen release occurs only at unfavorably high temperatures and may be accompanied by the release of toxic byproducts. Recently, however, it was shown that both the thermodynamics and the reaction kinetics of complex hydrides can be effectively influenced by confining them in scaffolds with nanoscopic pore sizes. We have therefore studied the effect of nanoconfining $LiBH_4$ in aerogel-like nitrogen-doped carbon scaffolds prepared by salt templating. Such scaffolds are easily prepared. They offer large pore volumes, are chemically stable, and their pore size can be effectively

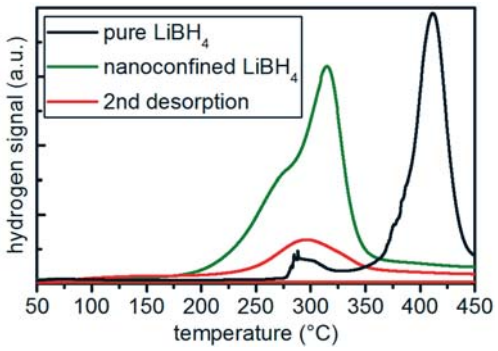

Fig. 3: Hydrogen mass spectrometry of pure $LiBH_4$ (black curve), $LiBH_4$ nanoconfined in the carbon scaffold with a loading of 40 wt. % (green), and the nanoconfined $LiBH_4$ after rehydrogenation at 100 bar hydrogen and 300 °C for 3 h (red).

tuned. Comprehensive investigations using differential scanning calorimetry (DSC), X-ray diffraction (XRD) and scanning transmission electron microscopy (STEM) in combination with electron energy loss spectroscopy (EELS) reveal, that for $LiBH_4$ loadings of 40 wt % the hydride is solely contained in the smallest pores of the carbon scaffold (pore diameters smaller < 5 nm) and that the $LiBH_4$ is amorphous. Thermogravimetric (TG) measurements and mass spectrometry (MS) confirm, that the hydrogen desorption temperature, which is above 400 °C for the bulk hydride, is reduced to 310 °C upon this nanoconfinement with an onset temperature as low as 200 °C (cf. Fig. 3) [7]. Partial rehydrogenation can be achieved under moderate conditions (60 bar hydrogen, 300 °C). In-situ STEM EELS measurements at temperatures up to 400 °C show, that the boron remains within the carbon scaffold also in the de-hydrogenated state. Unlike reports on $LiBH_4$ nanoconfined in highly ordered nanoporous carbon, an ejection of LiH from the carbon pores does not occur, neither in case of the in-situ heating in the electron microscope nor for the DSC heated sample. Apparently, both decomposition products (B and LiH) remain inside the pores of the carbon scaffold. The relatively small degree of rehydrogenation is, however, yet to be explained and will be a subject of further research.

[1] A. Manthiram et al., Chem. Rev. 114 (2014) 11751.
[2] J. Balach et al., J. Phys. Chem. C 119 (2015) 4580.
[3] J. Balach et al., Adv. Funct. Mater. 25 (2015) 5285.
[4] J. Balach et al., J. Power Sources 303 (2016) 317.
[5] U. Stoeck et al., J. Power Sources (2016) doi: 10.1016/j.jpowsour.2015.11.077.
[6] X. Yang et al., Langmuir 31 (2015) 8184.
[7] A. Surrey et al. Int. J. Hydrogen Energy (2016) accepted

Cooperations: Fraunhofer IWS; IKTS; IFAM Dresden; TU Bergakademie Freiberg; TU Dresden[1]; HZDR[2]; Universität der Bundeswehr, München[3]; MPI of Colloids and Interfaces, Potsdam[4]; Karlsruhe Institute of Technology[5]

Funding: German Federal Ministry of Education and Research (BMBF) within Excellent Battery – WING Center BamoSa "Batteries – mobile in Saxony" (03X4637C), German Research Foundation (DFG, Ec201/4), Reiner Lemoine Foundation

Research topic 2.6

Thermoelectric materials

People: L. Akinsinde[2], J. Garcia[1], M. Mohn[1], S. Neitsch[1], H. Reith[1], N. Perez Rodriguez[1], G. Schierning[1], H. Schlörb[1]
Responsible director: K. Nielsch[1]

Abstract: In this research topic we develop thermoelectric materials, processing techniques and intelligent concepts for device integration. Hereby, conventional tellurium-based compound semiconductors with high performance at room temperature serve as a thermoelectric model system to explore novel device strategies, both for generators or coolers. To develop integrated thick film devices, we employ electrochemical deposition of $(Bi_xSb_{1-x})_2Te_3$ which is a low-cost and easily scalable method. Although electrochemical deposition is not a standard process in semiconductor fabrication techniques, compatibility would be technologically feasible. Hence, this research topic benefits from the fruitful combination of long standing expertise in electrochemical deposition techniques and micro-manufacturing as well as measurement techniques at the IFW Dresden. In this article, we focus on work performed in the frame of an EU-funded project on Thermally Integrated smart Photonics Systems (TIPS).

Introduction

Next generation electronic devices require intelligent thermal management strategies in order to remove high density heat fluxes from the active electronic parts. The thermal challenge grows with advancing levels of integration. Jointing more and more functionality into ever-decreasing space increases the thermal budget, i.e. the heat flux densities. Especially optoelectronic devices demand a very precise thermal stabilization in order to produce a precisely defined wavelength. Hence, hardware solutions for a smart and efficient thermal management are sought for.

Fully integrated micro-scale coolers together with heat pumps, heat spreaders, heat exchangers and heat sinks are the envisioned combination for this problem within the TIPS project, addressing the multiple dimensions of heat transport. In case of success, high band-width optical communication could greatly benefit: An intelligent circuit which can control its own operations thermally could be up to five times more efficient than today's technology, is estimated within the ambitious objectives of the project.

One corner-stone of the thermal management strategy for future photonic communication systems are micro-scale thermoelectric coolers which are being developed at the IFW within the TIPS cooperation. The requirements with respect to thermoelectric material and fabrication technology are hereby manifold: The material needs to provide a high thermoelectric figure of merit at room temperature and be stable and reliable under operation. The fabrication should be done by a highly scalable, low-cost deposition technique and furthermore be fully compatible with CMOS fabrication requirements. Amongst the variety of thermoelectric materials and processing technologies, we picked electrochemical deposition of standard tellurium-based thermoelectric thick films combined with micro-structuring by lithography to best possible fulfil these high-end specifications.

Within this article we report on the electrochemical deposition of ternary $Bi_2(Te_xSe_{1-x})_3$ and $(Bi_xSb_{1-x})_2Te_3$ films. Hereby, the parameters of the electrochemical deposition were optimized to obtain defined film morphology and crystalline structure as well as best-possible thermoelectric properties. Smooth films of n-type and p-type doping are reliably produced. Their integration into micro-scale thermoelectric coolers is currently being developed.

Results and discussion

Electrochemical deposition of thick films

The previously reported bath chemistries and pulse plating procedures for both, the n-type material, $Bi_2(Te_xSe_{1-x})_3$, and the p-type material, $(Bi_xSb_{1-x})_2Te_3$ [1], were used as the starting point and optimized with regard on implementation in the device fabrication process. The desired composition of the ternary compounds and thus the Seebeck coefficient were adjusted by a careful selection of the pulse deposition potentials. In addition, an improvement of the p-type film compactness was achieved by applying longer pulse times for both the deposition as well as the relaxation step. The film thickness can be easily adapted by the number of pulses applied. Finally, the electrolyte composition was modified. In particular the addition of a small amount of a surfactant, namely sodium dodecyl sulfate (SDS), significantly reduced the surface roughness of the films (see Fig. 1) thereby strongly improving its suitability for further processing steps such as contacting.

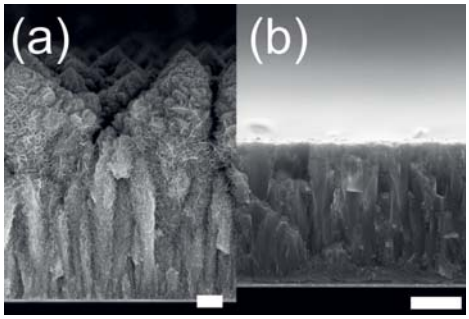

Fig 1: SEM cross section images of $(Bi_xSb_{1-x})_2Te_3$ electrodeposited samples. **(a)** Short pulse times results in dendritic growth. **(b)** Long pulse times and additives allow for leveled and compact growth. Scale bars are 2 µm.

Micro-structuring of thick films for device integration

The construction of the micro-scale thermoelectric cooler proposed in the TIPS project requires several lithographic steps in order to electrochemically deposit the different n-type and p-type chemical compositions of the thermoelectric materials next to each other. The masks for the electrochemical deposition were fabricated by means of micro-patterning. In order to achieve the optimal geometry complying with the requirements of device integration defined by the envisioned application, thick photoresist was used and the exposure parameters were optimized in order to achieve the best structure resolution. Due to substrate-mask-electrolyte interactions, the electrochemical deposition

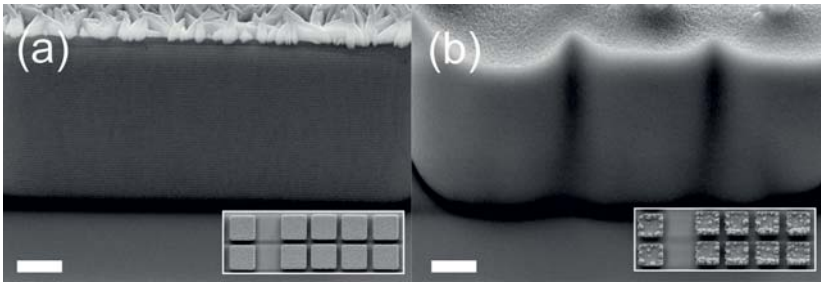

Fig 2: SEM cross section images of electrodeposited 20 µm x 20 µm squares of $Bi_2(Te_xSe_{1-x})_3$ **(a)** and $(Bi_xSb_{1-x})_2Te_3$ **(b)**. Scale bars are 2 µm. Insets show patterned array of the mentioned squares.

into a photo-pattered micrometer size cavity of the ternary systems of concern is not trivial. However, the electrochemical conditions were further optimized obtaining compact and well defined structures of both n- and p- type materials down to 20 µm x 20 µm feature size (Fig. 2). Subsequently, a two-step lithography was demonstrated for the successive deposition of both materials yielding well adhesive micro blocks suitable for further processing.

Thermoelectric properties

The transport properties of the thermoelectric $(Bi_xSb_{1-x})_2Te_3$ thick films can be sensitively adjusted by the choice of the parameters of the electrochemical deposition. This is demonstrated for the Seebeck coefficient exemplarily in Fig. 3 in which the off-potential E(off) is varied between 0 and 0.2 V. The variation of the off-potential results in detectable changes of the chemical composition of the sample evidenced in Fig. 3a by means of energy dispersive X-ray (EDX) analysis of the thick films. Within this series of samples, the tellurium content increased from 57 at.% to 70 at.% induced by the variation of the off-potential. This in turn results in a dramatic change of the Seebeck coefficient with maximum values around 140 µV K^{-1} and a minimum of -9 µV K^{-1}. Even the type of majority carriers changes from p-type to n-type (Fig. 3b). Fig. 3c combines both measurements to emphasize the dependence of the Seebeck coefficient on the tellurium content.

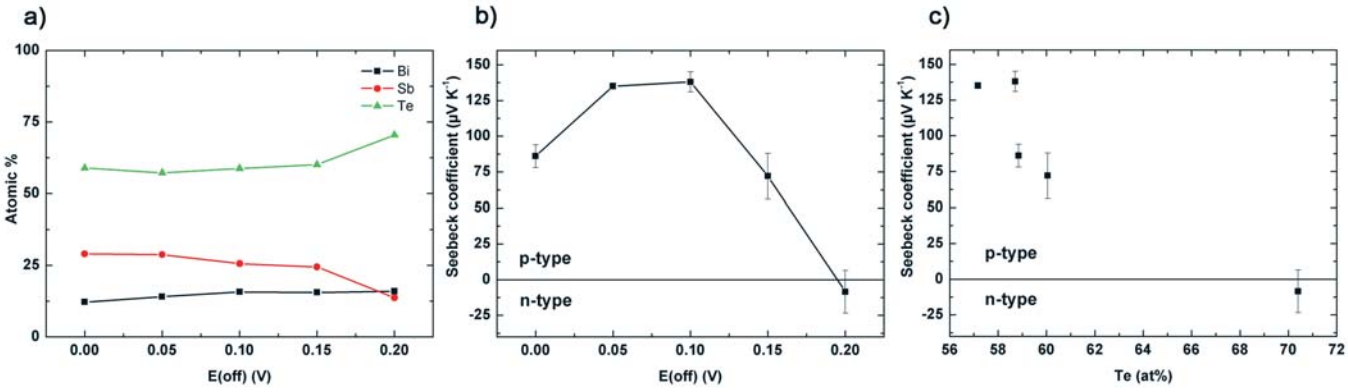

Fig. 3: Film composition obtained by EDX **(a)** and Seebeck coefficient **(b)** of electrodeposited Bi-Sb-Te thick films in dependence on the potential of the relaxation step ("off" potential) in the pulsed electrochemical deposition regime; **(c)** Dependence of Seebeck coefficient on the Te content of the as-deposited films showing the transition from p-type to n-type behavior.

The reason for the observed variations in the Seebeck coefficient is given by the defect chemistry of the material, tailored by the deposition process: Metal chalcogenides such as Bi_2Te_3, Sb_2Te_3 and the mixed crystals of the type $(Bi_xSb_{1-x})_2Te_3$ are usually intrinsically doped by antisite defects. Hereby, a Te- atom on a (Bi/Sb)-lattice site, $[Te]_{Bi}$, provides the crystal with one additional electron, while a (Bi/Sb)-atom on a Te-lattice site, $[Bi]_{Te}$, depletes the crystal by one electron. The tellurium-rich thick films therefore tend to show n-type behaviour, while tellurium-depleted thick films demonstrate p-type behaviour. The zero-crossing of the Seebeck coefficient is characterized by balanced concentrations of both types of defects, $[Te]_{Bi} \sim [Bi]_{Te}$.

The Bi/Sb ratio needs to be carefully tailored as well. The formation energies of the antisite defects depend on the specific chemical composition within the mixed crystal series, resulting in different concentrations of the antisite defects and therewith different doping levels, being directly reflected by the Seebeck coefficient. With the completely optimized parameter set (including electrolyte composition, pulse potentials, and pulse times) as-deposited p-type samples show a Te concentration of about 59 at.% and a Bi/Sb ratio of about 0.6 with a maximum value of the Seebeck coefficient of 163 ± 8 µV K^{-1}. The control of all parameters of the electrochemical deposition is therefore not only necessary to obtain a defined film morphology but also for optimal thermoelectric transport coefficients.

Outlook

The research topic 2.6, thermoelectric materials, is currently in its early stage of development. While the TIPS project already presents a strategic topic, combining the expertise of different teams within the IFW, new projects and collaboration will be fostered in 2016. These include innovative processes for the fabrication of bulk thermoelectric nanomaterials employing deformation methods typically used for metallic materials or functionalizing nanoparticles by a hybridization technique.

[1] Schumacher et.al., Adv. Energy Mater 3 (2013) 95

[1] Institute for Metallic Materials;
[2] Multifunctional Nanostructures, Physics Department, University of Hamburg

Funding: TIPS, European Union grant agreement No 644453 within Horizon 2020 Framework Programme for Research and Innovation.

Cooperations: Tyndall National Institute (TNI, Ireland), Centre National de la Recherche Scientifique (CNRS, France) with Lyon Institute of Nanotechnology (INL-CNRS, France), Institute of Light and Matter (ILM-CNRS, France), Materials Institute Jean Rouxel (IMN-CNRS, France), Communicraft (Ireland), Alcatel-Lucent Bell Labs (Ireland), Alcatel-Lucent Bell Labs (France), Alcatel Thales III-V Lab (France), LioniX BV (Netherlands), Stokes Laboratories (Ireland), University of Hamburg

Research topic 3.1

Designed Interfaces and heterostructures

People: K. Duschek, D. Efremov, S. Fabretti[5], S. Fähler, N. Heming, R. Hühne, V. Kataev, M. Knupfer, A. Koitzsch, K. Leistner, A. Petr, L. Schultz, H. Schlörb, A. Thomas, U. Treske, M. Uhlemann, L. Yang, J. Zehner, R. Zierold[4]
Responsible directors: B. Büchner, K. Nielsch, J. van den Brink

Abstract: In virtually all modern nanoscale devices interfaces play a crucial role. Genuine electronic and magnetic interface effects, not existent in bulk materials, emerge due to distinct electronic, compositional, as well as structural properties present at interfaces.
In the following we focus on three examples of ongoing research activities in this field in the IFW. The systems covered include polar oxide heterointerfaces, metal/oxide/electrolyte interfaces, as well as layered heterostructures for magnetic tunnel junctions (MTJ). Advanced deposition techniques as well as sophisticated measurement techniques that precisely reveal interface properties are used in order to understand and exploit the potential of these interface-dominated materials. Important scientific advances in the understanding of the electronic structure of polar oxide heterointerfaces have been made by combining density functional theory (DFT) calculations with orbital sensitive x-ray absorption spectroscopy (XAS). At solid/electrolyte interfaces, widely tunable interface magnetism has been detected by in situ Anomalous Hall Effect (AHE) and in situ Ferromagnetic Resonance (FMR) measurements. For MTJs, the precise preparation of a high performance thin film heterostructures is achieved by the combination of physical vapor deposition techniques (PVD) and atomic layer deposition (ALD).

1. Strain dependence of the electronic structure of polar oxide heterointerfaces

A conceptually appealing aspect of the research on polar oxide heterointerfaces is the possibility to design interface properties at will by the right choice of the constituent materials. For this to become truly operative numerical methods are needed that are reliable enough to predict key interface parameters - and guide, thereby, the materials development.

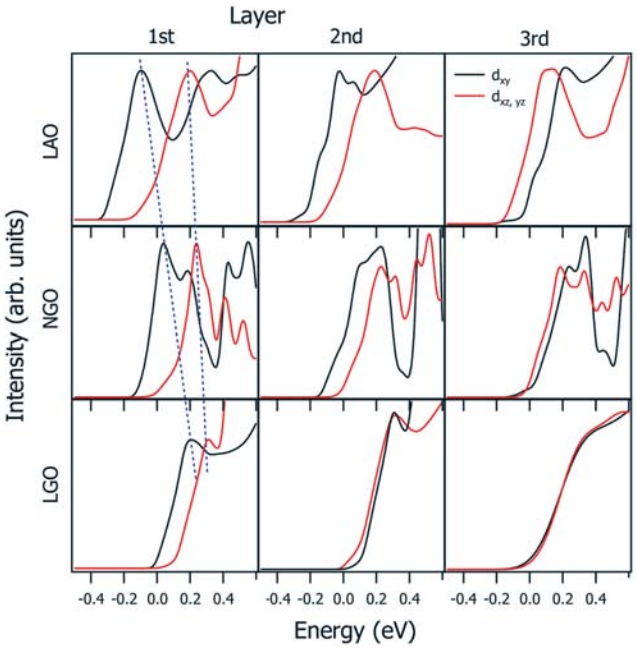

Fig. 1: Orbital resolved density of states for different materials and layers.

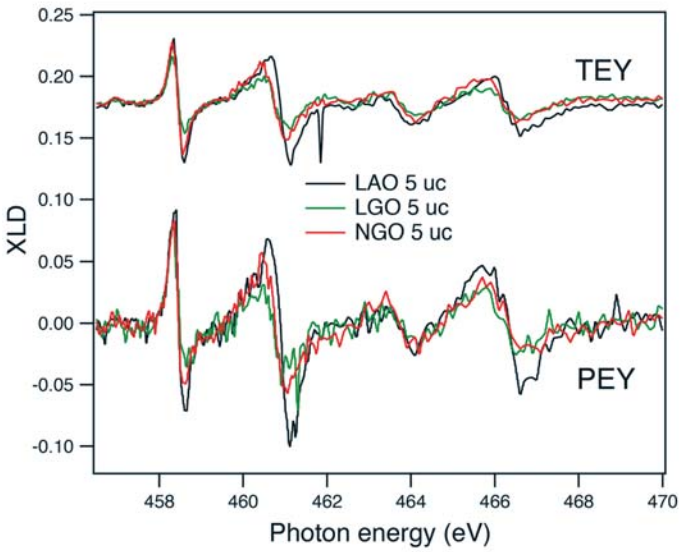

Fig. 2: X-ray linear dichroism in different yield modes at the Ti-L edge.

The most prominent property of polar oxide heterointerfaces is the appearance of a metallic state above a certain thickness threshold in $LaAlO_3/SrTiO_3$. This effect roots in the formation of a two-dimensional electron gas (2DEG) at the interface. The lowest d-level that becomes occupied is the d_{xy} orbital as has been explicitly shown by orbital sensitive XAS.

Here, we apply density functional theory (DFT) to calculate the orbital resolved electronic structure of the $LaAlO_3/SrTiO_3$, $NdGaO_3/SrTiO_3$, and $LaGaO_3/SrTiO_3$ series of interfaces, which all show a metal insulator transition at n = 4 unit cells. The system $(La,Nd)(Al,Ga)O_3$ is of model character due to its ionic, isovalent and isostructural character. We have previously investigated the electronic structure of this series by photoemission spectroscopy and found clear similarities among the materials. But an important difference is the lattice constant. Here we consider the influence of varying lattice mismatch and strain at the interface in an otherwise similar environment.

The splitting of the d-levels is a ground state property. Fig. 1 presents DFT calculations of the orbital and layer resolved density of states (DOS) for the 2 unit cells samples. The DOS has been normalized to the first peak in all cases, because we are interested in the states that become occupied first when the 2DEG forms at the interface. Indeed the degeneracy of the d_{xy} vs $d_{xz/yz}$ orbitals is lifted. The effect is most pronounced for the first layer, as expected, and decreases for deeper layers. The energy separation is largest for $LaAlO_3/SrTiO_3$ and smallest for $LaGaO_3/SrTiO_3$.

As mentioned above, the energy position of the d-levels can be measured by orbital sensitive XAS, which is most conveniently presented as x-ray linear dichroism (XLD). Fig. 2 presents the XLD spectra for all the materials and for different yield modes (partial electron yield – PEY, total electron yield – TEY), which are differently depth sensitive.

The spectra in Fig. 2 can be evaluated by the help of standard multiplet theory. The information thereby extracted from Fig. 2 is twofold: i) from the shape the d-level hierarchy is confirmed to be the same for all the compounds and led by the d_{xy} orbital. ii) The magnitude is largest for $LaAlO_3/SrTiO_3$ and smallest for $LaGaO_3/SrTiO_3$, which reflects the magnitude of the d_{xy} vs $d_{xz/yz}$ splitting in agreement to the DFT. The splitting is directly linked to the strain state at the interface.

This work represents a step towards the quantitative understanding of oxide heterointerfaces which could be exploited for future materials design.

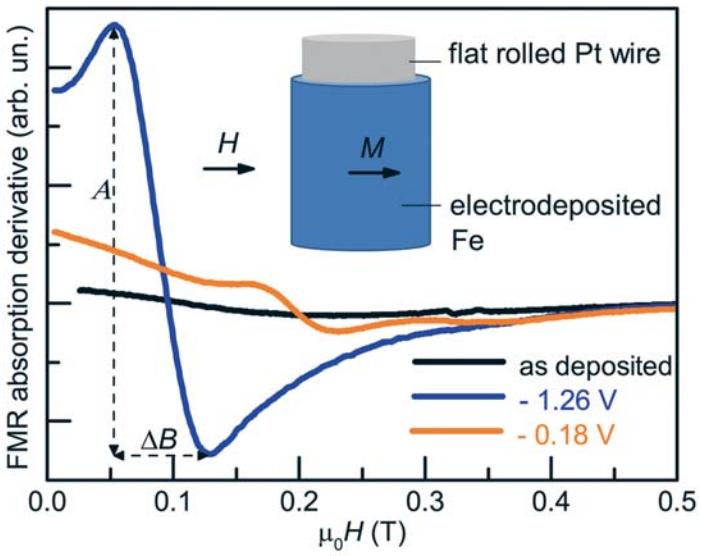

Fig. 3: FMR spectra of 10 nm electrodeposited Fe in as deposited state and during polarization at different voltages in 1 M KOH.

2. Interfacial control of magnetism in hybrid heterostructures by faradaic effects

Electric field control of magnetization at metal interfaces is of great interest for low power spintronic devices, nanofluidic systems as well as magneto-nanoelectromechanical systems [1]. The voltage dependency of interfacial properties of metals charged in solid or liquid electrolytes has already been successfully exploited for tunable monolayers or ultrathin metallic films. Changes of the electronic band filling in the uppermost atomic layers obtained by capacitive electronic charging, as well as a change of interface chemistry have been suggested as interfacial origin. The latter is related to electric field induced ion migration and charge-transfer, leading to a reversible change of the oxidation state of, e.g., Fe or Co species [2, 3]. These faradaic reactions at oxide/metal interfaces are not restricted to the uppermost atomic layers but depend on the reaction layer thickness. In principle, composition, phases, structure and microstructure can be changed, promising tremendously larger magnetic property changes achievable by electrochemical reactions than by sole electronic charging.

We demonstrated that voltage controlled tuning of surface magnetization of metal layers can be achieved in reaction volumes even well above monolayered regions. Liquid electrolytes are of advantage here, as ionic mobility is enhanced in comparison to solid electrolytes where heating or significantly higher voltages are required for measurable effects [2]. As a model system we chose several oxide/metal heterostructures polarized in liquid electrolytes. We are able to in situ characterize the voltage dependence of magnetism during polarization in the electrolyte by in situ FMR and in situ AHE measurements. To demonstrate all-electrochemical control, we investigated 10 nm thick electrodeposited Fe films with native oxide layer polarized in 1 M KOH. The measured FMR signal is depicted in Fig. 3. In the measurement geometry, the direction of the external magnetic field lies within the easy plane of the dominating part of the Fe film. Thus, for the most part, magnetization is collinear to the external magnetic field. This allows to correlate changes of the FMR intensity given by $A(\Delta B)^2$ with relative changes in saturation magnetization. More than 90 % change of magnetization is estimated when polarizing between -1.26 V and -0.18 V. This is a remarkably large impact, especially in comparison to 10 nm thick sputtered Fe film where only 13 % voltage-induced variation of magnetization was achieved. It can be concluded that defect-rich structures and a high surface/volume ratio, as present in our electrodeposited Fe films, favor kinetics of electrooxidation and electroreduction. In a volume appropriate for nanoscaled applications, large magnetization changes at room temperature and for a voltage change of merely 1 V are demonstrated.

3. HfO_2 based magnetic tunnel junctions

Magnetic tunnel junctions (MTJs) are generally prepared by physical vapor deposition (PVD) techniques such as sputtering, molecular beam epitaxy or thermal evaporation. In most cases, the tunnel barrier in these devices consists of magnesia or alumina. These alumina and magnesia based MTJs are well studied and show very good properties in many different applications. But it also leaves many opportunities for different barrier materials and some of these materials might require a non-PVD deposition technique. In general, atomic layer deposition (ALD) leads to high-quality, pinhole-free thin films with low impurity content because of its self-limiting, well-defined chemical reactions of gaseous precursors with the surface moieties of the substrate.

As an example for ALD/PVD heterostructures, we prepared HfO_2 based MTJs. HfO_2 has rarely been used as a barrier material and has a well-known ALD process. The electrodes of the MTJs were magnetron sputtered and the barrier was prepared from a tetrakis hafnium precursor.

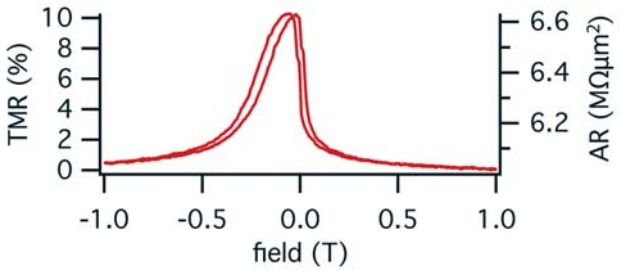

Fig. 4: Major loop of an HfO_2-based MTJ at 300 K and an applied bias voltage of 10 mV. The maximum observed TMR ratio was 10.3 %.

Figure 4 shows a major loop of the tunnel magnetoresistance (TMR) ratio as a function of the applied magnetic field at room temperature. We observed a TMR ratio of 10 % between the parallel and antiparallel magnetization states and an increase of the TMR ratio to 19 % was observed at 2 K. Both, the increase in the resistance and the increase in the TMR ratio with decreasing temperature have also been observed for MgO and Al_2O_3 based systems and can be explained in terms of magnon- and phonon-assisted tunneling modes.

Next, we measured the TMR ratio as a function of the applied bias voltage. Here, an asymmetry of the TMR ratio between negative and positive bias voltages was observed. This asymmetry might be attributable to the vacuum breaks between the sputtering of the lower stack and the ALD of the barrier oxide as well as after the ALD and before the sputtering of the top stack. This will be addressed by the next iteration of devices prepared in a thin film cluster tool without vacuum breaks.

We conclude that the proposed process is a very simple and reliable procedure for the fabrication of HfO_2-based MTJs, as HfO_2 is compatible with the commonly used processes for Si semiconductors. It also serves as a proof-of-concept for ALD/PVD heterostructures.

[1] F. Matsukura et al., Nature Nanotechn. 10, (2015) 209
[2] U. Bauer et al., Nature Mater. 14, (2015) 174
[3] K. Leistner et al., Phys. Rev. B 87 (2013) 224411
[4] S. Fabretti et al., Appl. Phys. Lett. 105 (2014) 132405

Funding: DFG Eigene Stelle, SPP 1538 (Topological Insulators), SPP 1666 (SpinCat), MIWF/NRW

Cooperations: [1]CNR SPIN, Complesso Universitario Monte S. Angelo, Napoli, Italy; [2]Dipartimento di Fisica, Universita „Federico II" di Napoli, Italy; [3]BESSY II, Berlin, Germany; [4]Univ. Hamburg, Inst. Appl. Phys., Hamburg, Germany; [5]Physics department, Univ. Bielefeld, Germany

Research topic 3.2

Quantum and nano-photonics

People: S. Böttner, H. Bryja, P. Chekhonin, Y. Chen, F. Ding, S. Engelhardt, E. S. Ghareh Naz, S. Giudicatti, B. Höfer, R. Hühne, Y. Huo, R. Keil, L. Ma, M. Mietschke, C. Ortix, H. Schröder, Y. Yin, E. Zallo, J. Zhang, Y. Zhang, M. Zopf
Responsible Directors: K. Nielsch, O. G. Schmidt, J. van den Brink

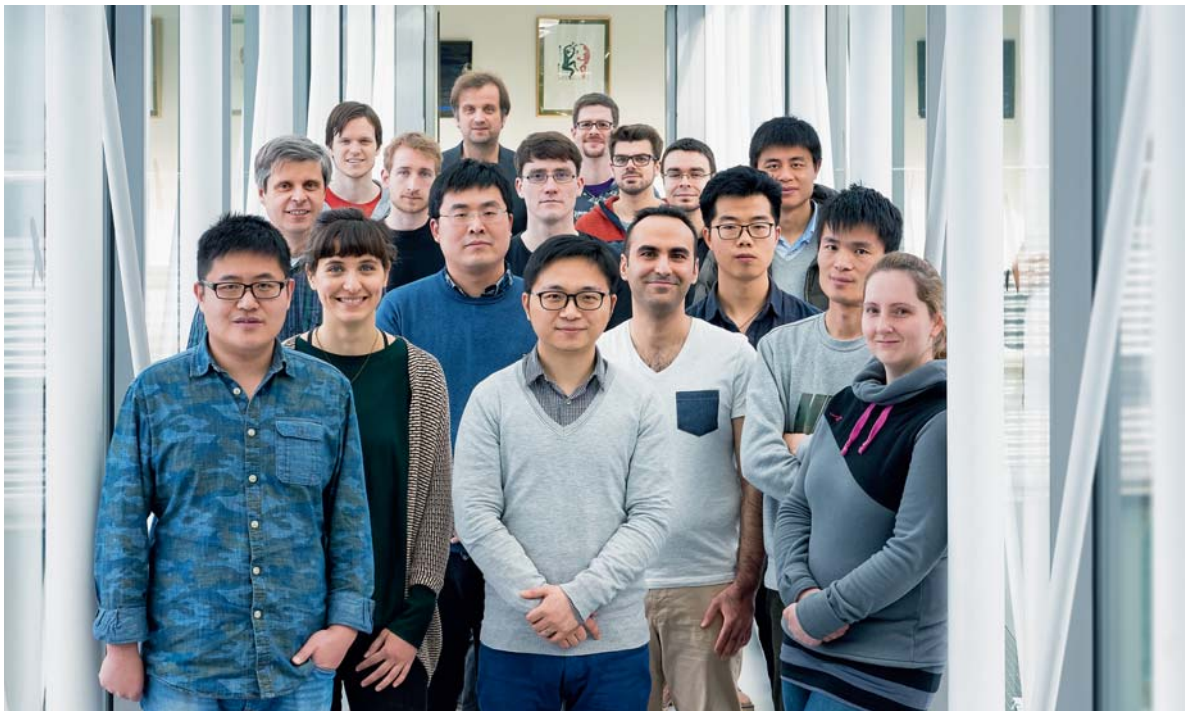

Hybrid plasmon-photon resonant mode in a microcavity

Abstract: The coupling between photon and plasmon in optical microcavities has attracted extensive interests from both fundamental and applied physics. Despite some preliminary reports, the role of light polarization in exciting hybrid plasmon-photon resonant modes in microcavities has not been clarified so far. Here we investigated polarization-dependent excitation of hybrid plasmon-photon resonant modes in a rolled-up microtube cavity coated with a gold nanocap. Two exceptional phenomena were revealed: 1) we demonstrated that the transverse magnetic polarized light predominantly excites hybrid resonant modes in optical microcavities; 2) it was found the thin wall of the microcavity significantly promotes optical energy transfer from the inner dielectric medium to the gold surface, resulting in a strongly enhanced exterior field. Both finite element method calculations and an effective potential approach confirm our experimental observations. Our work reveals the basic physical mechanisms responsible for exciting hybrid modes in opto-plasmonic microcavities and as such is relevant for both fundamental and applied studies in photonics and plasmonics, paving a way for enhanced light-matter interactions in optical microcavities.

Surface plasmon polaritons (SPPs), which can confine the electromagnetic (EM) field at metal surfaces, possess many unique properties. In particular, metal-coated optical cavities have been investigated to study SPPs in combination with optical whispering-gallery-mode (WGM) resonances, which result in SPP resonant and/or hybrid plasmon-photon modes localized at the metallic surface. These kinds of plasmonic resonant cavities are capable to accommodate intense resonant EM fields on the metal layer surfaces suitable for various applications such as enhanced light-matter interactions in a

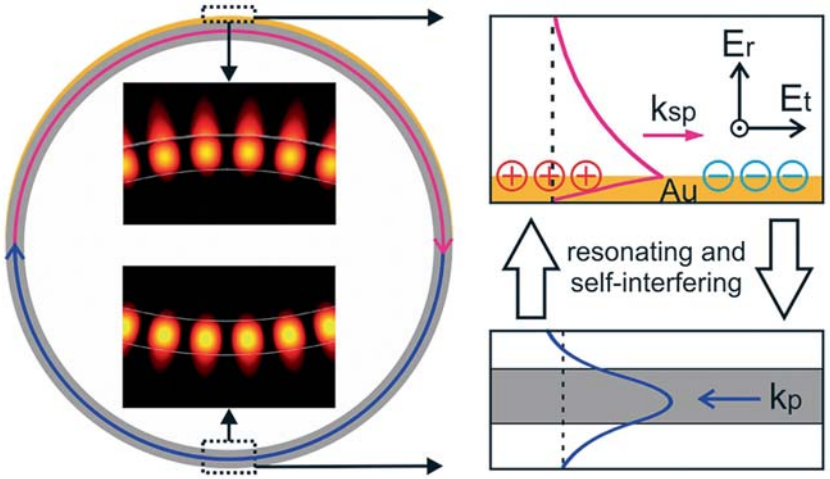

Fig.: Schematics of resonant light supported by a microtube cavity coated with a gold nanocap. As shown in the inset of the left panel, strongly hybridized resonant modes are formed in the gold-coated section compared to that without the gold coating. Right panel shows EM field distributions at the gold surface and within the dielectric tube wall.

microcavity. Despite some preliminary reports, the role of light polarization in exciting hybrid plasmon-photon resonant modes in microcavities has not been clarified so far. In this context, it is of fundamental interest to identify the basic factors, such as the polarization state and the distribution of the EM field in the cavity, which excite the hybrid plasmon-photon WGM modes in microcavities.

The microtube cavity was prepared by the roll-up of a prestrained nanomembrane. In brief, a photoresist sacrificial layer was patterned by lithography to obtain an array of specially designed U-shape profiles. A 30 nm thick SiO_x bilayer was then deposited onto the patterned photoresist by electron beam evaporation. The nanomembranes rolled up into microtubular structures (~ 5 μm in diameter) to release strain upon dissolving the photoresist sacrificial patterns. To increase the structural stability of the rolled-up microtubes, a 30 nm thick HfO_2 layer was conformally deposited on the microtubes via atomic layer deposition. Finally, an 8 nm thick gold layer was deposited by electron beam evaporation onto the top of the microtubes, resulting in a gold nanocap on the tubular cavity.

To clarify the role of light polarization in exciting hybrid plasmon-photon resonant mode, we investigated polarization-dependent excitation of hybrid resonant modes supported by a gold-coated microtube cavity. Both transverse magnetic (TM) and transverse electric (TE) modes were used to excite the hybrid resonant modes. In contrast to previous reports, we demonstrate that the TM polarized light is favorable for the excitation of hybrid plasmon-photon resonant modes. The distributions of the EM field energy densities were calculated by a finite-element analysis method, where the formation of hybrid modes is identified by the energy transfer from the inner dielectric tube wall to the gold surface, generating a greatly enhanced exterior field strength. The mechanism of the excitation of hybrid photon-plasmon modes was further explored by an effective potential approach to illustrate the influence of the tube wall thickness on the enhancement of the exterior field at the gold surface. In addition to the excitation polarization, the tube-wall thickness was found to play an important role in the formation of hybrid resonant modes. The investigation of the polarization-dependent excitation of hybrid modes in thin-walled microtubes is relevant to both fundamental and applied physics, paving the way for enhanced light-matter interactions in opto-plasmonic microcavities.

[1] Y. Yin, *et al.*, Phys. Rev. B **92** (2015) 241403(R).

High yield and ultrafast sources of electrically-triggered entangled-photon pairs based on strain-tunable quantum dots

Abstract: Entangled-light-emitting-diodes based on semiconductor quantum dots are among the most promising sources that can potentially address the communication tasks in quantum information science. However, entangled-light-emitting-diodes are plagued by a source of randomness, which results in a very low probability of finding quantum dots with sufficiently small fine-structure-splitting for entangled-photon-generation. We overcome this hurdle by introducing the first strain-tunable entangled-light-emitting-diodes that exploit piezoelectric-induced strains to tune quantum dots for entangled-photon-generation. We demonstrate that up to 30 % of the quantum dots in strain-tunable entangled-light-emitting-diodes emit polarization-entangled photons, and high entanglement-fidelity up to 0.83 has been achieved. Driven at the highest speed ever reported so far (400 MHz), strain-tunable entangled-light-emitting-diodes emerge as promising devices for high-data rate quantum applications.

We demonstrate a quantum device by integrating ELEDs onto a piezoelectric actuator featuring giant piezo-electric response and capable of delivering anisotropic strain fields. The device – which we call strain-tunable ELED (ST-ELED) – is schematically shown in Fig. 1a. A 440 nm-thick *n-i-p* nanomembrane containing InGaAs QDs is integrated onto a 0.3 mm-thick $[Pb(Mg_{1/3}Nb_{2/3})O_3]_{0.72}[PbTiO_3]_{0.28}$ (PMN-PT) single piezoelectric crystal. The detailed fabrication process is described elsewhere [2, 3]. In order to control the fine structure splitting (FSS) [4, 5] of the QDs embedded in the diode, the crystal axes [1-10] and [110] of the GaAs nanomembrane were aligned along the x and y axes of the PMN-PT actuator, respectively (see Fig. 1a). Representative plots of the FSS (s) of different QDs as a function of F_P are shown in Fig. 1b. We note that the tuning behavior is determined by the exciton polarization angle at zero strain fields (θ_0) with respect to the predefined direction of the strain. Fig. 1c-g show the exciton polarization direction θ_0 with respect to the strain axes for the five studied QDs. Specifically, owing to the exact alignment between the exciton polarization angle and the strain axes for dot D and E, their FSS can be reduced well below 1 μeV [3].

The ability to tune the FSS of the QDs to zero allows us to investigate the capability of the ST-ELED to generate polarization-entangled photon pairs with an ultrafast speed. Fig. 2a shows the results of polarization correlation measurements at 400 MHz for the

Fig. 1: (a) Sketch of the diode structure. **(b)** Representative variation of s as a function of F_P for five QDs. The insets show sketches of biexciton cascade. **(c – g)** s_0 and Θ_0 for the five studied QDs at F_P = 0 kV cm^{-1}.

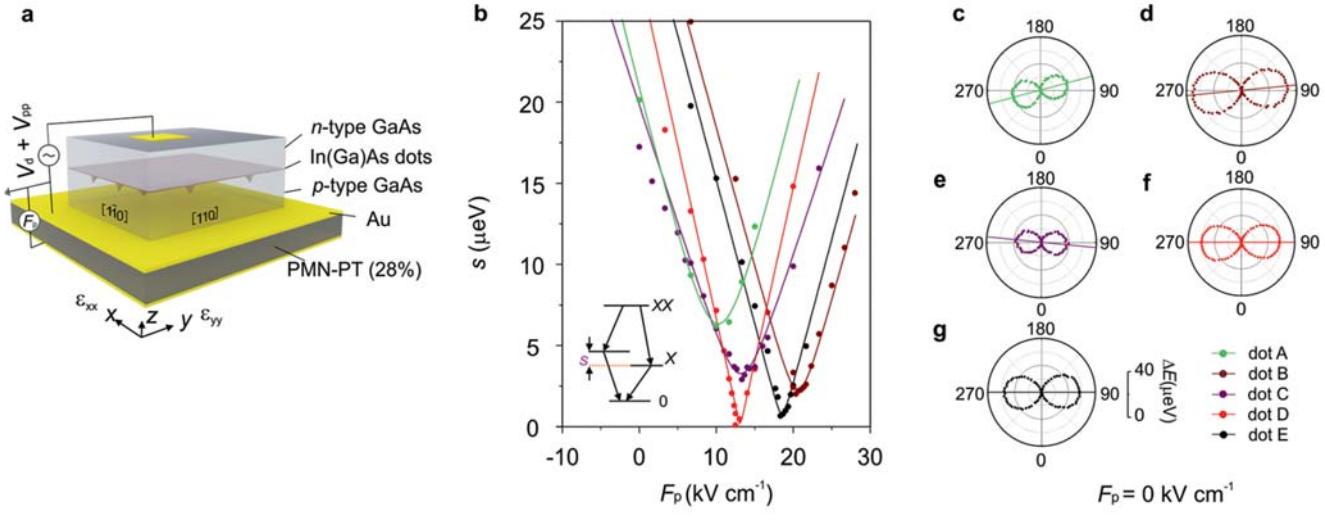

dot E. We observe correlations in the HV and DA bases and anti-correlation in the RL basis for co-polarized two photons. In Fig. 2b the degrees of correlation in given bases are reported. We find a state fidelity as high as 0.66 ± 0.02, which exceeds the classical limit of 0.5 and thus proves, for the first time, generation of entangled-photon pairs at 400 MHz[5]. Furthermore, a statistical study from 82 randomly selected QDs revealed that the majority of QDs in our ST-ELED device have θ_0 oriented close to the [1-10] crystal axis. To determine the entanglement fidelity as a function of the tuned FSS, polarization correlations were performed for each value of the FSS and entanglement was equivalently quantified by measuring the degree of correlation. As shown in Fig. 2c, the maximum fidelity $f^+ = 0.75 \pm 0.02$ is achieved when the FSS is tuned close to zero. For FSS values larger than 3 μeV, the fidelity decreases below the classical limit (see the dashed line). From the statistical investigation we find that 27 QDs can be tuned below 3 μeV (see Fig. 2d), which indicates a probability as high as 33 % of QDs that can be exploited as entangled-light emitters in our ST-ELEDs[3].

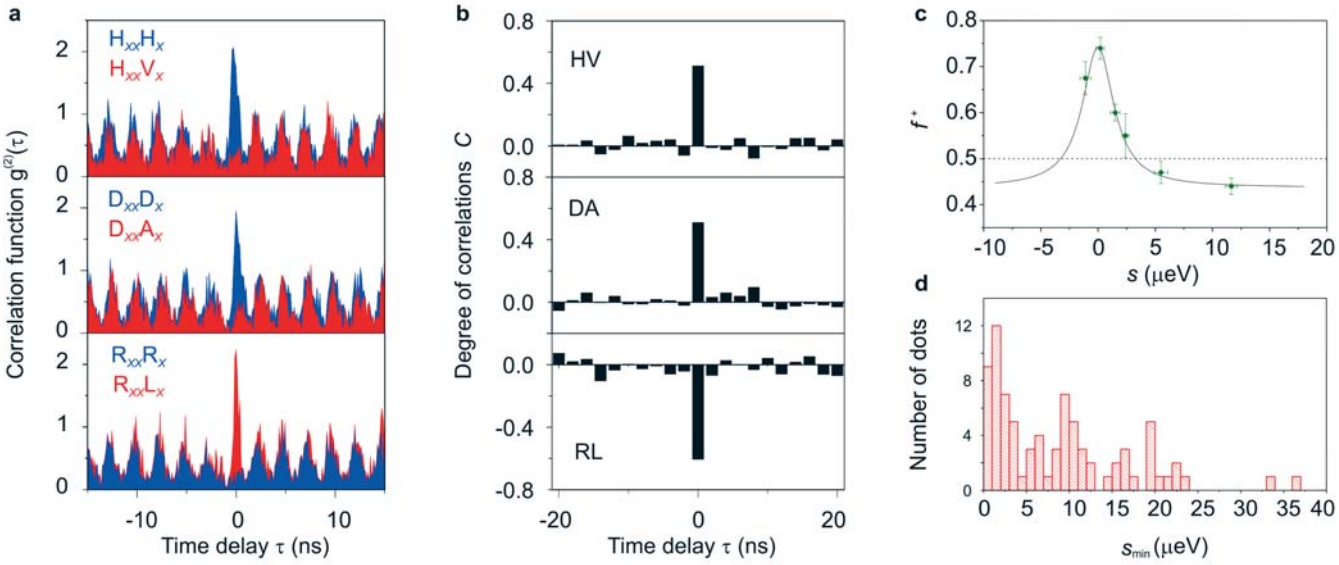

Fig. 2: (a) Normalized correlation functions with 400 MHz repetition rate. **(b)** Degree of correlation in given basis. **(c)** Fidelity as a function of FSS. **(d)** Histogram of the distribution of s_{min} tuned by the externally induced strain fields in the ST-ELED device.

We have presented ST-ELEDs in which anisotropic strain fields are used to tune QDs for entangled-photon generation. We have demonstrated that up to 30 % of QDs are capable of emitting polarization entangled-photon pairs and achieved triggered entangled-photon emission at a repetition rate of 400 MHz.

[1] O. Benson et al., Phys. Rev. Lett. 84 (2000) 2513.
[2] J. X. Zhang et al., Nano Lett. 13 (2013) 5808.
[3] J. X. Zhang et al., Nat. Commun. 6 (2015) 10067.
[4] D. Gammon et al., Phys. Rev. Lett. 76 (1996) 3005.
[5] M. Gong et al., Phys. Rev. B 89 (2014) 205312.

Funding: DFG FOR 1713, Volkswagen Foundation I/84072, Fellowships funded by the China Scholarship Council: Y. Yin.; BMBF QuaHL-Rep project, No. 01BQ1032 and No. 01BQ1034; Q.Com-H project, No. 16KIS0106; The European Union Seventh Framework Programme 209 (FP7/2007-2013) under Grant Agreement No. 601126 210 (HANAS); China Scholarship Council (CSC, No. 2010601008); DFG SPP 1599

Cooperations: J. Wildmann; R. Trotta; D. Hube; A. Rastelli; Institute of Semiconductor and Solid State Physics, Johannes Kepler University Linz, Austria; Fraunhofer IKTS Dresden, IAPP at TU Dresden, IBM Research Zurich/Switzerland

Research Topic 3.3

Functional molecular nanostructures and interfaces

Authors: F. Roth, M. Nohr, S. Hampel, B. Mahns, M. Knupfer, N. Samoylova, P. Machata, M. Zalibera, K. Junghans, A. Popov
Responsible Directors: B. Büchner, T. Gemming, O. G. Schmidt

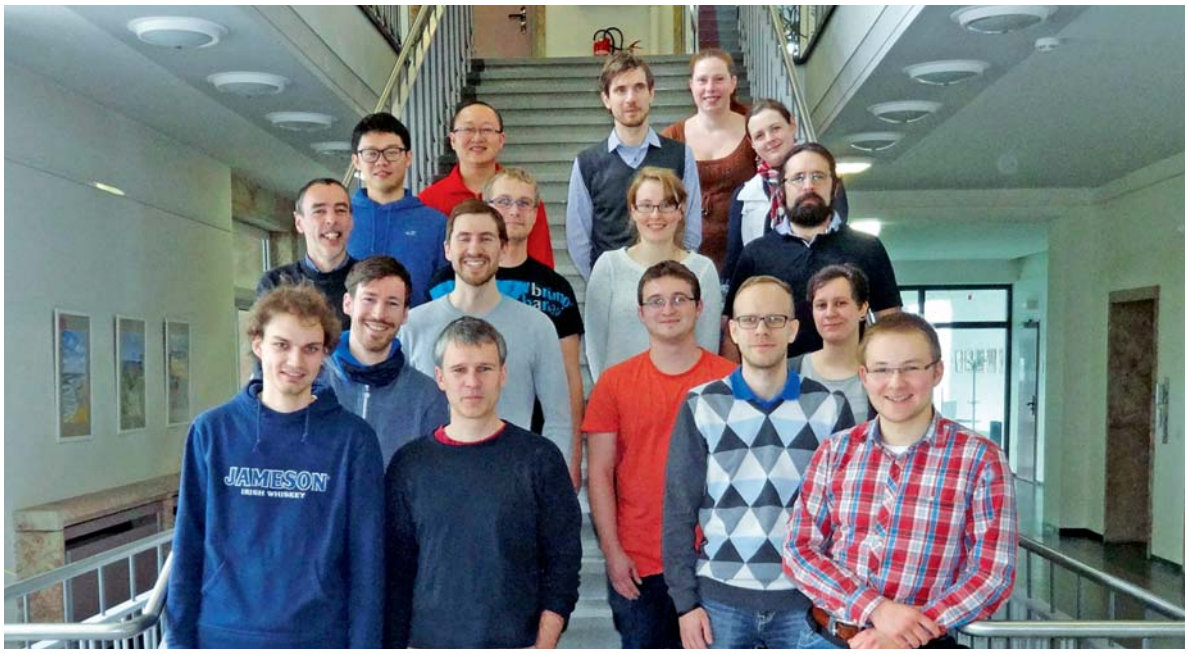

Abstract: Molecules and molecular solids characterized by π-derived electronic states are in the particular focus of research activities world-wide. The research activities in the IFW Dresden presently focus on the investigation of electronic properties of particular members of this large class of materials: endohedral metallofullerenes and organic semiconductors. We study these systems with a variety of techniques to provide a thorough understanding of their physical behavior. In the following we present selected results that have been achieved in the field recently.

Low energy exciton pocket at finite momentum in tetracene molecular solids

The excited state dynamics in organic semiconductors plays an important role for many processes associated with light absorption and emission. We have studied the momentum dependence of the lowest singlet excitons in tetracene molecular solids, an archetype system for other organic semiconductors [1]. Excitons are bound electron-hole pairs, and the character and dynamics of excitons are decisive for the photophysical behavior of the respective materials, also in view of potential applications in organic electronic devices [2].

We have applied electron energy-loss spectroscopy (EELS) in transmission [3] to obtain a comprehensive picture of the singlet exciton dispersion in tetracene along fundamental reciprocal lattice vectors at low temperature. Such studies require high quality single crystals of the materials under investigation, which have been grown in-house using physical vapor transport in an inert gas stream [4]. To illustrate our spectroscopic results, we show in Fig. 1 the excitation spectra of tetracene along the reciprocal lattice direction a*. Figure 1 summarizes selected excitation spectra in the left panel, and the full energy-momentum behavior (i.e. the dispersion) of the excitons in tetracene in the right panel.

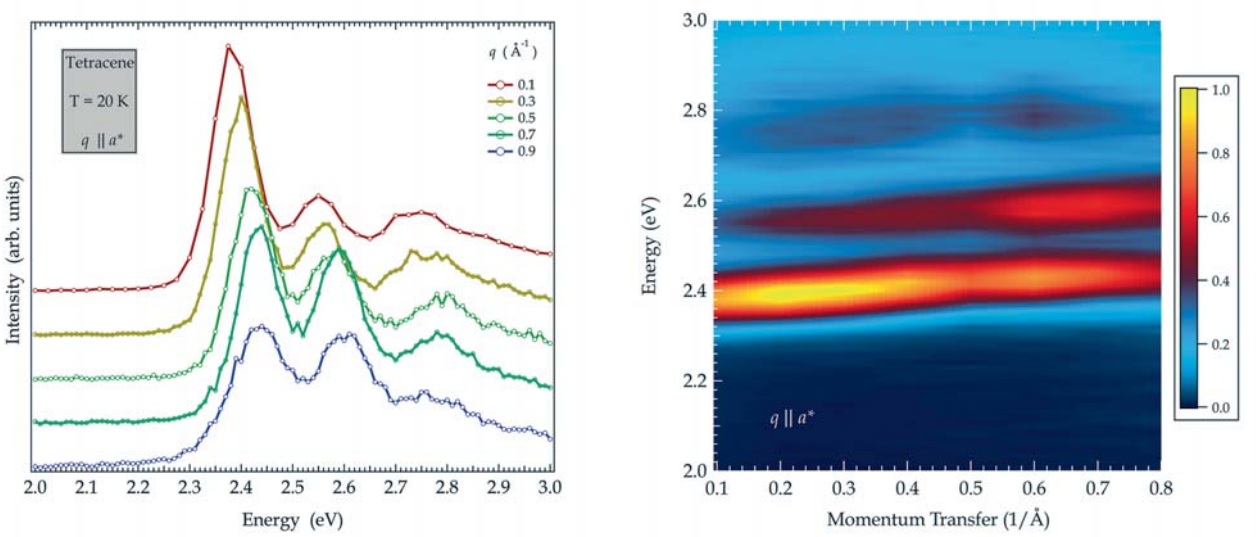

Fig. 1: Electronic excitation spectra of tetracene at low temperature (20 K) as a function of momentum transfer along the reciprocal lattice direction a* as obtained using EELS.

The excitation feature at lowest energy in the left panel of Fig. 1 represents the excitons in tetracene that have been studied in our work. The data clearly demonstrate that the lowest singlet exciton is characterized by a strong momentum dependence as it shifts to higher energies with increasing momentum. A strong dispersion has also been observed for other directions within the a*, b* reciprocal lattice plane.

The analysis of the exciton band structure along the two fundamental directions a* and b* is summarized in Fig. 2.

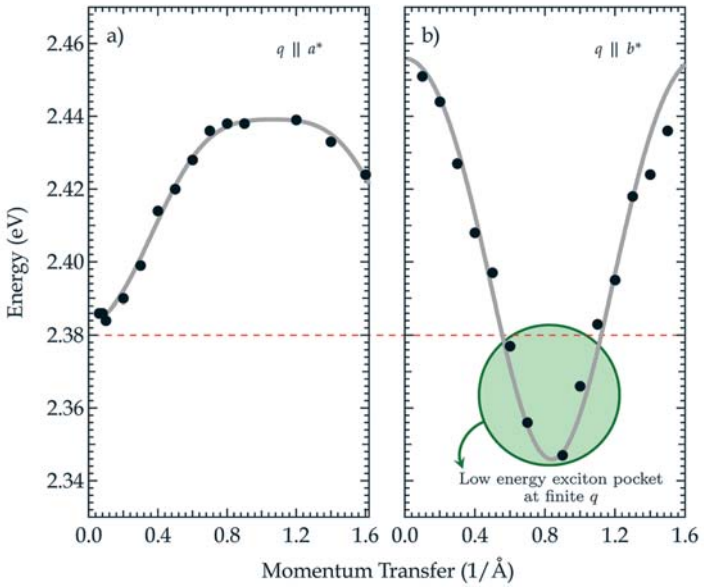

Fig. 2: Band structure of the energetically lowest (singlet) excitons in tetracene parallel to the two fundamental reciprocal lattice directions a* and b*. The gray lines are intended as a guide to the eye. The green shaded area denotes the low energy exciton pocket observed for momentum transfers along the b* direction.

Our data in Fig. 2 reveal a surprising new observation - the exciton for momentum transfers (q) along the b* direction arrives at an energy lower than the lowest excitation energy at very small momentum values (q ~ 0 $Å^{-1}$). The formation of a low energy exciton pocket as indicated in Fig. 2 can have important consequences for the photophysical behavior of tetracene. Excitations at higher energy might be able to relax into this pocket from where they cannot decay radiatively any more in a direct process due to momentum conservation. This would quench part of the fast photoluminescence and might be responsible for the differences between the behavior of tetracene and its close relative pentacene. In particular, in view of singlet fission as a process to generate multiple excitons and to achieve high efficient organic photovoltaic cells a momentum dependence of the excitons as revealed in Fig. 2 might be a disadvantage, since the relaxation into the low energy pockets can compete to the fission process. Our results emphasize the general importance of the exciton band structure for a thorough understanding of the photophysical behavior of organic semiconductors.

Crystal growth and charge transfer properties of new coronene charge transfer complexes

A revival of interest in organic charge-transfer (CT) systems in the last years is predominantly caused by their new applications in molecular electronics. A theoretical analysis of the charge transport performed for a series of CT mixed crystals revealed that the transfer integral can be much larger than in the best single-component semiconductors. A typical two-component charge-transfer complex consists of an electron-donor and electron-acceptor molecule, respectively. These partner molecules should have matching boundary orbitals and complementary spatial shapes to provide effective interaction and ordered structure. We have successfully grown high quality single crystals of novel charge transfer compounds based on coronene, a model system close to organic semiconductors, and F_4-TCNQ, a very strong electron acceptor [5]. These crystals have been obtained using physical vapor transport in closed quartz ampoules. Moreover, they have been thoroughly characterized by a number of methods, among them x-ray crystallography, IR-spectroscopy and electrochemistry.

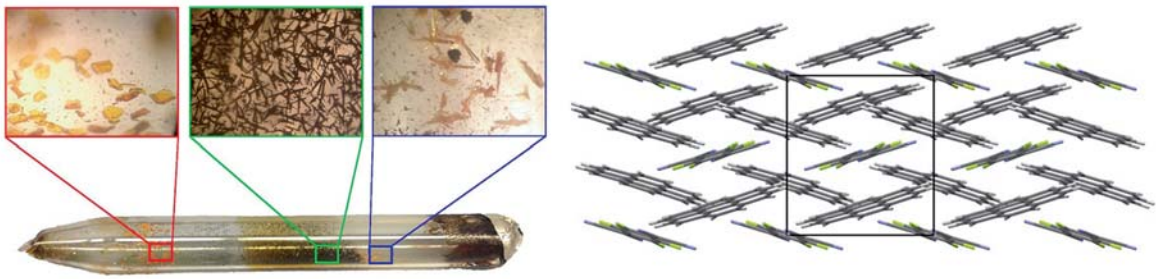

Fig. 3: Left panel: Quartz ampoule after growth procedure. The insets show a detailed view of the obtained crystals of pure coronene **(right)**, pure F_4-TCNQ **(left)** and coronene/F_4-TCNQ charge transfer crystals (2:1) **(middle)**.
Right panel: Fragments of crystal packing showing herring-bone packing in (Coronene)$_2$(F_4-TCNQ) crystals.

In Fig. 3, we show the result of the crystal growth in the ampoules as well as a fraction of the crystal structure of the novel charge transfer compound (Coronene)$_2$(F_4-TCNQ). These crystals demonstrate that novel charge transfer compounds based on polycyclic aromatic hydrocarbons can be grown with the prospect of new and interesting physical properties.

Selective synthesis of new family of endohedral fullerenes and charge transfer properties

Broad applications of endohedral metallofullerenes (EMFs) are still limited by the fact that their yield in the arc-discharge synthesis is only a fraction of that of empty fullerenes [6]. With this respect, development of the synthetic procedures aiming at improved selectivity and hence simplified work-up procedures are in focus of endohedral fullerene research. Recently, we have discovered a new type of endohedral metallofullerenes with the central carbon atom and a double Ti = C bond [7]. The first member of the family had the formulae $Lu_2TiC@C_{80}$ and its structure was unambiguously characterized by single crystal X-ray diffraction. In on-going efforts to increase the yield of such EMFs, we have found that the use of methane as a reactive gas in the arc-discharge process dramatically improves selectivity of the synthesis. The whole family of $M_2TiC@C_{80}$ carbide clusterfullerenes (M = Y, Nd, Gd, Dy, Er, Lu) has been synthesized as the main EMF products, whose isolation from the fullerene mixtures was then accomplished in a single chromatographic step (usually multistep chromatographic separation is required for such EMFs) [8].

Due to the predominant localization of the LUMO on the Ti atom, $M_2TiC@C_{80}$ clusterfullerenes have specific redox properties: the reduction of the compound changes the valence state of the endohedral Ti ion, whereas the fullerene cage serves as an electron- transparent "container". Interestingly, in spite of predominant localization of the LUMO on Ti, reduction potential of $M_2TiC@C_{80}$ exhibits pronounced dependence on the

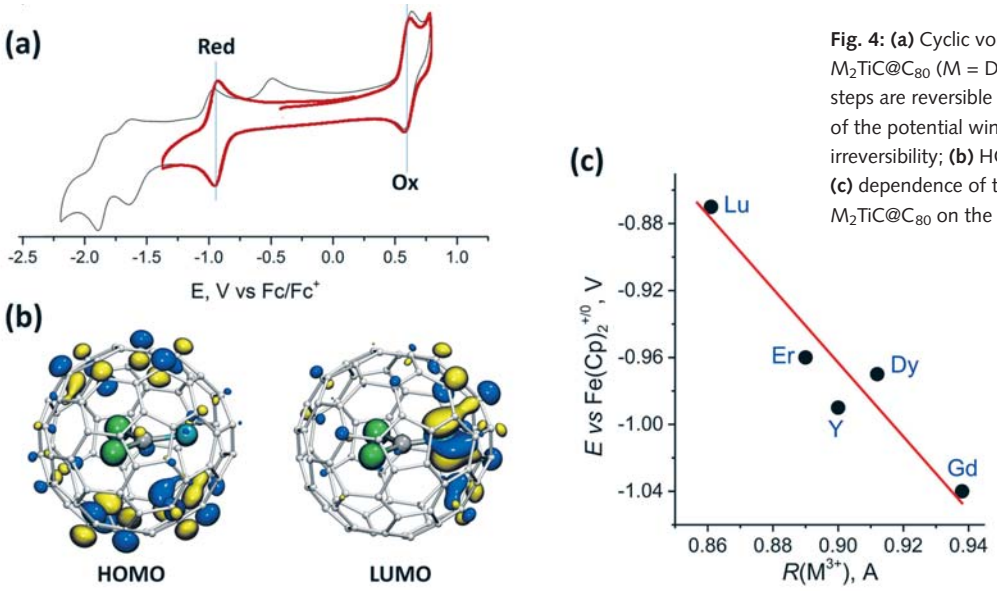

Fig. 4: (a) Cyclic voltammetry curve of the representative $M_2TiC@C_{80}$ (M = Dy): the first reduction and oxidation steps are reversible (thick red curve), whereas increase of the potential window in the kathodic range results in irreversibility; **(b)** HOMO and LUMO of $M_2TiC@C_{80}$; **(c)** dependence of the first reduction potential of $M_2TiC@C_{80}$ on the ionic radius of M^{3+}.

ionic size of the lanthanide (Fig. 4). The reason for such behaviour is in the increase of the ionic radius of Ti from 0.61 Å in Ti^{4+} (neutral $M_2TiC@C_{80}$) to 0.67 Å in Ti^{3+} (anion $M_2TiC@C_{80}^-$). As a result, the endohedral cluster becomes more strained and hence higher energy (more negative potential) is required to reduce the $M_2TiC@C_{80}$ containing larger lanthanides. At the same time, all $M_2TiC@C_{80}$ compounds exhibit almost identical oxidation potential assigned to the cage-localized HOMO.

Spectroelectrochemical study of the unconventional redox behaviour of perfluoroalkylated fullerene

Functionalization with electron-withdrawing groups, such as fluorine or perfluoralkyl radicals, is one of the common methods to increase an electron affinity and improve n-type properties of organic semiconductors. Perfluoroalkylated fullerenes, showing broad tunability of the electron accepting properties in dependence on the number of added CF_3 groups and their distribution on the fullerene surface, is one of the prominent examples [9]. Electrochemistry is a common tool to characterize electron accepting properties of molecular organic materials, whereas spectroelectrochemistry, the combination of in situ spectroscopy and electrochemistry, is a versatile tool in elucidation of redox mechanisms. In this work we studied the mechanism of the electrochemical reduction of the most abundant isomer of $C_{70}(CF_3)_{10}$, which is a rare example a perfluoroalkylated fullerene exhibiting electro-chemically irreversible reduction [10].

Fig. 5: (a) cyclic voltammetry of $C_{70}(CF_3)_{10}$ with different scan rates (irreversible reduction at 5 mV/s and reversible at 500 V/s); **(b)** in situ NMR spectroelectrochemistry (upper curves are measured during reduction, bottom curves – during reoxidation; thick red curve corresponds to the pristine compound, and thick green curve – to the reduced state; arrows show change of the intensity); **(c)** conclusion on the redox mechanism at moderate scan rates: reversible dimerization of the mono-anion radical.

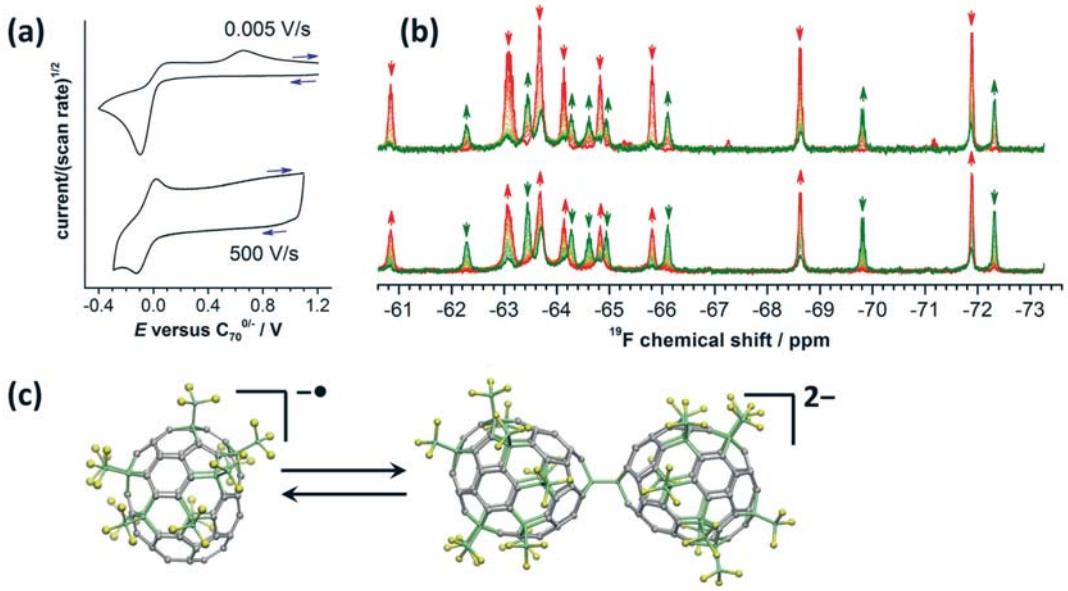

We showed that although reduction is irreversible at moderate scan rates, electrochemical reversibility is achieved at scan rates higher than 500 V/s (Fig. 5). This points to the follow-up chemical process following formation of the anion radical (so called EC mechanism). A plethora of spectroelectrochemical techniques was then applied to clarify the mechanism. Although *in situ* ESR spectroelectrochemistry proved formation of the ESR-active anion radical, quantitative ESR study showed that only a small fraction (less than 10 %) of the reduced $C_{70}(CF_3)_{10}$ is present in such form, whereas the rest of the compound is diamagnetic. To clarify the nature of the diamagnetic product, we developed and applied, for the first time, in situ ^{19}F NMR spectroelectrochemistry. This study showed that the reduced form of $C_{70}(CF_3)_{10}$ indeed exhibits the ^{19}F NMR spectrum typical for diamagnetic compounds, which is similar but still different from the spectrum of the neutral form. Detailed analysis of the spectrum proved that the number and positions of CF_3 groups are not changed upon electrochemical as well as chemical reduction. In combination with mass-spectrometry and DFT calculations, the spectroelectrochemical study revealed that the $C_{70}(CF_3)_{10}^-$ radical monoanion is in equilibrium with a singly-bonded diamagnetic dimeric dianion. The ^{19}F NMR spectroelectrochemistry developed in this work is shown to be a convenient and useful tool for studying redox reactions of fluorinated organic compounds.

[1] F. Roth et al., EPL 112, 37004 (2015)
[2] M. Pope, C.E. Swenberg, "Electronic Processes in Organic Crystals and Polymers", Oxford University Press, New York (1999)
[3] F. Roth et al., J. Electron Spectrosc. Relat. Phenom. 195, 85 (2014)
[4] M. Nohr, Bachelor Thesis (2012)
[5] O. Kataeva et al., Crystal Growth & Design, in press (2015)
[6] A. Popov et al., Chem. Rev. 113, 5989 (2013)
[7] A. Svitova et al., Nat. Commun. 5, 3568 (2014)
[8] K. Junghans et al. Angew. Chem. Int. Ed. 54, 13411 (2015)
[9] Boltalina et al. Chem. Rev. 115, 1051 (2015)
[10] Zalibera et al. Analyst 140, 7209 (2015)

Funding: Deutsche Forschungsgemeinschaft (DFG), European Research Council (ERC)

Cooperations: DESY Hamburg; A.E. Arbuzov Institute, Russian Academy of Sciences, Kazan; TU Bergakademie Freiberg; Kazan Federal University, Russia; Russian Academy of Sciences, Moscow

Research topic 4.1

Surface acoustic waves: Concepts, materials & applications

People: S. Biryukov, E. Brachmann, R. Brünig, A. Darinskii[1], C. Faust, T. Gemming, S. Harazim, V. Hoffmann, F. Kiebert, A. Kirchner, J. König, E. Lattner, G. Martin, S. Menzel, S. Oswald, G. K. Rane, H. Schmidt, M. Seifert, E. Smirnova[2], A. Sotnikov, M. Spindler, H. Turnow, U. Vogel, H. Wendrock, S. Wege, M. Weihnacht[3], R. Weser, A. Winkler
Responsible Directors: B. Büchner, K. Nielsch, T. Gemming, O. G. Schmidt

Abstract: The interdisciplinary research topic 4.1 on Surface Acoustic Waves (SAW) comprises the whole field of acoustoelectronics from fundamentals, e.g. effects of wave propagation, dynamic behavior of polar dielectrics and acoustofluidic interaction phenomena, to advanced applications with exploitation by innovation-oriented small and medium-sized enterprises. For the precision and lifetime of advanced SAW devices with increased temperature and power capability, incorporating piezoelectric substrates and thin film electrodes, material-related aspects are crucial. In 2015, the emphasis of this research topic was mainly put on i) emerging piezoelectric substrates, ii) appropriate electrode material systems and iii) SAW-driven microfluidics and aerosol generators.

i) Advanced piezoelectric substrate materials

Piezoelectric single crystals of the langasite (LGS) family are of current interest as very promising materials for microacoustic devices like bulk- and surface acoustic wave based sensors for harsh environments providing wireless interrogation as well as ID tag functionality. These crystals do not only survive at high temperatures and relevant gaseous atmosphere, but can be also operated in the extremely low (cryogenic) temperature range. Moreover, specific features of low temperature dielectric and elastic properties of LGS family materials are important for the basic understanding of the crystals' lattice dynamics.

Here, emerging piezoelectric single crystals from LGS family CTGS ($Ca_3TaGa_3Si_2O_{14}$) and SNGS ($Sr_3NbGa_3Si_2O_{14}$) as well as the parent material LGS ($La_3Ga_3SiO_{14}$) were characterized regarding their dielectric, elastic and piezoelectric properties in extra-wide

temperature range from 4.2 K to about 1173 K [1-4]. High precision measurements of acoustic wave velocities of longitudinal and shear bulk modes propagating in various crystallographic directions (X, Y, Z and Y ± 45°) allowed the precise derivation of the complete set of acoustic material constants including elastic and piezoelectric behavior as well as dielectric permittivity in an extra-wide temperature range. On the one hand a strong decrease of sound attenuation was found at cryogenic temperatures (Fig. 1a), while on the other hand, reasonably strong ultrasonic excitation using the 'internal' piezoelectric effect of the crystal was demonstrated as well. As for dielectric properties, it was shown for the first time that dielectric permittivity ε_{33} for CTGS and LGS crystals exhibit incipient (quantum) ferroelectric-like behavior (i.e. an increase with decreasing temperature followed by saturation at low temperatures, Fig. 1b) while SNGS demonstrates ordinary dielectric temperature dependence (i.e. dielectric permittivity decreases down to cryogenic temperatures).

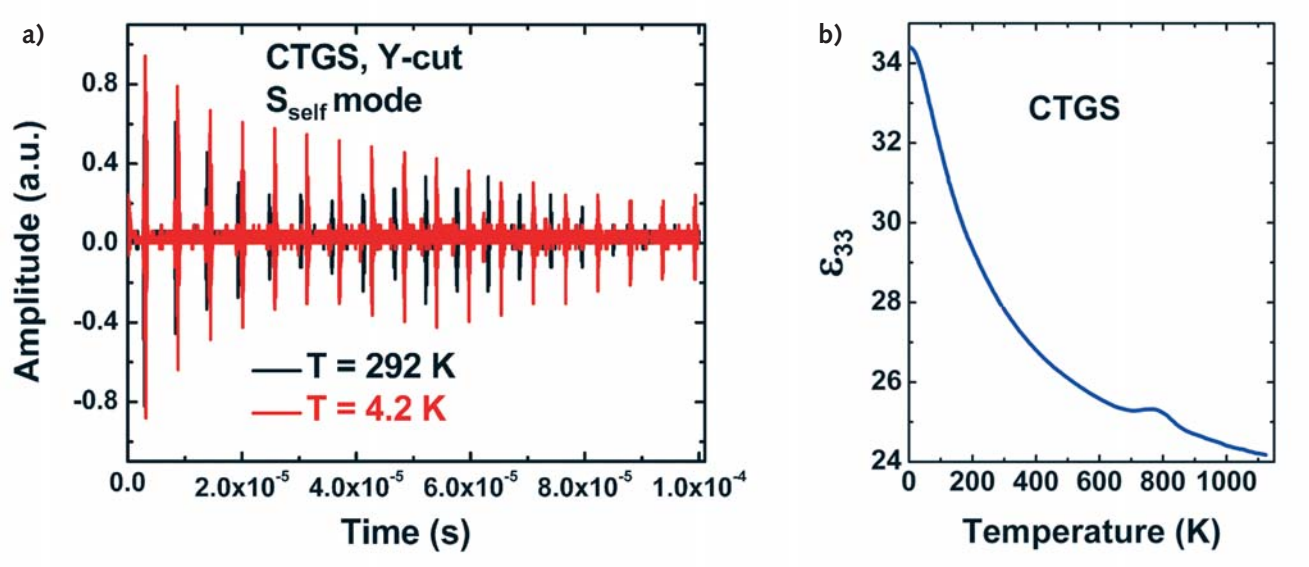

Fig. 1: a) Ultrasonic pulse-echo patterns for the shear mode propagating along Y crystallographic direction in CTGS single crystal at 292 K (black line) and at 4.2 K (red line); **b)** Temperature dependence of the dielectric permittivity e_{33} for CTGS single crystal in a wide temperature range starting at 4.2 K.

ii) Thin film electrode material systems with high thermal stability

At high operation temperatures, thin film electrodes of interdigital transducers undergo rapid degradation due to agglomeration, delamination or chemical interaction with the environment and the surrounding materials. Due to favorable properties including high-melting points (>2000 °C) as well as relatively low electrical resistivity (<50 µΩcm), metallization systems based on RuAl, W/Mo and TiAl including dedicated covering layers seem to be well suited for devices operating under these conditions and can be deposited as thin films via magnetron sputtering or electron-beam evaporation. The high temperature stability translates to minimal creep-related damages, improved compliance of the coefficient of thermal expansion as well as reliable operation over many temperature cycles.

In order to obtain a better understanding of the microstructure of the film-substrate composite under thermal treatment, chosen metallization systems deposited on high-temperature stable piezoelectric substrates LGS and CTGS have been studied up to a temperature of 800 °C. Thereby, different materials characterization techniques such as X-ray diffraction and reflectivity measurements, scanning and transmission electron microscopy (TEM), Auger electron spectroscopy and atomic force microscopy were carried out. Our studies reveal the stability of highly conductive W/Mo films on CTGS up to 800 °C under vacuum [5]. For LGS substrates, a diffusion barrier layer like sputtered alumina is required due to the inherent instability of the substrate with respect to Ga/O diffusion under vacuum annealing. Besides deposition, also structuring of the tungsten based interdigital transducer electrodes has been successfully performed using a wet-chemical etching process.

The material system RuAl was extensively studied during the last year. To inhibit the observed oxidation of RuAl on LGS and CTGS substrates after annealing in high vacuum at 800 °C for 10 h [6, 7], several possible barrier layer systems (SiO_2, Al_2O_3 and W) with thicknesses of 10 and 100 nm have been investigated. The heat treatment at 800 °C under high vacuum conditions showed a strong dependence of the RuAl film quality on the thickness and the material of the barrier layer. TEM investigation (Fig. 2) on the Al_2O_3 barrier system for 110 nm RuAl films on LGS prove that oxidation from the substrate side can be minimized using a thin SiO_2 barrier layer. In contrast to this, Al_2O_3 barrier layers do not sufficiently hinder the oxidation from the substrate side and a complete demixing into Al_2O_3 and Ru takes place. Thin W barrier layers, however, are strongly stressed and exhibit cracks after heat treatment, which makes them unsuitable as oxidation barriers, while thicker barriers are stable. Additional investigations were carried out to reduce oxidation of RuAl films via pre-annealing of the LGS substrates. For this, substrates were heated to 800 °C under high vacuum conditions, analyzed and subsequently coated with RuAl alloy films. A severe degradation of the LGS substrates was observed due to formation of cracks and a system of channels below the substrate surface, leading to enhanced outward diffusion of Ga [8].

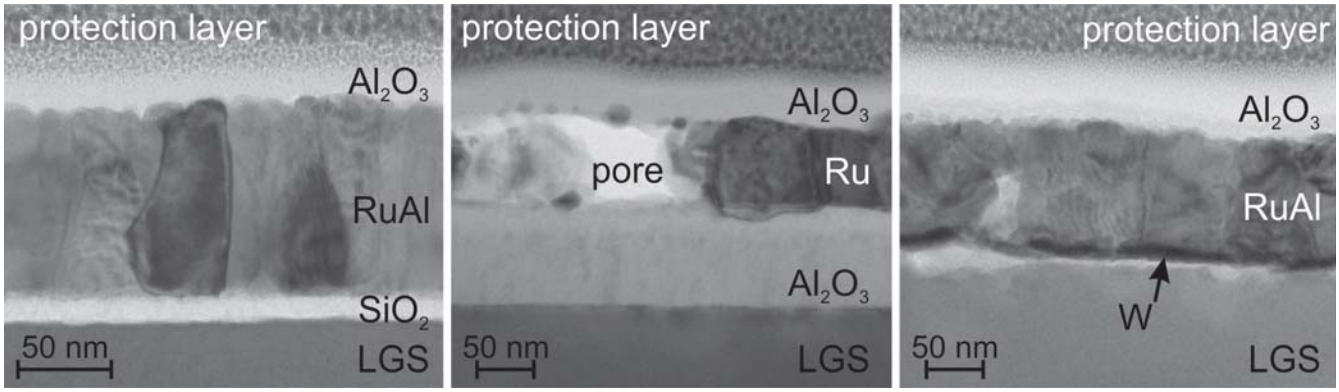

Fig. 2: TEM images of RuAl films on LGS with various barrier layers (SiO_2, Al_2O_3, W with thickness of 10 nm) after heat treatment at 800 °C for 10 h under high vacuum (protection layer used for focused ion beam analysis).

iii) Acoustofluidic fundamentals and applications

Microacoustic actuators enable the noninvasive manipulation of fluids in microfluidic vessels, whereby these fluids can additionally be loaded with particles or cells. Because of their small dimensions in combination with a high power density, SAW-based acoustic actuators are especially well suited for microfluidic applications like fluid mixing at low Reynolds numbers and acoustic tweezers. However, for designing an optimal acoustofluidic setup it is mandatory to choose proper operating parameters, e.g. the acoustic wavelength, geometric dimensions and surrounding material of the fluid reservoir. In order to ensure a comprehensive understanding of the acoustic and acoustofluidic interactions, investigations of involved physical phenomena were carried out via simulations and accompanying experiments (Fig. 3a) [9-11].

Furthermore, SAWs can be utilized to generate aerosols with micrometer-sized droplets without any moving parts or nozzles. As SAW chips show great potential for on-chip integration and can lead to an economic production of hand-held and even disposable devices, this technique could find versatile fields of applications including medical inhalators, thin film deposition systems, olfactory sources and mass-spectrometry. In order to exploit the full potential of SAW fluid atomization technique, a new approach for reliable and cost-effective mass-scale manufacturing of SAW atomizer chips with on-chip integrated fluid supply was developed [12]. Using this technique, a precise and stable fluid atomization with almost ideal aerosol plume geometry (Fig. 3b) and the *in-situ* alteration of the droplet size distribution can be achieved. Furthermore, an innovative thin film deposition method based on the SAW atomization principle [13] was developed.

This method can be divided into three subsequent steps: In a first step, high frequency surface acoustic waves atomize a metalorganic precursor solution (sol) into an ultra-fine aerosol. In a second step, the aerosol condensates on the substrate surface which is, in a third step, pyrolized into a crystalline thin film. The technique was demonstrated for the deposition of $La_2Zr_2O_7$ buffer layers on biaxial textured Ni5%W tapes, but is generally relevant for the deposition of other oxides. Aerosols with median droplet diameters of 4 and 7.5 µm were produced from Lanthanum/Zirconium precursor solutions based on propionic acid or water, respectively. X-ray diffraction studies of the crystallized films with a thickness of about 100 nm show a high crystalline quality with a strong (001)-orientation.

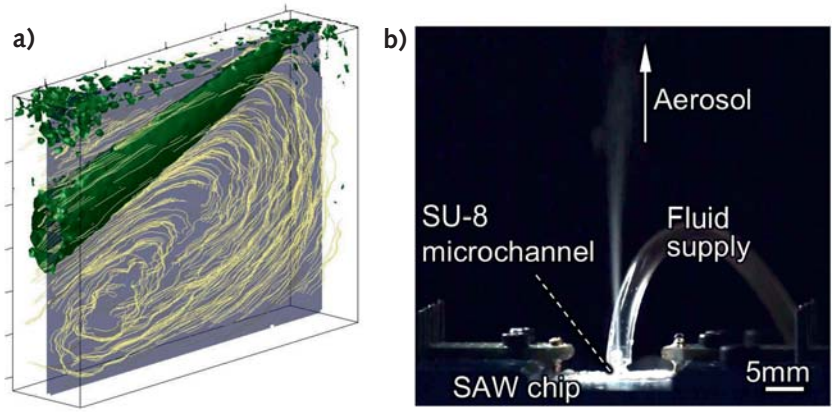

Fig. 3: a) Volumetric measurement of acoustic streaming in water induced by surface acoustic waves, yellow traces show particle trajectories obtained via particle image velocimetry, green zone (lobe) shows the area of maximum fluid velocity; **b)** Side view on SAW-based fluid atomization

[1] A.V. Sotnikov et.al., Phys. Solid State, 57 (2015), 1183.
[2] E. Smirnova et al., J. Phys. Chem. Solids, 85 (2015), 91.
[3] A. Sotnikov et. al., Proc. 2015 IEEE Int. Freq. Contr. Symp. (2015) 106.
[4] E.P. Smirnova et. al., Phys. Solid State, 57 (2015), 2241.
[5] G. K. Rane et al., Mater. Sci. Eng. B 202 (2015) 31.
[6] M. Seifert et al., Mater. Res. Express 2 (2015) 085001.
[7] M. Seifert et al., J. Alloys Compd. 664 (2016) 510.
[8] M. Seifert et al, Materials 8 (2015) 8868.
[9] A. N. Darinskii et al., Ultrasonics 56 (2015) 318.
[10] U. Vogel et al., Comsol Conf., Grenoble (2015) 29981.
[11] F. Kiebert et al., Phys. Proc. 70 (2015) 25.
[12] A. Winkler et al., Lab Chip 18, (2015) 3793.
[13] A. Winkler et al., J. Sol-Gel Sci. and Techn., (2015).

Funding: BMBF InnoProfile-Transfer (03IPT610A MiMi, 03IPT610Y HoBelAB), DFG (WI 4140/2-1, SO 1085/2-1), Vectron International, Creavac, SAW Components Dresden, Joint Initiative for Research and Innovation (SAW-2014-IFW-1)

Cooperations: TU Bergakademie Freiberg; BTU Cottbus; TU Dresden; Fraunhofer IPMS/CNT; [1]Institute for Crystallography RAS, Moscow, Russia; [2]Ioffe Physical Technical Institute RAS, St. Petersburg, Russia; Slovak University of Technology Bratislava, Slovakia; *Industry:* BelektroniG; Creavac; [3]InnoXacs; MLE Dresden; Prolatec; SAW Components Dresden; Sensortechnik Meinsberg; TSI; Vectron International

Research Topic 4.2

Materials for biomedical applications

People: M. Calin, A. Gebert, M. Guix, S. Hampel, F. Hebenstreit, V. Magdanz, M. Medina-Sánchez, A. K. Meyer, L. Schwarz, S. Weiz, H. Xu,
Responsible Directors: B. Büchner, T. Gemming, O. G. Schmidt

Abstract: Over the past few years, novel materials have drawn interest for use in various biomedical applications such as biosensing, dentistry, tissue engineering and therapeutics. This has resulted in a better understanding of the interactions between materials and biological entities, from the macro to the nanometric scale. At the IFW, interdisciplinary groups have dedicated numerous efforts to the development of new materials that exhibit particular properties (i.e. magnetism, superconductivity, low elastic modulus, excellent corrosion resistance, etc.) and applied them for diagnosis, targeted drug delivery, tissue regeneration and reproduction. The use of such materials represented a great progress in their respective fields in terms of biocompatibility, unique functionalities and ultra-sensitivity. One highlight topic of IFW is the project: 'Spermbots', a new type of hybrid micromotors that could help women trying to conceive. The important innovation of such micromotors is that they could be applied for *in vivo* fertilization, decreasing the risk of failure by preserving the natural microenvironment in which sperm and oocyte come together.

Artificially motorized sperm cells

Miniaturized vehicles that perform tasks and interact with living cells inside the human body appears to be one of the 20th century dreams that today's engineers finally become ready to tackle. In recent years, numerous approaches have emerged from various labs to employ such micromotors that can be powered and controlled on a scale that allows them to assist or interfere with cellular processes [1–3]. Most of these micromotors are directly inspired by their natural counterparts which are, for example, flagella or cilia of living microorganisms [4, 5]. These nature-approved propulsion strategies were mimicked successfully with the help of external power sources like electric or magnetic fields, ultrasound, light, or chemical fuels [6–8]. However, to carry out tasks in the complex surroundings of living cells requires more than just miniaturized motion alone. Active transport of microscopic cargo should be reasonably fast, and complex microcarrier movements should be directly controllable both spatially and chronologically. In

addition to these micro-engineering aspects, the operation in biologically active environments brings about a whole new set of problems that involves interactions with living matter that mostly happen on the nanoscale. Biocompatibility in this case not only means that the synthetic microcarrier must not be toxic to cells, but also implies that the microcarrier has to actively take part in cellular and biomolecular interactions in order to fulfill its task as biosensor, drug distributor, or micro-surgeon.

In our group, so-called 'Spermbots', have been introduced as a novel type of hybrid micromotor. Specifically, a spermatozoon was coupled to a ferromagnetic microtube as on-board power supply. The external magnetic field allows remote control while the sperm tail provides propulsion [9, 10]. This approach has opened up novel applications for micromotors such as new alternatives for assisted reproduction biology and related medical and fundamental studies [11].

The state-of-the-art of assisted reproduction methods involve artificial insemination, which is a relatively low-cost technique that has a limited success rate together with additional limitations such as the sperm motility requirement and obstacles in the female reproductive tract that sperms have to face. Moreover, in vitro fertilization and intracytoplasmic sperm injection have been widely used because of their effectiveness, when conventional methods like surgery or medication failed. However, these are complicated methods that require several steps, including hormones injection to initiate oocyte maturation, followed by their extraction from the body, fertilization in a petri dish, cultivation of embryos, and their reimplantation into the uterus. All these steps add to the stress that cells suffer along the procedure decrease the chance of conception.

'Spermbots' established a new approach that could be implemented for *in vivo* fertilization. Previous works have been focused on the use of microtubes made by rolled-up nanomembranes, which are coupled to motile sperm cells, serving as a guiding element to bring the sperm to the egg location in its natural state. To further this approach, we employ magnetic microhelices for active transportation of a sperm cell to the oocyte with the goal of fertilization. We show the capture and transportation of immotile, but otherwise functional, sperms [12, 13] to the oocyte by coupling them to artificial helical micromotors that can be actuated by rotating magnetic fields (see Fig. 1). Artificial propulsion of immotile sperms has potential for use in reproduction, because poor sperm motility is one of the major causes for male infertility, and despite numerous innovations in the field of assisted reproductive technology, can still not be countered in a satisfactory way [14, 15].

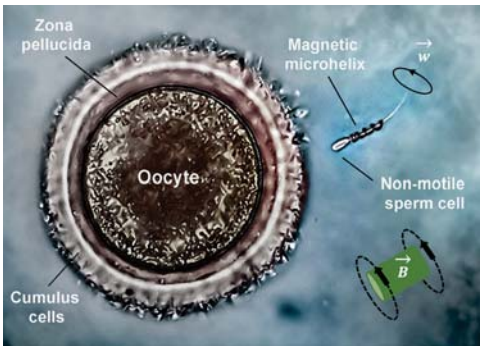

Fig. 1: An immotile sperm is captured by a remotely controlled magnetic helix and delivered to the oocyte for fertilization.

We have chosen magnetic helices as micromotors because of their relatively simple mechanism of motion that is widely understood and easy to control in 3D by a common setup of axial pairs of Helmholtz coils that create a rotating magnetic field. This control and actuation method is biocompatible [16, 17], which is crucial for its potential in *in vivo* applications.

We report the fabrication of polymer microhelices by direct laser writing [18], with soft-magnetic Ni/Ti bilayer coatings, which show controllable 3D motion with speeds comparable to fast microorganisms like sperms (up to 70 µm/s), under the influence of rotating magnetic fields that are generated by a customized set of Helmholtz coils. These microhelices are shown to be able to capture, transport, and release single live sperm cells under physiological conditions (in sperm medium with adapted viscosity and temperature). Successful delivery of sperm cells to the oocyte cell wall, in order to fertilize, was achieved. However, for successful *in vitro* fertilization further challenges to have the optimal experimental conditions should be addressed.

In order to use sperm-microhelix hybrid swimmers as a tool for assisted fertilization with immotile sperms requires proper means of sperm selection to distinguish immotile, but otherwise healthy, from completely infertile sperm cells. We chose the Hypoosmotic swelling test (HOS) for this purpose since it is a well-established method to indicate viable sperm cells without damaging them. HOS method is also reversible, which means that the sperm cell can return to its original state by changing the osmolarity of the surrounding media [19]. Swelled sperms in HOS medium and how the swelled tails correspond well to cell viability are shown in Fig. 2(a). Figure 2(b) shows the same for membrane integrity (blue = intact, green = damaged). As a side note, the partial curling of swelled sperm tails also facilitates sperm coupling significantly.

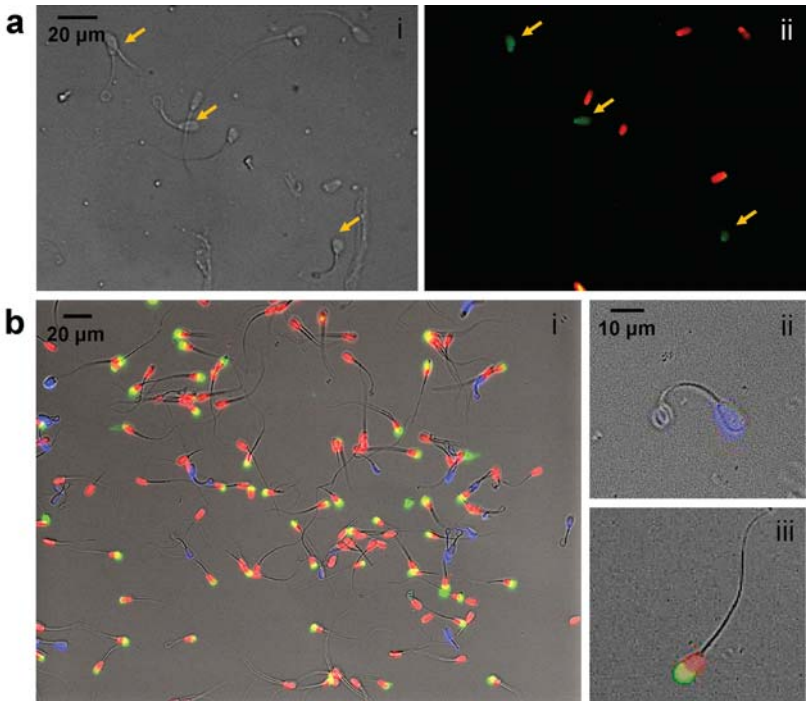

Fig. 2: Hypoosmotic swelling test (HOS), **a)** green: live sperm, red: dead sperm, **b)** blue: intact acrosome, green: defect acrosome, red: dead sperm.

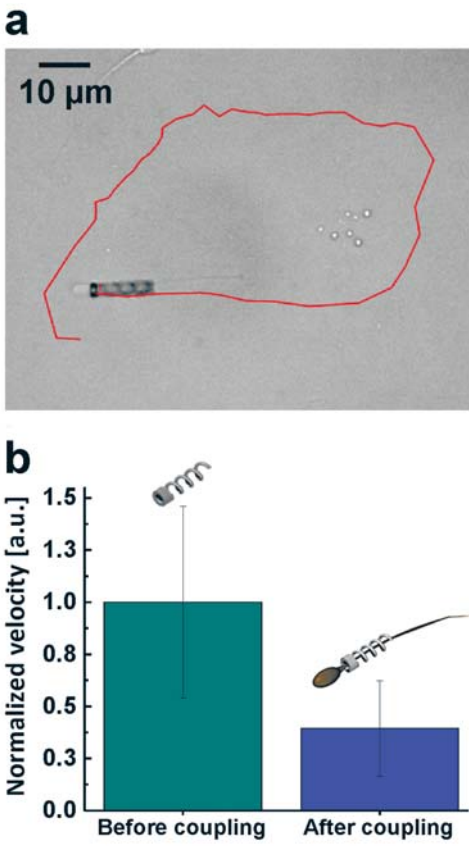

Fig. 3: a) Trajectory of a steered microhelix transporting a sperm cell over 18 sec, **b)** Velocity before and after coupling.

A sperm cell is successfully captured when its tail is confined inside the cylindrical lumen of the microhelix, while its head sticks out at the front end of the helix and is loosely bound by the front ring that acts like a noose to prevent the sperm head from slipping back through the helix (see Fig. 3(a)). This coupling mechanism is considered to be the most efficient since it does not involve any sticking or piercing mechanisms that could damage the sperm cell, while it also doesn't impair the helical propulsion of the artificial microswimmer in terms of helix rotation and steerability. A severe impairment of the helix movement would result in a drastic speed decrease, as well as a loss of directionality, i.e. the ability of the helix to follow the directions given by the orientation of the rotating magnetic field. Figure 3(b) compares speeds before and after coupling of six different cases and reveals an average speed decrease of the hybrid microswimmers to ca. 39.4 % of the initial helix velocity, with a relative standard deviation of 23.2 %. Such deviation is attributed to the variability of differently swelled sperms and their influence on the lose coupling between sperm tail and microhelix.

As next step, transportation of an immotile sperm cell to the oocyte cell wall is also demonstrated with the helical micromotors. In Figure 4, the sperm delivery procedure is shown in different steps: i) coupling, ii) transportation, iii) oocyte approach, and iv) sperm release. Although the helix velocity decreased due to the cell load and the disturbance caused by the sperm tail, it was possible to transport the sperm towards the oocyte and release it once it adhered to the oocyte wall by inverting the helix rotation via reversal of the magnetic field rotation.

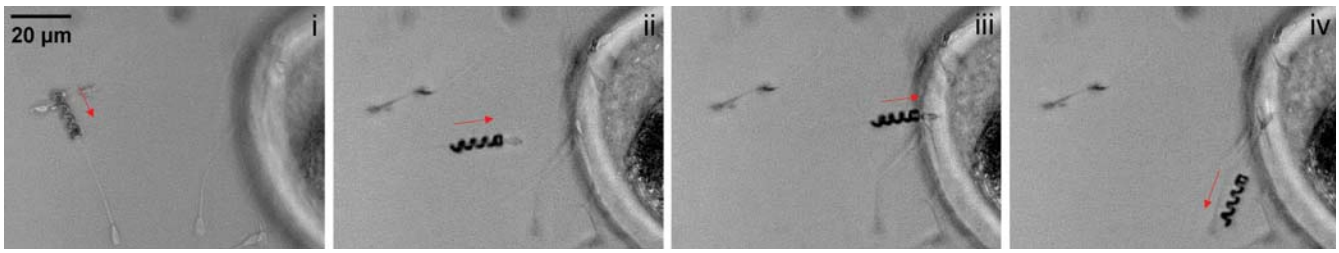

Fig. 4: Sperm cell coupling (i), transport (ii), approach to the oocyte membrane (iii), and release (iv).

We successfully fabricated biocompatible microhelices that can be actuated and controlled precisely in 3D by a customized Helmholtz coil set-up that generates a rotating magnetic field. We implemented these helices as microcarriers that can actively capture and transport single live sperm cells that would otherwise be immotile due to pathological defects. In order to set up an environment that would allow these artificially motorized sperm cells to fertilize an oocyte, we mimicked *in vivo* conditions and implemented hypoosmotic swelling as a method for sperm selection. Unfortunately, similar to many promising applications in biomedical engineering, it appears to be still a long way from artificially motorized sperm delivery to actual oocyte fertilization. There is a lot of future work to do, considering proper oocyte culturing, functionalization of helices to create important biochemical cues, and further improvement of targeted sperm capture and delivery, in order to achieve a critical rate of fertilization trials that would lead to successful *in vitro* fertilization. It remains to stress that, ultimately, the strength of this novel fertilization approach lies in its potential *in vivo* applicability, since it will not be necessary to explant (and re-implant) oocytes for artificial reproduction if we can target and fertilize the oocyte in its natural environment.

[1] K. E. Peyer, et al., Nanoscale (2013) 5
[2] Y. Man and E. Lauga, Phys. Fluids (2013) 25
[3] M. García, et al., Nanoscale (2013) 5
[4] A. W. Mahoney, et al., Appl. Phys. Lett. (2014) 104
[5] K. I. Morozov and A. M. Leshansky, Nanoscale (2014) 6
[6] M. Guix, et al., Chem. Rev. (2013) 114
[7] L. Zhang, et al., J.Appl. Phys. Lett. (2009) 94
[8] J. J. Abbott, et al., Int. J. Rob. Res. (2009) 28
[9] V. Magdanz, et al., Adv. Mater. (2013) 25
[10] V. Magdanz, et al., Adv. Funct. Mater. (2015) 25
[11] V. Magdanz, et al., Expert. Opin. Drug. Deliv. (2014) 11
[12] R. Nuñez-Calonge, et al., ISRN Urol. (2012)
[13] M. Nijs, et al., Hum. Reprod. (1996) 11
[14] C. Ortega, et al., Hum. Reprod. Update (2011) 17
[15] Z.P. Nagy, et al., Hum. Reprod. (1995) 10
[16] M. Feychting. Prog. Biophys. Mol. Biol. (2005) 87
[17] F. G. Shellock, and J. V. Crues, Radiology (2004) 232
[18] www.nanoscribe.de, Nanoscribe GmbH 2007–2015.
[19] C.B. Smikle, and P. J. Turek, Mol. Reprod. Dev. (1997) 47

Summarized version of the already published manuscript: M. Medina-Sánchez, et al., Nano Lett. (2015). DOI: 10.1021/acs.nanolett.5b04221

Cooperation: Dr. Jakop and Dr. Schön, Reproductive Cell Biology Unit at the Leibniz Institute for Animal Biology in Dummerstorf, IZW Berlin

Research topic 4.3

High strength materials / Leibniz Application Laboratory Amorphous Metals

People: B. Bartusch, S. Donath, J. Eckert, B. Escher, J. Freudenberger, M. Frey, A. Gebert, N. Geißler, P. F. Gostin, T. Gustmann, J. Hufenbach, S. Horn, R. Keller, H. Klauß, E. Knauer, K. Kosiba, U. Kühn, H. Merker, C. Mix, S. Neumann, S. Pauly, K. Gokuldoss Prashanth, J. Sander, K. Schröder, N. Schädlich, H. Schwab, S. Scudino, D. Seifert, F. Silze, M. Stoica, B. A. Sun, H.-P. Trinks, M. Uhlemann, Z. Wang, H. Wendrock, T. Wolf, J. Zeisig
Responsible Directors: K. Nielsch, T. Gemming, O. G. Schmidt

Abstract: The increasing demand of industry for equipment (tools, devices, machine parts, accessories etc.) with excellent durability under extreme loading conditions promotes the development of innovative materials possessing e.g. high strength, hardness, wear resistance, ductility and corrosion resistance. The basic idea is to transfer sophisticated technologies combined with specific newly developed materials towards industry. Besides the large variety of materials under investigation in this research area, the present report focusses on high strength lightweight hybrid structures, and new filler materials based on FeCrMoVC as well as Cu-Ag40-Ga10.

Hybrid nanostructured Aluminum alloy with unprecedented strength

Methods to strengthen aluminum alloys have been employed since the discovery of the age-hardening phenomenon in 1901. The upper strength limit of bulk Al alloys is ~0.7 GPa by conventional precipitation strengthening and increases to >1 GPa through grain refinement and amorphization. Unfortunately, the non-equilibrium state and the limited thermal stability of nanostructured and amorphous Al alloys limit their use at high temperatures. In order to overcome these limitations, we have developed a microstructural strategy for the production of high-strength Al-based alloys with good thermal stability.

Our processing strategy [1] consists of three steps: gas atomization, ball milling and hot pressing. Gas atomization is used to produce the amorphous particulate precursor with composition Al84Ni7Gd6Co3 (Fig. 1a). The rapidly cooled small gas atomized particles are amorphous, whereas the slowly cooled large particles display minor amounts of crystalline phases. The powders are then treated by ball milling, which has the purpose to designedly vary the microstructure and the crystallization behavior of the amorphous precursor (Fig. 1b). Finally, the powders are consolidated into highly dense bulk

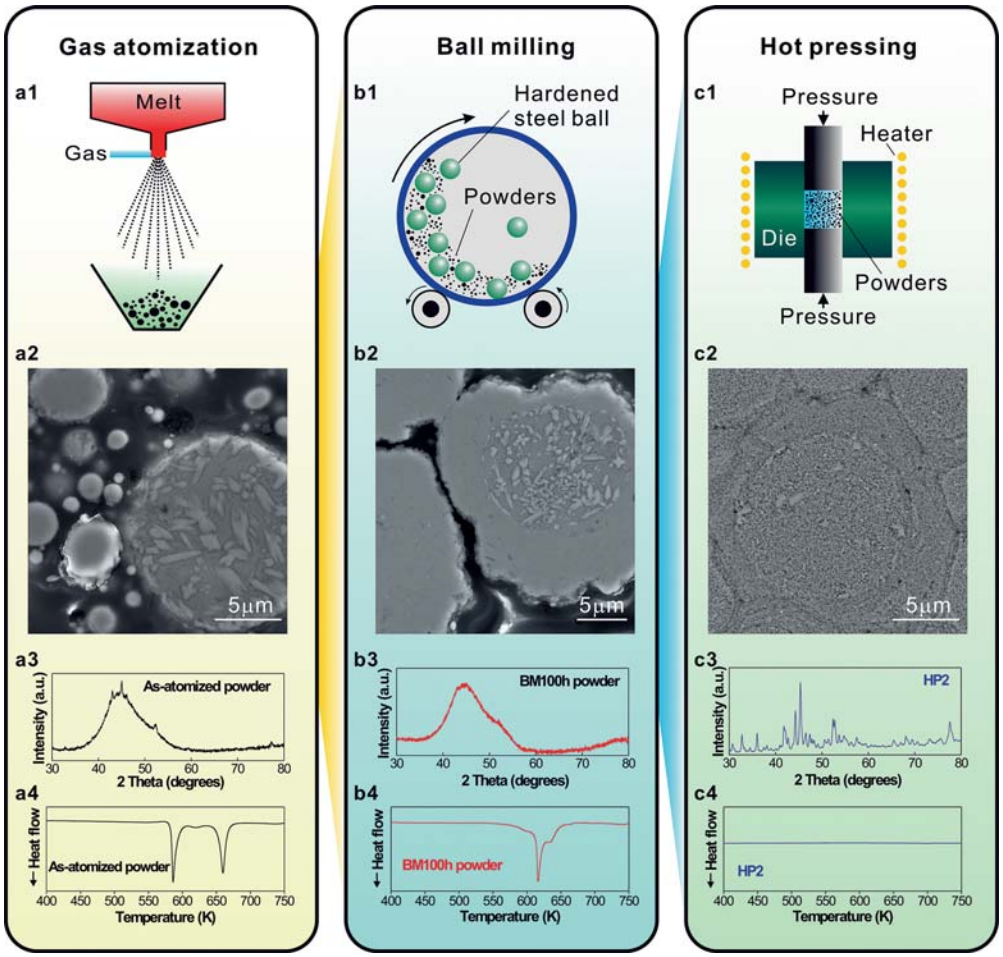

samples by hot pressing at a relatively high temperature, where the combined devitrification and consolidation of the amorphous particulate precursor take place (Fig. 1c).

The microstructure of the bulk samples clearly resembles the composite structure of the parent milled powder (compare Figs. 1b2 and 1c2) and consists of a bimodal-like microstructure with coarse and fine precipitates regions. At the nanoscale, the material exhibits hybrid structures composed of nanostructured fcc-Al and intermetallic compounds. Such a hybrid microstructure leads to high strength at both room and high temperatures along with large Young's modulus, which adds a new and promising region to the Ashby map of specific yield strength versus the specific Young's modulus (Fig. 2).

The basic principles for achieving such high strength are based on the composite structure and the effect of the mutual confinement between the nanosized phases. Confinement can effectively prevent the nanocrystalline fcc-Al and intermetallics from premature brittle fracture, thereby providing the possibility to deform plastically and to exhibit intrinsic strength rather than the flaw-controlled strength. The microstructural strategy can, in principle, be applicable to other materials and may thus provide a potential approach to developing high-performance hybrid materials.

Fig. 1: Processing of the Al84Ni7Gd6Co3 alloys: Gas atomization (a(1–4)), ball milling (b(1–4)) and hot pressing (c(1–4)). Schematic processing methods (a1, b1 and c1) and corresponding SEM backscattered electron (BSE) imaging (a2, b2 and c2), XRD (a3, b3 and c3) and differential scanning calorimetry (a4, b4 and c4) results of obtained microstructures.

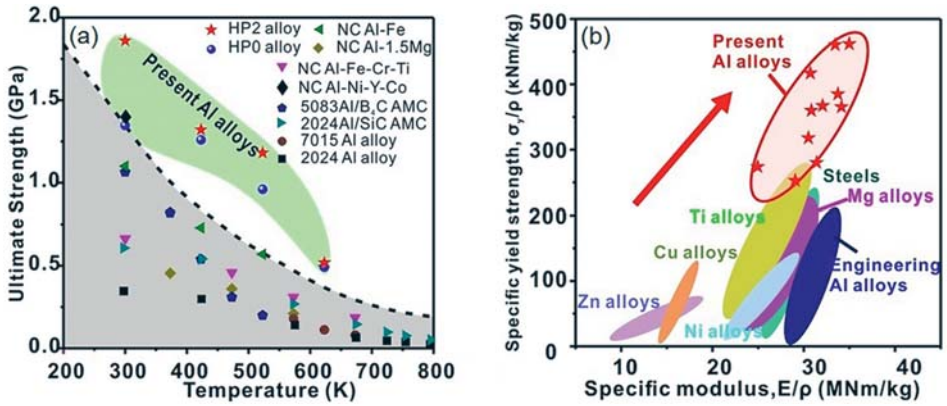

Fig. 2: (a) Comparison between the present alloys and other Al alloys with the compressive ultimate strength versus testing temperature. **(b)** Ashby map of specific yield strength versus specific Young's modulus.

Development of FeCrMoVC wires as novel filler material for hardfacing and repair welding of high-performance steel tools

The increasing processing of high-strength alloys and composites in automotive industry and mechanical engineering requires robust, high-performance tools. In order to extend the service lifetime of the highly loaded tool components, deposition and repair welding provides a cost-efficient and resource-conserving alternative compared to a continuous acquisition of new tool parts. By an appropriate welding process and a suitable filler material, hard surface layers with high strength, wear resistance and good toughness can be generated and worn areas as well as damaged edges can be rebuilt. Especially for complex profiles (e.g. mold inserts, punching plates) and localized geometries very thin filler wires with diameters down to 0.2 mm are required. Therefore, the manual laser welding is a favorable method due to the high local energy density and the possibility to focus the beam on a very small area.

At the IFW Dresden high-strength iron-based alloys are developed which exhibit high macrohardness (≥ 59 HRC), excellent compressive strength (up to 5500 MPa) and superior wear resistance already in the as-cast state [2-4]. Thereby, the patented Fe85Cr4Mo8V2C1 (wt%) cast alloy [5, 6] was already successfully applied as tool material for e. g. bucket teeth or cutting tools. Besides the outstanding mechanical properties first welding tests with thin Fe85Cr4Mo8V2C1 rods already demonstrated a very good weldability.

Within the framework of the ZIM project "EISI" (founded by Federal Ministry for Economic Affairs and Energy) innovative filler materials are developed and implemented in the repair and deposition welding process of high-performance tools in cooperation with the TU Chemnitz, LPT Laserpräzisionstechnik GmbH and quada V+F GmbH [7]. The developed processing technology allows to fabricate filler wires with diameters down to 0.3 mm out of Fe85Cr4Mo8V2C1 (Fig. 3). Furthermore, the laser welding process for different wire diameters was adjusted to transfer the excellent properties of the Fe85Cr4Mo8V2C1 alloy on the base material to get crack-free, wear-resistant deposition layers with a high hardness (≥ 60 HRC) (Fig. 4).

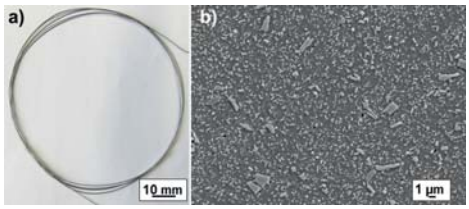

Fig. 3: (a) Fe85Cr4Mo8V2C1 wire with 0.3 mm in diameter and **(b)** scanning electron micrograph of its cross-section showing finely distributed carbides embedded in soft ferritic matrix.

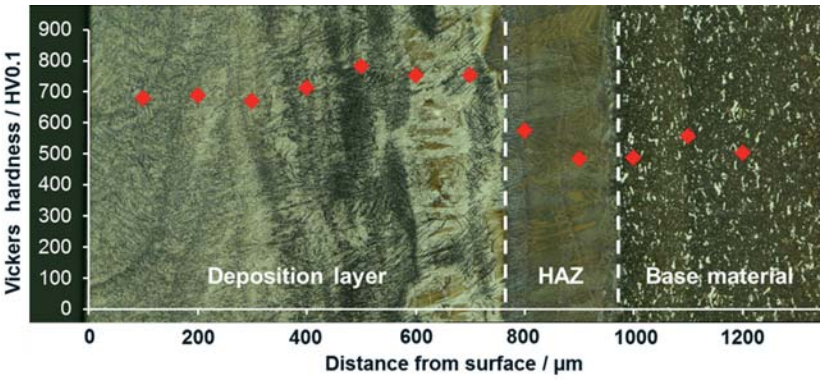

Fig. 4: Profile of Vickers microhardness over the Fe85Cr4Mo8V2C1 deposition layer, the heat-affected zone (HAZ) and the X155CrMo12-1 base material.

The forming technology of Fe85Cr4Mo8V2C1 wires was developed on an industrial scale. After casting a cylindrical bar the microstructure is composed of a complex carbide network and a mainly martensitic matrix leading to a very high hardness. By subsequent forging of the cast bar at about 900°C the carbide network breaks up and due to a tailored soft annealing process the hard martensitic phase is transformed into soft ferrite. Afterwards, wires with different thicknesses are produced with the help of an adjusted sequence of drawing/rotary swaging and annealing. The suitable laser parameters for the application of the FeCrMoVC wires were determined by parameter variation studies. By comprehensive welding tests with competing welding materials, a lower susceptibility to cracking and a higher hardness as well as an enhanced wear resistance of the Fe85Cr4Mo8V2C1 deposition layers could be confirmed. This opens up the possibility to introduce this alloy as a novel filler material for hardfacing and repair welding of high-performance steel tools.

New filler metal with improved properties

Many industrial applications demand versatile braze filler materials with optimized properties. Similar like welding, brazing is a widely-used joining technique to fabricate technical products with a variety of shapes. Also the combination of materials to be joined by means of brazing is vast. Hence, a multitude of materials properties have to be considered, which all affect the mechanisms occurring at the interface between the substrate and the braze filler during brazing. Understanding the mechanisms is crucial for the development of new braze fillers.

Together with Umicore AG & Co. KG a new Cu-based vacuum braze filler was created and patented [8]. The ternary alloy Cu-Ag40-Ga10 exhibits a similar behavior in terms of wetting and strength of the joint like the current standard braze fillers AgCu28. It fulfills all industrial requirements and consequently constitutes a suitable substitution of the eutectic, Ag-rich braze metal AgCu28.

One of the most important properties of braze fillers is the wetting behavior on the different substrates. According to the Young equation, the surface tension of the molten braze filler influences the contact angle and thus the wetting. Next to the viscosity and the vapor pressure also the surface tension of the new developed alloy was investigated in depth and compared with similar alloys. Reducing the Ag content increases the surface tension and the viscosity but the addition of Ga in turn improves the wetting behavior of the ternary alloy Cu-Ag40-Ga10 significantly.

Contact angle measurements verified that the new ternary alloy shows better wetting on steel substrates than the current standard alloys. In the next step, the wetting mechanism was investigated more in detail. During brazing the following processes occur at the liquid-solid interface (see Fig. 5): After melting Cu diffuses along the grain boundaries into the substrate (see Fig. 5b). This is followed by the diffusion of Ga from the liquid into the uppermost steel grains of the substrate. Simultaneously, the steel grains are depleted in Ni (Fig. 5c). Due to the modified composition inside the steel grains, a phase transformation from face-centered cubic (fcc, austenite) to body-centered cubic (bcc, ferrite) takes place (see Fig. 5d). This effect was confirmed by a detailed EBSD analysis (see Fig. 6). In those regions of the steel grains, where the Ga content rises, a bcc structure was detected [9, 10].

As a result of the phase transformation, the original steel surface is partially dissolved and also natural oxide layers disappear, which generally impede wetting. So next to the reduction of the Ag content by more than 40% in the new developed braze filler, which is of economical interest, also the wetting behavior has been understood in depth.

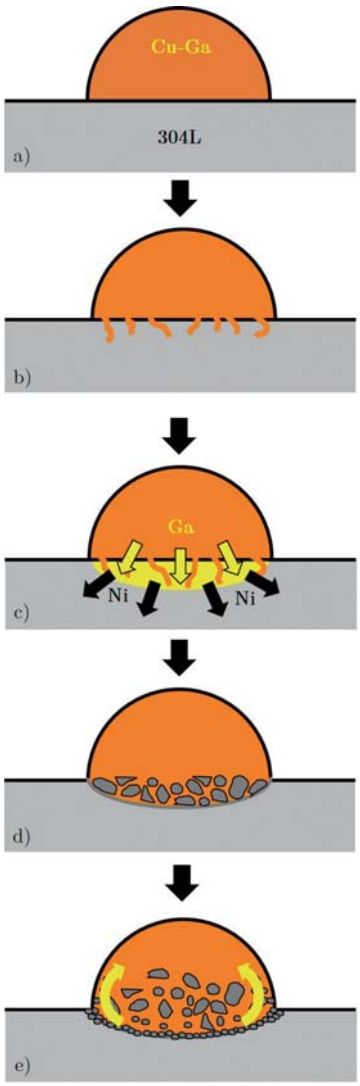

Fig. 5: Schematic process of the interfacial reactions: **a)** initial state; **b)** diffusion of Cu along the grain boundaries; **c)** diffusion of Ga into the steel grains, which is accompanied by a depletion in Ni; **d)** phase transformation of austenite to ferrite; **e)** separation of steel grains in the liquid braze filler.

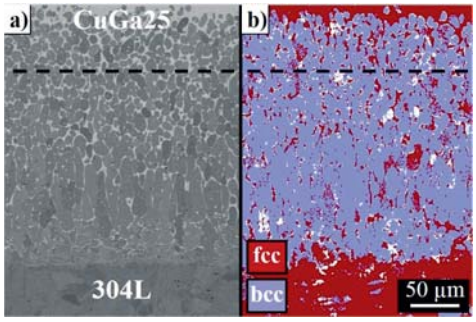

Fig. 6: SEM image **(a)** and EBSD mapping **(b)** of the CuGa25-304L interface in cross section after a spreading test (dashed line indicates former steel surface). While the steel and the Cu-based phase remain face-centered cubic (fcc, red), the new phase has a base-centered cubic (bcc) structure (purple).

[1] Z. Wang et al., Asia Mater. 7 (2015) e229.
[2] J. Hufenbach et al., J. Mater. Sci. 47 (2012) 267.
[3] J. Hufenbach et al., Acta Mater. 60 (2012) 4468.
[4] J. Hufenbach et al., Mater. Sci. Eng. A 586 (2013) 267.
[5] U. Kühn et al., Patent 11009 DE 10 2010 041 366.6 + 11009 PCT EP2011066283 (pending).
[6] U. Kühn et al., Appl. Phys. Lett. 90 (2007) 261901-1.
[7] J. Hufenbach et al.: Hochfeste Eisenlegierungen als Schweißzusatzwerkstoff für das Auftrag- und Verbindungsschweißen (patent application deposited).
[8] G. Wiehl; F. Silze; B. Kempf: Patent WO2014/111538, 24.07.2014.
[9] F. Silze et al. Metal. Mater. Trans. B 46 (2015) 1647-1653.
[10] F. Silze et al. Mater.Des. 91 (2016) 11-18.

Funding: ERC Advanced Grant: INTELHYB (ERC-2013-ADG-340025), EFRE and SAB: ADDE (SAB-Projektnummer: 14227/2337), Deutsche Forschungsgemeinschaft (EC 111/26-1), BMWi funded research ZIM (EISI - FKZ: KF2466405CK3)

Cooperations: TU Chemnitz, TU Dresden, TU Bergakademie Freiberg, quada V+F Laserschweißdraht GmbH, LPT Laserpräzisionstechnik GmbH, Umicore AG & Co. KG

Research topic 4.4

FlexMag: Development centre for flexible magnetoelectronic devices Imperceptible magnetic sense for everybody

People: D. Makarov[4], M. Melzer, M. Kaltenbrunner[1,2,3], Daniil Karnaushenko, Dmitriy Karnaushenko,
Responsible Directors: O. G. Schmidt

Abstract: Future electronic skin aims to mimic nature's original in both, functionality and appearance. While some of the multifaceted properties of human skin may remain exclusive to the biological system, electronics opens a unique path that leads beyond imitation and could equip us with unfamiliar senses. Here we demonstrate giant magnetoresistive sensor foils with high sensitivity, unmatched flexibility and mechanical endurance. They are less than 2 µm thick, extremely flexible, lightweight (≈ 3 g m^{-2}) and wearable as imperceptible magneto-sensitive skin that enables proximity detection, navigation and touchless control. On elastomeric supports, they can be stretched uniaxially or biaxially reaching strains of more than 270 % and endure over 1,000 cycles without fatigue. These ultrathin magnetic field sensors readily conform to ubiquitous objects including human skin and offer a new sense for soft robotics, safety and healthcare monitoring, consumer electronics and electronic skin devices.

Electronics of tomorrow will be compliant and will form a seamless link between soft, living beings and the digital world. Inspired by natures antetype, electronic skin is an intriguing technological platform already able to perceive temperature changes[1], mimic the sensation of touch [2] or monitor physiological conditions [3]. Concepts that enable even self-healing [4] will lead to durable, multifunctional artificial skin. Other functionalities, however, especially those which are unfamiliar to human beings, have hardly been addressed so far.

Magnetoception is a sense which allows for example insects and sharks to detect magnetic fields for orientation and navigation, humans are however unable to perceive magnetic fields naturally Electronic skin could soon help to gain access to this hidden medium in an intuitive and appealing manner. Soft and flexible sensorics to monitor physiological conditions are at the forefront of multidisciplinary research efforts bridging materials science, electrical engineering, and medicine. Magnetosensorics is

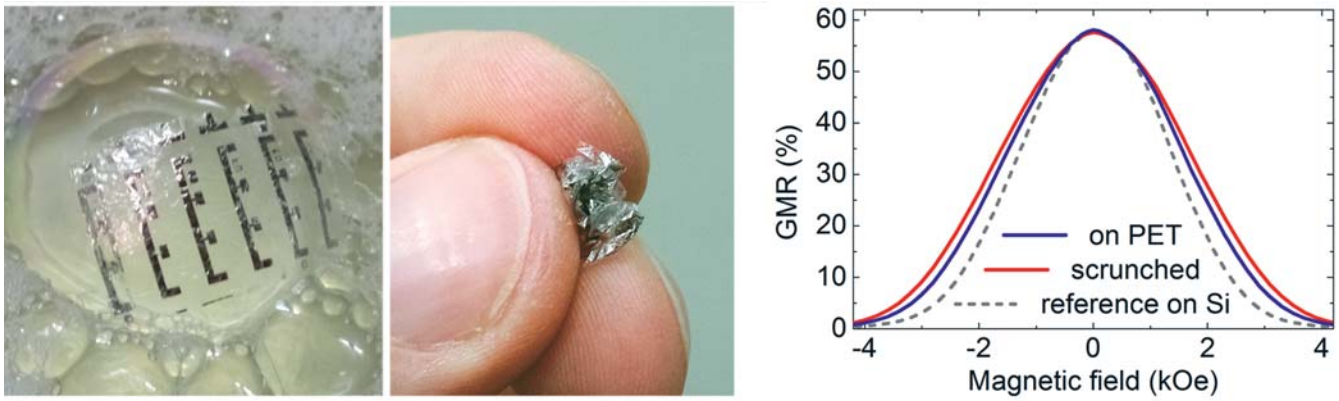

Fig. 1: GMR sensors on ultra-thin PET. **left:** Ultralight and compliant array of five Co/Cu multilayer elements on 1.4 µm-thick PET foil floating on a soap bubble, and (center) crumpled between fingertips. **right:** GMR characteristics of one element as prepared (blue curve), after crumpling as shown above (red curve) and in comparison to a reference sample on a rigid silicon wafer (dashed gray curve).

a versatile tool to monitor mechanical movements or implement navigation and orientation capabilities. On-skin and *in vivo* operation requires very specific mechanical properties of the sensing elements, such as high bendability, stretchabilities exceeding 100 % as well as a sensitivity for small magnetic fields, all of which are met by our recently demonstrated imperceptible magnetic sensors [5], making them ideally suited for wearable, yet unobtrusive orientation and manipulation aids.

With this development we go beyond just imitating the features of human physiology and introduce e-skins with a magneto-sensory system [5], that equips the recipient with a "sixth sense" able to perceive the presence of static or dynamic magnetic fields. We demonstrated an on-skin magnetic proximity detection systems for touch-less human-machine interaction, motion and displacement sensorics applicable for soft robots [6] or functional medical implants [7] as well as magnetic functionalities for epidermal electronics [8].

In this work, we constructed highly sensitive giant magnetoresistive (GMR) sensor elements on ultrathin, 1.4 µm polyethylene terephthalate (PET) foils. The substrate foil is commodity scale, commercially available PET (Mylar® 1.4 CW02) that is fully compatible with lithographic processes, which allows for accurately patterned individual devices, yet large area and low-cost manufacture. Weight and flexibility are key figures of merit for large area electronics or robotic skin, as they critically influence the mechanical response and perception of the artificial sensory system. With just about 1.5 µm total thickness, the imperceptible magneto-electronic foils are light ($\approx$3 g m^{-2}) and unmatched in flexibility (radii of curvature < 3 µm). The extreme light-weight and compliant nature of the sensor elements is demonstrated in the top of Fig. 1, where an array of magnetic field sensors is floating on a spherical soap bubble. Impressively, the magnetoelectronic devices adapt their shape readily to the soft and fragile surface, rather than *vice versa*. Despite their imperceptible design, our GMR sensors exhibit excellent magnetoresistive properties, identical to their counterparts on rigid Si/SiO2 wafer substrates. Nevertheless, our sensor foil is so flexible yet highly durable; it can withstand for example severe crumpling between the fingertips without performance degradation, as corroborated by comparative GMR characteristics on the bottom of Fig. 1.

Imperceptible magnetoelectronics can be readily worn directly on the skin (*e.g.* the palm) as demonstrated in Fig. 2. Here, a set of GMR sensors intimately conforms to the inner hand and unobtrusively follows the motions and deformations of the skin when the hand

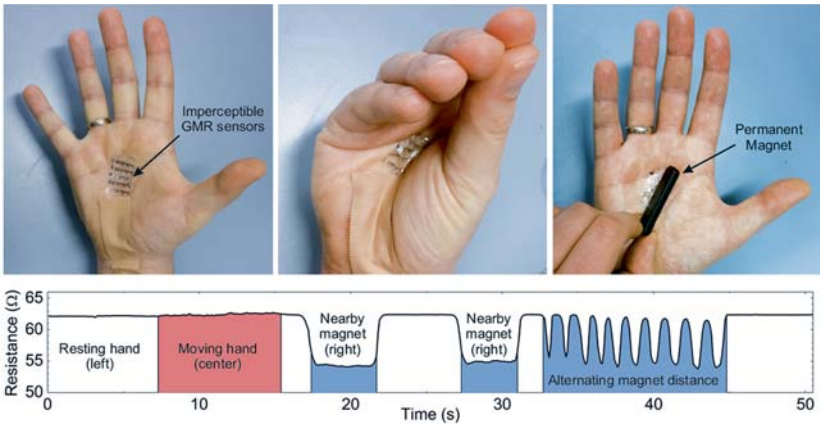

Fig. 2: Imperceptible on-skin magnetic detection. Imperceptible GMR sensor array on a human palm with one element connected to a readout circuit during rest **(right)**, moving the hand (center) and in proximity to a permanent magnet **(left)** as well as the recorded resistance of the sensor element **(bottom)**.

is moved. The resistance of one on-skin sensor element is recorded while moving the fingers and opening and closing the hand, which shows a stable signal during these motions. Applying a magnetic field with a permanent magnet induces a strong resistance drop and alternating the distance of the magnet results in a corresponding real-time signal.

Biological skin is soft and flexible but also stretchable, a feature that is most desirable for an artificial equivalent. Imperceptible electronic foils [9] offer an elegant route to facilitate very high levels of strain without any sacrifices in device performance by a facile one-step post fabrication transfer onto a pre-strained elastomer, which also provides an encapsulation of the functional magnetic nanomembrane. The magnetosensitive capabilities of the presented elements are not affected by this process. The top of Fig. 3 shows a stretchable GMR sensing element, mounted into the stretching stage and contacted for *in situ* magnetoelectrical characterization in a relaxed and stretched state. The very high stretchability is demonstrated by GMR curves recorded at different tensile strain levels, which are congruent with each other. Hence, the prepared sensors can reversibly attain tensile strains up to 270% with no influence on their magnetosensitive capabilities. The progression of the GMR magnitude and the relative resistance change of the sensor are presented as a function of the uniaxial deformation in bottom of Fig. 3. Both values remain unchanged, which highlights the strain-invariant behavior of the prepared sensor elements.

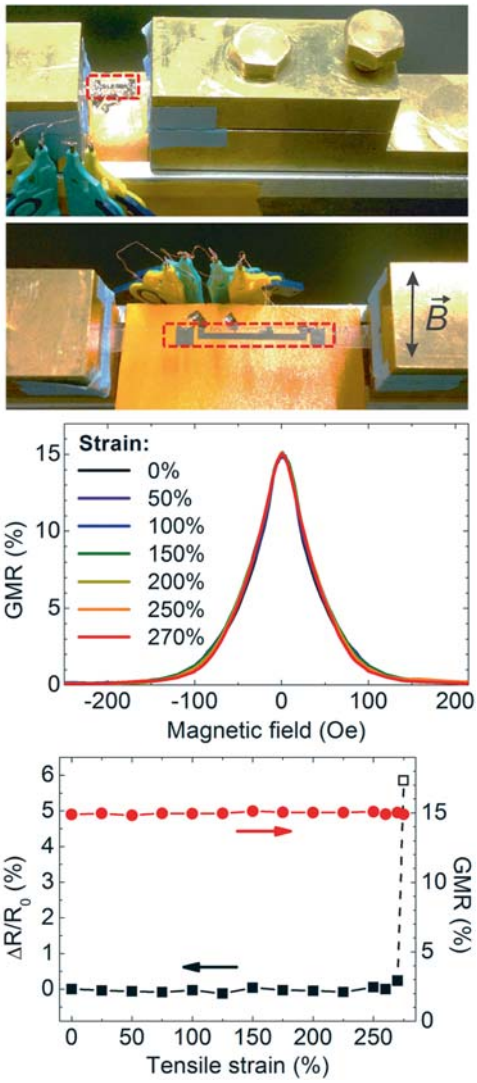

Fig. 3: Stretchable GMR sensors. **top:** Stretchable Py/Cu sensor stripe (in red frame) contacted and mounted to the in situ stretching stage relaxed and fully elongated. **center:** GMR curves recorded for increasing uniaxial strains along the stripe up to 270%. **bottom:** GMR magnitude (red dots) and resistance change normalized to 0% strain (black squares) as a function of applied strain.

Further experiments [5] revealed a remarkable long-term durability with 1,000 extensive stretching cycles showing no fatigue, which renders the presented imperceptible and stretchable GMR elements suitable for "real world" electronic skin applications. The outstanding resilience against high mechanical deformations is attributed in particular to the ductile properties of the materials [10] involved in the GMR multilayer stacks. In addition, biaxial stretchability as well as the real-time monitoring of a soft diaphragm actuator was demonstrated.

In conclusion, these ready-to-use imperceptible and highly sensitive magnetic field sensors with unique mechanical properties extend the cognition of electronic skin systems to a medium that by no means can be detected by human beings. They are ultra-light weight, conform to arbitrary surfaces and seamlessly follow deformations or distortions without performance degradation. For the emerging field of stretchable magnetoelectronics, the here presented GMR sensors outperform all previously introduced elements [11, 12] in terms of stretchability, reliability and fabrication potential by a multiple. The device structure can be adapted and scaled to meet the requirements for specific applications and design concepts. Future work will focus on optimizations to interface electrically and mechanically with other electronic components enabling for example wireless readout and remote sensing. The integration of magnetoelectronics with

other ultrathin functional elements like solar cells [13], light emitting diodes [14], transistors [15] as well as temperature [10] and tactile sensor arrays [9], will enable autonomous and versatile smart systems with a multitude of sensing and actuation features. In the scope of the FlexMag initiative that was launched by the IFW Dresden, new facilities for roll-to-roll fabrication should validate this and other recently introduced technology platforms for shapeable magnetic sensorics [16, 17] towards economically feasible large-scale production and initialize development efforts for specific application scenarios with industry participation. Several companies already evinced their interest in this novel sensorics and first collaborations have been established. We foresee our work to inspire a diverse number of devices that will benefit from a "sixth sense" magnetoception.

[1] R. C. Webb *et al.*, Nat. Mater. 12 (2013) 938.
[2] D. J. Lipomi *et al.*, Nat. Nanotechnol. 6 (2011) 788.
[3] X. Huang *et al.*, Biointerphases 7 (2012).
[4] B. C. K. Tee *et al.*, Nat. Nanotechnol. 7 (2012) 825.
[5] M. Melzer *et al.*, Nat. Commun. 6 (2015) 6080.
[6] D. Rus, and M. T. Tolley, Nature 521 (2015) 467.
[7] D. H. Kim *et al.*, Nat. Mater. 9 (2010) 511.
[8] D. H. Kim *et al.*, Science 333 (2011) 838.
[9] M. Kaltenbrunner *et al.*, Nature 499 (2013) 458.
[10] M. Drack *et al.*, Adv. Mater. 27 (2015) 34.
[11] M. Melzer *et al.*, Adv. Mater. 24 (2012) 6468.
[12] M. Melzer *et al.*, Adv. Mater. 27 (2015) 1333.
[13] M. Kaltenbrunner *et al.*, Nat. Mater. 14 (2015) 1032.
[14] M. S. White *et al.*, Nat. Photonics 7 (2013) 811.
[15] G. A. Salvatore *et al.*, Nat. Commun. 5 (2014) 2982.
[16] D. Karnaushenko *et al.*, Adv. Mater. 27 (2015) 880.
[17] M. Melzer *et al.*, Adv. Mater. 27 (2015) 1274.

Funding: This work was funded in part by the Nanett project of the German Federal Ministry of Education and Research (BMBF) and European Research Council under the European Union's Seventh Framework Programme (FP7/2007-2013)/ERC grant agreement n° 306277. The work in Tokyo was supported by the JST Someya Bio-Harmonized ERATO grant.

Cooperations: [1] Department of Soft Matter Physics, Johannes Kepler University Linz, Austria; [2] Electrical and Electronic Engineering and Information Systems, The University of Tokyo, Japan; [3] Exploratory Research for Advanced Technology (ERATO), Japan Science and Technology Agency (JST), Tokyo, Japan; [4] Intelligente Werkstoffe und Funktionselemente, Helmholtz-Zentrum Dresden-Rossendorf, Dresden

Research Topic 4.5

Concepts and materials for superconducting applications

People: A. Berger, D. Berger, U. Besold, P. Chekhonin, T. Espenhahn, U. Fiedler, G. Fuchs, V. Grinenko, S. Hameister, W. Häßler, A. Horst, R. Hühne, A. Kirchner, M. Kühnel, K. Nenkov, K. Nielsch, P. Pahlke, K. Peukert, J. Scheiter, L. Schultz, M. Sieger, M. Sparing, R. Uhlemann, F. Wall, A. Winkler

Responsible Director: K. Nielsch

Abstract: Superconducting materials are so far mainly used as high field research magnets and moderate field MRI magnets for medical diagnostics. High temperature superconductors have the potential to drastically extend the application range towards power systems like motors, cables, fault current limiters as well as ultra-high field magnets and levitation based applications. Therefore, the central aim of this research topic is to tailor the properties of these materials for the envisaged applications and to develop selected demonstrator systems with superconducting components. Some highlights of our work performed in the last year are summarized in the following.

Improved YBCO coated conductors

The work on this topic is embedded in the framework of the European project *Eurotapes,* where 20 partners from universities, research centers and industry aim to integrate the advanced materials development on *RE*$Ba_2Cu_3O_{7-x}$ high temperature superconductors into longer length coated conductors. The main focus of our contributions in the last year was on the preparation of thick $YBa_2Cu_3O_{7-x}$ (YBCO) layers with artificial pinning centers on buffered textured templates provided by industrial partners. These tapes were either based on Ni-W substrates prepared by the rolling biaxially textured substrates (RABiTS) approach or on ion-beam textured YSZ layers deposited on stainless steel using the alternating beam assisted deposition (ABAD) scheme. The superconducting layers were grown at IFW with pulsed laser deposition from mixed targets with $BaHfO_3$ (BHO) or $Ba_2Y(Nb,Ta)O_6$ (BYNTO) additions. Some recent results are given in the following section.

At first, we realized 1.6 µm thick BYNTO doped YBCO films on fully CSD-buffered Ni5W substrates with a reasonable growth rate of 1.6 nm/s [1]. Nanosized BYNTO rods parallel to the YBCO *c*-axis and BYNTO as well as Y_2O_3 plates parallel to the YBCO *ab*-plane are incorporated with biaxial orientation into the YBCO matrix (Fig. 1). Inductive

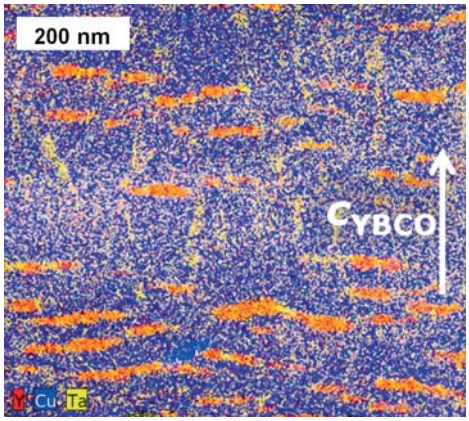

Fig. 1: TEM-EDX analysis of BYNTO doped YBCO on Ni-5at.%W tape showing a rich distribution of nanosized Y_2O_3 or BYNTO plates and BYNTO nanorods.

measurements show only a slight decrease in the critical temperature T_c for the doped film. An improved local homogeneity of the critical current density J_c over the sample was evaluated from trapped field profiles measured using a scanning Hall probe microscope. The mean J_c in rolling direction of the tape is 1.8 MA/cm^2 (77 K) and doubles the value of the undoped sample. Angular dependent measurements of the critical current density, $J_c(\theta)$, show a decreased anisotropy of the doped film for various magnetic fields at 77 K as well as 64 K. At lower temperatures, a *c*-axis peak becomes visible. Adjustment of the deposition parameters temperature and growth rate are on the way and might further enhance the $J_c(B,\theta)$ characteristics of BYNTO-doped YBCO films on biaxially textured Ni-W tapes.

Secondly, 6 mol% BHO doping was successfully implemented into YBCO based coated conductors prepared on CeO_2 buffered ABAD-YSZ templates [2]. The self-field J_c at 77 K reaches 1.1 MA/cm^2 in the doped sample compared to 2.5 MA/cm^2 in pure YBCO, at a film thickness of around 1 μm. Above a magnetic field of 2.2 T along the $B//c$ direction, the J_c of the BHO-doped sample exceeds the J_c of the undoped film. In general, the J_c anisotropy curves of the doped sample show a large and broad peak at $B//c$ and a strongly reduced anisotropy at all temperatures and fields compared to the pure sample. As a result, the BHO sample shows at 40 K and 4 T a better performance at all angles in comparison to the undoped reference sample (Fig. 2). A complex defect structure with $YBa_2Cu_4O_8$ intergrowths, Y_2O_3 precipitates and BHO nanocolumns with a fan-shaped structure is observed by TEM investigations, which can explain the measured $J_c(B,\theta)$ behavior.

Finally, major efforts were directed to study the influence of granularity on the local current transport in YBCO layers prepared on technical substrates. Therefore, high resolution EBSD measurements were performed on superconducting YBCO layers prepared on Ni-RABiTS tapes as well as on ABAD-YSZ based templates [3]. Whereas the orientation of YBCO on the Ni-9at.%W substrate varies strongly from grain to grain (Fig. 3), which is attributed to the different orientation of the Ni substrate grains with regard to the surface normal, orientation variations were observed on the sub-micrometer scale only for YBCO on ABAD-YSZ originating from the finer granularity of this template. Presently, the structural data are compared to micro-Hall scans performed by our cooperation partner at the Technical University Vienna to correlate the local J_c in such YBCO layers to the structural data.

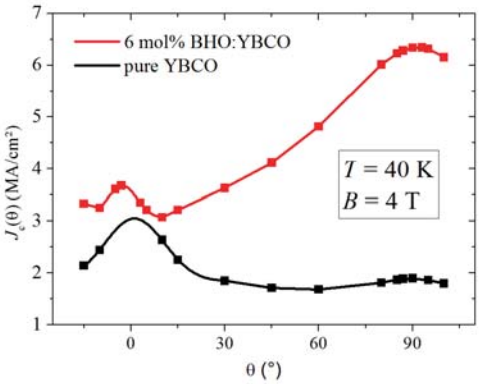

Fig. 2: $J_c(\theta)$-curve for the pure and the BHO doped YBCO sample at an magnetic field of 4 T and a temperature of 40 K.

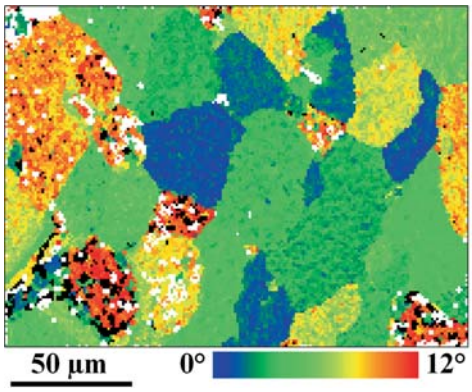

Fig. 3: EBSD mapping (step size 1 μm) of YBCO deposited on Ni-9at.% W tape showing the absolute misorientation from the ideal cube texture. White dots are non-indexed areas; at black dots the misorientation exceeds 12°.

Superconducting magnetic bearings in rotating high-speed textile machines

The unique properties of superconducting magnetic bearings (SMB) - passive load bearing and contact-less motion - have been intensely studied in recent years e.g. for motors, flywheel energy storage systems and other high-speed rotating machines. In the framework of a joint DFG project with the Institute of Textile Machinery and High Performance Material Technology (ITM) at the TU Dresden we investigated the replacement of the conventional ring traveler twist element in ring spinning machines with a superconducting magnetic bearing. The limiting process factors in the industrial production of short staple yarn by ring spinning are frictional wear and heat in the twist element.

We developed and built a SMB, consisting of a permanent-magnetic NdFeB ring acting as yarn driven traveler and a stationary superconducting $YBa_2Cu_3O_{7-x}$ ring cooled on 77 K in a flow-through cryostat. It allows spinning yarn with up to 25.000 rpm, which is the current production speed limit [4, 5] (Fig. 4). The yarn properties and the interaction between the yarn and the SMB were both describe theoretically and measured experimentally. Polyester yarn spun with the SBM twist element has similar properties to conventional yarn. Furthermore, the yarn surface of the SMB-yarn is more even and less hairy due to the reduced friction and heat in the SMB twist element. The decay constant δ of the SMB was found to depend strongly not only on the field cooling

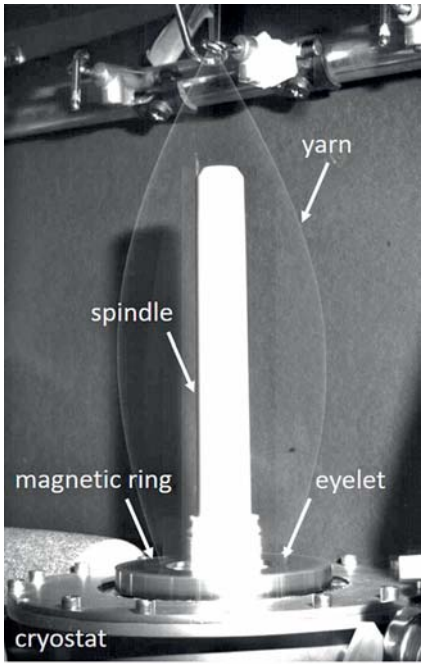

Fig. 4: Yarn spining at 15 000 rpm with superconducting magnetic bearing twist element (high speed camera image).

distance but also on the initial radial displacement Δr. Since damping in SMB is caused by the depinning of flux lines during oscillation, the linear increase of δ with Δr can be attributed to an increase of the average number of pinning centers within the displacement distance [6].

The newly developed ring spinning machine with superconducting magnetic bearing twist element was exhibited at the world leading International Textile Machinery Exhibition ITMA in Milan (Italy) in November 2015 and created a large interest on this new technological solution.

Large Scale Application: SupraTrans II

The test drive facility SupraTrans II was continuously used to study the behavior of magnetic levitation under practical operation conditions and to develop new components such as electromagnetic tracks and fast switchable electromagnetic turnouts. A first prototype of an electromagnetic track was realized using superconducting tapes to create the magnetomotive force needed. This prototype is used for field and force measurements in order to confirm the topology modelled and optimized by FEM simulations. Simultaneously, the test drive facility is constantly used for a general dissemination of superconductivity to the wider public (pupils, students, vocational training etc.) as well as for professional presentations to contact potential users of this new technology.

Within the last year, a monorail levitation system was realized in cooperation with industrial partners for Lexus International using existing track segments of the SupraTrans II test facility. The system allowed studying new track elements as segments with gradients, slopes, water covered tracks or lateral twists as well as the influence of interrupted tracks on such a transport system. Therefore, the track was installed in a specially designed skate park near Barcelona/Spain, where an impressive PR movie was created showing the possibilities of magnetic levitation based on superconducting materials using a levitating hoverboard (Fig. 5).

Fig. 5: Superconducting hoverboard using track components of Supratrans II. ©Lexus International.

[1] M. Sieger et al., IEEE Trans. Appl. Supercond. **26** (2016) submitted.
[2] P. Pahlke et al., IEEE Trans. Appl. Supercond. **26** (2016) submitted.
[3] P. Pahlke et al., IEEE Trans. Appl. Supercond. **26** (2016) submitted.
[4] M. Sparing et al., IEEE Trans. Appl. Supercond. **25** (2015) 3600504.
[5] A. Berger et al., IEEE Trans Appl. Supercond. **26** (2016) accepted.
[6] M. Sparing et al., IEEE Trans. Appl. Supercond. **26** (2016) accepted.

Funding: EU (Eurotapes); DFG; DAAD PPP PROBRAL; ERA.Net Rus; Chi&Partner; THEVA GmbH

Cooperations: Bruker HTS GmbH, Alzenau, Germany; THEVA GmbH, Ismaning, Germany; Deutsche Nanoschicht GmbH Rheinbach, Germany, University of Cambridge, United Kingdom; ICMAB Barcelona, Spain; University of Vienna, Austria; University of Antwerp, Belgium; COPPE/UFRJ, Rio de Janeiro, Brazil; evico GmbH, Dresden, Germany; Institute of Textile Machinery and High Performance Material Technology at the TU Dresden; Festo AG & Co KG, Esslingen, Germany; KIT, Karlsruhe, Germany; Siemens, Erlangen, Germany; IEE Bratislava, Slovakia; University Niigata, Japan

Publications 2015

Journal Papers

1) M.A. Abdulmalic, A. Aliabadi, A. Petr, Y. Krupskaya, V. Kataev, B. Buechner, R. Zaripov, E. Vavilova, V. Voronkova, K. Salikov, T. Hahn, J. Kortus, F. Eya'ane Meva, D. Schaarschmidt, T. Rueffer, *Magnetic superexchange interactions: trinuclear bis(oxamidato) versus bis(oxamato) type complexes*, Dalton Transactions 44 (2015) Nr. 17, S. 8062-8079.
2) F. Ahrend, D. Holzinger, M. Fohler, S. Pofahl, U. Wolff, M. DeKieviet, R. Schaefer, A. Ehresmann, *Stray fields above artificial magnetic in-plane domains*, Journal of Magnetism and Magnetic Materials 381 (2015), S. 292-296.
3) J. Akola, B. Beuneu, R.O. Jones, P. Jovari, I. Kaban, J. Kolar, I. Voleska, T. Wagner, *Structure of amorphous Ag/Ge/S alloys: experimentally constrained density functional study*, Journal of Physics: Condensed Matter 27 (2015) Nr. 48, S. 485304/1-10.
4) A. Alfonsov, B. Peters, F.Y. Yang, B. Buechner, S. Wurmehl, *Nuclear magnetic resonance study of thin $Co_2FeAl_{0.5}Si_{0.5}$ Heusler films with varying thickness*, Physical Review B 91 (2015) Nr. 6, S. 64421/1-7.
5) A. Aliabadi, R. Zaripov, K. Salikhov, V. Voronkova, E. Vavilova, M.A. Abdulmalic, T. Rueffer, B. Buechner, V. Kataev, *Electron Spin Density on the N-Donor Atoms of Cu(II) - (Bis)oxamidato Complexes As Probed by a Pulse ELDOR Detected NMR*, Journal of Physical Chemistry B 119 (2015) Nr. 43, S. 13762-13770.
6) R. Arayanarakool, A.K. Meyer, L. Helbig, S. Sanchez, O.G. Schmidt, *Tailoring three-dimensional architectures by rolled-up nanotechnology for mimicking microvasculatures*, Lab on a Chip 15 (2015) Nr. 14, S. 2981-2989.
7) H. Attar, L. Loeber, A. Funk, M. Calin, L.C. Zhang, K.G. Prashanth, S. Scudino, Y.S. Zhang, J. Eckert, *Mechanical behavior of porous commercially pure Ti and Ti-TiB composite materials manufactured by selective laser melting*, Materials Science and Engineering A 625 (2015), S. 350-356.
8) H. Attar, K.G. Prashanth, A.K. Chaubey, M. Calin, L.C. Zhang, S. Scudino, J. Eckert, *Comparison of wear properties of commercially pure titanium prepared by selective laser melting and casting processes*, Materials Letters 142 (2015), S. 38-41.
9) H. Attar, K.G. Prashanth, L.-C. Zhang, M. Calin, I.V. Okuloy, S. Scudino, C. Yang, J. Eckert, *Effect of Powder Particle Shape on the Properties of In Situ Ti-TiB Composite Materials Produced by Selective Laser Melting*, Journal of Materials Science & Technology 31 (2015) Nr. 10, S. 1001-1005.
10) M.A. Awad, A.M. Ahmed, V.O. Khavrus, E.M.M. Ibrahim, *Tuning the morphology of ZnO nanostructure by in doping and the associated variation in electrical and optical properties*, Ceramics International 41 (2015) Nr. 8, S. 10116-10124.
11) A. Bachmatiuk, J. Boeckl, H. Smith, I. Ibrahim, T. Gemming, S. Oswald, W. Kazmierczak, O.G. Schmidt, J. Eckert, L. Fu, M.H. Rummeli, *Vertical Graphene Growth from Amorphous Carbon Films Using Oxidizing Gases*, The Journal of Physical Chemistry C 119 (2015) Nr. 31, S. 17965-17970.
12) A. Bachmatiuk, J. Zhao, S.M. Gorantla, I.G. Gonzalez Martinez, J. Wiedermann, C. Lee, J. Eckert, M.H. Rummeli, *Low Voltage Transmission Electron Microscopy of Graphene*, Small 11 (2015) Nr. 5, S. 515-542.
13) S.-H. Baek, D.V. Efremov, J.M. Ok, J.S. Kim, J. van den Brink, B. Buechner, *Orbital-driven nematicity in FeSe*, Nature Materials 14 (2015), S. 210-214.
14) S.-H. Baek, Y. Utz, M. Huecker, G.D. Gu, B. Buechner, H.-J. Grafe, *Magnetic field induced anisotropy of La^{139} spin-lattice relaxation rates in stripe ordered $La_{1.875}Ba_{0.125}CuO_4$*, Physical Review B 92 (2015) Nr. 15, S. 155144/1-6.
15) S. Baessler, B. Hamdou, P. Sergelius, A.-K. Michel, R. Zierold, H. Reith, J. Gooth, K. Nielsch, *One-dimensional edge transport on the surface of cylindrical $Bi_xTe_{3-y}Se_y$ nanowires in transverse magnetic fields*, Applied Physics Letters 107 (2015) Nr. 18, S. 181602/1-5.
16) J. Balach, T. Jaumann, M. Klose, S. Oswald, J. Eckert, L. Giebeler, *Mesoporous Carbon Interlayers with Tailored Pore Volume as Polysulfide Reservoir for High-Energy Lithium-Sulfur Batteries*, The Journal of Physical Chemistry C 119 (2015) Nr. 9, S. 4580-4587.
17) J. Balach, T. Jaumann, M. Klose, S. Oswald, J. Eckert, L. Giebeler, *Functional Mesoporous Carbon-Coated Separator for Long-Life, High-Energy Lithium-Sulfur Batteries*, Advanced Functional Materials 25 (2015) Nr. 33, S. 5285-5291.
18) O. Balci, K.G. Prashanth, S. Scudino, D. Agaogullari, I. Duman, M.L. Oevecoglu, V. Uhlenwinkel, J. Eckert, *Effect of Milling Time and the Consolidation Process on the Properties of Al Matrix Composites Reinforced with Fe-Based Glassy Particles*, Metals 5 (2015) Nr. 2, S. 669-685.
19) A. Barla, H. Wilhelm, M.K. Forthaus, C. Strohm, R. Rueffer, M. Schmidt, K. Koepernik, U.K. Roessler, M.M. Abd-Elmeguid, *Pressure-Induced Inhomogeneous Chiral-Spin Ground State in FeGe*, Physical Review Letters 114 (2015) Nr. 1, S. 16803/1-5.
20) A. Bateni, E. Erdem, S. Repp, S. Acar, I. Kokal, W. Haessler, S. Weber, M. Somer, *Electron paramagnetic resonance and Raman spectroscopy studies on carbon-doped MgB2 superconductor nanomaterials*, Journal of Applied Physics 117 (2015) Nr. 15.
21) M. Belesi, L. Giebeler, C.G.F. Blum, U.K. Roessler, B. Buechner, S. Wurmehl, *Local magnetism and structural properties of Heusler Ni_2MnGa alloys*, Physical Review B 91 (2015) Nr. 13, S. 134415/1-10.
22) A. Benke, E. Mehner, M. Rosenkranz, E. Dmitrieva, T. Leisegang, H. Stoecker, W. Pompe, D.C. Meyer, *Pyroelectrically Driven OH Generation by Barium Titanate and Palladium Nanoparticles*, The Journal of Physical Chemistry C 119 (2015) Nr. 12, S. 18278-18286.

23) H. Bih, I. Saadoune, L. Bih, M. Mansori, H. ToufiK, H. Fuess, H. Ehrenberg, *Synthesis, Rietveld refinements, Infrared and Raman spectroscopy studies of the sodium diphosphate $NaCr_yFe_{1-y}P_2O_7$ (0 <= y <= 1)*, Journal of Molecular Structure 1103 (2015), S. 103-109.

24) V. Bisogni, K. Wohlfeld, S. Nishimoto, C. Monney, J. Trinckauf, K. Zhou, R. Kraus, K. Koepernik, C. Sekar, V. Strocov, B. Buechner, T. Schmitt, J. van den Brink, J. Geck, *Orbital Control of Effective Dimensionality: From Spin-Orbital Fractionalization to Confinement in the Anisotropic Ladder System $CaCu_2O_3$*, Physical Review Letters 114 (2015) Nr. 9, S. 96402/1-6.

25) F. Bittner, L. Schultz, T.G. Woodcock, *Twin-like defects in $L1_0$ ordered Tau-MnAl-C studied by EBSD*, Acta Materialia 101 (2015), S. 48-54.

26) M. Bleckmann, J. Gleinig, J. Hufenbach, H. Wendrock, L. Giebeler, J. Zeisig, U. Diekmann, J. Eckert, U. Kuehn, *Effect of cooling rate on the microstructure and properties of FeCrVC*, Journal of Alloys and Compounds 634 (2015), S. 200-207.

27) I.S. Blokhin, S.Yu. Gavrilkin, B.P. Gorshunov, V.A. Dravin, E.S. Zhukova, O.M. Ivanenko, K. Aida, S.I. Krasnosvobodtsev, F. Kurt, K.V. Mitsen, A.Yu. Tsvetkov, *Effect of nonmagnetic defects on superconducting and transport properties of $Ba(Fe_{1-x}Co_xAs)_2$ high-T_c superconductors*, Journal of Experimental and Theoretical Physics 121 (2015) Nr. 5, S. 853-859.

28) I.S. Blokhin, S.Yu. Gavrilkin, B.P. Gorshunov, V.A. Dravin, E.S. Zhukova, O.M. Ivanenko, K. Iida, S.I. Krasnosvobodtsev, F. Kurth, K.V. Mitsen, A.Yu. Tsvetkov, *Effect of radiation defects on the magnetotransport properties of $Ba(Fe_{1-x}Co_xAs)_2$ high-temperature superconductor*, JETP Letters 101 (2015) Nr. 4, S. 247-250.

29) C.G.F. Blum, A. Holcombe, M. Gellesch, M.I. Sturza, S. Rodan, R. Morrow, A. Maljuk, P. Woodward, P. Morris, A.U.B. Wolter, B. Buechner, S. Wurmehl, *Flux growth and characterization of Sr_2NiWO_6 single crystals*, Journal of Crystal Growth 421 (2015), S. 39-44.

30) M. Boenisch, M. Calin, J. van Humbeeck, W. Skrotzki, J. Eckert, *Factors influencing the elastic moduli, reversible strains and hysteresis loops in martensitic Ti-Nb alloys*, Materials Science and Engineering C 48 (2015), S. 511-520.

31) F. Boerrnert, H. Mueller, M. Linck, A. Horst, A.I. Kirkland, B. Buechner, H. Lichte, *Approaching the „Lab in the Gap": First Results from a Versatile In-situ (S)TEM*, Microscopy and Microanalysis 21 (2015) Nr. Suppl. 3, S. 99-100.

32) F. Boerrnert, H. Mueller, T. Riedel, M. Linck, A.I. Kirkland, M. Haider, B. Buechner, H. Lichte, *A flexiblemulti-stimuli in situ (S)TEM: Concept, optical performance, and outlook*, Ultramicroscopy 151 (2015), S. 31-36.

33) N.A. Bogdanov, V.M. Katukuri, J. Romhanyi, V. Yushankhai, V. Kataev, B. Buechner, J. van den Brink, L. Hozoi, *Orbital reconstruction in nonpolar tetravalent transition-metal oxide layers*, Nature Communications 6 (2015), S. 7306/1-9.

34) A. Bogusz, D. Blaschke, D. Buerger, O.G. Schmidt, H. Schmidt, *Morphological transformations of top electrodes on $YMnO_3$ caused by filamentary resistive switching in the oxide matrix*, Advanced Materials Research 1101 (2015), S. 120-123.

35) O.V. Boltalina, A.A. Popov, I.V. Kuvychko, N.B. Shustova, S.H. Strauss, *Perfluoroalkylfullerenes*, Chemical Reviews 115 (2015) Nr. 2, S. 1051-1105.

36) A. Bonatto Minella, S. Garroni, C. Pistidda, M. Dolors Baro, O. Gutfleisch, T. Klassen, M. Dornheim, *Sorption properties and reversibility of Ti(IV) and Nb(V)-fluoride doped-$Ca(BH_4)_2$-MgH_2 system*, Journal of Alloys and Compounds 622 (2015), S. 989-994.

37) C. Bonavolonta, C. de Lisio, M. Valentino, F. Laviano, G.P. Pepe, F. Kurth, K. Iida, A. Ichinose, I. Tsukada, *Influence of Fe Buffer Layer on Co-Doped $BaFe_2As_2$ Superconducting Thin Films*, Advances in Condensed Matter Physics (2015), S. 753108/1-8.

38) L. Braunschweig, A.K. Meyer, L. Wagenfuehr, A. Storch, *Oxygen regulates proliferation of neural stem cells through Wnt/ß-catenin signalling*, Molecular and Cellular Neuroscience 67 (2015), S. 84-92.

39) M. Brehm, M. Grydlik, T. Tayagaki1, G. Langer, F. Schaeffler, O.G. Schmidt, *Photoluminescence investigation of strictly ordered Ge dots grown on pit-patterned Si substrates*, Nanotechnology 26 (2015) Nr. 22, S. 225202/1-11.

40) W. Brzezicki, M. Daghofer, A.M. Oles, *Hole Propagation in the Orbital Compass Models*, Acta Physica Polonica A 127 (2015) Nr. 2, S. 263-265.

41) K. Buchkov, M. Polichetti, K. Nenkov, E. Nazarova, D. Mancusi, N. Balchev, D. Kovacheva, A. Zahariev, S. Pace, *Investigation of the vortex dynamics of $Fe_{1.02}Se$ crystals by fundamental and 3rd harmonic ac magnetic susceptibility analysis*, Superconductor Science and Technology 28 (2015), S. 35009/1-13.

42) F. Cao, Y. Jia, K.G. Prashanth, P. Ma, J. Li, S. Scudino, F. Huang, J. Eckert, J. Sun, *Evolution of microstructure and mechanical properties of as-cast Al-50Si alloy due to heat treatment and P modifier content*, Materials and Design 74 (2015), S. 150-156.

43) A. Castro Nava, M. Cojoc, C. Peitzsch, G. Cirillo, I. Kurth, S. Fuessel, K. Erdmann, D. Kunhardt, O. Vittorio, S. Hampel, A. Dubrovska, *Development of novel radiochemotherapy approaches targeting prostate tumor progenitor cells using nanohybrids*, International Journal of Cancer 137 (2015) Nr. 10, S. 2492-2503.

44) T. Cetner, A. Morawski, D. Gajda, W. Haessler, M. Rindfleisch, M. Tomsic, A. Zaleski, T. Czujko, E. Zuchowska, P. Przyslupski, *Hot isostatic pressing of multifilamentary MgB_2 wires in solid state media for large scale application*, Superconductor Science and Technology 28 (2015) Nr. 14, S. 45009/1-6.

45) A. Charnukha, D.V. Evtushinsky, C.E. Matt, N. Xu, M. Shi, B. Buechner, N.D. Zhigadlo, B. Batlogg, S.V. Borisenko, *High-temperature superconductivity from fine-tuning of Fermi-surface singularities in iron oxypnictides*, Scientific Reports 5 (2015), S. 18273/1-6.

46) A. Charnukha, S. Thirupathaiah, V.B. Zabolotnyy, B. Buechner, N.D. Zhigadlo, B. Batlogg, A.N. Yaresko, S.V. Borisenko, *Interaction-induced singular Fermi surface in a high-temperature oxypnictide superconductor*, Scientific Reports 5 (2015), S. 10392/1-7.

47) A.K. Chaubey, S. Scudino, K.G. Prashanth, J. Eckert, *Microstructure and mechanical properties of Mg-Al-based alloy modified with cerium*, Materials Science and Engineering A 625 (2015), S. 46-49.

48) P. Chekhonin, J. Engelmann, M. Langer, C.-G. Oertel, B. Holzapfel, W. Skrotzki, *Strain inhomogeneities in epitaxial $BaFe_2As_2$ thin films*, Crystal Research and Technology 50 (2015) Nr. 11, S. 891-902.

49) X.M. Chen, A.J. Miller, C. Nugroho, G.A. de la Pena, Y.I. Joe, A. Kogar, J.D. Brock, J. Geck, G.J. MacDougall, S.L. Cooper, E. Fradkin, D.J. Van Harlingen, P. Abbamonte, *Influence of Ti doping on the incommensurate charge density wave in $1T$-TaS_2*, Physical Review B 91 (2015) Nr. 24, S. 245113/1-6.

50) P. Cimalla, T. Werner, K. Winkler, C. Mueller, S. Wicht, M. Gaertner, M. Mehner, J. Walther, B. Rellinghaus, D. Wittig, M.O. Karl, M. Ader, R.H.W. Funk, E. Koch, *Imaging of nanoparticle-labeled stem cells using magnetomotive optical coherence tomography, laser speckle reflectometry, and light microscopy*, Journal of Biomedical Optics 20 (2015) Nr. 3, S. 36018/1-9.

51) T.T. Clikeman, S.H.M. Deng, A.A. Popov, X.-B. Wang, S.H. Strauss, O.V. Boltalina, *Fullerene cyanation does not always increase electron affinity: an experimental and theoretical study*, Physical Chemistry Chemical Physics 17 (2015) Nr. 1, S. 551-556.

52) A.I. Cocemasov, D.L. Nika, V.M. Fomin, D. Grimm, O.G. Schmidt, *Phonon-engineered thermal transport in Si wires with constant and periodically modulated cross-sections: A crossover between nano- and microscale regimes*, Applied Physics Letters 107 (2015) Nr. 1, S. 11904/1-5.

53) M. Curcio, U.G. Spizzirri, G. Cirillo, O. Vittorio, N. Picci, F.P. Nicoletta, F. Iemma, S. Hampel, *On demand delivery of ionic drugs from electro-responsive CNT hybrid films*, RSC Advances 5 (2015) Nr. 56, S. 44902-44911.

54) J. Cwik, Y. Koshkid'ko, A. Mikhailova, N. Kolchugina, K. Nenkov, A. Hackamer, M. Miller, *Magnetic properties and transformation of crystal structure in the $ErFe_2$-$ErAl_2$ system*, Journal of Applied Physics 117 (2015) Nr. 12, S. 123912/1-9.

55) J. Cwik, Y. Koshkid'ko, I. Tereshina, N. Kolchugina, K. Nenkov, A. Hackemer, J. Lyubina, T. Palewski, G.S. Burkhanov, M. Miller, *Role of lanthanum in modifying the magnetic state in RNi_2 solid solutions with R = Tb, Dy, Ho*, Journal of Alloys and Compounds 649 (2015), S. 417-425.

56) A.N. Darinskii, M. Weihnacht, H. Schmidt, *Surface acoustic wave reflection/transmission at vertical borders of piezoelectric substrates*, Ultrasonics 56 (2015), S. 318-324.

57) S. Das, A. Herklotz, E. Pippel, E.J. Guo, D. Rata, K. Doerr, *Strain dependence of antiferromagnetic interface coupling in $La_{0.7}Sr_{0.3}MnO_3$/$SrRuO_3$ superlattices*, Physical Review B 91 (2015) Nr. 13, S. 134405/1-7.

58) E. Demencik, F. Grilli, A. Kario, R. Nast, A. Jung, M. Vojenciak, J. Scheiter, W. Goldacker, *AC Magnetization Loss and Transverse Resistivity of Striated YBCO Coated Conductors*, IEEE Transactions On Applied Superconductivity 25 (2015) Nr. 3, S. 8201405/1-5.

59) Q. Deng, K. Junghans, A.A. Popov, *Carbide clusterfullerenes with odd number of carbon atoms: molecular and electronic structures of $Sc_4C@C_{80}$, $Sc_4C@C_{82}$, and $Sc_4C_3@C_{80}$*, Theoretical Chemistry Accounts 134 (2015) Nr. 2, S. 10/1-12.

60) Q. Deng, A.A. Popov, *Prato and Bingel-Hirsch cycloaddition to heptagon-containing $LaSc_2N@C_s(hept)$-C_{80}: importance of pentalene units*, Chemical Communications 51 (2015) Nr. 26, S. 5637-5640.

61) A. Diestel, R. Niemann, B. Schleicher, S. Schwabe, L. Schultz, S. Faehler, *Field-temperature phase diagrams of freestanding and substrate-constrained epitaxial Ni-Mn-Ga-Co films for magnetocaloric applications*, Journal of Applied Physics 118 (2015) Nr. 2, S. 23908/1-11.

62) J. Dijkmans, M. Dusselier, D. Gabriels, K. Houthoofd, P.C.M.M. Magusin, S. Huang, Y. Pontikes, M. Trekels, A. Vantomme, L. Giebeler, S. Oswald, B.F. Sels, *Cooperative Catalysis for Multistep Biomass Conversion with Sn/Al Beta Zeolite*, ACS Catalysis 5 (2015) Nr. 2, S. 928-940.

63) A.P. Dioguardi, M.M. Lawson, B.T. Bush, J. Crocker, K.R. Shirer, D.M. Nisson, T. Kissikov, S. Ran, S.L. Bud'ko, P.C. Canfield, S. Yuan, P.L. Kuhns, A.P. Reyes, H.-J. Grafe, N.J. Curro, *NMR evidence for inhomogeneous glassy behavior driven by nematic fluctuations in iron arsenide superconductors*, Physical Review B 92 (2015) Nr. 16, S. 165116/1-8.

64) S. Doering, D. Reifert, N. Hasan, S. Schmidt, F. Schmidl, V. Tympel, F. Kurth, K. Iida, B. Holzapfel, T. Wolf, P. Seidel, *Excess currents in planar $Ba(Fe_{1-x}Co_x)2As_2$/TiO_x/Pb Josephson junctions*, Physica Status Solidi B 252 (2015) Nr. 12, S. 2858-2866.

65) S. Doering, S. Schmidt, D. Reifert, M. Feltz, M. Monecke, N. Hasan, V. Tympel, F. Schmidl, J. Engelmann, F. Kurth, K. Iida, I. Moench, B. Holzapfel, P. Seidel, *Hybrid Josephson Junctions with Iron-based and Conventional Superconductor Electrodes*, Journal of Superconductivity and Novel Magnetism 28 (2015) Nr. 3, S. 1117-1121.

66) C. Du, I. Lee, R. Adur, Y. Obukhov, C. Hamann, B. Buechner, J. McCord, D.V. Pelekhov, P.C. Hammel, *Imaging interfaces defined by abruptly varying internal magnetic fields by means of scanned nanoscale spin wave modes*, Physical Review B 92 (2015) Nr. 21, S. 214413/1-5.

67) N. Du, M. Kiani, C.G. Mayr, T. You, D. Buerger, I. Skorupa, O.G. Schmidt, H. Schmidt, *Single pairing spike-timing dependent plasticity in $BiFeO_3$ memristors with a time window of 25ms to 125mys*, Frontiers in Neuroscience 9 (2015), S. 227/1-10.

68) B. Dutta, T. Hickel, J. Neugebauer, C. Behler, S. Faehler, A. Behler, A. Waske, N. Teichert, J.M. Schmalhorst, A. Huetten, *Interplay of strain and interdiffusion in Heusler alloy bilayers*, Physica Status Solidi - Rapid Research Letters 9 (2015) Nr. 5, S. 321-325.

69) D. Elefant, R. Schaefer, *Low-temperature resistivity, magnetoresistance, and domain-wall resistance of highly pure single- and polycrystalline iron*, Physical Review B 91 (2015) Nr. 6, S. 64403/1-15.

70) M. Enachi, M. Guix, T. Braniste, V. Postolache, V. Ciobanu, V Ursaki, O.G. Schmidt, I. Tiginyanu, *Photocatalytic Properties of TiO_2 Nanotubes Doped with Ag, Au and Pt or Covered by Ag, Au and Pt Nanodots*, Elektronnaya Obrabotka Materialov (Surface Engineering and Applied Electrochemistry) 51 (2015) Nr. 1, S. 3-8.

71) M. Erbe, J. Haenisch, R. Huehne, T. Freudenberg, A. Kirchner, L. Molina-Luna, C. Damm, G. van Tendeloo, S. Kaskel, L. Schultz, B. Holzapfel, *$BaHfO_3$ artificial pinning centres in TFA-MOD-derived YBCO and GdBCO thin films*, Superconductor Science and Technology 28 (2015) Nr. 11, S. 114002/1-13.

72) A. Federov, C.S. Praveen, N.I. Verbitskiy, D. Haberer, D. Usachov, D.V. Vyalikh, A. Nefedov, C. Woell, L. Petaccia, S. Piccinin, H. Sachdev, M. Knupfer, B. Buechner, S. Fabris, A. Grueneis, *Efficient gating of epitaxial boron nitride monolayers by substrate functionalization*, Physical Review B 92 (2015) Nr. 12, S. 125440/1-7.

73) F.S. Federov, P. Dunne, A. Gebert, M. Uhlemann, *Influence of Cu^{2+} Ion Concentration on the Uniform Electrochemical Growth of Copper Nanowires in Ordered Alumina Template*, Journal of The Electrochemical Society 162 (2015) Nr. 12, S. D568-D574.

74) M. Fehrenbacher, S. Winnerl, H. Schneider, J. Doering, S.C. Kehr, L.M. Eng, Y. Huo, O.G. Schmidt, K. Yao, Y. Liu, M. Helm, *Plasmonic superlensing in doped GaAs*, Nano Letters 15 (2015), S. 1057-1061.

75) J. Fink, *Supraleitung bei Raumtemperatur?*, Physik Journal 14 (2015) Nr. 3, S. 18-19.

76) J. Fink, A. Charnukha, E.D.L. Rienks, Z.H. Liu, S. Thirupathaiah, I. Avigo, F. Roth, H.S. Jeevan, P. Gegenwart, M. Roslova, I. Morozov, S. Wurmehl, U. Bovensiepen, S. Borisenko, M. Vojta, B. Buechner, *Non-Fermi-liquid scattering rates and anomalous band dispersion in ferropnictides*, Physical Review B 92 (2015) Nr. 20, S. 201106/1-6.

77) V.M. Fomin, A.A. Balandin, *Phonon Spectrum Engineering in Rolled-up Micro- and Nano-Architectures*, Applied Sciences 5 (2015) Nr. 4, S. 728-746.

78) B. Gadgil, P. Damlin, E. Dmitrieva, T. Aeaeritalo, C. Kvarnstroem, *ESR/UV-Vis-NIR spectroelectrochemical study and electrochromic contrast enhancement of a polythiophene derivative bearing a pendant viologen*, RSC Advances 5 (2015) Nr. 53, S. 42242-42249.

79) B. Gadgil, E. Dmitrieva, P. Damlin, T. Aeritalo, C. Kvarnstroem, *Redox reactions in a linear polyviologen derivative studied by in situ ESR/UV-vis-NIR spectroelectrochemistry*, Journal of Solid State Electrochemistry 19 (2015) Nr. 1, S. 77-83.

80) U. Gaitzsch, C. Rodig, C. Damm, L. Schultz, *Elongated grains in Ni5W(Ag) RABiTS tapes*, Journal of Alloys and Compounds 623 (2015), S. 132-135.

81) D. Gajda, A. Morawski, A.J. Zaleski, W. Haessler, K. Nenkov, M.A. Rindfleisch, E. Zuchowska, G. Gajda, T. Czujko, T. Cetner, M.S.A. Hossain, *The critical parameters in in-situ MgB_2 wires and tapes with ex-situ MgB_2 barrier after hot isostatic pressure, cold drawing, cold rolling and doping*, Journal of Applied Physics 117 (2015) Nr. 17, S. 173908/1-9.

82) R.R. Gareev, V. Zbarsky, J. Landers, I. Soldatov, R. Schaefer, M. Muenzenberg, H. Wende, P. Gruenberg, *The role of weak interlayer coupling in the spin-reorientation of perpendicular ultrathin Co-Fe-B/MgO-based heterostructures*, Applied Physics Letters 106 (2015) Nr. 13, S. 132408/1-5.

83) P. Gargarella, C.S. Kiminami, E.M. Mazzer, R.D. Cava, L.A. Basilio, C. Bolfarini, W.J. Botta, J. Eckert, T. Gustmann, S. Pauly, *Phase Formation, Thermal Stability and Mechanical Properties of a Cu-Al-Ni-Mn Shape Memory Alloy Prepared by Selective Laser Melting*, Materials Research 18 (2015) Nr. Suppl. 2, S. 35-38.

84) P. Gargarella, S. Pauly, M.F. de Oliveira, U. Kuehn, J. Eckert, *Glass formation in the Ti-Cu system with and without Si additions*, Journal of Alloys and Compounds 618 (2015), S. 413-420.

85) P. Gargarella, S. Pauly, M. Stoica, G. Vaughan, C.R.M. Afonso, U. Kuehn, J. Eckert, *Structural evolution in Ti-Cu-Ni metallic glasses during heating*, APL materials 3 (2015) Nr. 1, S. 16101/1-6.

86) I.A. Garifullin, P.V. Leksin, N.N. Garifyanov, A.A. Kamashev, Y.V. Fominov, J. Schumann, Y. Krupskaya, V. Kataev, O.G. Schmidt, B. Buechner, *The superconducting spin valve and triplet superconductivity*, Journal of Magnetism and Magnetic Materials 373 (2015), S. 18-22.

87) A. Gebert, S. Oswald, A. Helth, A. Voss, P.F. Gostin, M. Rohnke, J. Janek, M. Calin, J. Eckert, *Effect of indium (In) on corrosion and passivity of a beta-type Ti-Nb alloy in Ringer's solution*, Applied Surface Science 335 (2015), S. 213-222.

88) P. Gentile, M. Cuoco, C. Ortix, *Edge States and Topological Insulating Phases Generated by Curving a Nanowire with Rashba Spin-Orbit Coupling*, Physical Review Letters 115 (2015) Nr. 25, S. 256801/1-5.

89) G. Giannopoulos, L. Reichel, A. Markou, I. Panagiotopoulos, V. Psycharis, C. Damm, S. Faehler, I. Khan, J. Hong, D. Niarchos, *Optimization of $L1_0$ FePt/$Fe_{45}Co_{55}$ thin films for rare earth free permanent magnet applications*, Journal of Applied Physics 117 (2015) Nr. 22, S. 223909/1-7.

90) G. Giannopoulos, L. Reichel, A. Markou, W. Wallisch, M. Stoeger-Pollach, I. Panagiotopoulos, V. Psycharis, S. Faehler, Fidler. J., D. Niarchos, *Structural and magnetic properties of strongly carbon doped Fe-Co thin films*, Journal of Magnetism and Magnetic Materials 393 (2015), S. 479-483.

91) G. Giovannetti, M., van den Brink, J. Capone, C. Ortix, *Kekule textures, pseudospin-one Dirac cones, and quadratic band crossings in a graphene-hexagonal indium chalcogenide bilayer*, Physical Review B 91 (2015) Nr. 12, S. 121417/1-5.

92) P.F. Gostin, D. Eigel, D. Grell, J. Eckert, E. Kerscher, A. Gebert, *Comparing the pitting corrosion behavior of prominent Zr-based bulk metallic glasses*, Journal of Materials Research 30 (2015) Nr. 2, S. 233-241.

93) P.F. Gostin, D. Eigel, D. Grell, M. Uhlemann, E. Kerscher, J. Eckert, A. Gebert, *Stress-Corrosion Interactions in Zr-Based Bulk Metallic Glasses*, Metals 5 (2015) Nr. 3, S. 1262-1278.

94) P.F. Gostin, D. Eigel, D. Grell, M. Uhlemann, E. Kerscher, J. Eckert, A. Gebert, *Stress corrosion cracking of a Zr-based bulk metallic glass*, Materials Science and Engineering: A 639 (2015), S. 681-690.

95) P. Graczyk, R. Schaefer, B. Mroz, *Magnetoelastic coupling between NiFe thin film and $LiCsSO_4$ studied by Kerr microscopy*, Journal of Physics D: Applied Physics 48 (2015) Nr. 42, S. 425002/1-6.

96) H.-J. Grafe, W. Loeser, S. Schmitz, M. Sakaliyska, S. Wurmehl, S. Eisert, B. Reichenbach, J. Acker, A. Rietig, J. Ducke, T. Mueller, *NMR investigation of boron impurities in refined metallurgical grade silicon*, Physica Status Solidi A 212 (2015) Nr. 9, S. 2031-2036.

97) P. Gruendler, L. Dunsch, *Thermal switching of redox reactions at gold electrodes*, Journal of Solid State Electrochemistry 19 (2015) Nr. 1, S. 23-29.

98) M.E. Gruner, W. Keune, B. Roldan Cuenya, C. Weis, J. Landers, S.I. Makarov, D. Klar, M.Y. Hu, E.E. Alp, J. Zhao, M. Krautz, O. Gutfleisch, H. Wende, *Element-Resolved Thermodynamics of Magnetocaloric $LaFe_{13-x}Si_x$*, Physical Review Letters 114 (2015) Nr. 5, S. 57202/1-6.

99) M. Grydlik, M. Brehm, T. Tayagaki, G. Langer, O.G. Schmidt, F. Schaeffler, *Optical properties of individual site-controlled Ge quantum dots*, Applied Physics Letters 106 (2015) Nr. 25, S. 251904/1-5.

100) J. Gubicza, Z. Hegedues, J.L. Labar, A. Kauffmann, J. Freudenberger, V. Subramanya Sarma, *Solute redistribution during annealing of a cold rolled Cu-Ag alloy*, Journal of Alloys and Compounds 623 (2015), S. 96-103.

101) J. Gubicza, K. Sitarama Raju, V. Subramanya Serma, A. Kauffmann, Z. Hegedues, M. Peterlechner, J. Freudenberger, G. Wilde, *The effect of thermomechanical treatment on the microstructure and the mechanical behavior of a supersaturated Cu-Ag alloy*, Materials Science Forum 812 (2015), S. 53-58.

102) Z. Guguchia, A. Amato, J. Kang, H. Luetkens, P.K. Biswas, G. Prando, F. von Rohr, Z. Bukowski, A. Shengelaya, H. Keller, E. Morenzoni, R.M. Fernandes, R. Khasanov, *Direct evidence for a pressure-induced nodal superconducting gap in the $Ba_{0.65}Rb_{0.35}Fe_2As_2$ superconductor*, Nature Communications 6 (2015), S. 8863/1-8.

103) E.-J. Guo, R. Roth, A. Herklotz, D. Hesse, K. Doerr, *Ferroelectric 180° Domain Wall Motion Controlled by Biaxial Strain*, Advanced Materials 27 (2015) Nr. 9, S. 1615-1618.

104) E.J. Guo, R. Roth, S. Das, A. Herklotz, K. Doerr, *Strain-induced improvement of retention loss in $PbZr_{0.2}Ti_{0.8}O_3$ films*, Applied Physics Letters 106 (2015) Nr. 7, S. 72904/1-4.

105) C. Habenicht, M. Knupfer, B. Buechner, *Investigation of the dispersion and the effective masses of excitons in bulk 2H-MoS_2 using transition electron energy-loss spectroscopy*, Physical Review B 91 (2015) Nr. 24, S. 245203/1-6.

106) J. Haenisch, K. Lida, F. Kurth, E. Reich, C. Tarantini, J. Jaroszynski, T. Foerster, G. Fuchs, R. Huehne, V. Grinenko, L. Schultz, B. Holzapfel, *High field superconducting properties of $Ba(Fe_{1-x}Co_x)_2As_2$ thin films*, Scientific Reports 5 (2015), S. 17363/1-11.

107) W. Haessler, C. Rodig, C. Damm, J. Scheiter, L. Schultz, A. Aubele, B. Sailer, K. Schlenga, *Increased critical current density of in-situ MgB_2 wires by Mg deficiency*, Physica C 510 (2015), S. 8-12.

108) F. Hammerath, M. Moroni, L. Bossoni, S. Sanna, R. Kappenberger, S. Wurmehl, A.U.B. Wolter, M.A. Afrassa, Y. Kobayashi, M. Sato, B. Buechner, P. Carretta, *Enhancement of low-frequency fluctuations and superconductivity breakdown in Mn-doped $La_{1-y}Y_yFeAsO_{0.89}F_{0.11}$ superconductors*, Physical Review B 92 (2015) Nr. 2, S. 20505/1-5.

109) N. Harshavardhana, N.R. Gorhe, J. Freudenberger, M.P. Gururajan, P. Pant, *Comparison of Room Temperature and Cryo-Deformation Effects on Mechanical Properties and Microstructure of Copper*, Transactions of the Indian Institute of Metals 68 (2015) Nr. Suppl. 2, S. 131-135.

110) J. He, N. Mattern, I. Kaban, F. Dai, K. Song, Z. Yan, J. Zhao, D.H. Kim, J. Eckert, *Enhancement of glass-forming ability and mechanical behavior of zirconium-lanthanide two-phase bulk metallic glasses*, Journal of Alloys and Compounds 618 (2015), S. 795-802.

111) M.D. Heinemann, V. Efimova, R. Klenk, B. Hoepfner, M. Wollgarten, T. Unold, H.-W. Schock, C.A. Kaufmann, *Cu(In,Ga)Se_2 superstrate solar cells: prospects and limitations*, Progress in Photovoltaics 23 (2015) Nr. 10, S. 1228-1237.

112) M. Hoffmann, U. Schroeder, T. Schenk, T. Shimizu, H. Funakubo, O. Sakata, D. Pohl, M. Drescher, C. Adelmann, R. Materlik, A. Kersch, T. Mikolajick, *Stabilizing the ferroelectric phase in doped hafnium oxide*, Journal of Applied Physics 118 (2015) Nr. 7, S. 72006/1-9.

113) M. Hoffmann, M. Zier, S. Oswald, J. Eckert, *Challenges for lithium species identification in complementary Auger and X-ray photoelectron spectroscopy*, Journal of Power Sources 288 (2015), S. 434-440.

114) S. Horn, S. Oswald, M. Stoica, M. Uhlemann, A. Gebert, *Complex microshaping of bulk metallic glass surfaces by electrochemical means*, Journal of Materials Research 30 (2015) Nr. 22, S. 3493-3501.

115) J. Hu, B.A. Sun, Y. Yang, C.T. Liu, S. Pauly, Y.X. Weng, J. Eckert, *Intrinsic versus extrinsic effects on serrated flow of bulk metallic glasses*, Intermetallics 66 (2015), S. 31-39.

116) X. Hu, M. Ma, R.G. Mendes, M. Zeng, Q. Zhang, Y. Xue, T. Zhang, M.H. Ruemmeli, L. Fu, *Li-storage performance of binder-free and flexible iron fluoride@graphene cathodes*, Journal of Materials Chemistry A 3 (2015) Nr. 47, S. 23930-23935.

117) M. Huang, S.G. Hickey, B. Hoefer, F. Ding, S. He, O.G. Schmidt, A. Eychmueller, S. Miao, *Band-Emission Evolutions from Magic-sized Clusters to Nanosized Quantum Dots of Cd_3As_2 in the Hot-Bubbling Synthesis*, The Journal of Physical Chemistry C 119 (2015) Nr. 28, S. 16390-16395.

118) H. Huckfeldt, F. Ahrend, D. Holzinger, H. Klein, D. Engel, M. Melzer, D. Makarov, O.G. Schmidt, T. Fuhrmann-Lieker, A. Ehresmann, *Selective Alignment of Molecular Glass Wrinkles by Engineered Magnetic Field Landscapes*, Advanced Functional Materials 25 (2015) Nr. 43, S. 6768-6774.

119) A. Hynowska, A. Blanquer, E. Pellicer, J. Fornell, S. Surinach, M.D. Baro, A. Gebert, M. Calin, J. Eckert, C. Nogues, E. Ibanez, L. Barrios, J. Sort, *Nanostructured Ti-Zr-Pd-Si-(Nb) bulk metallic composites: Novel biocompatible materials with superior mechanical strength and elastic recovery*, Journal of Biomedical Materials Research Part B: Applied Biomaterials 103 (2015) Nr. 8, S. 1569-1579.

120) M. Iakovleva, E. Vavilova, H.-J. Grafe, S. Zimmermann, A. Alfonsov, H. Luetkens, H.-H. Klauss, A. Maljuk, S. Wurmehl, B. Buechner, V. Kataev, *Ground state and low-energy magnetic dynamics in the frustrated magnet $CoAl_2O_4$ as revealed by local spin probes*, Physical Review B 91 (2015) Nr. 14, S. 144419/1-11.

121) I. Ibrahim, J. Kalbacova, V. Engemaier, J. Pang, R.D. Rodriguez, D. Grimm, T. Gemming, D.R.T. Zahn, O.G. Schmidt, J. Eckert, M.H. Ruemmeli, *Confirming the Dual Role of Etchants during the Enrichment of Semiconducting Single Wall Carbon Nanotubes by Chemical Vapor Deposition*, Chemistry of Materials 27 (2015) Nr. 17, S. 5964-5973.

122) J.J. Ipus, J.M. Borrego, J.S. Blazquez, M. Stoica, V. Franco, A. Conde, *Influence of hot compaction on microstructure and magnetic properties of mechanically alloyed Fe(Co)-based amorphous compositions*, Journal of Alloys and Compounds 653 (2015), S. 546-551.

123) A.C. Jacko, C. Janani, K. Koepernik, B.J. Powell, *Emergence of quasi-one-dimensional physics in a nearly-isotropic three-dimensional molecular crystal: Ab initio modeling of $Mo_3S_7(dmit)3$*, Physical Review B 91 (2015) Nr. 12, S. 125140/1-5.

124) J.-P. Jahn, M. Munsch, L. Beguin, A.V. Kuhlmann, M. Renggli, Y. Huo, F. Ding, R. Trotta, M. Reindl, O.G. Schmidt, A. Rastelli, P. Treutlein, R.J. Warburton, *An artificial Rb atom in a semiconductor with lifetime-limited linewidth*, Physical Review B 92 (2015) Nr. 24, S. 245439/1-.

125) T. Jaumann, J. Balach, M. Klose, S. Oswald, U. Langklotz, A. Michaelis, J. Eckert, L. Giebeler, *SEI-component formation on sub 5 nm sized silicon nanoparticles in Li-ion batteries: the role of electrode preparation, FEC addition and binders*, Physical Chemistry Chemical Physics 17 (2015) Nr. 38, S. 24956-24967.

126) T. Jaumann, M. Herklotz, M. Klose, K. Pinkert, S. Oswald, J. Eckert, L. Giebeler, *Tailoring hollow Silicon-Carbon nanocomposites as high-performance anodes in secondary Lithium-based batteries through economical chemistry*, Chemistry of Materials 27 (2015), S. 37-43.

127) L. Jin, Y. Shuai, X. Ou, W.B. Luo, C.G. Wu, W.L. Zhang, D. Buerger, I. Skorupa, T. You, N. Du, O.G. Schmidt, H. Schmidt, *Transport properties of Ar^+ irradiated resistive switching $BiFeO_3$ thin films*, Applied Surface Science 336 (2015), S. 354-358.

128) P. Jovari, S. Cui, V. Nazabal, I. Kaban, B. Beuneu, M. Dussauze, C. Boussard, B. Bureau, *Network Rearrangement in AgI-Doped $GeTe_4$ Glasses*, Journal of the American Ceramic Society 98 (2015) Nr. 3, S. 1034-1039.

129) H.Y. Jung, S.J. Choi, K.G. Prashanth, M. Stoica, S. Scudino, S. Yi, U. Kuehn, D.H. Kim, K.B. Kim, J. Eckert, *Fabrication of Fe-based bulk metallic glass by selective laser melting: A parameter study*, Materials and Design 86 (2015), S. 703-708.

130) H.Y. Jung, M. Stoica, S. Yi, D.H. Kim, J. Eckert, *Crystallization kinetics of $Fe_{76.5-x}C_{6.0}Si_{3.3}B_{5.5}P_{8.7}Cux$ (x = 0, 0.5, and 1 at. pct) bulk amorphous alloy*, Metallurgical and Materials Transactions A 46 (2015) Nr. 6, S. 2415-2421.

131) H.Y. Jung, M. Stoica, S.H. Yi, D.H. Kim, J. Eckert, *Influence of Al on glass forming ability and nanocrystallization behavior of cast-iron based bulk amorphous alloy*, Journal of Materials Research 30 (2015) Nr. 06, S. 818-824.

132) K. Junghans, C. Schlesier, A. Kostanyan, N.A. Samoylova, Q. Deng, M. Rosenkranz, S. Schiemenz, R. Westerstroem, T. Greber, B. Buechner, A.A. Popov, *Methane as a Selectivity Booster in the Arc-Discharge Synthesis of Endohedral Fullerenes: Selective Synthesis of the Single-Molecule Magnet $Dy_2TiC@C_{80}$ and Its Congener $Dy_2TiC_2@C_{80}$*, Angewandte Chemie 54 (2015) Nr. 45, S. 13411-13415.

133) I. Kaban, P. Jovari, B. Escher, D.T. Tran, G. Svensson, M.A. Webb, T.Z. Regier, V. Kokotin, B. Beuneu, T. Gemming, J. Eckert, *Atomic structure and formation of CuZrAl bulk metallic glasses and composites*, Acta Materialia 100 (2015), S. 369-376.

134) A.E. Karakozov, B.P. Gorshunov, Ya.G. Ponomarev, A.S. Prokhorov, V.S. Nozdrin, M.V. Magnitskaya, E.S. Zhukova, K. Iida, M. Dressel, S. Zapf, S. Haindl, *Study of the structure of a superconducting state of Co-doped $BaFe_2As_2$ multiband compounds*, JETP Letters 100 (2015) Nr. 5, S. 328-335.

135) D. Karnaushenko, L. Baraban, D. Ye, I. Uguz, R.G. Mendes, M.H. Ruemmeli, J.A.G.M. de Visser, O.G. Schmidt, G. Cuniberti, D. Makarov, *Monitoring microbial metabolites using an inductively coupled resonance circuit*, Scientific Reports 5 (2015), S. 12878/1-13.

136) D. Karnaushenko, B. Ibarlucea, S. Lee, G. Lin, L. Baraban, S. Pregl, M. Melzer, D. Makarov, W.M. Weber, T. Mikolajick, O.G. Schmidt, G. Cuniberti, *Light Weight and Flexible High-Performance Diagnostic Platform*, Advanced Healthcare Materials 4 (2015) Nr. 10, S. 1517-1525.

137) D. Karnaushenko, D.D. Karnaushenko, D. Makarov, S. Baunack, R. Schaefer, O.G. Schmidt, *Self-Assembled On-Chip-Integrated Giant Magneto-Impedance Sensorics*, Advanced Materials 27 (2015) Nr. 42, S. 6582-6589.

138) D. Karnaushenko, D. Makarov, M. Stoeber, D.D. Karnaushenko, S. Baunack, O.G. Schmidt, *High-performance magnetic sensorics for printable and flexible electronics*, Advanced Materials 27 (2015), S. 880-885.

139) D. Karnaushenko, N. Muenzenrieder, D.D. Karnaushenko, B. Koch, A.K. Meyer, S. Baunack, L. Petti, G. Troester, D. Makarov, O.G. Schmidt, *Biomimetic Microelectronics for Regenerative Neuronal Cuff Implants*, Advanced Materials 27 (2015) Nr. 43, S. 6797-6805.

140) D.D. Karnaushenko, D. Karnaushenko, D. Makarov, O.G. Schmidt, *Compact helical antenna for smart implant applications*, NPG Asia Materials 7 (2015), S. e188/1-10.

141) D. Kasinathan, K. Koepernik, L.H. Tjeng, M.W. Haverkort, *SmO thin films: A flexible route to correlated flat bands with nontrivial topology*, Physical Review B 91 (2015) Nr. 19, S. 195127/1-8.

142) E.Y. Kataev, D.M. Itkis, A.V. Fedorov, B.V. Senkovsky, D.Y. Usachov, N.I. Verbitskiy, A. Grueneis, A. Barinov, D.Y. Tsukanova, A.A. Volykhov, K.V. Mironovich, V.A. Krivchenko, M.G. Rybin, E.D. Obraztsova, C. Laubschat, D.V. Vyalikh, L.V. Yashina, *Oxygen Reduction by Lithiated Graphene and Graphene-Based Materials*, ACS Nano 9 (2015) Nr. 1, S. 320-326.

143) V.M. Katukuri, S. Nishimoto, I. Rousochatzakis, H. Stoll, J. van den Brink, L. Hozoi, *Strong magnetic frustration and anti-site disorder causing spin-glass behavior in honeycomb Li_2RhO_3*, Scientific Reports 5 (2015), S. 14718/1-8.

144) A. Kauffmann, J. Freudenberger, H. Klauss, W. Schillinger, V. Subramanya Sarma, L. Schultz, *Efficiency of the refinement by deformation twinning in wire drawn single phase copper alloys*, Materials Science and Engineering A 624 (2015), S. 71-78.

145) I.S.M. Khalil, V. Magdanz, S. Sanchez, O.G. Schmidt, S. Misra, *Precise localization and control of catalytic janus micromotors using weak magnetic fields*, International Journal of Advanced Robotic Systems 12 (2015) Nr. 2, S. 1-7.

146) F. Kiebert, J. Koenig, C. Kykal, H. Schmidt, *Measurements of Streams Agitated by Fluid Loaded SAW-devices Using a Volumetric 3-component Measurement Technique (V3V)*, Physics Procedia 70 (2015), S. 25-29.

147) K. Kikoin, S.-L. Drechsler, K. Koepernik, J. Malek, J. van den Brink, *Magnetic moment formation due to arsenic vacancies in LaFeAsO-derived superconductors*, Scientific Reports 5 (2015), S. 11280/.

148) B.H. Kim, J. van den Brink, *Resonant inelastic x-ray scattering on single magnons at oxygen K edges*, Physical Review B 92 (2015) Nr. 8, S. 81105/1-5.

149) K.C. Kim, S.H. Park, M.Y. Na, H.J. Chang, W.T. Kim, N. Mattern, J. Eckert, Y. Yokoyama, K.B. Kim, D.H. Kim, *Formation of nano-porous GeO_x by de-alloying of an Al-Ge-Mn amorphous alloy*, Scripta Materialia 104 (2015), S. 49-52.

150) B. Koch, A.K. Meyer, L. Helbig, S.M. Harazim, A. Storch, S. Sanchez, O.G. Schmidt, *Dimensionality of Rolled-up Nanomembranes Controls Neural Stem Cell Migration Mechanism*, Nano Letters 15 (2015) Nr. 8, S. 5530-5538.

151) T. Kosub, M. Kopte, F. Radu, O.G. Schmidt, D. Makarov, *All-Electric Access to the Magnetic-Field-Invariant Magnetization of Antiferromagnets*, Physical Review Letters 115 (2015) Nr. 9, S. 97201/1-5.

152) A. Krause, W.M. Weber, D. Pohl, B. Rellinghaus, A. Kersch, T. Mikolajick, *Investigation of band gap and permittivity of the perovskite $CaTiO_3$ in ultrathin layers*, Journal of Physics D: Applied Physics 48 (2015) Nr. 41, S. 415304/1-7.

153) M. Krautz, A. Funk, K.P. Skokov, T. Gottschall, J. Eckert, O. Gutfleisch, A. Waske, *A new type of $La(Fe,Si)_{13}$-based magnetocaloric composite with amorphous metallic matrix*, Scripta Materialia 95 (2015), S. 50-53.

154) F. Kurth, C. Tarantini, V. Grinenko, J. Haenisch, J. Jaroszynski, E. Reich, Y. Mori, A. Sakagami, T. Kawaguchi, J. Engelmann, L. Schultz, B. Holzapfel, H. Ikuta, R. Huehne, K. Iida, *Unusually high critical current of clean P-doped $BaFe_2As_2$ single crystalline thin film*, Applied Physics Letters 106 (2015) Nr. 7, S. 72602/1-5.

155) S. Lamrani, A. Guittoum, R. Schaefer, M. Hemmous, V. Neu, S. Pofahl, T. Hadjersi, N. Benbrahim, *Morphology, structure and magnetic study of permalloy films electroplated on silicon nanowires*, Journal of Magnetism and Magnetic Materials 396 (2015), S. 263-267.

156) A. Lau, C. Ortix, J. van den Brink, *Topological Edge States with Zero Hall Conductivity in a Dimerized Hofstadter Model*, Physical Review Letters 115 (2015) Nr. 21, S. 216805/1-5.

157) A. Lau, C. Ortix, J. van den Brink, *One-dimensional Dirac electrons on the surface of weak topological insulators*, Physical Review B 91 (2015) Nr. 8, S. 85106/1-7.

158) P.V. Leksin, N.N. Garifyanov, A.A. Kamashev, Ya.V. Fominov, J. Schumann, C. Hess, V. Kataev, B. Buechner, I.A. Garifullin, *Superconducting spin-valve effect and triplet superconductivity in CoO_x/Fe1/Cu/Fe2/Cu/Pb multilayer*, Physical Review B 91 (2015) Nr. 21, S. 214508/1-12.

159) B.S. Li, H. Shakur Shahabi, S. Scudino, J. Eckert, J.J. Kruzic, *Designed heterogeneities improve the fracture reliability of a Zr-based bulk metallic glass*, Materials Science and Engineering: A 646 (2015), S. 242-248.

160) H.-F. Li, C. Cao, A. Wildes, W. Schmidt, K. Schmalz, B. Hou, L.-P. Regnault, C. Zhang, P. Meuffels, W. Loeser, G. Roth, *Distinct itinerant spin-density waves and local-moment antiferromagnetism in an intermetallic $ErPd_2Si_2$ single crystal*, Scientific Reports 5 (2015), S. 7968/1-7.

161) X. Li, C. Yan, J. Wang, A. Graff, S.L., Sprafke, A. Schweizer, O.G. Schmidt, R.B. Wehrspohn, *Stable Silicon Anodes for Lithium-Ion Batteries Using Mesoporous Metallurgical Silicon*, Advanced Energy Materials 5 (2015) Nr. 4.

162) G. Lin, V.M. Fomin, D. Marakov, O.G. Schmidt, *Supervised discriminant analysis for droplet micro-magnetofluidics*, Microfluidics and Nanofluidics 19 (2015) Nr. 2, S. 457-464.

163) G. Lin, D. Makarov, M. Medina-Sanchez, M. Guix, L. Baraban, G. Cuniberti, O.G. Schmidt, *Magnetofluidic platform for multidimensional magnetic and optical barcoding of droplets*, Lab on a Chip 15 (2015), S. 216-224.

164) G. Lin, D. Makarov, O.G. Schmidt, *Strong Ferromagnetically-Coupled Spin Valve Sensor Devices for Droplet Magnetofluidics*, Sensors 15 (2015) Nr. 6, S. 12526-12538.

165) J. Linnemann, J. Giorgio, K. Wagner, G. Mathieson, G.G. Wallace, D.L. Officer, *A simple one step process for enhancement of titanium foil dye sensitised solar cell anodes*, Journal of Materials Chemistry A 3 (2015) Nr. 7, S. 3266-3270.

166) X. Liu, J. Zhang, W. Si, L. Xi, B. Eichler, C. Yan, O.G. Schmidt, *Sandwich Nanoarchitecture of Si/Reduced Graphene Oxide Bilayer Nanomembranes for Li-Ion Batteries with Long Cycle Life*, ACS Nano 9 (2015) Nr. 2, S. 1198-1205.

167) X. Liu, J. Zhang, W. Si, L. Xi, S. Oswald, C. Yan, O.G. Schmidt, *High-rate amorphous SnO_2 nanomembrane anodes for Li-ion batteries with a long cycling life*, Nanoscale 7 (2015) Nr. 1, S. 282-288.

168) Z.-H. Liu, T.K. Kim, A. Sala, H. Ogino, J. Shimoyama, B. Buechner, S.V. Borisenko, *Electronic structure of $(Ca_{0.85}La_{0.15})FeAs_2$*, Applied Physics Letters 106 (2015) Nr. 5, S. 52602/1-5.

169) Z.H. Liu, Y.G. Zhao, Y. Li, L.L. Jia, Y.P. Cai, S. Zhou, T.L. Xia, B. Buechner, S.V. Borisenko, S.C. Wang, *Orbital characters and electronic correlations in KCo_2Se_2*, Journal of Physics: Condensed Matter 27 (2015) Nr. 29.

170) S. Loos, D. Gruner, M. Abdel-Hafiez, J. Seidel, R. Huettl, A.U.B. Wolter, K. Bohmhammel, F. Mertens, *Heat capacity (C_p) and entropy of olivine-type $LiFePO_4$ in the temperature range (2 to 773) K*, Journal of Chemical Thermodynamics 85 (2015), S. 77-85.

171) E. Lopatina, I. Soldatov, V. Budinsky, M. Marsilius, L. Schultz, G. Herzer, R. Schaefer, *Surface crystallization and magnetic properties of $Fe_{84.3}Cu_{0.7}Si_4B_8P_3$ soft magnetic ribbons*, Acta Materialia 96 (2015), S. 10-17.

172) R. Lou, Z. Liu, W. Jin, H. Wang, Z. Han, K. Liu, X. Wang, T. Qian, Y. Kushnirenko, S.-W. Cheong, R.M. Osgood, H. Ding, S. Wang, *Sudden gap closure across the topological phase transition in $Bi_{2-x}In_xSe_3$*, Physical Review B 92 (2015) Nr. 11, S. 115150/1-5.

173) X. Lu, J. Deng, W. Si, X. Liu, B. Liu, L. Liu, S. Oswald, S. Baunack, H.J. Grafe, C. Yan, O.G. Schmidt, *High-Performance Li-O_2 Batteries with Trilayered Pd/MnO_x/Pd Nanomembranes*, Advanced Science 2 (2015) Nr. 9, S. 1500113/1-6.

174) X. Lu, W. Si, X. Sun, J. Deng, L. Xi, B. Liu, C. Yan, O.G. Schmidt, *Curly MnOx nanomembranes as cathode materials for rechargeable lithium-oxygen battery systems*, Journal of Power Sources 295 (2015), S. 197-202.

175) V. Lukes, P. Rapta, L. Goetzke, A. Packalen, E. Dmitrieva, J.K. Clegg, K. Gloe, K. Gloe, J.J. Weigand, *5,7,8,10,15,17,18, 20-Octaphenyl-21,23-dithiaporphyrin: Synthesis, structure and spectroelectrochemistry*, Journal of Solid State Electrochemistry 19 (2015), S. 123-134.

176) Q. Luo, G. Garbarino, B. Sun, D. Fan, Y. Zhang, Z. Wang, Y. Sun, J. Jiao, X. Li, P. Li, N. Mattern, J. Eckert, J. Shen, *Hierarchical densification and negative thermal expansion in Ce-based metallic glass under high pressure*, Nature Communications 6 (2015), S. 5703/1-9.

177) A. Madani, M. Kleinert, D. Stolarek, L. Zimmermann, L. Ma, O.G. Schmidt, *Vertical optical ring resonators fully integrated with nanophotonic waveguides on silicon-oninsulator substrates*, Optics Letters 40 (2015) Nr. 16, S. 3826-3829.

178) M. Madian, L. Giebeler, M. Klose, T. Jaumann, M. Uhlemann, A. Gebert, S. Oswald, N. Ismail, A. Eychmueller, J. Eckert, *Self-Organized TiO_2/CoO Nanotubes as Potential Anode Materials for Lithium Ion Batteries*, ACS Sustainable Chemisty & Engineering 3 (2015) Nr. 5, S. 909-919.

179) V. Magdanz, B. Koch, S. Sanchez, O.G. Schmidt, *Sperm dynamics in tubular confi nement*, Small 11 (2015), S. 781-785.

180) V. Magdanz, M. Medina-Sanchez, Y. Chen, M. Guix, O.G. Schmidt, *How to Improve Spermbot Performance*, Advanced Functional Materials 25 (2015) Nr. 18, S. 2763-2770.

181) S.I. Makarov, M. Krautz, S. Salamon, K. Skokov, C.S. Teixeira, O. Gutfleisch, H. Wende, W. Keune, *Local electronic and magnetic properties of pure and Mn-containing magnetocaloric $LaFe_{13-x}Si_x$ compounds inferred from Mössbauer spectroscopy and magnetometry*, Journal of Physics D: Applied Physics 48 (2015) Nr. 30, S. 305006/1-12.

182) S. Makharza, O. Vittorio, G. Cirillo, S. Oswald, E. Hinde, M. Kavallaris, B. Buechner, M. Mertig, S. Hampel, *Graphene Oxide - Gelatin Nanohybrids as Functional Tools for Enhanced Carboplatin Activity in Neuroblastoma Cells*, Pharmaceutical Research 32 (2015) Nr. 16, S. 2132-2143.

183) K. Manna, A.K. Bera, M. Jain, S. Elizabeth, M.S. Yusuf, P.S. Anil Kumar, *Structural-modulation-driven spin canting and reentrant glassy magnetic phase in ferromagnetic Lu_2MnNiO_6*, Physical Review B 91 (2015) Nr. 22, S. 224420/1-7.

184) L.A.B. Marcal, M.-I. Richard, R. Magalhaes-Paniago, F. Cavallo, M.G. Lagally, O.G. Schmidt, T.U. Schuelli, Ch. Deneke, A. Malachias, *Direct evidence of strain transfer for InAs island growth on compliant Si substrates*, Applied Physics Letters 106 (2015) Nr. 15, S. 151905/1-5.

185) D. Marko, I. Soldatov, M. Tekielak, R. Schaefer, *Stray-field-induced Faraday contributions in wide-field Kerr microscopy and -magnetometry*, Journal of Magnetism and Magnetic Materials 396 (2015), S. 9-15.

186) P. Marra, R. Citro, C. Ortix, *Fractional quantization of the topological charge pumping in a one-dimensional superlattice*, Physical Review B 91 (2015) Nr. 12, S. 125411/1-7.

187) M. Matczak, R. Schaefer, M. Urbaniak, B. Szymanski, P. Kuswik, A. Jarosz, M. Schmidt, J. Aleksiejew, S. Jurga, F. Stobiecki, *Domain wall generated by graded interlayer coupling in Co/Pt/Co film with perpendicular anisotropy*, Applied Physics Letters 107 (2015) Nr. 1, S. 12404/1-4.

188) P. Materne, S. Kamusella, R. Sarkar, T. Goltz, J. Spehling, H. Maeter, L. Harnagea, S. Wurmehl, B. Buechner, H. Luetkens, C. Timm, H.-H. Klauss, *Coexistence of superconductivity and magnetism in $Ca_{1-x}Na_xFe_2As_2$: Universal suppression of the magnetic order parameter in 122 iron pnictides*, Physical Review B 92 (2015) Nr. 13, S. 134511/1-15.

189) Ph. Materne, C. Koz, U.K. Roessler, M. Doerr, T. Goltz, H.H. Klauss, U. Schwarz, S. Wirth, S. Roessler, *Solitonic Spin-Liquid State Due to the Violation of the Lifshitz Condition in $Fe_{1+y}Te$*, Physical Review Letters 115 (2015) Nr. 17, S. 177203/1-5.

190) T. Matsuda, S. Partzsch, T. Tsuyama, E. Schierle, E. Weschke, J. Geck, T. Saito, S. Ishiwata, Y. Tokura, H. Wadati, *Observation of a Devil's Staircase in the Novel Spin-Valve System $SrCo_6O_{11}$*, Physical Review Letters 114 (2015) Nr. 23, S. 236403/1-5.

191) P. Mcguiness, O. Akdogan, A. Asali, S. Bance, F. Bittner, J.M.D. Coey, N.M. Dempsey, J. Fidler, D. Givord, O. Gutfleisch, M. Katter, D. Le Roy, S. Sanvito, T. Schrefl, L. Schultz, C. Schwoebl, M. Soderznik, S. Sturm, P. Tozman, K. Uestuener, M. Venkatesan, T.G. Woodcock, K. Zagar, S. Kobe, *Replacement and Original Magnet Engineering Options (ROMEOs): A European Seventh Framework Project to Develop Advanced Permanent Magnets Without, or with Reduced Use of, Critical Raw Materials*, JOM 67 (2015) Nr. 6, S. 1306-1317.

192) M. Melzer, M. Kaltenbrunner, D. Makarov, D.D. Karnaushenko, D. Karnaushenko, T. Sekitani, T. Someya, O.G. Schmidt, *Imperceptible magnetoelectronics*, Nature Communications 6 (2015), S. 6080/1-8.

193) M. Melzer, D. Karnaushenko, G. Lin, S. Baunack, D. Makarov, O.G. Schmidt, *Direct transfer of magnetic sensor devices to elastomeric supports for stretchable electronics*, Advanced Materials 27 (2015), S. 1333-1338.

194) M. Melzer, J.I. Moench, D. Makarov, Y. Zabila, G.S.C. Bermudez, D. Karnaushenko, S. Baunack, F. Bahr, C. Yan, M. Kaltenbrunner, O.G. Schmidt, *Wearable magnetic field sensors for flexible electronics*, Advanced Materials 27 (2015), S. 1274-1280.

195) R.G. Mendes, B. Koch, A. Bachmatiuk, X. Ma, S. Sanchez, C. Damm, O.G. Schmidt, T. Gemming, J. Eckert, M.H. Ruemmli, *A size dependent evaluation of the cytotoxicity and uptake of nanographene oxide*, Journal of Materials Chemistry B 3 (2015) Nr. 12, S. 2522-2529.

196) S. Miao, D. Chen, A. Madani, M.R. Jorgensen, V.A. Bolanos Quinones, L. Ma, G.H. Hickey, A. Eychmueller, O.G. Schmidt, *Optofluidic Sensor: Evaporation Kinetics Detection of Solvents Dissolved with Cd_3P_2 Colloidal Quantum Dots in a Rolled-Up Microtube*, Advanced Optical Materials 3 (2015) Nr. 2, S. 187-193.

197) M. Mietschke, S. Oswald, S. Faehler, L. Schultz, R. Huehne, *Tuning structure in epitaxial $Pb(Mg_{1/3}Nb_{2/3})O_3$-$PbTiO_3$ thin films by using miscut substrates*, Thin Solid Films 589 (2015), S. 792-797.

198) D. Mikhailova, J.M. Engel, M. Schmidt, A.A. Tsirlin, H. Ehrenberg, *Copper(II) perrhenate $Cu(C_3H_7OH)_2(ReO_4)_2$: Synthesis from isopropanol and $CuReO_4$, structure and properties*, Journal of Solid State Chemistry 232 (2015), S. 264-269.

199) D. Mikhailova, A. Voss, S. Oswald, A.A. Tsirlin, M. Schmidt, A. Senyshyn, J. Eckert, H. Ehrenberg, *Lithium Insertion into Li_2MoO_4: Reversible Formation of $(Li_3Mo)O_4$ with a Disordered Rock-Salt Structure*, Chemistry of Materials 27 (2015) Nr. 12, S. 4485-4492.

200) V.A. Miluykov, I.A. Bezkishko, L.R. Kochetkova, O.N. Kataeva, T.P. Gerasimova, S.A. Katsyuba, O.G. Sinyashin, P. Loennecke, E. Hey-Hawkins, A. Parameswaran, Y. Krupskaya, Kataevc V., B. Buechner, *Synthesis and magnetic properties of manganese carbonyl complexes with different coordination modes of 3,4,5-triaryl-1,2-diphospholide ligands*, Dalton Transactions 44 (2015) Nr. 22, S. 10259-10266.

201) T. Mix, K.-H. Mueller, L. Schultz, T.G. Woodcock, *Formation and magnetic properties of the $L1_0$ phase in bulk, powder and hot compacted Mn-Ga alloys*, Journal of Magnetism and Magnetic Materials 391 (2015), S. 89-95.

202) I.J. Moench, F. Bahr, M. Melzer, D. Karnaushenko, D. Makarov, W. Hofmann, O.G. Schmidt, *Flexible Hall Sensorics for Flux-Based Control of Magnetic Levitation*, IEEE Transactions on Magnetics 51 (2015) Nr. 11, S. 1-4.

203) S. Molatta, S. Haindl, S. Trommler, M. Schulze, S. Wurmehl, R. Huehne, *Interface control by homoepitaxial growth in pulsed laser deposited iron chalcogenide thin films*, Scientific Reports 5 (2015), S. 16334/1-7.

204) M. Molina, M. Asadian-Birjand, J. Balach, J. Bergueiro, E. Miceli, M. Calderon, *Stimuli-responsive nanogel composites and their application in nanomedicine*, Chemical Society Reviews 44 (2015) Nr. 17, S. 6161-6186.

205) L. Molina-Luna, M. Duerrschnabel, S. Turner, M. Erbe, G.T. Martinez, S. van Aert, B. Holzapfel, G. van Tendeloo, *Atomic and electronic structures of $BaHfO_3$-doped TFA-MOD-derived $YBa_2Cu_3O_{7-delta}$ thin films*, Superconductor Science and Technology 28 (2015) Nr. 11.

206) M. Moore, A. Gebert, M. Stoica, M. Uhlemann, W. Loser, *A route for recycling Nd from Nd-Fe-B magnets using Cu melts*, Journal of Alloys and Compounds 647 (2015), S. 997-1006.

207) M. Moore, S. Roth, A. Gebert, L. Schultz, O. Gutfleisch, *The effect of surface grain reversal on the AC losses of sintered Nd-Fe-B permanent magnets*, Journal of Magnetism and Magnetic Materials 375 (2015), S. 43-48.

208) E. Mueller, B. Mahns, B. Buechner, M. Knupfer, *An electron energy-loss study of picene and chrysene based charge transfer salts*, The Journal of Chemical Physics 142 (2015) Nr. 18, S. 184702/1-4.

209) G. Mutschke, K. Tschulik, M. Uhlemann, J. Froehlich, *Numerical simulation of the mass transfer of magnetic species at electrodes exposed to small-scale gradients of the magnetic field*, Magnetohydrodynamics 51 (2015) Nr. 2, S. 369-374.

210) S. Nayak, S. Thota, D.C. Joshi, M. Krautz, A. Waske, A. Behler, J. Eckert, T. Sarkar, M.S. Andersson, R. Mathieu, V. Narang, M.S. Seehra, *Magnetic compensation, field-dependent magnetization reversal, and complex magnetic ordering in Co_2TiO_4*, Physical Review B 92 (2015) Nr. 21, S. 214434/1-10.

211) E. Nazarova, N. Balchev, K. Nenkov, K. Buchkov, D. Kovacheva, A. Zahariev, G. Fuchs, *Improvement of the superconducting properties of polycrystalline FeSe by silver addition*, Superconductor Science and Technology 28 (2015) Nr. 12, S. 125013/1-8.

212) E. Nazarova, N. Balchev, K. Nenkov, K. Buchkov, D. Kovacheva, A. Zahariev, G. Fuchs, *Transport and pinning properties of Ag doped $FeSe_{0.94}$*, Superconductor Science and Technology 28 (2015) Nr. 2, S. 25013/1-8.

213) E. Nazarova, K. Buchkov, S. Terzieva, K. Nenkov, A. Zahariev, D. Kovacheva, N. Balchev, G. Fuchs, *The effect of Ag addition on the superconducting properties of $FeSe_{0.94}$*, Journal of Superconductivity and Novel Magnetism 28 (2015), S. 1135-1138.

214) D. Niarchos, G. Giannopoulos, M. Gjoka, C. Sarafidis, V. Psycharis, J. Rusz, A. Edstroem, O. Eriksson, P. Toson, J. Fidler, E. Anagnostopoulou, U. Sanyal, F. Ott, L.-M. Lacroix, G. Viau, C. Bran, M. Vazquez, L. Reichel, L. Schultz, S. Faehler, *Toward Rare-Earth-Free Permanent Magnets: A Combinatorial Approach Exploiting the Possibilities of Modeling, Shape Anisotropy in Elongated Nanoparticles, and Combinatorial Thin-Film Approach*, JOM 67 (2015) Nr. 6, S. 1318-1328.

215) S. Nishimoto, S.-L. Drechsler, R. Kuzian, J. Richter, J. van den Brink, *Interplay of interchain interactions and exchange anisotropy: Stability and fragility of multipolar states in spin-1/2 quasi-one-dimensional frustrated helimagnets*, Physical Review B 92 (2015) Nr. 21, S. 214415/1-15.

216) S. Nishimoto, M. Nakamura, *Non-symmetry-breaking ground state of the S=1 Heisenberg model on the kagome lattice*, Physical Review B 92 (2015) Nr. 14, S. 140412/1-5.

217) S. Niyomsoan, P. Gargarella, N. Chomsaeng, P. Termsuksawad, U. Kuehn, J. Eckert, *Phase Separation in Rapid Solidified Ag-rich Ag-Cu-Zr Alloys*, Materials Research 18 (2015) Nr. Supl. 1.

218) F.S. Nogueira, A. Sudbo, I. Eremin, *Higgs mechanism, phase transitions, and anomalous Hall effect in three-dimensional topological superconductors*, Physical Review B 92 (2015) Nr. 22, S. 224507/1-9.

219) C. Nowka, L. Veyrat, S. Gorantla, U. Steiner, B. Eichler, O.G. Schmidt, H. Funke, J. Dufouleur, B. Buechner, R. Griaud, S. Hampel, *Catalyst-free Growth of Single Crystalline Bi_2Se_3 Nanostructures for Quantum Transport Studies*, Crystal Growth and Design 15 (2015) Nr. 9, S. 4272-4278.

220) Z. Nussinov, J. van den Brink, *Compass models: Theory and physical motivations*, Reviews of Modern Physics 87 (2015) Nr. 1, S. 1-59.

221) T. Oka, H. Ota, T. Shimoda, J. Ogawa, S. Fukui, T. Sato, K. Yokoyama, A. Murakami, M. Langer, *Preferential Magnetic Flux Invasion and Heat Generation Owing to Macrostructure in HTS Bulk Magnets in Pulse Field Magnetization Processes*, IEEE Transactions on Applied Superconductivity 25 (2015) Nr. 3, S. 6800904/1-4.

222) I.V. Okulov, M.F. Sarmanova, A.S. Volegov, A. Okulov, U. Kuehn, W. Skrotzki, J. Eckert, *Effect of boron on microstructure and mechanical properties of multicomponent titanium alloys*, Materials Letters 158 (2015), S. 111-114.

223) I.V. Okulov, I.V. Soldatov, M.F. Sarmanova, I. Kaban, T. Gemming, K. Edstroem, J. Eckert, *Flash Joule heating for ductilization of metallic glasses*, Nature Communications 6 (2015), S. 7932/1-6.

224) I.V. Okulov, H. Wendrock, A.S. Volegov, H. Attar, U. Kuehn, W. Skrotzki, J. Eckert, *High strength beta titanium alloys: New design approach*, Materials Science and Engineering: A 628 (2015), S. 297-302.

225) R.B. Onyancha, J. Shimoyama, S.J. Singh, H. Ogino, V.V. Srinivasu, *Observation of a Structure and Line Shape Evolution of Non-resonant Microwave Absorption in a SmFeAs(O, F) Polycrystalline Iron Pnictide Superconductor*, Journal of Superconductivity and Novel Magnetism 28 (2015) Nr. 10, S. 2927-2934.

226) B. Op de Beeck, M. Dusselier, J. Geboers, J. Holsbeek, E. Morre, S. Oswald, L. Giebeler, B.F. Sels, *Direct catalytic conversion of cellulose to liquid straight-chain alkanes*, Energy and Environmental Science 8 (2015), S. 230-240.

227) C. Ortix, *Quantum mechanics of a spin-orbit coupled electron constrained to a space curve*, Physical Review B 91 (2015) Nr. 24, S. 245412/1-4.

228) M. Oschatz, M. Zeiger, N. Jaeckel, P. Strubel, L. Borchardt, R. Reinhold, W. Nickel, J. Eckert, V. Presser, S. Kaskel, *Emulsion soft templating of carbide-derived carbon nanospheres with controllable porosity for capacitive electrochemical energy storage*, Journal of Materials Chemistry A 3 (2015) Nr. 35, S. 17983-17990.

229) S. Oswald, *Binding energy referencing for XPS in alkali metal-based battery materials research (I): Basic model investigations*, Applied Surface Science 351 (2015), S. 492-503.

230) C. Pacchierotti, V. Magdanz, M. Medina-Sánchez, O.G. Schmidt, D. Prattichizzo, S. Misra, *Intuitive control of self-propelled microjets with haptic feedback*, Journal of Micro-Bio Robotics 10 (2015) Nr. 1, S. 37-53.

231) P. Pahlke, M. Hering, M. Sieger, M. Lao, M. Eisterer, A. Usoskin, J. Stroemer, B. Holzapfel, L. Schultz, R. Huehne, *Thick high J_c YBCO films on ABAD-YSZ templates*, IEEE Transactions on Applied Superconductivity 25 (2015) Nr. 3, S. 6603804/1-4.

232) S. Pan, Y. Zhao, G. Huang, J. Wang, S. Baunack, T. Gemming, M. Li, L. Zheng, O.G. Schmidt, Y. Mei, *Highly photocatalytic TiO_2 interconnected porous powder fabricated by sponge-templated atomic layer deposition*, Nanotechnology 26 (2015) Nr. 36, S. 364001/1-6.

233) J. Pang, A. Bachmatiuk, L. Fu, R.G. Mendes, M. Libera, D. Placha, G.S. Martynkova, B. Trzebicka, T. Gemming, J. Eckert, M.H. Ruemmeli, *Direct synthesis of graphene from adsorbed organic solvent molecules over copper*, RSC Advances 5 (2015) Nr. 75, S. 60884-60891.

234) J. Pang, A. Bachmatiuk, L. Fu, C. Yan, M. Zeng, J. Wang, B. Trzebicka, T. Gemming, J. Eckert, M.H. Rummeli, *Oxidation as A Means to Remove Surface Contaminants on Cu Foil Prior to Graphene Growth by Chemical Vapor Deposition*, The Journal of Physical Chemistry C 119 (2015) Nr. 23, S. 13363-13368.

235) A. Panigrahi, M. Boenisch, T. Waitz, E. Schafler, M. Calin, J. Eckert, W. Skrotzki, M. Zehetbauer, *Phase transformations and mechanical properties of biocompatible Ti-16.1Nb processed by severe plastic deformation*, Journal of Alloys and Compounds 628 (2015), S. 434-441.

236) J.M. Park, K.H. Park, E.S. Park, S.-M. Hong, S.Y. Kim, S.S. Jee, E.S. Lee, S.J. Kim, K.B. Kim, D.H. Kim, J. Eckert, *Effect of Metallic Glass Particle Size on the Contact Resistance of Ag/Metallic Glass Electrode*, Metallurgical and Materials Transactions A 46 (2015) Nr. 6, S. 2443-2448.

237) R. Parthiban, M. Stoica, I. Kaban, R. Kumar, J. Eckert, *Viscosity and fragility of the supercooled liquids and melts from the Fe-Co-B-Si-Nb and Fe-Mo-P-C-B-Si glass-forming alloy systems*, Intermetallics 66 (2015), S. 48-55.

238) C. Pauly, B. Rasche, K. Koepernik, M. Liebmann, M. Pratzer, M. Richter, J. Kellner, M. Eschbach, B. Kaufmann, L. Plucinski, C.M. Schneider, M. Ruck, J. van den Brink, M. Morgenstern, *Subnanometre-wide electron channels protected by topology*, Nature Physics 11 (2015) Nr. 4, S. 338-343.

239) O. Perevertov, J. Thielsch, R. Schaefer, *Effect of applied tensile stress on the hysteresis curve and magnetic domain structure of grain-oriented transverse Fe-3%Si steel*, Journal of Magnetism and Magnetic Materials 385 (2015), S. 358-367.

240) N. Perez, M. Melzer, D. Makarov, O. Ueberschaer, R. Ecke, S.E. Schulz, O.G. Schmidt, *High-performance giant magnetoresistive sensorics on flexible Si membranes*, Applied Physics Letters 106 (2015) Nr. 15, S. 153501/1-5.

241) I. Pethes, I. Kaban, R.-P. Wang, B. Luther-Davies, P. Jovari, *Short range order in Ge-As-Se glasses*, Journal of Alloys and Compounds 623 (2015), S. 454-459.

242) U. Pfaff, A. Hildebrandt, M. Korb, D. Schaarschmidt, M. Rosenkranz, A. Popov, H. Lang, *Five-Membered Heterocycles as Linking Units in Strongly Coupled Homobimetallic Group 8 Metal Half-Sandwich Complexes*, Organometallics 34 (2015) Nr. 12, S. 2826-2840.

243) A.A. Piarristeguy, M. Micoulaut, R. Escalier, P. Jovari, I. Kaban, J. van Eijk, J. Luckas, S. Ravindren, P. Boolchand, A. Pradel, *Structural singularities in Ge_xTe_{100-x} films*, The Journal of Chemical Physics 143 (2015) Nr. 7, S. 74502/1-9.

244) G. Pireddu, A. Valentoni, C. Bonatto Minella, C. Pistidda, C. Milanese, S. Enzo, G. Mulas, S. Garroni, *Comparison of the thermochemical and mechanochemical transformations in the $2NaNH_2$-MgH_2 system*, International Journal of Hydrogen Energy 40 (2015) Nr. 4, S. 1829-1835.

245) D. Pohl, S. Schneider, J. Rusz, B. Rellinghaus, *Electron vortex beams prepared by a spiral aperture with the goal to measure EMCD on ferromagnetic films via STEM*, Ultramicroscopy 150 (2015), S. 16-22.

246) G. Pollefeyt, A. Meledin, C. Pop, S. Ricart, R. Huehne, G. van Tendeloo, I. van Driessche, *Chemical stability of $YBiO_3$ buffer layers for implementation in $YBa_2Cu_3O_{7-delta}$ coated conductors*, Acta Materialia 100 (2015), S. 224-231.

247) G. Prando, T. Hartmann, W. Schottenhammel, Z. Guguchia, S. Sanna, F. Ahn, I. Nekrasov, C.G.F. Blum, A.U.B. Wolter, S. Wurmehl, R. Khasanov, I. Eremin, B. Buechner, *Mutual Independence of Critical Temperature and Superfluid Density under Pressure in Optimally Electron-Doped Superconducting $LaFeAsO_{1-x}F_x$*, Physical Review Letters 114 (2015) Nr. 24, S. 247004/1-6.

248) G. Prando, G. Profeta, A. Continenza, R. Khasanov, A. Pal, V.P.S. Awana, B. Buechner, S. Sanna, *Common effect of chemical and external pressures on the magnetic properties of RCoPO (R = La, Pr, Nd, Sm). II.*, Physical Review B 92 (2015) Nr. 14, S. 144414/1-9.

249) G. Prando, S. Sanna, R. Khasanov, A. Pal, E.M. Bruening, M. Mazzani, V.P.S. Awana, B. Buechner, R. De Renzi, *Effect of external pressure on the magnetic properties of RCoAsO (R=La, Pr, Sm): a mySR study*, Journal of Physics and Chemistry of Solids 84 (2015), S. 63-69.

250) K.G. Prashanth, H. Shakur Shahabi, H. Attar, V.C. Srivastava, N. Ellendt, V. Uhlenwinkel, J. Eckert, S. Scudino, *Production of high strength $Al_{85}Nd_8Ni5Co_2$ alloy by selective laser melting*, Additive Manufacturing 6 (2015), S. 1-5.

251) K. Prokes, M. Schulze, S. Hartwig, N. Schaefer, S. Landsgesell, C.G.F. Blum, D. Abou-Ras, M.Y. Hacisalihoglu, E. Ressouche, B. Ouladdiaf, B. Buechner, S. Wurmehl, *Structural inhomogeneities in $FeTe_{0.6}Se_{0.4}$: Relation to superconductivity*, Journal of Crystal Growth 432 (2015), S. 95-104.

252) B. Pulko, J. Tusek, J.D. Moore, B. Weise, K. Skokov, O. Mityashkin, A. Kitanovski, C. Favero, P. Fajfar, O. Gutfleisch, A. Waske, A. Poredos, *Epoxy-bonded La-Fe-Co-Si magnetocaloric plates*, Journal of Magnetism and Magnetic Materials 375 (2015), S. 65-73.

253) O.V. Pylypovskyi, V.P. Kravchuk, D.D. Sheka, D. Makarov, O.G. Schmidt, Y. Gaididei, *Coupling of Chiralities in Spin and Physical Spaces: The Moebius Ring as a Case Study*, Physical Review Letters 114 (2015) Nr. 19, S. 197204/1-5.

254) X.M. Qin, J. Tan, C.J. Li, X.C. Wang, Y.H. Jiang, R. Zhou, *On the formation, mechanical properties and crystallization behaviors of a $Zr_{56}Co_{24}Al_{20}$ bulk metallic glass*, Journal of Alloys and Compounds 647 (2015), S. 204-208.

255) H.T. Quang, A. Bachmatiuk, A. Dianat, F. Ortmann, J. Zhao, J.H. Warner, J. Eckert, G. Cunniberti, M.H. Ruemmeli, *In Situ Observations of Free-Standing Graphene-like Mono- and Bilayer ZnO Membranes*, ACS Nano 9 (2015) Nr. 11, S. 11408-11413.

256) G.K. Rane, S. Menzel, M. Seifert, T. Gemming, J. Eckert, *Tungsten/molybdenum thin films for application as interdigital transducers on high temperature stable piezoelectric substrates $La_3Ga_5SiO_{14}$ and $Ca_3TaGa_3Si_2O_{14}$*, Materials Science and Engineering B 202 (2015), S. 31-38.

257) C.F. Reiche, J. Koerner, B. Buechner, T. Muehl, *Introduction of a co-resonant detection concept for mechanical oscillation-based sensors*, Nanotechnology 26 (2015) Nr. 33, S. 335501/1-9.

258) C.F. Reiche, S. Vock, V. Neu, L. Schultz, B. Buechner, T. Muehl, *Bidirectional quantitative force gradient microscopy*, New Journal of Physics 17 (2015), S. 13014/1-10.

259) L. Reichel, L. Schultz, S. Faehler, *Lattice relaxation studies in strained epitaxial Fe-Co-C films*, Journal of Applied Physics 117 (2015) Nr. 17, S. 17C712/1-4.

260) L. Reichel, L. Schultz, D. Pohl, S. Oswald, S. Faehler, M. Werwinski, A. Edstroem, E.K. Delczeg-Czirjak, J. Rusz, *From soft to hard magnetic Fe-Co-B by spontaneous strain: a combined first principles and thin film study*, Journal of Physics: Condensed Matter 27 (2015) Nr. 47, S. 1-14.

261) S. Reja, R. Ray, J. van den Brink, S. Kumar, *Coupled spin-charge order in frustrated itinerant triangular magnets*, Physical Review B 91 (2015) Nr. 14, S. 140403/1-5.

262) R.O. Rezaev, E.A. Levchenko, O.G. Schmidt, V.M. Fomin, *Dynamics of the Abrikosov Vortices on Cylindrical Microtubes*, Russian Physics Journal 58 (2015) Nr. 5, S. 623-628.

263) H. Richert, H. Schmidt, S. Lindner, M. Lindner, B. Wenzel, R. Holzhey, R. Schaefer, *Dynamic Magneto-Optical Imaging of Domains in Grain-Oriented Electrical Steel*, Steel Research International online first (2015).

264) C. Rieger, D. Kunhardt, A. Kaufmann, D. Schendel, D. Huebner, K. Erdmann, S. Propping, M.P. Wirth, B. Schwenzer, S. Fuessel, S. Hampel, *Characterization of different carbon nanotubes for the development of a mucoadhesive drug delivery system for intravesical treatment of bladder cancer*, International Journal of Pharmaceutics 479 (2015) Nr. 2, S. 357-363.

265) T. Ritschel, J. Trinckauf, K. Koepernik, B. Buechner, M. von Zimmermann, H. Berger, Y.I. Joe, P. Abbamonte, J. Geck, *Orbital textures and charge density waves in transition metal dichalcogenides*, Nature Physics 11 (2015), S. 328-331.

266) P. Robaschik, M. Fronk, M. Toader, S. Klyatskaya, F. Ganss, P.F. Siles, O.G. Schmidt, M. Albrecht, M. Hietschold, M. Ruben, D.R.T. Zahn, G. Salvan, *Tuning the magneto-optical response of $TbPc_2$ single molecule magnets by the choice of the substrate*, Journal of Materials Chemistry C 3 (2015) Nr. 31, S. 8039-8049.

267) S. Roessler, C. Koz, L. Jiao, U.K. Roessler, F. Steglich, U. Schwarz, S. Wirth, *Emergence of an incipient ordering mode in FeSe*, Physical Review B 92 (2015) Nr. 6, S. 60505/1-5.

268) J. Romhanyi, G. Burkard, A. Palyi, *Subharmonic transitions and Bloch-Siegert shift in electrically driven spin resonance*, Physical Review B 92 (2015) Nr. 5, S. 54422/1-15.

269) J. Romhanyi, K. Penc, R. Ganesh, *Hall effect of triplons in a dimerized quantum magnet*, Nature Communication 6 (2015), S. 6805/1-6.

270) F. Roth, M. Herzig, C. Lupulescu, E. Darlatt, A. Gottwald, M. Knupfer, W. Eberhardt, *Electronic properties of Mn-phthalocyanine-C_{60} bulk heterojunctions: Combining photoemission and electron energy-loss spectroscopy*, Journal of Applied Physics 118 (2015) Nr. 18, S. 185310/1-6.

271) F. Roth, M. Knupfer, *Electronic excitation spectrum of doped organic thin films investigated using electron energy-loss spectroscopy*, Journal of Electron Spectroscopy and Related Phenomena 204 (2015) Nr. Part A, S. 23-28.

272) F. Roth, M. Knupfer, *Impact of potassium doping on the electronic structure of tetracene and pentacene: An electron energy-loss study*, The Journal of Chemical Physics 143 (2015) Nr. 15, S. 154708/1-5.

273) F. Roth, M. Nohr, S. Hampel, M. Knupfer, *Low-energy exciton pocket at finite momentum in tetracene molecular solids*, epl 112 (2015) Nr. 3, S. 37004/1-5.

274) K.O. Ruotsalainen, C.J. Sahle, T. Ritschel, J. Geck, M. Hosoda, C. Bell, Y. Hikita, H.Y. Hwang, T.T. Fister, R.A. Gordon, K. Haemaelaeinen, M. Hakala, S. Huotari, *Inelastic x-ray scattering in heterostructures: electronic excitations in $LaAlO_3/SrTiO_3$*, Journal of Physics: Condensed Matter 27 (2015) Nr. 33, S. 335501/1-10.

275) M. Samadi Khoshkhoo, S. Scudino, T. Gemming, J. Thomas, J. Freudenberger, M. Zehetbauer, C.C. Koch, J. Eckert, *Nanostructure formation mechanism during in-situ consolidation of copper by room-temperature ball milling*, Materials and Design 65 (2015), S. 1083-1090.

276) K.L. San, T.T. Clikeman, C. Dubceac, A.A. Popov, Y.-S. Chen, M.A. Petrukhina, S.H. Strauss, O.V. Boltalina, *Corannulene Molecular Rotor with Flexible Perfluorobenzyl Blades: Synthesis, Structure and Properties*, Chemistry - A European Journal 21 (2015) Nr. 26, S. 9488-9492.

277) L.K. San, E.V. Bukovsky, B.W. Larson, J.B. Whitaker, S.H.M. Deng, N. Kopidakis, G. Rumbles, A.A. Popov, Y.-S. Chen, X.-B. Wang, O.V. Boltalina, S.H. Strauss, *A faux hawk fullerene with PCBM-like properties*, Chemical Science 6 (2015) Nr. 3, S. 1801-1815.

278) B. Sarac, D. Sopu, E. Park, J.K. Hufenbach, S. Oswald, M. Stoica, J. Eckert, *Mechanical and Structural Investigation of Porous Bulk Metallic Glasses*, Metals 5 (2015) Nr. 2, S. 920-933.

279) S. Sawatzki, T.G. Woodcock, K. Gueth, K.-H. Mueller, O. Gutfleisch, *Calculation of remanence and degree of texture from EBSD orientation histograms and XRD rocking curves in Nd-Fe-B sintered magnets*, Journal of Magnetism and Magnetic Materials 382 (2015), S. 219-224.

280) V. Sayevich, N. Gaponik, M. Ploetner, M. Kruszynska, T. Gemming, V.M. Dzhagan, S. Akhavan, D.R.T. Zahn, H.V. Demir, A. Eychmueller, *Stable Dispersion of Iodide-Capped PbSe Quantum Dots for High-Performance Low-Temperature Processed Electronics and Optoelectronics*, Chemistry of Materials 27 (2015) Nr. 12, S. 4328-4337.

281) B. Schleicher, R. Niemann, A. Diestel, R. Huehne, L. Schultz, S. Faehler, *Epitaxial Ni-Mn-Ga-Co thin films on PMN-PT substrates for multicaloric applications*, Journal of Applied Physics 118 (2015) Nr. 5, S. 53906/1-6.

282) C. Schliebe, T. Gemming, J. Noll, L. Mertens, M. Mehring, A. Seifert, S. Spange, H. Lang, *Zirconium and Hafnium Twin Monomers for Mixed Oxides*, ChemPlusChem 80 (2015) Nr. 3, S. 559-567.

283) C. Schliebe, U. Pfaff, T. Gemming, C. Lochenie, B. Weber, H. Lang, *$Si(OCH_2Fc)_4$: Synthesis, Electrochemical Behavior, and Twin Polymerization*, European Journal of Inorganic Chemistry 23 (2015), S. 3850-3860.

284) F. Schmidt, D. Pohl, L. Schultz, B. Rellinghaus, *Segregation phenomena in Nd-Fe-B nanoparticles*, Journal of Nanoparticle Research 14 (2015) Nr. 4, S. 17:170/1-15.

285) S. Schoenecker, X. Li, K. Koepernik, B. Johansson, L. Vitos, M. Richter, *Metastable cubic and tetragonal phases of transition metals predicted by density-functional theory*, RSC Advances 5 (2015) Nr. 85, S. 69680-69689.

286) S. Schoenecker, M. Richter, K. Koepernik, H. Eschrig, *Prediction of first-order martensitic transitions in strained epitaxial films*, New Journal of Physics 17 (2015), S. 23005/1-7.

287) F.J.R. Schuelein, E. Zallo, P. Atkinson, O.G. Schmidt, R. Trotta, A. Rastelli, A. Wixforth, H.J. Krenner, *Fourier synthesis of radiofrequency nanomechanical pulses with different shapes*, Nature Nanotechnology Letter 10 (2015) Nr. 6, S. 512-516.

288) R. Schuster, J. Trinckauf, C. Habenicht, M. Knupfer, B. Buechner, *Anisotropic Particle-Hole Excitations in Black Phosphorus*, Physical Review Letters 115 (2015) Nr. 2, S. 26404/1-5.

289) H. Schwab, K.G. Prashanth, L. Loeber, U. Kuehn, J. Eckert, *Selective Laser Melting of Ti-45Nb Alloy*, Metals 5 (2015) Nr. 2, S. 686-694.

290) T. Schwarz, R. Woelbing, C.F. Reiche, B. Mueller, M.J. Martínez-Perez, T. Muehl, B. Buechner, R. Kleiner, D. Koelle, *Low-Noise $YBa_2Cu_3O_7$ Nano-SQUIDs for Performing Magnetization-Reversal Measurements on Magnetic Nanoparticles*, Physical Review Applied 3 (2015) Nr. 4, S. 44011/1-10.

291) K. Schwedtmann, S. Schulz, F. Hennersdorf, T. Strassner, E. Dmitrieva, J.J. Weigand, *Synthesis and EPR/UV/Vis-NIR Spectro-electrochemical Investigation of a Persistent Phosphanyl Radical Dication*, Angewandte Chemie 127 (2015) Nr. 38, S. 11206-11210.

292) S. Scudino, H. Shakur Shahabi, M. Stoica, I. Kaban, B. Escher, U. Kuehn, G.B.M. Vaughan, J. Eckert, *Structural features of plastic deformation in bulk metallic glasses*, Applied Physics Letters 106 (2015) Nr. 3, S. 31903/1-5.

293) S. Scudino, M. Stoica, I. Kaban, K.G. Prashanth, G.B.M. Vaughan, J. Eckert, *Length scale-dependent structural relaxation in $Zr_{57.5}Ti_{7.5}Nb_5Cu_{12.5}Ni_{10}Al_{7.5}$ metallic glass*, Journal of Alloys and Compounds 639 (2015), S. 465-469.

294) S. Scudino, C. Unterdoerfer, K.G. Prashanth, H. Attar, N. Ellendt, V. Uhlenwinkel, J. Eckert, *Additive manufacturing of Cu-10Sn bronze*, Materials Letters 156 (2015), S. 202-204.

295) M. Seifert, S.B. Menzel, G.K. Rane, H. Hoffmann, T. Gemming, *RuAl thin films on high-temperature piezoelectric substrates*, Materials Research Express 2 (2015) Nr. 8, S. 85001/1-7.

296) M. Seifert, G.K. Rane, B. Kirbus, S.B. Menzel, T. Gemming, *Surface Effects and Challenges for Application of Piezoelectric Langasite Substrates in Surface Acoustic Wave Devices Caused by High Temperature Annealing under High Vacuum*, Materials 8 (2015) Nr. 12, S. 8868-8876.

297) H. Shakur Shahabi, S. Scudino, I. Kaban, M. Stoica, U. Ruett, U. Kuehn, J. Eckert, *Structural aspects of elasto-plastic deformation of a Zr-based bulk metallic glass under uniaxial compression*, Acta Materialia 95 (2015), S. 30-36.

298) A.K. Sharifabadi, A. Madani, M. Raoufi, *The Influence of Cu^{+2} Concentration on the Magnetic Properties and Microstructure of Pulse Electrodeposited $Co_x Cu_{1-x}$ Nanowire Arrays*, Journal of Nanoscience and Nanotechnology 15 (2015) Nr. 9, S. 6699-6703.

299) D.A. Shishkin, A.V. Proshkin, N.V. Selezneva, E.G. Gerasimov, P.B. Terentev, A.M. Chirkova, K. Nenkov, L. Schultz, N.V. Baranov, *Effect of rapid quenching on the magnetic state, electrical resistivity and thermomagnetic properties of Gd_3Co*, Journal of Alloys and Compounds 647 (2015), S. 481-485.

300) M. Sieger, J. Haenisch, P. Pahlke, M. Sparing, U. Gaitzsch, K. Iida, R. Nast, E. Reich, L. Schultz, B. Holzapfel, R. Huehne, *BaHfO3-doped thick $YBa_2Cu_3O_{7-delta}$ films on highly alloyed textured Ni-W tapes*, IEEE Transactions on Applied Superconductivity 25 (2015) Nr. 3, S. 6602604/1-4.

301) F. Silze, G. Wiehl, I. Kaban, U. Kuehn, J. Eckert, S. Pauly, *Effect of Ga on the Wettability of CuGa10 on 304L Steel*, Metallurgical and Materials Transactions B 46 (2015) Nr. 4, S. 1647-1653.

302) L. Simkova, E. Dmitrieva, J. Klima, L. Dunsch, J. Ludvik, *(Spectro) Electrochemical investigation of reduction mechanism of a new energetic molecule 2,2-dinitroethene-1,1-diamine (FOX-7) in aprotic solvents*, Journal of Solid State Electrochemistry 19 (2015), S. 103-112.

303) S.J. Singh, R. Beck, S. Wurmehl, C. Hess, B. Buechner, *Granular behavior observed in the polycrystalline superconducting LiFeAs*, Superconductor Science and Technology 28 (2015) Nr. 2, S. 25006/1-7.

304) S.J. Singh, J. Shimoyama, H. Ogino, K. Kishio, *Thermoelectric properties of FeAs based superconductors, with thick perovskite- and Sm-O fluorite-type blocking layers*, Physica C-Superconductivity and Its Applications 518 (2015), S. 18-22.

305) E. Smirnova, A. Sotnikov, H. Schmidt, M. Weihnacht, S. Sakharov, *Low-temperature dielectric behavior of disordered and ordered langasite family single crystals LGS, LGT, SNGS and STGS*, Journal of Physics and Chemistry of Solids 85 (2015), S. 91-95.

306) E.P. Smirnova, A.V. Sotnikov, N.V. Zaitseva, H. Schmidt, M. Weihnacht, *Dielectric properties of $SrTiO_3$-$DyScO_3$ solid solutions*, Physics of the Solid State 57 (2015) Nr. 11, S. 2241-2245.

307) L. Smykalla, P. Shukrynau, C. Mende, H. Lang, M. Knupfer, M. Hietschold, *Photoelectron spectroscopy investigation of the temperature-induced deprotonation and substrate-mediated hydrogen transfer in a hydroxyphenyl-substituted porphyrin*, Chemical Physics 450-451 (2015), S. 39-45.

308) I.H. Son, J.H. Park, S. Kwon, S. Park, M.H. Ruemmeli, A. Bachmatiuk, H.J. Song, J. Ku, J.W. Choi, J.-M. Choi, S.-G. Doo, H. Chang, *Silicon carbide-free graphene growth on silicon for lithium-ion battery with high volumetric energy density*, Nature Communications 6 (2015), S. 7393/1-8.

309) K.K. Song, D.Y. Wu, S. Pauly, C.X. Peng, L. Wang, J. Eckert, *Thermal stability of B2 CuZr phase, microstructural evolution and martensitic transformation in Cu-Zr-Ti alloys*, Intermetallics 67 (2015), S. 177-184.

310) D. Sopu, K. Albe, *Influence of grain size and composition, topology and excess free volume on the deformation behavior of Cu-Zr nanoglasses*, Beilstein Journal of Nanotechnology 6 (2015), S. 537-545.

311) D. Sopu, M. Stoica, J. Eckert, *Deformation behavior of metallic glass composites reinforced with shape memory nanowires studied via molecular dynamics simulations*, Applied Physics Letters 106 (2015) Nr. 21, S. 211902/1-4.

312) A.V. Sotnikov, E.P. Smirnova, H. Schmidt, M. Weihnacht, *Low-temperature elastic properties of $Sr_3NbGa_3Si_2O_{14}$ single crystals*, Physics of the Solid State 57 (2015) Nr. 6, S. 1183-1187.

313) M. Sparing, M. Hossain, D. Berger, A. Berger, A. Abdkader, G. Fuchs, C. Cherif, L. Schultz, *Superconducting magnetic bearing as twist element in textile machines*, IEEE Transactions on Applied Superconductivity 25 (2015) Nr. 3, S. 3600504/1-4.

314) U.G. Spizzirri, S. Hampel, G. Cirillo, M.V. Mauro, O. Vittorio, P. Cavalcanti, C. Giraldi, M. Curcio, N. Picci, F. Iemma, *Functional Gelatin-Carbon Nanotubes Nanohybrids With Enhanced Antibacterial Activity*, International Journal of Polymeric Materials and Polymeric Biomaterials 64 (2015) Nr. 9, S. 439-447.

315) F. Steckel, R. Beck, M. Roslova, M. Abdel-Hafiez, A.U.B. Wolter, I. Morozov, S. Wurmehl, C. Hess, B. Buechner, *Characterization of doped $Na(Fe_{1-x}T_x)As$ single crystals with T = Pd, Ni, Cr, and Mn*, Journal of Superconductivity and Novel Magnetism 28 (2015) Nr. 3, S. 1123-1127.

316) F. Steckel, M. Roslova, R. Beck, I. Morozov, S. Aswartham, D. Evtushinsky, C.G.F. Blum, M. Abdel-Hafiez, D. Bombor, J. Maletz, S. Borisenko, A.V. Shevelkov, Wolter A.U.B., C. Hess, S. Wurmehl, B. Buechner, *Crystal growth and electronic phase diagram of 4d-doped $Na_{1-delta}Fe_{1-x}Rh_xAs$ in comparison to 3d-doped $Na_{1-delta}Fe_{1-x}Co_xAs$*, Physical Review B 91 (2015) Nr. 18, S. 184516/1-9.

317) D. Steil, O. Schmitt, R. Fetzer, T. Kubota, H. Naganuma, M. Oogane, Y. Ando, S. Rodan, C.G.F. Blum, B. Balke, S. Wurmehl, M. Aeschlimann, M. Cinchetti, *Impact of local order and stoichiometry on the ultrafast magnetization dynamics of Heusler compounds*, Journal of Physics D: Applied Physics 48 (2015) Nr. 16, S. 164016/1-7.

318) M. Stoica, P. Ramasamy, I. Kaban, S. Scudino, M. Nicoara, G.B.M. Vaughan, J. Wright, R. Kumar, J. Eckert, *Structure evolution of soft magnetic $(Fe_{36}Co_{36}B_{19.2}Si_{4.8}Nb_4)_{100-x}Cu_x$ (x=0 and 0.5) bulk glassy alloys*, Acta Materialia 95 (2015), S. 335-342.

319) R. Streubel, P. Fischer, M. Kopte, O.G. Schmidt, D. Makarov, *Magnetization dynamics of imprinted non-collinear spin textures*, Applied Physics Letters 107 (2015) Nr. 11, S. 112406/1-4.

320) R. Streubel, L. Han, M-Y. Im, F. Kronast, U.K. Roessler, F. Radu, R. Abrudan, G. Lin, O.G. Schmidt, P. Fischer, D. Makarov, *Manipulating Topological States by Imprinting Non-Collinear Spin Textures*, Scientific Reports 5 (2015), S. 8787/1-7.

321) R. Streubel, F. Kronast, P. Fischer, D. Parkinson, O.G. Schmidt, D. Makarov, *Retrieving spin textures on curved magnetic thin films with full-field soft X-ray microscopies*, Nature Communications 6 (2015), S. 7612/1-11.

322) R. Streubel, F. Kronast, U.K. Roessler, O.G. Schmidt, D. Makarov, *Reconfigurable large-area magnetic vortex circulation patterns*, Physical Review B 92 (2015) Nr. 10, S. 104431/1-8.

323) C. Struzzi, N.I. Verbitskiy, A.V. Fedorov, A. Nefedov, O. Frank, Kalbac, M., G. Di Santo, M. Panighel, A. Goldoni, J. Gaertner, W. Weber, M. Weinl, M. Schreck, Ch. Woell, H. Sachdev, A. Grueneis, L. Petaccia, *High-quality graphene on single crystal Ir(111) films on Si(111) wafers: Synthesis and multi-spectroscopic characterization*, Carbon 81 (2015), S. 167-173.

324) R. Sueptitz, S. Horn, M. Stoica, M. Uhlemann, A. Gebert, *Electrochemical micromachining of passive electrodes - Application to bulk metallic glasses*, Journal of Materials Processing Technology 219 (2015), S. 193-198.

325) R. Sueptitz, S. Sawatzki, M. Moore, M. Uhlemann, O. Gutfleisch, A. Gebert, *Effect of DyF3 on the corrosion behavior of hot-pressed Nd-Fe-B permanent magnets*, Materials and Corrosion 66 (2015) Nr. 2, S. 152-157.

326) J. Sun, Y. Chen, M.K. Priydarshi, Z. Chen, A. Bachmatiuk, Z. Zou, Z. Chen, X. Song, Y. Gao, M.H. Ruemmeli, Y. Zhang, Z. Liu, *Direct Chemical Vapor Deposition-Derived Graphene Glasses Targeting Wide Ranged Applications*, Nano Letters 15 (2015) Nr. 9, S. 5846-5854.

327) X. Sun, W. Si, L. Xi, B. Liu, X. Liu, C. Yan, O.G. Schmidt, *In Situ-Formed, Amorphous, Oxygen-Enabled Germanium Anode with Robust Cycle Life for Reversible Lithium Storage*, ChemElectroChem 2 (2015) Nr. 5, S. 737-742.

328) A.H. Taghvaei, J. Bednarcik, J. Eckert, *Influence of annealing on microstructure and magnetic properties of cobalt-based amorphous/nanocrystalline powders synthesized by mechanical alloying*, Journal of Alloys and Compounds 632 (2015), S. 296-302.

329) A.H. Taghvaei, F. Ghajari, D. Marko, K.G. Prashanth, *Influence of milling time on microstructure and magnetic properties of $Fe_{80}P_{11}C_9$ alloy produced by mechanical alloying*, Journal of Magnetism and Magnetic Materials 395 (2015), S. 354-360.

330) T.H. Taghvaei, H. Shakur Shahabi, J. Bednarcik, J. Eckert, *Inhomogeneous thermal expansion of metallic glasses in atomic-scale studied by in-situ synchrotron X-ray diffraction*, Journal of Applied Physics 117 (2015) Nr. 4, S. 44902/1-7.

331) Z. Taleat, K. Mathwig, E.J.R. Sudhoelter, L. Rassaei, *Detection strategies for methylated and hypermethylated DNA*, TrAC Trends in Analytical Chemistry 66 (2015), S. 80-89.

332) L. Tan, J. Han, R.G. Mendes, M.H. Ruemmeli, J. Liu, Q. Wu, X. Leng, T. Zhang, M. Zeng, L. Fu, *Self-Aligned Single-Crystalline Hexagonal Boron Nitride Arrays: Toward Higher Integrated Electronic Devices*, Advanced Electronic Materials 1 (2015) Nr. 11.

333) L. Tan, M. Zeng, Q. Wu, L. Chen, J. Wang, T. Zhang, J. Eckert, M.H. Ruemmeli, L. Fu, *Direct Growth of Ultrafast Transparent Single-Layer Graphene Defoggers*, Small 11 (2015) Nr. 15, S. 1840-1846.

334) N. Teichert, A. Boehnke, A. Behler, B. Weise, A. Waske, A. Huetten, *Exchange bias effect in martensitic epitaxial Ni-Mn-Sn thin films applied to pin CoFeB/MgO/CoFeB magnetic tunnel junctions*, Applied Physics Letters 106 (2015) Nr. 19, S. 192401/1-4.

335) N. Teichert, D. Kucza, O. Yildirim, E. Yuzuak, I. Dincer, A. Behler, B. Weise, L. Helmich, A. Boehnke, S. Klimova, A. Waske, Y. Elerman, A. Huetten, *Structure and giant inverse magnetocaloric effect of epitaxial Ni-Co-Mn-Al films*, Physical Review B 91 (2015) Nr. 18, S. 184405/1-7.

336) B. Terlan, A.A. Levin, F. Boerrnert, F. Simon, M. Oschatz, M. Schmidt, R. Cardoso-Gil, T. Lorenz, I.A. Baburin, J.-O. Joswig, A. Eychmueller, *Effect of Surface Properties on the Microstructure, Thermal, and Colloidal Stability of VB_2 Nanoparticles*, Chemistry of Materials 27 (2015) Nr. 14, S. 5106-5115.

337) A. Thomas, S. Niehoerster, S. Fabretti, N. Shepheard, O. Kuschel, K. Kuepper, J. Wollschlaeger, P. Krzysteczko, E. Chicca, *Tunnel junction based memristors as artificial synapses*, Frontiers in Neuroscience (2015), S. 241/1-9.

338) D. Thomas, M. Zeilinger, D. Gruner, R. Huettl, J. Seidel, A.U.B. Wolter, T.F. Faessler, F. Mertnes, *The heat capacity and entropy of the lithium silicides $Li_{17}Si_4$ and $Li_{16.42}Si_4$ in the temperature range from (2 to 873) K*, Journal of Chemical Thermodynamics 85 (2015), S. 178-190.

339) D.I. Tosa, V.A. Serban, C. Codrean, D. Buzdugan, M. Stoica, *Dual phase bulk metallic glasses fabricated by hot pressing using two different types of glassy alloy powder*, Journal of Optoelectronics and Advanced Materials 17 (2015) Nr. 7-8, S. 1026-1031.

340) U. Treske, N. Heming, M. Knupfer, B. Buechner, E. Di Gennaro, A. Khare, U.S. Di Uccio, F.M. Granozio, S. Krause, A. Koitzsch, *Universal electronic structure of polar oxide hetero-interfaces*, Scientific Reports 5 (2015), S. 14506/1-11.

341) S. Trommler, S. Molatta, J. Haenisch, K. Iida, L. Schultz, R. Huehne, *Strain dependence of critical fields - studied on piezoelectric substrates*, IEEE Transactions on Applied Superconductivity 25 (2015) Nr. 3, S. 8400404/1-4.

342) R. Trotta, J. Martin-Sanchez, I. Daruka, C. Ortix, A. Rastelli, *Energy-Tunable Sources of Entangled Photons: A Viable Concept for Solid-State-Based Quantum Relays*, Physical Review Letters 114 (2015) Nr. 15, S. 150502/1-5.

343) K. Tschulik, K. Ngamchuea, C. Ziegler, M.G. Beier, C. Damm, A. Eychmueller, R.G. Compton, *Core-Shell Nanoparticles: Characterizing Multifunctional Materials beyond Imaging - Distinguishing and Quantifying Perfect and Broken Shells*, Advanced Functional Materials 25 (2015) Nr. 32, S. 5149-5158.

344) N.G. Tsierkezos, P. Szroeder, R. Fuge, U. Ritter, *Electrochemical studies on novel films consisting of phosphorus-doped multi-walled carbon nanotubes*, Ionics 21 (2015) Nr. 4, S. 1081-1088.

345) G.A. Ummarino, S. Galasso, P. Pecchio, D. Daghero, R.S. Gonnelli, F. Kurth, K. Iida, B. Holzapfel, *Resistivity in $Ba(Fe_{1-x}Co_x)_2As_2$: Comparison of thin films and single crystals*, Physica Status Solidi (B) 252 (2015) Nr. 4, S. 821-827.

346) D. Usachov, A. Fedorov, M.M. Otrokov, A. Chikina, O. Vilkov, A. Petukhov, A.G. Rybkin, Y.M. Koroteev, E.V. Chulkov, V.K. Adamchuk, A. Grueneis, C. Laubschat, D.V. Vyalikh, *Observation of Single-Spin Dirac Fermions at the Graphene/Ferromagnet Interface*, Nano Letters 15 (2015) Nr. 4, S. 2396-2401.

347) D.Y. Usachov, A.V. Fedorov, A.E. Petukhov, O.Y. Vilkov, A.G. Rybkin, M.M. Otrokov, A. Arnau, E.V. Chulkov, L.V. Yashina, M. Farjam, V.K. Adamchuk, B.V. Senkovskiy, C. Laubschat, D.V. Vyalikh, *Epitaxial B-Graphene: Large-Scale Growth and Atomic Structure*, ACS Nano 9 (2015) Nr. 7, S. 7314-7322.

348) Y. Utz, F. Hammerath, S. Nishimoto, C. Hess, N. Sekhar Beesetty, R. Saint-Martin, A. Revcolevschi, B. Buechner, H.-J. Grafe, *Suppression of the impurity-induced local magnetism by the opening of a spin pseudogap in Ni-doped Sr_2CuO_3*, Physical Review B 92 (2015) Nr. 6, S. 60405/1-5.

349) M. Valldor, U.K. Roessler, Y. Prots, J.-Y. Kuo, J.-C. Chiang, Z. Hu, T.-W. Pi, R. Kniep, L.H. Tjeng, *Synthesis and Characterization of Ba[CoSO]: Magnetic Complexity in the Presence of Chalcogen Ordering*, Chemistry - A European Journal 21 (2015) Nr. 30, S. 10821–10828.

350) N.I. Verbitskiy, A.V. Fedorov, G. Profeta, A. Stroppa, L. Petaccia, B. Senkovskiy, A. Nefedov, C. Woell, D.Y. Usachov, D.V. Vyalikh, L.V. Yashina, A.A. Eliseev, T. Pichler, A. Grueneis, *Atomically precise semiconductor–graphene and hBN interfaces by Ge intercalation*, Scientific Reports 5 (2015), S. 17700/1-9.

351) L. Veyrat, F. Iacovella, J. Dufouleur, C. Nowka, H. Funke, M. Yang, W. Escoffier, M. Goiran, B. Eichler, O.G. Schmidt, B. Buechner, S. Hampel, R. Giraud, *Band Bending Inversion in Bi_2Se_3 Nanostructures*, Nano Letters 15 (2015) Nr. 11, S. 7503-7507.

352) H. Vinzelberg, J. Schumann, *CrSi(O,N)-based cermet-like material for high-ohmic thin film resistor applications*, Physica Status Solidi A online first (2015).

353) S. Vock, K. Tschulik, M. Uhlemann, C. Hengst, S. Faehler, L. Schultz, V. Neu, *Magnetostatic nearest neighbor interactions in a $Co_{48}Fe_{52}$ nanowire array probed by in-field magnetic force microscopy*, Journal of Applied Physics 118 (2015) Nr. 23, S. 233901/1-6.

354) U. Vogel, E. Brachmann, S. Oswald, S. Menzel, T. Gemming, J. Eckert, *Evaluation of a mobile vacuum transfer system for in vacuo XPS analysis using as-deposited Ti thin-films*, Vacuum 117 (2015), S. 81-84.

355) M. Vojenciak, A. Kario, B. Ringsdorf, R. Nast, D.C. van der Laan, J. Scheiter, A. Jung, B. Runtsch, F. Goemoery, W. Goldacker, *Magnetization ac loss reduction in HTS CORC® cables made of striated coated conductors*, Superconductor Science and Technology 28 (2015) Nr. 10, S. 104006 /1-9.

356) M. Voronov, V. Hoffmann, D. Birus, C. Engelhard, W. Buscher, *Investigation of the electrical properties of standard and low-gas-flow ICPs using novel probes for the direct measurements of RF voltage and current in the load coil and the corresponding calculation of the ICP power*, Journal of Analytical Atomic Spectrometry 30 (2015) Nr. 10, S. 2089-2098.

357) L. Wagenfuhr, A.K. Meyer, L. Braunschweig, L. Marrone, A. Storch, *Brain oxygen tension controls the expansion of outer subventricular zone-like basal progenitors in the developing mouse brain*, Development 142 (2015) Nr. 17, S. 2904-2915.

358) Z. Wang, K.G. Prashanth, A.K. Chaubey, L. Loeber, F.P. Schimansky, F. Pyczak, W.W. Zhang, S. Scudino, J. Eckert, *Tensile properties of Al-12Si matrix composites reinforced with Ti-Al-based particles*, Journal of Alloys and Compounds 630 (2015), S. 256-259.

359) Z. Wang, S. Scudino, M. Stoica, W. Zhang, J. Eckert, *Al-based matrix composites reinforced with short Fe-based metallic glassy fiber*, Journal of Alloys and Compounds 651 (2015), S. 170-175.

360) A. Waske, L. Giebeler, B. Weise, A. Funk, M. Hinterstein, M. Herklotz, K. Skokov, S. Faehler, O. Gutfleisch, J. Eckert, *Asymmetric first-order transition and interlocked particle state in magnetocaloric La(Fe,Si)$_{13}$*, Physica Status Solidi - Rapid Research Letters 9 (2015) Nr. 2, S. 136-140.

361) F. Wasser, A. Schneidewind, Y. Sidis, S. Wurmehl, S. Aswartham, B. Buechner, M. Braden, *Spin reorientation in $Ba_{0.65}Na_{0.35}Fe_2As_2$ studied by single-crystal neutron diffraction*, Physical Review B 91 (2015) Nr. 6, S. 60505/1-5.

362) T. Wei, F. Liu, S. Wang, X. Zhu, A.A. Popov, S. Yang, *An Expanded Family of Dysprosium-Scandium Mixed-Metal Nitride Cluster-fullerenes: The Role of the Lanthanide Metal on the Carbon Cage Size Distribution*, Chemistry - A European Journal 21 (2015) Nr. 15, S. 5750-5759.

363) Z. Wei, P. Ma, H. Wang, C. Zou, S. Scudino, K. Song, K.G. Prashanth, W. Jiang, J. Eckert, *The thermal expansion behaviour of SiC_p/ Al- 20Si composites solidified under high pressures*, Materials and Design 65 (2015), S. 387-394.

364) R. Westerstroem, A.-C. Uldry, R. Stania, J. Dreiser, C. Piamonteze, M. Muntwiler, F. Matsui, S. Rusponi, H. Brune, S. Yang, A. Popov, B. Buechner, B. Delley, T. Greber, *Surface Aligned Magnetic Moments and Hysteresis of an Endohedral Single-Molecule Magnet on a Metal*, Physical Review Letters 114 (2015) Nr. 8, S. 87201/1-5.

365) Z. Whang, R.T. Qu, S. Scudino, B.A. Sun, K.G. Prashanth, D.V. Louzguine-Luzgin, M.W. Chen, Z.F. Zhang, J. Eckert, *Hybrid nanostructured aluminum alloy with super-high strength*, NPG Asia Materials 7 (2015), S. e229/1-8.

366) S. Wicht, V. Neu, L. Schultz, V. Mehta, S. Jain, J. Reiner, O. Mosendz, O. Hellwig, D. Weller, B. Rellinghaus, *Modification of the structural and magnetic properties of granular FePt films by seed layer conditioning*, Journal of Applied Physics 117 (2015) Nr. 1, S. 13907/1-9.

367) J.S. Wildmann, R. Trotta, J. Martin-Sanchez, E. Zallo, M. O'Steen, O.G. Schmidt, A. Rastelli, *Atomic clouds as spectrally selective and tunable delay lines for single photons from quantum dots*, Physical Review B 92 (2015) Nr. 23, S. 235306/1-6.

368) B. Willenberg, H. Ryll, K. Kiefer, D.A. Tennant, F. Groitl, K. Rolfs, P. Manuel, D. Khalyavin, K.C. Rule, A.U.B. Wolter, S. Suellow, *Luttinger liquid behavior in the alternating spin-chain system copper nitrate*, Physical Review B 91 (2015) Nr. 6, S. 60407/1-5.

369) J. Wind, J.E. Auckett, R.L. Withers, R.O. Piltz, A. Maljuk, C.D. Ling, *Type II $Bi_{1-x}W_xO_{1.5+1.5x}$: a (3 + 3)-dimensional commensurate modulation that stabilizes the fast-ion conducting delta phase of bismuth oxide*, Acta Crystallographica Section B 71 (2015) Nr. 6, S. 679-687.

370) A. Winkler, S.M. Harazim, S.B. Menzel, H. Schmidt, *SAW-based fluid atomization using mass-producible chip devices*, Lab on a Chip 15 (2015) Nr. 18, S. 3793-3799.

371) D. Wu, K. Song, C. Cao, R. Li, G. Wang, J. Wu, F. Wan, F. Ding, Y. Shi, X. Bai, I. Kaban, J. Eckert, *Deformation-Induced Martensitic Transformation in Cu-Zr-Zn Bulk Metallic Glass Composites*, Metals 5 (2015) Nr. 4, S. 2134-2147.

372) L. Xi, I. Kaban, R. Nowak, B. Korpala, G. Bruzda, N. Sobczak, N. Mattern, J. Eckert, *High-temperature wetting and interfacial interaction between liquid Al and TiB_2 ceramic*, Journal of Materials Science 50 (2015) Nr. 7, S. 2682-2690.

373) Z. Yan, Y. Hu, K. Song, F. Dai, J. He, J. Eckert, *Vickers-indentation-induced crystallization in a metallic glass*, Applied Physics Letters 106 (2015) Nr. 10, S. 101909/1-5.

374) X. Yang, F. Karnbach, M. Uhlemann, S. Odenbach, K. Eckert, *Dynamics of Single Hydrogen Bubbles at a Platinum Microelectrode*, Langmuir 31 (2015), S. 8184-8193.

375) G. Yin, V. Brackmann, V. Hoffmann, M. Schmid, *Enhanced performance of ultra-thin Cu(In,Ga)Se_2 solar cells deposited at low process temperature*, Solar Energy Materials and Solar Cells 132 (2015), S. 142-147.

376) Y. Yin, S.L. Li, S. Giudicatti, C.Y. Jiang, L.B. Ma, O.G. Schmidt, *Strongly hybridized plasmon-photon modes in optoplasmonic microtubular cavities*, Physical Review B 92 (2015) Nr. 24, S. 241403/1-4.

377) Y. Yokoyama, *Development of an Automatic Fabrication System for Cast Glassy Alloys*, Metallurgical and Materials Transactions B 46 (2015) Nr. 2, S. 893-205.

378) S. Yoon, S.-H. Baek, A. Balodhi, W.-J. Balodhi, K.-Y. Choi, I. Watanabe, J.S. Lord, B. Buechner, B.J. Suh, Y. Singh, *Spin dynamics in $Na_{4-x}Ir_3O_8$ (x=0.3 and 0.7) investigated by ^{23}Na NMR and mySR*, Journal of Physics: Condensed Matter 27 (2015) Nr. 48, S. 485603/1-6.

379) T. You, X. Ou, G. Niu, F. Baerwolf, G. Li, N. Du, D. Buerger, I. Skorupa, Q. Jia, W. Yu, X. Wang, O.G. Schmidt, H. Schmidt, *Engineering interface-type resistive switching in $BiFeO_3$ thin film switches by Ti implantation of bottom electrodes*, Scientific Reports 5 (2015), S. 18623/1-9.

380) F. Yuan, K. Iida, M. Langer, J. Haenisch, A. Ichinose, I. Tsukada, A. Sala, M. Putti, R. Huehne, L. Schultz, Z. Shi, *Influence of substrate type on transport properties of superconducting $FeSe_{0.5}Te_{0.5}$ thin films*, Superconductor Science and Technology 28 (2015) Nr. 6, S. 65005/1-7.

381) F.F. Yuan, Y. Sun, W. Zhou, X. Zhou, Q.P. Ding, K. Iida, R. Huehne, L. Schultz, T. Tamegai, Z.X. Shi, *Anisotropy of iron-platinum-arsenide $Ca_{10}(Pt_nAs_8)(Fe_{2-x}Pt_xAs_2)_5$ single crystals*, Applied Physics Letters 107 (2015) Nr. 1, S. 12602/1-5.

382) M. Zalibera, P. Machata, T.T. Clikeman, M. Rosenkranz, S.H. Strauss, O.V. Boltalina, A.A. Popov, *^{19}F NMR-, ESR-, and vis-NIR-spectroelectrochemical study of the unconventional reduction behaviour of a perfluoroalkylated fullerene: dimerization of the $C_{70}(CF_3)_{10}$- radical anion*, Analyst 140 (2015) Nr. 21, S. 7209-7216.

383) H. Zhang, Y. Huo, K. Lindfors, Y. Chen, O.G. Schmidt, A. Rastelli, M. Lippitz, *Narrow-line self-assembled GaAs quantum dots for plasmonics*, Applied Physics Letters 106 (2015) Nr. 10, S. 101110/1-4.

384) J. Zhang, M. Brehm, M. Grydlik, O.G. Schmidt, *Evolution of epitaxial semiconductor nanodots and nanowires from supersaturated wetting layers*, Chemical Society Reviews 44 (2015), S. 26-39.

385) J. Zhang, J.S. Wildmann, F. Ding, R. Trotto, Y. Huo, E. Zallo, D. Huber, A. Rastelli, O.G. Schmidt, *High yield and ultrafast sources of electrically triggered entangled-photon pairs based on strain-tunable quantum dots*, Nature Communications 6 (2015), S. 10067/1-7.

386) J. Zhang, Y. Huo, A. Rastelli, M. Zopf, B. Hoefer, Y. Chen, F. Ding, O.G. Schmidt, *Single photons on-demand from light-hole excitons in strain-engineered quantum dots*, Nano Letters 15 (2015), S. 422-427.

387) P. Zhang, X. Lu, Y. Huang, J. Deng, L. Zhang, F. Ding, Z. Su, G. Wei, O.G. Schmidt, *MoS_2 nanosheets decorated with gold nanoparticles for rechargeable Li-O_2 batteries*, Journal of Materials Chemistry A 3 (2015) Nr. 28, S. 14562-14566.

388) X. Zhang, T. Hickel, J. Rogal, S. Faehler, R. Drautz, J. Neugebauer, *Structural transformations among austenite, ferrite and cementite in Fe-C alloys: A unified theory based on ab initio simulations*, Acta Materialia 99 (2015), S. 281-289.

389) Y. Zhang, K.B. Ghiassi, Q. Deng, N.A. Samoylova, M.M. Olmstead, A.L. Balch, A.A. Popov, *Synthesis and Structure of $LaSc_2N@Cs(hept)$-C_{80} with One Heptagon and Thirteen Pentagons*, Angewandte Chemie 54 (2015) Nr. 2, S. 495-499.

390) Y. Zhang, D. Krylov, M. Rosenkranz, S. Schiemenz, A.A. Popov, *Magnetic anisotropy of endohedral lanthanide ions: paramagnetic NMR study of $MSc_2N@C_{80}$-I_h with M running through the whole 4f row*, Chemical Science 6 (2015) Nr. 4, S. 2328-2341.

391) J. Zhao, Q. Deng, T.H. Ly, G.H. Han, G. Sandeep, M.H. Ruemmeli, *Two-dimensional membrane as elastic shell with proof on the folds revealed by three-dimensional atomic mapping*, Nature Communications 6 (2015), S. 8935/1-6.

392) P. Zhu, Y. Zhu, Y. Hidaka, L. Wu, J. Cao, H. Berger, J. Geck, R. Kraus, S. Pjerov, Y. Shen, R.I. Tobey, J.P. Hill, X.J. Wang, *Femtosecond time-resolved MeV electron diffraction*, New Journal of Physics 17 (2015), S. 63004/1-6.

393) S. Ziemak, K. Kirshenbaum, S.R. Saha, R. Hu, J.-P. Reid, R. Gordon, L. Taillefer, D. Evtushinsky, S. Thirupathaiah, B. Buechner, S.V. Borisenko, A. Ignatov, D. Kolchmeyer, G. Blumberg, J. Paglione, *Isotropic multi-gap superconductivity in $BaFe_{1.9}Pt_{0.1}As_2$ from thermal transport and spectroscopic measurements*, Superconductor Science and Technology 28 (2015) Nr. 1, S. 14004/1-12.

394) D. Zilic, L. Andros, Y. Krupskaya, V. Kataev, B. Buechner, *Magnetic anisotropy of Cr(III) ions in polymeric oxalate complexes as revealed by HF-ESR spectroscopy*, Applied Magnetic Resonance 46 (2015), S. 309-321.

395) E.A. Zvereva, V.B. Nalbandyan, M.A. Evstigneeva, H.-J. Koo, M.-H. Whangbo, A.V. Ushakov, B.S. Medvedev, L.I. Medvedeva, N.A. Gridina, G.E. Yalovega, A.V. Churikov, A.N. Vasiliev, B. Buechner, *Magnetic and electrode properties, structure and phase relations of the layered triangular-lattice tellurate Li_4NiTeO_6*, Journal of Solid State Chemistry 225 (2015), S. 89-96.

396) E.A. Zvereva, I.A. Presniakov, M.-H. Whangbo, H.-J. Koo, T.V. Frantsuzenko, O.A. Savelieva, A.V. Sobolev, V.B. Nalbandyan, P.-S. Shih, J.-C. Chiang, J.-M. Lee, J.-M. Chen, J.-Y. Lin, B. Buechner, A.N. Vasiliev, *Crucial Role of Site Disorder and Frustration in Unusual Magnetic Properties of Quasi-2D Triangular Lattice Antimonate Na_4FeSbO_6*, Applied Magnetic Resonance 46 (2015) Nr. 10, S. 1121-1145.

397) M. Zwiebler, J.E. Hamann-Borrero, M. Vafaee, P. Komissinskiy, S. Macke, R. Sutarto, F. He, B. Buechner, G.A. Sawatzky, L. Alff, J. Geck, *Electronic depth profiles with atomic layer resolution from resonant soft x-ray reflectivity*, New Journal of Physics 17 (2015), S. 83046/1-15.

Contributions to conference proceedings and monographs

1) B. Betz, P. Rauscher, R. Siebert, R. Schaefer, A. Kaestner, H. Van Swygenhoven, E. Lehmann, C. Gruenzweig, *Visualization of bulk magnetic properties by Neutron grating interferometry*, Proceedings of the 10th World Conference on Neutron Radiography (WCNR-10) Grindelwald, Switzerland October 5–10, 2014, in: Physics Procedia, 69, 399-403 (2015).

2) D. Eigel, P.-F. Gostin, A. Eychmueller, A. Gebert, V. Hoffmann, *Oberflaechenmodifizierung von Ti-Nb-Legierungen durch Plasma-Elektrolyse-Oxidation fuer biokompatible Anwendungen*, Kongress des Zentralverbands fuer Oberflaechentechnik (ZVO), Berlin/ Germany, 23.-24.9.15 (2015).

3) J. Fink, *High Temperature Superconductivity at Room Temperature?*, in: European Superconductivity News Forum (global edition), 32 (2015).

4) V.M. Fomin, *Theory of Catalytic Micro- and Nanoengines: From Self-propulsion Mechanisms to Remediation of Polluted Water*, 3rd International Conference on Nanotechnologies and Biomedical Engineering, in: IFMBE Proceedings, 55, 25-29 (2015).

5) C. Gruenzweig, R. Siebert, B. Betz, P. Rauscher, R. Schaefer, E. Lehmann, *Determination of Bulk Magnetic Volume Properties by Neutron Dark-Field Imaging*, Proceedings of the 10th World Conference on Neutron Radiography (WCNR-10) Grindelwald, Switzerland October 5–10, 2014, in: Physics Procedia, 69, 413-419 (2015).

6) J. Koenig, F. Kiebert, H. Schmidt, C. Kykal, *Volumetrische Messung der durch akustische Oberflächenwellen induzierten Partikelbewegung in Flüssigkeiten*, in: Lasermethoden in der Strömungsmesstechnik - 23. Fachtagung, Dresden /Germany, 8.-10.9.15 (2015).

7) I. Manke, N. Kardjilov, R. Schaefer, A. Hilger, R. Grothausmann, M. Strobl, M. Dawson, C. Gruenzweig, C. Toetzke, C. David, A. Kupsch, A. Lange, M.P. Hentschel, J. Banhart, *Three-Dimensional Imaging of Magnetic Domains with Neutron Grating Interferometry*, Proceedings of the 10th World Conference on Neutron Radiography (WCNR-10) Grindelwald, Switzerland October 5–10, 2014, in: Physics Procedia, 69, 404-412 (2015).
8) J. Massing, J. Koenig, F. Kiebert, S. Wege, H. Schmidt, C. Cierpka, *3D3C Geschwindigkeitsmessungen mittels Astigmatismus Particle Tracking Velocimetry (APTV) in SAW-basierten mikrofluidischen Mischern*, in: Lasermethoden in der Strömungsmesstechnik - 23. Fachtagung, Dresden /Germany, 8.-10.9.15, 13/1-9 (2015).
9) K. Nektarios, J. Koenig, L. Buettner, J. Czarske, *Flow-Field Measurements Through Phase-Boundaries Using Wavefront Shaping*, Wavefront Sensing and Adaptive Optics, in: Frontiers in Optics 2015, OSA Technical Digest (online) (Optical Society of America, 2015), FTu5D.3 (2015).
10) A. Panigrahi, M. Boenisch, T. Waitz, M. Calin, W. Skrotzki, J. Eckert, M. Zehetbauer, *Thermal stability of HPT-induced omega phase in biocompatible Ti-16.1Nb alloys*, 7th International Conference on Solid-Solid Phase Transformations in Inorganic Materials (PTM) 2015, 28.6.-3.7.2015, Whistler, BC, Canada, in: Proceedings of the 7th International Conference on Solid-Solid Phase Transformations in Inorganic Materials (PTM) 2015, 263-268 (2015).
11) P. Rapta, E. Dmitrieva, A.A. Popov, L. Dunsch, *Chapter 3. In Situ Spectroelectrochemistry of Organic Compounds*, in: Organic Electrochemistry, 169-190 (2015).
12) H. Schmidt, A. Sotnikov, S.V. Biryukov, M. Weihnacht, *Precise Microacoustic Characterization of new Piezoelectric Crystals for High-Temperature Sensors*, AMA Conferences 2015, Nuremberg/ Germany, 19.-21.5.15, in: Proceedings SENSOR 2015, 396-401 (2015).
13) A. Sotnikov, E. Smirnova, H. Schmidt, M. Weihnacht, J. Gotze, S. Sakharov, *Langasite family crystals as promising materials for microacoustic devices at cryogenic temperatures*, Joint Conference of the IEEE International Frequency Control Symposium & the European Frequency and Time Forum (FCS) 2015, Denver/ USA, 12.-16.4.15, in: Frequency Control Symposium & the European Frequency and Time Forum (FCS), 2015 Joint Conference of the IEEE International, 106-110 (2015).

Invited Talks 2015

1) F. Bittner, T. Mix, K.-H. Mueller, L. Schultz, T.G. Woodcock, *Mn-Based Permanent Magnets with the L10 Structure*, TMS Annual Meeting 2015/ Symposium: Magnetic Materials for Energy Applications V, Orlando/ USA, 16.-19.03.15 (2015).
2) M. Boenisch, A. Panigrahi, M. Calin, F. Senftleben, M. Stoica, M. Zehetbauer, T. Waitz, W. Skrotzki, J. Eckert, *Selected aspects relating to the martensitic transformations in Ti-Nb alloys*, BioTiNet Workshop, Universitaet Wien, Vienna/ Austria, 7.-10.4.15 (2015).
3) F. Boerrnert, *Approaching graphene devices inside a TEM*, SFB-Kolloquium, Universitaet Ulm, Ulm/ Germany, 3.7.15 (2015).
4) F. Boerrnert, *A multi-stimuli in-situ (S)TEM: Concept, optical performance, and outlook*, Fritz-Haber-Institut der Max-Planck-Gesellschaft, Berlin/ Germany, 17.3.15 (2015).
5) F. Boerrnert, *A multi-stimuli in-situ (S)TEM: Concept, optical performance, and outlook*, Universitaet Ulm, Ulm/ Germany, 13.5.15 (2015).
6) F. Boerrnert, *Towards graphene devices in the TEM*, 5th SALVE Summer Workshop, Hirschegg/ Austria, 30.6.15 (2015).
7) F. Boerrnert, H. Mueller, M. Linck, A. Horst, A.I. Kirkland, B. Buechner, H. Lichte, *Approaching the „Lab in the Gap": First Results from a Versatile In-Situ (S)TEM*, Microscopy Conference (MC) 2015, Goettingen/ Germany, 6.-11.9.15 (2015).
8) S.V. Borisenko, *Experimental realization of TRS-breaking type II Weyl semimetal*, The 15th International Conference on the Formation of Semiconductor Interfaces (ICFSI-15), Hiroshima/ Japan, 15.-20.11.15 (2015).
9) S.V. Borisenko, *Materials Architecture: Design of Functional Systems in Reciprocal Space*, Institut für Festkörperphysik (IFP) / Karlsruher Institut für Technologie (KIT), Karlsruhe/ Germany, 29.5.15 (2015).
10) S.V. Borisenko, *Spin-orbit interaction vs. nematicity in multiband iron-based superconductors as seen by ARPES*, Plenary talk at Quantum in Complex Matter: Superconductivity, Magnetism and Ferroelectricity, Ischia/ Italy, 15.-17.6.15 (2015).
11) S.V. Borisenko, *Experimental realization of TRS-breaking Weyl state*, International Conference on Materials for Advanced Technologies (ICMAT 2015) 2015, MRS Singapore, Singapore/ Singapore, 27.6.-4.7.15 (2015).
12) S.V. Borisenko, *Can ARPES help to design new materials?*, 19th Hiroshima International Symposium on Synchrotron Radiation Hiroshima Synchrotron Radiation Center, Hiroshima/ Japan, 4.-9.3.15 (2015).
13) S.V. Borisenko, *Graphene-like electronic structure in one and three dimensions*, General Physics Colloquium Ruhr Universität Bochum, Bochum/ Germany, 19.1.15 (2015).
14) B. Buechner, *NMR studies of nanoscale electronic order in high temperature*, V. International Symposium on Strong Nonlinear Vibronic and Electronic Interactions in Solids, Tartu/ Estland, 30.4.-2.5.15 (2015).
15) B. Buechner, *Correlated Metals: Electronic Order, Orbitals and Hund's Coupling*, THz to Soft X-ray Workshop, HZB Berlin, Berlin/ Germany, 7.-8.12.15 (2015).
16) B. Buechner, *Fe based Superconductors: Materials, phase diagrams, and spectroscopy (Lectures)*, XIX Training Course in the Physics of Strongly Correlated Systems, Salerno/ Italy, 12.-16.10.15 (2015).

17) B. Buechner, *Tunable sub-THz ESR spectroscopy of complex transition metal oxides*, COST TO-BE spring meeting, Aveiro/ Portugal, 30.3.-2.4.15 (2015).
18) B. Buechner, *The Iron Age of High Temperature Superconductivity*, Hamburg Photon Science Colloquium, Hamburg/ Germany, 26.6.15 (2015).
19) B. Buechner, *Orbital-driven nematicity and superconductivity in FeSe: NMR study*, SUPERSTRIPES 2015, Ischia/ Italy, 14.-18.6.15 (2015).
20) B. Buechner, *Orbital-driven nematicity in FeSe*, 11th Conference on Materials and Mechanisms of Superconductivity (M2S 2015), Geneve/ Swiss, 23.-28.8.15 (2015).
21) M. Calin, S. Abdi, F.P. Gostin, A. Gebert, J. Eckert, *Ti-based glassy alloys as prospective biomaterials*, Workshop BioTiNet, University of Vienna, Vienna/ Austria, 7.-10.4.15 (2015).
22) M. Calin, S. Abdi, N. Zheng, F.P. Gostin, A. Gebert, J. Eckert, *Compositional-induced structural change and deformation behavior of glassy Ti-Zr-based alloys with potential for biomedical applications*, 22nd International Symposium on Metastable, Amorphous and Nanostructured Materials (ISMANAM 2015), Paris/ France, 13.-17.7.15 (2015).
23) M. Calin, M. Boenisch, A. Helth, S. Abdi, F.P. Gostin, A. Gebert, J. Eckert, *Novel Ti-Based Metastable Alloys for Biomedical Applications*, The 9th International Conference on Materials Science & Engineering - Bramat 2015, Brasov/ Romania, 5.-7.3.15 (2015).
24) M. Calin, A. Gebert, S. Abdi, A. Helth, S. Pilz, J. Eckert, *Property optimization of Ti-based biomaterials by structural design*, Colloquium of Materials Science and Enginerring Faculty, University Politehnica Bucharest, Bucharest/ Romania, 11.-12.11.15 (2015).
25) M. Calin, A. Gebert, F.P. Gostin, A. Helth, M. Boenisch, S. Pilz, R. Schmidt, U. Hempel, M. Zehetbauer, J. Eckert, *Tailoring the microstructures and surfaces of metastable Ti-based alloys at the nano-scale for implant applications*, 1st. International Symposium on Physics of Surfaces and Interfaces, from Fundamentals to Sustainable Applications (SIPS 2015), Antalya/ Turkey, 4.-9.10.15 (2015).
26) Y. Chen, *Wavelength tunable entangled photons from silicon integrated III-V quantum dots*, 3rd International Workshop on Engineering of Quantum Emitter Properties (EQE2015), Linz/ Austria, 17.-18.12.15 (2015).
27) F. Ding, *Quantum photonic engineering with semiconductor quantum dots*, Colloquium, Leibniz University Hannover, Hannover/ Germany, 11.6.15 (2015).
28) F. Ding, *Semiconductor nanomembranes: A novel playground for quantum photonics*, The AVS Shanghai Thin Film Conference Shanghai, Shanghai/ China, 24.-25.10.15 (2015).
29) J. Eckert, K.G. Prashanth, S. Scudino, M. Stoica, S. Pauly, U. Kuehn, *Selective Laser Melting of Metallic Glasses*, The Minerals, Metals and Materials Society Annual Meeting 2015 (TMS 2015), Orlando/ USA, 15.-19.3.15 (2015).
30) S. Faehler, *Origin of hysteresis in multicaloric materials*, Middle East - Mediterranean Materials Congress (MEMA 2015), Doha/ Quatar, 11.-14.1.15 (2015).
31) S. Faehler, M.E. Gruner, H. Seiner, R. Niemann, L. Schultz, *Origin of hysteresis in multicaloric materials*, ICM, Barcelona/ Spain, 5.-10.7.15 (2015).
32) S. Faehler, R. Niemann, C. Behler, A. Diestel, M.E. Gruner, H. Seiner, O. Heczko, L. Schultz, *Formation of a hierarchical martensitic microstructure*, From Grain Boundaries to Stochastic Homogenization: PIRE Workshop, Leipzig/ Germany, 20.-23.7.15 (2015).
33) S. Faehler, R. Niemann, C. Behler, A. Diestel, M.E. Gruner, H. Seiner, O. Heczko, L. Schultz, *Formation of a hierarchical martensitic microstructure in epitaxial Ni-Mn-Ga films*, European Symposium on Martensitic Transformations (ESOMAT), Antwerpen/ Belgium, 14.-18.9.15 (2015).
34) J. Fink, *Non-Fermi-liquid scattering rates and anomalous band dispersions in ironpnictides and ironchalcogenides - an ARPES study*, Seminarvortrag, Universitaet Zuerich, Zurich/ Switzerland, 25.11.15 (2015).
35) J. Fink, *Non-Fermi-liquid scattering rates and anomalous band dispersions in ironpnictides and ironchalcogenides - an ARPES study*, Seminarvortrag, Universitaet Genf, Geneva/ Switzerland, 26.11.15 (2015).
36) J. Fink, *Non-Fermi-liquid scattering rates and anomalous band dispersions in ironpnictides and ironchalcogenides - an ARPES study*, Kolloquiumsvortrag, Universitaet Lausanne (EPFL), Lausanne/ Switzerland, 27.11.15 (2015).
37) J. Fink, *Non-Fermi-liquid scattering rates and anamolous band dispersion in ferropnictides-an ARPES study*, Superstripes 2015, Ischia/ Italy, 13.-18.6.15 (2015).
38) J. Fink, *From a spectroscopist to a spectroscopist, new ARPES results on unconventional superconductors*, Geburtstagskolloquium Prof. Kuzmany, University of Vienna, Vienna/ Austria, 10.9.15 (2015).
39) J. Fink, *Non-Fermi-liquid scattering rates and anomalous band dispersions in ironpnictides and ironchalcogenides - an ARPES study*, Seminarvortrag, Vancouver/ Canada, 17.11.15 (2015).
40) J. Fink, *Angle-resolved photoemission spectroscopy (ARPES)-a many body spectroscopy*, Bonn-Cologne Graduate School, Cologne/ Germany, 12.-16.10.15 (2015).
41) J. Fink, *Experimente zur Hochtemperatursupraleitung, Werner Webers Beitraege und neuere Entwicklungen*, Gedenkkolloquium fuer Werner Weber, Dortmund/ Germany, 7.4.15 (2015).
42) V.M. Fomin, *Topological effects in quantum rings*, Seminar, Pusan National University, Pusan/ Republic of Korea, 12.2.15 (2015).

43) V.M. Fomin, *Dynamics of vortices in self-organized superconductor micro- and nanostructures*, Seminar, Department of Low Temperature Physics and Superconductivity, Faculty of Physics, Lomonosov Moscow State University, Moscow/ Russia, 18.6.15 (2015).
44) V.M. Fomin, *Theory of catalytic micro- and nanoengines: From self-propulsion mechanisma to remediation of polluted water*, 3rd International Conference on Nanotechnologies and Biomedical Engineering (ICNBME-2015), Chisinau/ Republic of Moldova, 24.9.15 (2015).
45) V.M. Fomin, *Impact of topology on electronic properties of solid-state micro- and nanostructures*, Seminar, Bogoliubov Laboratory of Theoretical Physics, Joint Institute for Nuclear Research Dubna, Moscow Region/ Russia, 18.2.15 (2015).
46) V.M. Fomin, *The fascination of quantumn rings: From fundamentals to recent advances*, Moldo-Japanese Autumn School Nano-Bioengineering-2015, Chisinau/ Republic of Moldova, 22.9.15 (2015).
47) V.M. Fomin, *Vortex dynamics in self-assembled superconductor micro- and nanostructures*, Seminar, Instituto de Ciencia de Materiales Nicolas Cabrera, Universidad Autonoma de Madrid, Madrid/ Spain, 9.6.15 (2015).
48) V.M. Fomin, *Impact of topology on electronic properties of micro- and nanostructures*, Seminar, Instituto de Microelectronica de Madrid, CNM-CSIC, Madrid/ Spain, 11.6.15 (2015).
49) V.M. Fomin, *Theory of vortices in self-assembled superconducting micro- and nanostructures*, Seminar, Institute of Electronic Engineering and Nanotechnologies, Academy of Sciences of Moldova, Chisinau/ Republic of Moldova, 26.3.15 (2015).
50) J. Freudenberger, *Ver- und Umformung fuer ein besseres Verstaendnis von Werkstoffen*, Kolloquium des IAM-WK (KIT), Karlsruhe/ Germany, 5.5.15 (2015).
51) J. Freudenberger, A. Kauffmann, F. Thiel, S. Yin, F. Bittner, H. Klauß, *High strength conductors for pulsed high field magnets: development of CuAgZr materials*, Kolloquium des internationalen Hochfeldlabors Wroclaw, Wroclaw /Poland, 12.11.15 (2015).
52) A. Gebert, *A straight-forward route for recycling of Nd from Nd-Fe-B magnets based on melt extraction*, MCARE 2015, Jeju/ Korea, 23.-27.2.15 (2015).
53) A. Gebert, S. Horn, R. Sueptitz, P.F. Gostin, M. Stoica, J. Eckert, M. Uhlemann, *Electrochemical micromachining of bulk metallic glasses*, 227th Electrochemical Society Meeting (ECS), Chicago/ USA, 25.-28.5.15 (2015).
54) A. Gebert, S. Horn, R. Sueptitz, M. Stoica, J. Eckert, M. Uhlemann, *Electrochemical micromachining of passive Fe-based bulk metallic glasses*, TMS Annual Meeting 2015, Orlando/ USA, 15.-19.3.15 (2015).
55) D. Geissler, J. Freudenberger, A. Kauffmann, S. Martin, D. Rafaja, *Eine kritische Auseinandersetzung mit der gegenwaertigen thermodynamischen Beschreibung der Stapelfehlerenergie*, 36. Adelbodener Werkstoffseminar des Instituts fuer Angewandte Materialien - Werkstoffkunde (IAM-WK), Karlsruher Institut fuer Technologie (KIT), Adelboden/ Schweiz, 7.-14.3.15 (2015).
56) M. Gellesch, A. Omar, *Crystal growth of Heusler compounds - Kristallzuechtung von Heuslerverbindungen*, 4. Seminar der Jungen DGKK, Frankfurt am Main, 3.-4.3.15 (2015).
57) H.-J. Grafe, *Spin fluctuations and inhomogeneities in iron pnictide superconductors as probed by NMR and NQR*, Modern Development of Magnetic Resonance, Kazan/ Russia, 22.-26.9.15 (2015).
58) H.-J. Grafe, *Determination of the local structure of high temperature superconductors by NMR and NQR*, Seminar talk, Institut fuer Strukturphysik, TU Dresden, Dresden/ Germany, 12.5.15 (2015).
59) H.-J. Grafe, *Nuclear Magnetic Resonance in unconventional superconductors - and the role of inhomogeneites*, Seminar talk, 3. Physikalisches Institut, Universitaet Stuttgart, Stuttgart/ Germany, 15.7.15 (2015).
60) T. Gustmann, U. Kuehn, S. Pauly, J. Eckert, P. Gargarella, C.S. Kiminami, C. Bolfarini, *Selektives Laserstrahlschmelzen von kupferbasierten Formgedaechtnislegierungen*, Symposium zum 3D-Druck, Erding/ Germany, 14.-15.10.15 (2015).
61) J.E. Hamann-Borrero, *Studying emergent phenomena at surfaces and interfaces of complex matter using resonant soft x-ray reflectivity*, Superstripes, Ischia/ Italy, 13.-18.6.15 (2015).
62) C. Hess, *Quasiparticle interference and gap spectroscopy of the unconventional superconductor LiFeAs*, APCTP 2015 Workshop on „Impurity induced states and quasiparticle interference in unconventional superconductors and strong spin-orbit coupled systems (ISQUS15)“, Asia Pacific Center for Theoretical Physics (APCTP), Pohang/ South-Korea, 18.-23.10.15 (2015).
63) C. Hess, *Unconventional superconductivity in LiFeAs as seen by scanning tunneling microscopy and spectroscopy*, 598. WE-Heraeus-Seminar: „Frontiers in Scanning Probe Microscopy“, 1.-5.11.15 (2015).
64) C. Hess, *High-temperature heat transport in spin-1/2 quantum magnets*, Center for Novel States of Complex Materials Research, Seoul National University, Seoul/ South-Korea, 23.10.15 (2015).
65) C. Hess, *Scanning tunneling spectroscopy of the unconventional superconductor LiFeAs*, International Workshop & Seminar „Quantum Design“, Max-Planck-Institut fuer Physik komplexer Systeme, Dresden/ Germany, 17.-24.7.15 (2015).
66) C. Hess, *Spin and charge excitations probed by transport and tunneling experiments*, Kolloquium, Karlsruher Institut fuer Technologie, Karlsruhe/ Germany, 22.5.15 (2015).
67) C. Hess, *Spin Heat Transport of low-dimensional Quantum Magnets*, Solid State Physics Seminar, ETH Zurich, Zurich/ Swiss, 16.4.15 (2015).
68) C. Hess, *Rastertunnelspektroskopie an dem unkonventionellen Supraleiter LiFeAs*, Kolloquium, Universitaet Augsburg, Zentrum fuer elektronische Korrelationen und Magnetismus, Augsburg/ Germany, 22.6.15 (2015).

69) V. Hoffmann, E. Steers, S. Mushtaq, J. Pickering, C. Gonzalez Gago, P. Smid, T. Hofmann, C. Venzago, W. Gruner, *Measurement of Oxygen in Solid Samples using Analytical Glow Discharges with Optical and Mass Spectrometric Detection*, SciX 2015, Rhode Island/ USA, 27.9.-2.10.15 (2015).
70) R. Huehne, B. Holzapfel, *Supraleitende Motoren und Generatoren*, 3. Workshop „Materialien fuer die Energietechnik": Magnetwerkstoffe, Dresden, 22.4.15 (2015).
71) J. Hufenbach, U. Kuehn, J. Eckert, *Development of high-strength iron-based alloys for tooling applications*, Korea Institute for Rare Metals (Incheon Research Center), Incheon/ South Korea, 22.4.15 (2015).
72) Y.H. Huo, *Novel GaAs quantum dots grown by droplet etching*, Seminar, Department of Physics and Astronomy, University of Sheffield, Sheffield/ United Kingdom, 25.2.15 (2015).
73) Y.H. Huo, *Excitonic signature of QDs with light hole ground state*, Seminar, Department of Electronic & Electrical Engineering, University College London, London/ United Kingdom, 27.2.15 (2015).
74) Y.H. Huo, *Symmetric quantum dots grown on (001) substrate*, Seminar, School of Engineering & Physical Sciences, Heriot-Watt University, Edinburgh/ United Kingdom, 23.2.15 (2015).
75) Y.H. Huo, *GaAs quantum dots grown by droplet etching*, Seminar, School of Physics, Harbin Institute of Technology, Harbin/ China, 27.3.15 (2015).
76) T. Jaumann, *Si/C nanocomposites through economical chemistry as advanced anode in Li -ion and Li -S batteries*, Freiberger Siliziumtage 2015, Freiberg/ Germany, 19.6.15 (2015).
77) I. Kaban, *Topological and chemical short-range order in Cu47.5Zr47.5Al5 metallic glass*, German-Korean Workshop on Bulk Metallic Glasses and Nanostructured Materials, Munich/ Germany, 10.-11.7.15 (2015).
78) I. Kaban, *Structural studies of CuZr-based metallic glasses*, 588. WE-Heraeus Seminar „Element specific structure determination in materials on nanometer and sub-nanometer scales using modern X-ray and neutron techniques", Bad Honnef/ Germany, 26.-30.4.15 (2015).
79) I. Kaban, *Structural studies of Ge-Te alloys in liquid and glassy state*, Chinese-German symposium 'Electronic and Memory Materials', RWTH Aachen, Aachen/ Germany, 2.-5.11.15 (2015).
80) D. Karnaushenko, *Shapeable electronics*, Special Seminar, Osaka University, Osaka/ Japan, 25.11.15 (2015).
81) D. Karnaushenko, *Artrendering science (3D special effects)*, Special Seminar, Institute for Materials Science, TU Dresden, Dresden/ Germany, 10.9.15 (2015).
82) D. Karnaushenko, *Compact biomimetic microelectronics*, Special seminar, Center for Engineering Innovation, The University of Texas at Dallas, Dallas/ USA, 14.4.15 (2015).
83) V. Kataev, *Exotic spin phases in the low-dimensional quantum magnet LiCuSbO4 as seen by high-field NMR and ESR spectroscopies*, International Conference „Modern Development of Magnetic Resonance 2015", Kazan/ Russia, 22.-26.9.15 (2015).
84) V. Kataev, *Interplay of disorder and spin frustration near the critical point: A case study of CoAl2O4 by local spin probe techniques*, International Conference Superstripes 2015, Ischia/ Italy, 13.-18.6.15 (2015).
85) M. Knupfer, *Dispersion of plasmons and excitons in layered materials from electron energy-loss spectroscopy*, Seminar, Institut fuer Physik, TU Chemnitz, Chemnitz/ Germany, 26.6.15 (2015).
86) J. Koenig, *Multidimensional near-electrode flow measurements during copper magneto-electrolysis using an advanced interferometric technique*, 116th Annual Meeting of the DGaO, Brno/Czech Republic, 26.-39.5.15 (2015).
87) M. Kopte, *Structure of magnetic domain walls*, Seminar, Experimentalphysik IV, Universitaet Augsburg, Augsburg, 5.3.15 (2015).
88) U. Kuehn, D. Geißler, T. Gustmann, H. Schwab, J. Sander, J.K. Hufenbach, *Metallische Leichtbaustrukturen hergestellt durch selektives Laserstrahlschmelzen*, Treffpunkt Zukunft „Moderne Werkstoffe" im Rahmen der „Werkstoffwoche 2015" der DGM e.V. und des Stahlinstituts VdEh in Dresden, Dresden/ Germany, 15.9.15 (2015).
89) G. Lin, *Magnetoresistive sensing technologies for droplet digital microfluidics*, 50. Zakopane School of Physics - breaking frontiers: Submicron structures in physics and biology, Zakopane/ Poland, 18.-23.5.15 (2015).
90) L. Ma, *Rolled up microtube cavities with three dimensional optical confinement for label free sensing*, The AVS Shanghai Thin Film Conference Shanghai, Shanghai/ China, 24.-25.10.15 (2015).
91) D. Makarov, *Curved magnetic nanomembranes*, Laser- und Quantenoptikseminar, Technische Universitaet Kaiserslautern, Kaiserslautern/ Germany, 6.2.15 (2015).
92) D. Makarov, *Curvilinear magnetism*, Seminar, Poggio Lab, University of Basel, Basel/ Switzerland, 28.4.15 (2015).
93) D. Makarov, *3D curved magnetic surfaces*, 20th International Conference on Magnetism (ICM2015), Barcelona/ Spain, 5.-10.7.15 (2015).
94) D. Makarov, *Magnetic functionalities for flexible interactive electronics*, Seminar, Soochow University Suzhou/ China, 3.7.15 (2015).
95) D. Makarov, *Active and passive electronics for smart implants*, International Workshop on Thin-films for Electronics, Electro-Optics, Energy and Sensors (TFE3S), Suzhou/ China, 4.-6.7.15 (2015).
96) D. Makarov, *Curvilinear magnetism*, Seminar, Department Materials for Green Spintronics, HZB, BESSY II, Berlin/ Germany, 13.7.15 (2015).
97) D. Makarov, *3D magnetic surfaces*, SPIE NanoScience + Engineering Conferences 2015, Spintronics VIII, San Diego/ USA, 9.-13.8.15 (2015).

98) D. Makarov, *Active and passive electronics for smart implants*, 3rd International Conference on Nanotechnologies and Biomedical Engineering (ICNBME-2015), Chisinau/ Republic of Moldova, 23.-26.9.15 (2015).
99) D. Makarov, *Curved magnetic nanomembranes*, Colloquium, University of Bayreuth, Bayreuth/ Germany, 15.1.15 (2015).
100) D. Makarov, *3D magnetic surfaces*, Evaluation of the SPEEM Beamline, HZB, BESSY II, Berlin/ Germany, 10.2.15 (2015).
101) D. Makarov, *3D curved architectures: From curvilinear magnetism to biomimetic microelectronics* , Colloquium, Helmholtz-Zentrum Dresden-Rossendorf, Rossendorf/ Germany, 4.6.15 (2015).
102) D. Makarov, *Smart biomimetic microelectronics*, The AVS Shanghai Thin Film Conference Shanghai, Shanghai/ China, 24.-25.10.15 (2015).
103) D. Makarov, *3D magnetic architectures*, Seminar, Experimental Physics IV, University of Augsburg, Augsburg/ Germany, 28.5.15 (2015).
104) S. Menzel, *Migration processes in structured thin films*, Workshop Morphologie und Mikrostruktur Duenner Schichten und deren Beeinflussung, Dresden EFDS/FhG-IWS, Dresden, 12.3.15 (2015).
105) V. Neu, S. Vock, *Principles and possibilities of quantitative magnetic force microscopy*, Gruppenseminar am Institut fuer Physik (Experimentalphysik IV), Universitaet Kassel, Kassel/ Germany, 27.1.15 (2015).
106) R. Niemann, A. Backen, C. Behler, A. Diestel, J. Romberg, L. Schultz, S. Faehler, J. Kopeczek, O. Heczko, J. Baro, E. Vives, L. Manosa, A. Planes, *Two dimensional localization of acoustic emission during the martensitic transformation*, Seminar im Dipartimento di Matematica, Politecnico di Milano, Milano/ Italy, 26.3.15 (2015).
107) R. Niemann, A. Diestel, B. Schleicher, S. Kauffmann-Weiss, C. Behler, A. Backen, U.K. Roessler, H. Seiner, O. Heczko, S. Hahn, M.F.-X. Wagner, L. Schultz, S. Faehler, *Epitaxial magnetic shape memory films for magnetocaloric applications*, Donostia International Workshop on Energy, Materials and Nanotechnology, San Sebastian/ Spain, 1.-4.9.15 (2015).
108) R. Niemann, S. Kauffmann-Weiss, C. Behler, A. Diestel, A. Backen, U.K. Roessler, H. Seiner, O. Heczko, S. Hahn, M.F.-X. Wagner, L. Schultz, S. Faehler, *Phase nucleation in ferroic thin films for cooling applications*, Edgar Luescher Seminar 2015, Klosters-Serneus/ Schweiz, 7.-13.2.15 (2015).
109) R. Niemann, J. Romberg, L. Schultz, S. Faehler, J. Kopeczek, O. Heczko, J. Baro, L. Manosa, A. Planes, *Microstructural origin of martensitic avalanches*, Seminar „Magnetische Nanostrukturen" der AG Farle, Universitaet Duisburg-Essen, Duisburg-Essen, 4.5.15 (2015).
110) D. Pohl, S. Schneider, J. Rusz, P. Tiemeijer, B Rellinghaus, *Electron vortex beams for EMCD measurements on ferromagnetic nanoparticles via STEM*, National Center for Electron Microscopy, (NCEM), Lawrence Berkeley National Laboratory, Berkeley/ USA, 14.4.15 (2015).
111) D. Pohl, S. Schneider, J. Rusz, P. Tiemeijer, B. Rellinghaus, *EMCD measurements on ferromagnetic nanoparticles using electron vortex probes*, DPG 2015/ Fruehjahrstagung der Sektion Kondensierte Materie (SKM), Berlin, 15.-20.3.15 (2015).
112) D. Pohl, S. Schneider, J. Rusz, P. Tiemeijer, B. Rellinghaus, *Electron vortex beams for EMCD measurements on ferromagnetic samples via STEM*, Seminar NCEM Berkeley, Berkeley/ USA, 13.3.15 (2015).
113) D. Pohl, S. Schneider, J. Rusz, P. Tiemeijer, B. Rellinghaus, *Electron vortex beams for magnetic measurements on ferromagnetic samples via STEM*, Microscopy and Microanalysis 2015, Portland/ USA, 2.-6.8.15 (2015).
114) A. Popov, *Metallofullerenes with Single Carbon Atom in the Endohedral Cluster*, 227th Electrochemical Society Meeting, Chicago/ USA, 24.-28.5.15 (2015).
115) A. Popov, *Interior design of metallofullerenes for single molecular magnetism and endohedral electron transfer*, University of Zuerich, Zuerich/ Switzerland, 2015 (2015).
116) A. Popov, *Metallofullerenes as single molecular magnetism*, Technical University of Berlin, Berlin/ Germany, 2015 (2015).
117) A. Popov, *Methane as a reactive gas in the synthesis of endohedral metallofullerenes*, The International Chemical Congress of Pacific Basin Societies (PACIFICHEM) 2015, Hawaii/ USA, 15.-20.12.15 (2015).
118) G. Prando, *Recent my^{+}SR studies of frustrated metallic pyrochlores and pnictide superconductors*, GRK 1621 Seminar Series, TU Dresden, Dresden/ Germany, 20.1.15 (2015).
119) G. Prando, *mySR under pressure: investigations of magnetism and superconductivity in iron-based pnictides*, 3rd ERC Symposium QuantumPuzzle, Vienna University of Technology, Vienna/ Austria, 30.-31.5.15 (2015).
120) C.F. Reiche, *Scanning force microscopy based on resonant oscillations of carbon nanotubes*, Seminar des Physikalischen Instituts, Karlsruher Institut für Technologie, Karlsruhe/ Germany, 19.10.2015 (2015).
121) C.F. Reiche, J. Koerner, B. Buechner, T. Muehl, *Bidirectional scanning force microscopy probes with co-resonant sensitivity enhancement*, IEEE 15th International Conference on Nanotechnology (IEEE-NANO), Rome/ Italy, 27.-30.6.15 (2015).
122) L. Reichel, R. Salikhov, G. Giannopoulos, A. Edstroem, E.K. Delczeg-Czirjak, M. Werwinski, J. Rusz, M. Farle, L. Schultz, S. Faehler, *High magnetic anisotropy of strained epitaxial Fe-Co-X films - buffer induced distortion versus spontaneous strain*, IEEE International Magnetics Conference 2015 (INTERMAG Asia), Bejing/ China, 11.-15.5.15 (2015).
123) B. Rellinghaus, *Probing the physical properties of nanomagnets at the atomic scale*, XXIV International Materials Research Congress (IMRC 2015), Cancun/ Mexico, 16.-20.8.15 (2015).
124) B. Rellinghaus, D. Pohl, A. Surrey, S. Schneider, E. Mohn, L. Schultz, *Unveiling the physical properties of nanomagnets at the atomic scale: Status quo and perspectives*, TEM Inauguration Day -MRC Workshop, IBM Research, Zuerich, Rueschlikon/ Schweiz, 30.1.15 (2015).

125) B. Rellinghaus, D. Pohl, A. Surrey, S. Schneider, L. Schultz, *Probing the physical properties of nanomagnets at the atomic scale: Status quo and perspectives*, BIT's 4th Annual Conference and Expo of AnalytiX 2015, Nanjing/ China, 25.-28.4.15 (2015).
126) F. Rhein, S. Vock, U. Wolff, H. Stopfel, V. Neu, D.S. Inosov, Y. Liu, C. Lin, H.J. Hug, N. Joshi, S. Oezer, L. Schultz, *Quantitative magnetic force microscopy: A method to determine the physical properties of superconducting materials by means of deconvolution*, Seminar Physikinstitut, Universitaet Kassel, Kassel, 26.-28.1.15 (2015).
127) M. Richter, *Hands-on-FPLO*, Tutorial at the European School on Magnetism, ESM 2015, Cluj-Napoca/ Hungary, 24.8.-4.9.15 (2015).
128) M. Richter, *Electronic structure calculations for magnetic systems*, Lecture at the European School on Magnetism, ESM 2015, Cluj-Napoca/ Hungary, 24.8.-4.9.15 (2015).
129) M. Richter, S. Schoenecker, X. Li, K. Koepernik, B. Johansson, L. Vitos, *An excursion along Bain paths of the transition metal elements*, VI Workshop on Novel Methods for Electronic Structure Calculations, La Plata/ Argentina, 12.-14.11.15 (2015).
130) J. Rusz, J.-C. Idrobo, D. Pohl, J. Spiegelberg, A. Edstroem, S. Schneider, B. Rellinghaus, *Towards measurement of magnetic properties of soingle atomic columns*, European Congress and Exhibition on Advanced Materials and Processes (EUROMAT) 2015, Warsaw/ Poland, 20.-24.9.15 (2015).
131) J. Sander, *Verarbeitung und Anwendbarkeit hochfester Stahlbauteile aus dem SLM Verfahren*, Symposium zum 3D-Druck, Erding/ Germany, 14.-15.10.15 (2015).
132) R. Schaefer, *Grains, grain boundaries and magnetic domains*, PIRE Workshop „From grain boundaries to stochastic homogenization", Max Planck Institute for Mathematics in the Sciences, Leibzig, Leipzig/ Germany, 20.-23.7.15 (2015).
133) R. Schaefer, *Magneto-optical Kerr microscopy*, Seminar an National Cheng Kung University, Department of Materials Science and Engineering, Tainan/ Taiwan, 26.8.15 (2015).
134) R. Schaefer, *Magneto-optical Kerr microscopy*, Seminar bei Advanced Technology & Materials Co., Ltd (AT&M), Peking/ China, 1.4.15 (2015).
135) R. Schaefer, *Magneto-optical Kerr microscopy*, Seminar an National Chung-Hsing University, Department of Physics, Taichung/ Taiwan, 10.3.15 (2015).
136) R. Schaefer, *Magnetic materials and applications*, Blockvorlesung an 2015 IEEE Magnetics Summer School, Minneapolis/ USA, 14.-19.6.15 (2015).
137) R. Schaefer, *Magneto-optical microscopy: basics, developments and applications*, Characterization of Magnetic Materials Workshop, at TMS 2015 Annual Meeting & Exhibition, Orlando/ USA, 15.3.15 (2015).
138) R. Schaefer, *Kerr Microscopy*, Seminar Vortrag, Silesian Center for Education and Interdisciplinary Research, Chorzow/ Poland, 23.10.15 (2015).
139) R. Schaefer, *Magneto-optical Kerr microscopy*, Seminarvortrag, Ural State University, Department of Magnetism and Magnetic Nanomaterials, Physics Department, Yekaterinburg/ Russia, 24.2.15 (2015).
140) R. Schaefer, *Magnetic Domains*, Vorlesung im Dept. of Physics, Simon Fraser University, Burnaby/ Canada, 18.9.15 (2015).
141) R. Schaefer, *Progress in Magneto-optical Domain Imaging*, Seminar am National Center for Mathematics and Physics, King Abdulaziz City for Science and Technology, Riyadh/ Saudi Arabia, 21.12.15 (2015).
142) R. Schaefer, *Progress in magneto-optical domain imaging*, Seminar an Wright-Patterson Air Force Base, Dayton/ USA, 24.9.15 (2015).
143) R. Schaefer, I. Soldatov, C. Becker, *Progress in magneto-optical domain imaging*, Donostia International Workshop on Energy, Materials, Nanotechnology (DINEMN) 2015, San Sebastian/ Spain, 1.-4.9.15 (2015).
144) R. Schaefer, I. Soldatov, C. Becker, *Progress in magneto-optical domain imaging*, Soft Magnetic Materials Conference SMM 22, Sao Paulo/ Brasil, 13.-16.9.15 (2015).
145) H. Schmidt, *More-than-Memory functionalities of memristive BiFeO3 thin film structures*, Kolloquium, Technische Universitaet Dresden, Dresden/ Germany, 5.5.15 (2015).
146) H. Schmidt, *Designing smart carriers for biosensors, tissue engineering, and directed cell growth by teaming up semiconductor wafers from micro/nano-electronics and polymer supports from biotechnology*, World Bio Summit & Expo 2015, Dubai/ United Arab Republic, 2.-4.11.15 (2015).
147) H. Schmidt, *Magnetic ZnO films with stable bound magnetic polarons*, Energy Materials Nanotechology (EMN) Istanbul Meeting, Istanbul/ Turkey, 1.-4.7.15 (2015).
148) H. Schmidt, *More-than-Moore functionalities of multiferroic BiFeO3 MIM structures*, Kolloquium, University of California, Department of Physics, San Diego/ USA, 16.4.15 (2015).
149) H. Schmidt, A. Sotnikov, S.V. Biryukov, M. Weihnacht, *Precise Microacoustic Characterization of new Piezoelectric Crystals for High-Temperature Sensors*, AMA Conferences 2015, Nuremberg/ Germany, 19.-21.5.15, in: Proceedings SENSOR 2015, 396-401 (2015).
150) H. Schmidt, A. Sotnikov, M. Weihnacht, S. Biryukov, *Precise characterization of crystals by means of surface acoustic waves*, 17th Scientific Seminar of the Dresden Fraunhofer Cluster Nanoanalysis (DFCNA), Dresden, 4.3.15 (2015).
151) O.G. Schmidt, *Hybrid nanomembranes: From imperceptible magnetoelectronics to micro-biorobotics*, The 5th International Conference on Manipulation, Manufacturing, and Measurement on the Nanoscale, Changchun/ China, 5.-9.10.15 (2015).

152) O.G. Schmidt, *Inorganic nanomembranes: From imperceptable magnetoelectronics to microautonomous systems*, Seminar, Ningbo Institute of Materials Technology and Engineering, CAS, Ningbo/ China, 18.5.15 (2015).
153) O.G. Schmidt, *3D assembly of microtubular nanomembrane devices*, NanoDay 2015, UNAM- National Nanotechnology Research Center, Ankara/ Turkey, 15.5.15 (2015).
154) O.G. Schmidt, *3D Nanomembrane architectures for physical, chemical and biomedical applications*, Seminar, Chinese University of Hong Kong, Hong Kong/ China, 12.10.15 (2015).
155) O.G. Schmidt, *Mikroroehren mit ungewoehnlichen Anwendungen*, Vorlesung, Seniorenakademie TU Dresden, Dresden, 26.2.15 (2015).
156) O.G. Schmidt, *Inorganic Nanomembranes: From imperceptible magnetoelectronics to hybrid micro-biomotors*, Seminar, Ecole Polytechnique de Montreal, Montreal, Canada, 5.2.15 (2015).
157) O.G. Schmidt, *3D nanomembrane architectures*, The 10th Annual IEEE International Conference on Nano/Micro Engineered and Molecular Systems (IEEE-NEMS 2015), Xi'an/ China, 7.-11.4.15 (2015).
158) O.G. Schmidt, *3D nanomembrane architectures: From lab-in-a-tube systems to micro-biorobotics*, Colloquium, University of Kiel, Kiel/ Germany, 7.8.15 (2015).
159) O.G. Schmidt, *Inorganic Nanomembranes: From flexible magnetoelectronics to micromotorized reproduction technologies*, Seminar, Soochow University, Suzhou/ China, 24.4.15 (2015).
160) O.G. Schmidt, *Tubular nanomembranes: 3D architectures for photonics, electronics, energy storage and micro-biorobotics*, SPIE Micro Technologies, Barcelona/ Spain, 4.-6.5.15 (2015).
161) O.G. Schmidt, *Straining and shaping nanomembranes: From concepts to applications*, Seminar, National Chiao Tung University, Hsinchu/ Taiwan, 22.5.15 (2015).
162) O.G. Schmidt, *Playing with inorganic nanomembranes*, Colloquium, University of Regensburg, Regensburg/ Germany, 12.1.15 (2015).
163) O.G. Schmidt, *Straining nanomembranes: From concepts to applications*, Zhong-Guan-Cun Forum on Condensed Matter Physics, Institute of Physics, CAS, Beijing/ China, 20.5.15 (2015).
164) O.G. Schmidt, *Playing with nanomembranes*, 581. WE-Heraeus-Seminar on Flexible, Stretchable and Printable High Performance Electronics, Bad Honnef/ Germany, 12.-14.1.15 (2015).
165) O.G. Schmidt, *Inorganic nanomembrane architectures*, IMPRS Workshop „Micro to Macro", Schloss Ringberg/ Germany, 9.-13.2.15 (2015).
166) O.G. Schmidt, *Progress in tubular micromotors and spermbots*, IEEE International Conference on Robotics and Automation 2015 (ICRA 2015), Seattle/ USA, 26.-30.5.15 (2015).
167) O.G. Schmidt, *Microtube optical ring resonators for integrated photonic and optofluidic applications*, SPIE Photonics West, San Francisco/ USA, 7.-12.2.15 (2015).
168) L. Schultz, *Interaction of Ferromagnetic and Superconducting Permanent Magnets: Superconducting Levitation*, Seminar of the Materials Sciences Division, Lawrence Berkeley National Laboratory, Berkeley/ USA, 12.10.15 (2015).
169) L. Schultz, *Vom Schweben auf Magnetfeldern: die wundersame Welt der Supraleiter*, 49. Metallographietagung der DGM, Dresden/ Germany, 16.-18.9.15 (2015).
170) L. Schultz, *Interaction of Ferromagnetic and Superconducting Permanent Magnets: Superconducting Levitation*, Seminar CIC nanoGUNE, San Sebastian/ Spain, 11.9.15 (2015).
171) L. Schultz, *Interaction of Ferromagnetic and Superconducting Permanent Magnets: Superconducting Levitation*, Condensed Matter and Nanophysdics Seminar, Department of Physics and Astronomy, University of Delaware, Newark, Delaware/USA, 9.11.15 (2015).
172) L. Schultz, *Interaction of Ferromagnetic and Superconducting Permanent Magnets: Superconducting Levitation*, IEEE Magnetics Society Distinguished Lecture, National Institute of Standards and Technology, Gaithersburg/ USA, 6.11.15 (2015).
173) L. Schultz, *Interaction of Ferromagnetic and Superconducting Permanent Magnets: Superconducting Levitation*, Electrical Engineering Department Seminar, University of Cambridge, Cambridge/ England, 10.3.15 (2015).
174) L. Schultz, *Interaction of Ferromagnetic and Superconducting Permanent Magnets: Superconducting Levitation*, Seminar, University of South Florida, Tampa, Florida/USA, 2.11.15 (2015).
175) L. Schultz, *Interaction of Ferromagnetic and Superconducting Permanent Magnets: Superconducting Levitation*, Physics Colloquium, University of York, York/ England, 14.4.15 (2015).
176) L. Schultz, *Interaction of Ferromagnetic and Superconducting Permanent Magnets: Superconducting Levitation*, Interaction of Ferromagnetic and Superconducting Permanent Magnets: Superconducting Levitation, Teddington/ England, 14.4.15 (2015).
177) L. Schultz, *Interaction of Ferromagnetic and Superconducting Permanent Magnets: Quantum Suspension*, Tyndall Lecture Series, Tynadall National Institute, Cork/ Ireland, 20.4.15 (2015).
178) L. Schultz, *Interaction of Ferromagnetic and Superconducting Permanent Magnets: Superconducting Levitation*, Fall Research Workshop, Center for Materials for Information Technology (MINT), University of Alabama, Tuscaloosa/ USA, 28.10.15 (2015).
179) L. Schultz, *Interaction of Ferromagnetic and Superconducting Permanent Magnets: Superconducting Levitation*, Seminar, Brooklyn College, City University of New York (CUNY), New York/ USA, 11.11.15 (2015).

180) L. Schultz, *Interaction of Ferromagnetic and Superconducting Permanent Magnets: Quantum Suspension*, International Conference on Materials for Advanced Technologies (ICMAT) 2015 and International Union of Materials Research Societies, International Conference in Asia (IUMRS-ICA) 2015, Singapore/ Singapore, 29.6.-3.7.15 (2015).
181) L. Schultz, *Interaction of Ferromagnetic and Superconducting Permanent Magnets: Quantum Suspension*, Physics Seminar, Imperial College, London/ England, 24.4.15 (2015).
182) L. Schultz, *Interaction of Ferromagnetic and Superconducting Permanent Magnets: Superconducting Levitation*, Physics Seminar, National University of Singapore, Singapore/ Singapore, 2.7.15 (2015).
183) L. Schultz, *Interaction of Ferromagnetic and Superconducting Permanent Magnets: Quantum Suspension*, Seminar Institut Louis Néel, CNRS Grenoble, Grenoble/ France, 28.8.15 (2015).
184) L. Schultz, *Interaction of Ferromagnetic and Superconducting Permanent Magnets: Quantum Suspension*, Donostia Int. Workshop on Energy, Materials and Nanotechnology, University of Basque Country, San Sebastian/ Spain, 1.-5.9.15 (2015).
185) L. Schultz, *Interaction of Ferromagnetic and Superconducting Permanent Magnets: Superconducting Levitation*, Seminar in memoriam Patricia Crespo, Instituto de Magnetismo Aplicado, Universidad Complutense, Madrid/ Spain, 7.9.15 (2015).
186) L. Schultz, *Interaction of Ferromagnetic and Superconducting Permanent Magnets: Superconducting Levitation*, Seminar Instituto de Ciencia de Materiales, CSIC and Universidad Autonoma Madrid, Madrid/ Spain, 8.9.15 (2015).
187) L. Schultz, *Interaction of Ferromagnetic and Superconducting Permanent Magnets: Superconducting Levitation*, Solid State Physics Seminar, Argonne National Laboratory, Argonne/ USA, 15.6.15 (2015).
188) L. Schultz, *Interaction of Ferromagnetic and Superconducting Permanent Magnets: Superconducting Levitation*, Seminar, Iowa State University, Ames/ USA, 17.6.15 (2015).
189) L. Schultz, *Interaction of Ferromagnetic and Superconducting Permanent Magnets: Superconducting Levitation*, IEEE DL Seminar, Seagate Company, Minneapolis/ USA, 18.6.15 (2015).
190) L. Schultz, *Interaction of Ferromagnetic and Superconducting Permanent Magnets: Superconducting Levitation or: The Physics Behind the „Back to the Future" Hoverboard*, Physics Colloquium, Jozef Stefan Institute, Ljubljana/ Slovenia, 16.12.15 (2015).
191) L. Schultz, *Interaction of Ferromagnetic and Superconducting Permanent Magnets: Superconducting Levitation or: The Physics Behind the „Back to the Future" Hoverboard*, Physikalisches Kolloquium, TU Graz and University of Graz, Graz/ Austria, 15.12.15 (2015).
192) L. Schultz, *Interaction of Ferromagnetic and Superconducting Permanent Magnets: Superconducting Levitation or: The Physics Behind the „Back to the Future" Hoverboard*, Seminar, Erich-Schmid-Institute and Montanuniversität Leoben, Leoben/ Austria, 14.12.15 (2015).
193) L. Schultz, *Superconducting Levitation: Physics and Applications or: The Physics Behind the „Back to the Future" Hoverboard*, Seminarium Naukowe, Uniwersytet Wroclawski, Wroclaw/ Poland, 11.12.15 (2015).
194) L. Schultz, *Riding on Magnetic Fields - the Miraculous World of Superconductivityor: The Physics Behind the „Back to the Future" Hoverboard*, Visiting Professor Public DL Seminar, Fundusz Scientiae Wratislavienses, City of Wroclaw, Wroclaw/ Poland, 11.12.15 (2015).
195) L. Schultz, *Electric and Magnetic Functional Materials for Energy-Related Applications*, Visiting Professor Seminar, Fundusz Scientiae Wratislavienses, International Laboratory of High Magnetic Fields and Low Temperatures Wroclaw, Wroclaw/ Poland, 10.12.15 (2015).
196) L. Schultz, *Superconducting Levitation: Physics and Applications or: The Physics Behind the „Back to the Future" Hoverboard*, Seminar, Polytechnical University of Wroclaw, Wroclaw/ Poland, 8.12.15 (2015).
197) L. Schultz, *Interaction of Ferromagnetic and Superconducting Permanent Magnets: Superconducting Levitation or: The Physics Behind the „Back to the Future" Hoverboard*, Materials Science Colloquium, TU Darmstadt, Darmstadt/ Germany, 4.12.15 (2015).
198) L. Schultz, *Magnetic Levitation: The Physics Behind the „Back to the Future" Hoverboard*, Seminar, Carnegie Mellon University, Pittsburgh/ USA, 16.11.15 (2015).
199) L. Schultz, *Interaction of Ferromagnetic and Superconducting Permanent Magnets: Superconducting Levitation*, IEEE DL Seminar, Boston Chapter of IEEE Magnetics Society, Northeastern University, Boston/ USA, 12.11.15 (2015).
200) L. Schultz, *Interaction of Ferromagnetic and Superconducting Permanent Magnets: Superconducting Levitation*, Instituto Nacional de Tecnica Aerospacial (INTA), Torrejon de Ardoz, Madrid/ Spain, 9.9.15 (2015).
201) L. Schultz, *Prospects of High Temperature Superconductors*, IEEE Taiwan Chapter Meeting, International Forum, National Taiwan University, Taipei/ Taiwan, 29.-30.6.15 (2015).
202) L. Schultz, *Interaction of Ferromagnetic and Superconducting Permanent Magnets: Superconducting Levitation*, Seminar Departamento de Fisica, Universidad Publica de Navarra, Pamplona/ Spain, 4.9.15 (2015).
203) L. Schultz, *Interaction of Ferromagnetic and Superconducting Permanent Magnets: Superconducting Levitation*, Seminar, YAZAKI Technology Center America, Camarill/ USA, 15.10.15 (2015).
204) L. Schultz, *Interaction of Ferromagnetic and Superconducting Permanent Magnets: Superconducting Levitation*, Seminar, National High Magnetic Field Laboratory, Florida State University at Tallahassee, Tallahassee/ USA, 30.10.15 (2015).
205) L. Schultz, *Interaction of Ferromagnetic and Superconducting Permanent Magnets: Superconducting Levitation*, Seminar Instituto de Ciencia de Materiales de Aragón, Universidad de Zaragoza, Zaragoza/ Spain, 3.9.15 (2015).

206) L. Schultz, *Interaction of Ferromagnetic and Superconducting Permanent Magnets: Superconducting Levitation*, Nebraska Center for Matewrials and Nanoscience, University of Nebraska at Lincoln, Lincoln, Nebraska/ USA, 26.10.15 (2015).
207) L. Schultz, *Interaction of Ferromagnetic and Superconducting Permanent Magnets: Superconducting Levitation*, Physics Seminar, University of Wyoming at Laramie, Laramie/ USA, 23.10.15 (2015).
208) L. Schultz, *Interaction of Ferromagnetic and Superconducting Permanent Magnets: Superconducting Levitation*, Physics Seminar, Colorado State University, Fort Collins/ USA, 22.10.15 (2015).
209) L. Schultz, *Interaction of Ferromagnetic and Superconducting Permanent Magnets: Superconducting Levitation*, Colloquium, University of Colorado at Boulder and NIST Boulder, Boulder/ USA, 21.10.15 (2015).
210) L. Schultz, *Interaction of Ferromagnetic and Superconducting Permanent Magnets: Superconducting Levitation*, Physics Colloquium, University of Denver, Denver/ USA, 20.10.15 (2015).
211) L. Schultz, *Interaction of Ferromagnetic and Superconducting Permanent Magnets: Superconducting Levitation*, Seminar, University of Colorado at Colorado Springs, Colorado Springs/ USA, 19.10.15 (2015).
212) L. Schultz, *Interaction of Ferromagnetic and Superconducting Permanent Magnets: Superconducting Levitation*, Seminar, Oregon State University, Corvallis/ USA, 9.10.15 (2015).
213) L. Schultz, *Interaction of Ferromagnetic and Superconducting Permanent Magnets: Superconducting Levitation*, Seminar of the Center for Magnetic Recording Research, University of California at San Diego (UCSD), La Jolla/ USA, 16.10.15 (2015).
214) L. Schultz, *Interaction of Ferromagnetic and Superconducting Permanent Magnets: Superconducting Levitation*, Physics Seminar, University of California at Davis, Davis/ USA, 13.10.15 (2015).
215) L. Schultz, *Interaction of Ferromagnetic and Superconducting Permanent Magnets: Superconducting Levitation*, Seminar, Stanford Institute for Materials & Energy Sciences, Stanford University and SLAC, Stanford/ USA, 13.10.15 (2015).
216) L. Schultz, *Interaction of Ferromagnetic and Superconducting Permanent Magnets: Superconducting Levitation*, 8th IEEE Magnetics Society Summer School, University of Minnesota, Minnesota/ USA, 18.6.15 (2015).
217) L. Schultz, *Interaction of Ferromagnetic and Superconducting Permanent Magnets: Superconducting Levitation*, 7th International Workshop on Amorphous and Nanostructured Magnetic Materials ANMM'2015, Iasi/ Romania, 21.-24.9.15 (2015).
218) L. Schultz, *Interaction of Ferromagnetic and Superconducting Permanent Magnets: Superconducting Levitation*, Seminar ICMAB, Universidad Autonoma, Bellaterra/ Spain, 23.6.15 (2015).
219) L. Schultz, *Interaction of Ferromagnetic and Superconducting Permanent Magnets: Superconducting Levitation*, IEEE Taiwan Chapter Meeting, National Taiwan University, Taipei/ Taiwan, 29.-30.6.15 (2015).
220) L. Schultz, *Interaction of Ferromagnetic and Superconducting Permanent Magnets: Superconducting Levitation*, Seminar Facultad de Ciencia y Tecnologia, Universidad del Pais Vasco, Bilbao/ Spain, 10.9.15 (2015).
221) L. Schultz, D. Berger, *Interaction of Ferromagnetic and Superconducting Permanent Magnets: Quantum Suspension*, Wing Konferenz, BMBF, Dresden/ Germany, 27.-28.4.15 (2015).
222) L. Schultz, S. Kauffmann-Weiss, *Interaction of Ferromagnetic and Superconducting Permanent Magnets: Quantum Levitation*, Advanced Seminar on Condensed Matter Physics, Universitaet Heidelberg, 6.2.15 (2015).
223) L. Schultz, A. Kirchner, *Interaction of Ferromagnetic and Superconducting Permanent Magnets: Superconducting Levitation*, Kolloquium des Instituts für Technische Physik, Karlsruhe Institut für Technologie (KIT), Karlsruhe/ Germany, 28.4.15 (2015).
224) L. Schultz, A. Kirchner, *Interaction of Ferromagnetic and Superconducting Permanent Magnets: Superconducting Levitation*, Physics Seminar, Universite de Lorraine und CNRS, Nancy/ Frankreich, 29.4.15 (2015).
225) L. Schultz, L. Klodt, *Interaction of Ferromagnetic and Superconducting Permanent Magnets: Superconducting Levitation*, Magnetism and Spin Electronics Group Seminar, Trinity College, Dublin/ Ireland, 21.4.15 (2015).
226) L. Schultz, J. Thielsch, *Vom Schweben auf Magnetfeldern: die wundersame Welt der Supraleiter*, Explore Science 2015 (Veranstaltung der Klaus-Tschirra-Stiftung), Mannheim/ Germany, 6.-12.7.15 (2015).
227) L. Schultz, K. Tschulik, *Interaction of Ferromagnetic and Superconducting Permanent Magnets: Superconducting Levitation*, Colloquium of the Materials Department, University of Oxford, Oxford/ England, 23.4.15 (2015).
228) H. Schwab, J. Eckert, F. Palm, U. Kuehn, *Selektives Laserstrahlschmelzen von Titanlegierungen - Herausforderungen und Perspektiven*, Symposium zum 3D-Druck, Erding/ Germany, 14.-15.10.15 (2015) (2015).
229) H. Schwab, U. Kuehn, F. Palm, J. Eckert, *Selektives Laserstrahlschmelzen der Legierung Ti-5553: Chancen und Herausforderungen*, Werkstoffwoche 2015: „Werkstoffe der Zukunft", Dresden/ Germany, 14.-17.9.15 (2015).
230) S. Scudino, *Effect of mechanical pretreatment on the mechanical behavior of bulk metallic glasses*, 2nd Industry-Network Meeting – VitriMetTech ITN, "Mechanical Properties of Vitrified Metals", IFW Dresden, Dresden/ Germany, 14.-17.9.15 (2015).
231) S. Scudino, H. Shakur Shahabi, M. Stoica, I. Kaban, G. Vaughan, U. Kuehn, J. Eckert, *Strain Analysis of Plastically-deformed Bulk Metallic Glasses*, 22nd International Symposium on Metastable, Amorphous and Nanostructured Materials (ISMANAM 2015), Paris/ France, 13.-17.7.15 (2015).
232) M. Sparing, D. Berger, A. Berger, M. Hossain, A. Abdkader, C. Chokri, L. Kuehn, T. Espenhahn, G. Fuchs, L. Schultz, *Superconducting Magnetic Bearings*, Magnetics in a Green Future (UKMagSoc), Copenhagen/ Denmark, 2.-3.11.15 (2015).
233) M. Stoica, *Mechanical properties of bulk glassy alloys studied by means of X-ray diffraction*, Seminar of the Department of Physics, University of Balearic Islans, Palma de Mallorca/ Spain, 11.11.15 (2015).

234) M. Stoica, *Preparation of Bulk Metallic Glasses*, The seminar of the Institute of Metallurgy and Materials Science, Polish Academy of Sciences, Krakow/ Poland, 2.10.15 (2015).
235) M. Stoica, *Structure evolution of {[(Fe0.5Co0.5)0.75Si0.05B0.20]0.96Nb0.04}100-xCux (x = 0 and 0.5) bulk glassy alloys*, Joint CMAC-Intelhyb workshop, Dresden/ Germany, 30.9.15 (2015).
236) M. Stoica, *Bulk Metallic Glasses (BMGs) and their composites*, The seminar of the Institute of advanced manufacturing technology, Krakow/ Poland, 8.10.15 (2015).
237) M. Stoica, *(Fe36Co36B19.2Si4.8Nb4)100-xCux (x = 0 and 0.5) BMGs, Crystallisation Behavior and magnetic properties*, XXIV International Materials Research Congress, Cancun/ Mexico, 16.-20.8.15 (2015).
238) M. Stoica, S. Scudino, I. Kaban, P. Ramasamy, M. Nicoara, J. Eckert, *(Fe36Co36B19.2Si4.8Nb4)100-xCux (x = 0 and 0.5) Bulk Amorphous Alloys, Structure Evolution and Soft Magnetic Properties*, Global Research Laboratory Korea- Germany Workshop on Bulk Metallic Glasses and Nanostructured Materials, Munich/ Germany, 10.-11.7.15 (2015).
239) M. Stoica, S. Scudino, I. Kaban, P. Ramasamy, M. Nicoara, J. Eckert, *Structure evolution and soft magnetic properties of Cu-free and Cu-added Fe-Co-B-Si-Nb BMGs*, Advanced Materials and Structures AMS'15, Timisoara/ Romania, 16.-17.10.15 (2015).
240) M. Stoica, S. Scudino, I. Kaban, P. Ramasamy, M. Nicoara, J. Eckert, *(Fe36Co36B19.2Si4.8Nb4)100-xCux (x = 0 and 0.5) Bulk Amorphous Alloys, Structure Evolution and Soft Magnetic Properties*, 22nd International Symposium on Metastable, Amorphous and Nanostructured Materials (ISMANAM 2015), Paris/ France, 13.-17.7.15 (2015).
241) R. Streubel, *Imaging spin textures on curved magnetic surfaces*, Seminar, Helmholtz-Zentrum Dresden-Rossendorf, Dresden/ Germany, 18.6.15 (2015).
242) R. Streubel, D. Makarov, *Curved magnetic nanomembranes*, International Magnetics Conference (INTERMAG), Beijing/ China, 11.-15.5.15 (2015).
243) A. Surrey, C. Bonatto Minella, N. Fechler, M. Antonietti, L. Schultz, B. Rellinghaus, *Nanocrystalline MgH2 and nanoconfined LiBH4 for solid state hydrogen storage*, ANM2015 1st International conference on Hydrogen Energy, Aveiro/ Portugal, 20.-22.7.15 (2015).
244) J. van den Brink, *Resonant Inelastic X-ray Scattering on high Tc cuprates and magnetic iridates*, Nordita Physics Seminar, Stockholm/ Sweden, 15.12.15 (2015).
245) J. van den Brink, *Magnetic Resonant Inelastic X-ray Scattering - an overview*, 9th international conference on Inelastic X-ray Scattering, Hsinchu/ Taiwan, 22.11.15 (2015).
246) J. van den Brink, *Resonant Inelastic X-ray Scattering on high Tc cuprates and magnetic iridates*, V International Symposium on Strong Nonlinear Vibronic and Electronic Interactions in Solids, University of Tartu, Tartu/ Estonia, 1.5.15 (2015).
247) J. van den Brink, *Resonant Inelastic X-ray Scattering on high Tc cuprates and magnetic iridates*, BIT's 4th Annual World Congress of Advanced Materials, Chongqing/ China, 29.5.15 (2015).
248) J. van den Brink, *Insights into the electronic and magnetic structure of iridates from Resonant Inelastic X-ray Scattering and Quantum Chemistry*, Workshop on Competing Interactions and Colossal Responses in Transition Metal Oxides, Telluride/ USA, 6.6.15 (2015).
249) J. van den Brink, *40 years of Resonant Inelastic X-ray Scattering - accomplishments and remaining challanges*, Kai Siegbahn Prize Ceremony, Uppsala/ Sweden, 14.9.15 (2015).
250) J. van den Brink, *The quantum nature of skyrmions and half-skyrmions in Cu_2OSeO_3*, APS March Meeting Invited Talk, San Antonio/ USA, 4.3.15 (2015).
251) J. van den Brink, *Magnetic Resonant Inelastic X-ray Scattering*, 5th Annual Niels Bohr International Academy Workshop-School on ESS Science: Condensed Matter Theory and Advanced software, Copenhagen/ Denmark, 11.11.15 (2015).
252) J. van den Brink, *Spin-orbital separation in the quasi-one-dimensional Mott insulator Sr_2CuO_3*, Physics Colloquium, University of Toronto, Toronto/ Canada, 12.2.15 (2015).
253) J. van den Brink, *Spin-orbital separation in the quasi-one-dimensional Mott insulator Sr_2CuO_3*, Condensed-Matter Physics and Materials Science Seminar, Brookhaven National Laboratries, Brookhaven/ USA, 9.2.15 (2015).
254) J. van den Brink, *Resonant Inelastic X-ray Scattering on high Tc cuprates and magnetic iridates*, Physics Seminar, University of Toronto, Toronto/ Canada, 12.2.15 (2015).
255) J. van den Brink, *Resonant Inelastic X-ray Scattering on high Tc cuprates and magnetic iridates*, COST TO-BE Spring Meeting Plenary Presentation, University of Avero, Avero/ Portugal, 1.4.15 (2015).
256) J. van den Brink, *Spin-orbital separation in the quasi-one-dimensional Mott insulator Sr_2CuO_3*, Leopold Infeld Colloquium, University of Warsaw, Warsaw/ Poland, 22.10.15 (2015).
257) J. van den Brink, *Resonant Inelastic X-ray Scattering on high Tc cuprates and magnetic iridates*, Transregio Seminar, University of Augsburg, Augsburg/ Germany, 28.4.15 (2015).
258) U. Vogel, M. Spindler, S. Wege, T. Gemming, *Calculation of surface acoustic waves on a piezoelectric substrate using Amazon Cloud Computing*, Comsol Conference, Italy/ Grenoble, 14.-16.10.15 (2015).
259) S. Wicht, V. Neu, L. Schultz, V. Metha, S. Jain, S.H. Wee, O. Hellwig, D. Weller, B. Rellinghaus, *The relevance of structure information at the atomic level for a better understanding of FePt-based media*, The 26th Magnetic Recording Conference (TMRC 2015), Minneapolis/ USA, 17.-19.8.15 (2015).

260) A. Winkler, *Einfuehrung in die akustoelektronische Mikrofluidik*, Einzelvorlesung im Rahmen der Vorlesung Mikrobiologie der TU Dresden (ILBT), TU Dresden, Institut fuer Lebensmittel und Bioverfahrenstechnik, Dresden, 5.2.15 (2015).
261) U. Wolff, *The variety of scanning probe methods - investigating magnetic and superconducting structures*, BIT's 1st Annual World Congress of Smart Materials-2015, Busan/ South Korea, 23.-26.3.15 (2015).
262) T.G. Woodcock, *The Influence of Atomic-Scale Microstructural Features on the Properties of Permanent Magnets*, Seminar at the Institute of Ion Beam Physics and Materials Research, Helmoltz-Zentrum Dresden-Rossendorf, Dresden, 22.4.15 (2015).
263) S. Wurmehl, *Disentanglement of intrinsic and extrinsic properties in highly functional Heusler materials*, Physics colloquium, TU Dresden. Dresden/ Germany, 21.7.15 (2015).
264) S. Wurmehl, *Complex, novel materials for modern applications- A crystal growth perspective*, IKZ Berlin and HU Berlin, Berlin/ Germany, 19.2.15 (2015).
265) S. Wurmehl, *Disentanglement of intrinsic and extrinsic properties in highly functional Heusler materials*, Kolloqium, Uni Bielefeld, Bielefeld/ Germany, 23.-24.11.15 (2015).
266) S. Wurmehl, L. Harnagea, S. Aswartham, I. Morozov, A. Wolter-Giraud, H.-J. Grafe, F. Steckel, U. Graefe, D. Bombor, C. Hess, B. Borisenko, B. Buechner, *Crystal growth and properties of pnictide superconductors*, International Conference on Magnetic and Superconducting Materials (MSM), Antalya/ Turkey, 30.4.-3.5.15 (2015).
267) S. Wurmehl, C. Hess, H.-J. Grafe, V. Kataev, S. Borisenko, L. Harnegea, S. Aswartham, R. Beck, I. Morozov, F. Hammerath, F. Steckel, D. Bombor, D. Evtushinskiy, B. Buechner, *Pnictide superconductors-a crystal growth perspective*, 14th International Union of Materials Research Societies-International Conference on Advanced Materials 2015 (IUMRS-ICAM), Jeju Island/ South Korea, 25.-29.10.15 (2015).
268) F. Zhu, *Novel organic nanostructure devices based on rolled-up nanomembranes*, Seminar, Changchun Institute of Applied Chemistry, Chinese Academy of Sciences, Changchun/ China, 2.11.15 (2015).
269) F. Zhu, *Novel organic/hybrid electronic devices based on rolled-up nanomembranes*, The AVS Shanghai Thin Film Conference Shanghai, Shanghai/ China, 24.-25.10.15 (2015).
270) F. Zhu, *Organic thin film engineering and novel organic/hybrid electronic devices*, Seminar, University of Electronic Science and Technology of China, Chengdu/ China, 29.10.15 (2015).

Patents

Issues of patents (issue decision date)

DE 10 2009 002 308 (10909 DE)	Verfahren und Anordnung zum Anregen von elektroakustischen Aktuatoren (09.10.2015) *Inventors:* Raimund Brünig, Hagen Schmidt, Karsten Mensel
EP 2422347 (10914 AT)	Magnetisches Legierungsmaterial und Verfahren zu seiner Herstellung (08.06.2015) *Inventors:* Julia Lyubina, Oliver Gutfleisch
EP 2422347 (10914 CH/LI)	Magnetisches Legierungsmaterial und Verfahren zu seiner Herstellung (08.06.2015) *Inventors:* Julia Lyubina, Oliver Gutfleisch
EP 2422347 (10914 DE)	Magnetisches Legierungsmaterial und Verfahren zu seiner Herstellung (08.06.2015) *Inventors:* Julia Lyubina, Oliver Gutfleisch
EP 2422347 (10914 FR)	Magnetisches Legierungsmaterial und Verfahren zu seiner Herstellung (08.06.2015) *Inventors:* Julia Lyubina, Oliver Gutfleisch
EP 2422347 (10914 GB)	Magnetisches Legierungsmaterial und Verfahren zu seiner Herstellung (08.06.2015) *Inventors:* Julia Lyubina, Oliver Gutfleisch
DE 10 2014 222 535.3 (11415 DE)	Ultrakompakter Mikrokondensator und Verfahren zu seiner Herstellung (01.12.2015) *Inventors:* Daniel Grimm, Martin Bauer, Oliver G. Schmidt
DE 10 2014 223 873.0 (11429 DE)	Verfahren zur Herstellung eines aufgerollten elektrischen oder elektronischen Bauelementes (16.10.2015) *Inventors:* Daniel Grimm, Dmitriy Karnaushenko, Martin Bauer, Daniil Karnaushenko, Denys Makarov, Oliver G. Schmidt
CH 001321_2013 (11137 CH/LI)	Aufspul- und Dralleinrichtung einer Ringspinn- oder Ringzwirnmaschine sowie Ringspinn- und Ringzwirnverfahren (15.09.2015) *Inventors:* Anwar Abdkader, Dietmar Berger, Chokri Cherif, Oliver De Haas, Lars Kühn, Ludwig Schultz
US 13/202,228 (10903 US)	ISOLATIONSMATERIAL FÜR INTEGRIERTE SCHALTKREISE UND DEREN VERWENDUNG (25.08.2015) *Inventors:* Ehrenfried Zschech, Helmut Hermann, Konstantin Zagarodniy, Gotthard Seifert
DE 10 2012 206 393.5 (11207 DE)	Akustisches Oberflächenbauelement (10.04.2015) *Inventors:* Günter Martin, Bernd Steiner
DE 10 2010 028 007.0 (11006 DE)	Wandler mit natürlicher Unidirektionalität für akustische Oberflächenwellen (24.02.2015) *Inventors:* Günter Martin, Manfred Weihnacht, Sergey Biryukov, Alexander Darinski, Bert Wall

Patent applications (application date)

PCT/EP2015/077070 (11429PCT)	Verfahren zur Herstellung eines aufgerollten elektrischen oder elektronischen Bauelementes (19.11.2015) *Inventors:* Daniel Grimm, Dmitriy Karnaushenko, Martin Bauer, Daniil Karnaushenko, Denys Makarov, Oliver G. Schmidt
PCT/EP2015/075822 (11415 PCT)	Ultrakompakter Mikrokondensator und Verfahren zu seiner Herstellung (05.11.2015) *Inventors:* Daniel Grimm, Martin Bauer, Oliver G. Schmidt
DE 10 2015 224 938.7 (11528 DE)	Verfahren und Vorrichtung zur Ermittlung von Kraftfeldern, Kraftfeldgradienten, Materialeigenschaften oder Massen mit einem System aus gekoppelten, schwingungsfähigen, balkenartigen Komponenten (11.12.2015) *Inventors:* Christopher Reiche, Thomas Mühl, Julia Körner
PCT/EP2015/068723 (11413 PCT)	Hochfeste, mechanische Energie absorbierende und korrosionsbeständige Formkörper aus Eisenlegierungen und Verfahren zu deren Herstellung (14.08.2015) *Inventors:* Josephine Zeisig, Julia Kristin Hufenbach, Uta Kühn, Jürgen Eckert
DE 10 2015 221 268.8 (11520 DE)	Verfahren und Vorrichtung zur Regelung des Spaltmaßes in supraleitenden Magnetlagern (30.10.2015) *Inventors:* Dirk Lindackers, Christoph Mühsig

PCT/EP2015/073540 (11426 PCT)	Kompakter Kondensator und Verfahren zu seiner Herstellung (12.10.2015) *Inventor:* Oliver G. Schmidt
DE 10 2015 219 696.8 (11521 DE)	Verfahren zur Herstellung eines kompakten Mikro- oder Nano-Kondensators und kompakter Mikro- oder Nano-Kondensator (12.10.2015) *Inventor:* Oliver G. Schmidt
DE 10 2015 220 766.8 (11523 DE)	Verfahren zur Herstellung eines umgeformten Körpers aus vollkristallinen, metastabilen Materialien und umgeformter Körper aus vollkristallinen, metastabilen Materialien (23.10.2015) *Inventors:* Simon Pauly, Konrad Kosiba, Uta Kühn, Jürgen Eckert
EP 15 193 411.4 (11430 EP)	Vorrichtung zur Flüssigkeitszerstäubung und Verfahren zu ihrer Herstellung (06.11.2015) *Inventors:* Andreas Winkler, Stefan Harazim, Jürgen Eckert, Oliver G. Schmidt
PCT/EP2015/063638 (11414 PCT)	Batterieträger (17.06.2015) *Inventors:* Markus Herklotz, Jonas Weiß, Lars Giebeler, Michael Knapp
PCT/EP2015/051650 (11402 PCT)	Verfahren zur Herstellung der Beweglichkeit von immobilen Zellen (28.01.2015) *Inventor*: Oliver G. Schmidt
DE 10 2015 108 950.5 (11432 DE)	Keramische Drucksensoren mit im thermischen Ausdehnungskoeffizient an die Keramik angepasstem Aktivhartlot (08.06.2015) *Inventors:* Andreas Roßberg, Elke Schmidt, Markus Rettenmayr, Peter Siegmund, Uta Kühn, Simon Pauly
DE 10 2015 203 272.8 (11501 DE)	Magnetoelektrische Funktionselemente (24.02.2015) *Inventors:* Tobias Kosub, Denys Makarov, Oliver G. Schmidt
DE 10 2015 214 177.2 (11508 DE)	Drehbarer Batterieträger (27.07.2015) *Inventors:* Markus Herklotz, Jonas Weiß, Eike Ahrens, Lars Giebeler
DE 10 2015 204 112.3 (11503 DE)	Biologisch abbaubare Eisenbasislegierungen und ihre Verwendung (06.03.2015) *Inventors:* Julia Kristin Hufenbach, Uta Kühn, Annett Gebert, Jürgen Eckert
DE 10 2015 205 443.8 (11506 DE)	Anodenmaterial für Lithium-Ionen-Batterien (25.03.2015) *Inventors:* Maik Scholz, Rüdiger Klingeler, Marcel Haft, Sabine Wurmehl, Silke Hampel, Franziska Hammerath, Bernd Büchner
DE 10 2015 200 643.3 (11410 DE)	Verfahren zur Herstellung von neuronale Zellen enthaltenden strangförmigen Kapseln und strangförmige Kapseln (16.01.2015) *Inventors:* Andreas Winkler, Anne K. Meyer

Graduation of young researchers

Habilitations

Dr. Mihai Stoica	Fe-based bulk metallic glasses: alloy optimization, focused on understanding the influences of impurities on the glass formation, Politehnica University Timisoara, Romania
Dr. Steffen Sykora	Interferenz von Quasiteilchen als Zugang zum Paarungs-Mechanismus eisenbasierter Supraleiter, TU Dresden

PhD Theses

Somayeh Abdi	Investigation of new Ti-based metallic glasses with improved mechanical properties and corrosion resistance for implant applications, TU Dresden
Stefan Böttner	Rolled-Up Vertical Microcavities Studied by Evanescent Wave Coupling and Photoluminescence Spectroscopy, TU Chemnitz
André Fischer	Advanced cluster methods for correlated-electron systems, TU Dresden
Arne Helth	Optimierung der biofunktionellen Eigenschaften der Legierung Ti-40Nb für Knochenersatzanwendungen, TU Dresden
Deng Junwen	Strain engineered nanomembranes as anodes for lithium ion batteries, TU Chemnitz
Vamshi Mohan Katukuri	Quantum chemical approach to spin-orbit excitations and magnetic interactions in iridium oxides, TU Dresden
Jin Young Kim	Synthesis and characterization of bulk metallic glasses, composites and hybrid porous structures by powder metallurgy of Ni59Zr20Ti16Si2Sn3 glassy powders, TU Dresden
Markus Klose	Zur Verwendung einer metallorganischen Gerüstverbindung als Präkursor für poröse, kohlenstoffbasierte Energiespeichermaterialien, TU Dresden
Fritz Kurth	High Magnetic Field Properties of Fe - Pnictide Thin Films, TU Dresden
Shilong Li	Probing and modeling of optical resonances in rolled-up structures, TU Chemnitz
Lukas Löber	Werkstoffwissenschaftliche Aspekte des Leichtbaus von laserstrahlgeschmolzenen Titanaluminiden, TU Dresden
Benjamin Mahns	Elektronische Eigenschaften dotierter polyzyklischer aromatischer Kohlenwasserstoffe, TU Dresden
Sami Makharza	Graphene Oxide Nanohybrids as Platforms for Carboplatin Loading and Delivery, TU Dresden
Janek Maletz	Low-energy electronic structure of iron chalcogenide superconductors, TU Dresden
Pasquale Marra	Theoretical approach to direct resonant inelastic X-ray scattering on magnets and superconductors, TU Dresden
Michael Melzer	Stretchable Magnetoelectronics, TU Chemnitz
Rafael Gregorio Mendes	Synthesis, characterization and toxicological evaluation of carbon-based nanostructures, TU Dresden
Robert Niemann	Nukleation und Wachstum des adaptiven Martensits in epitaktischen Schichten der Formgedächtnislegierung Ni-Mn-Ga, TU Dresden
Ilya Okulov	Microstructure and mechanical Properties of new composite structured Ti-based alloys, TU Dresden
Santosh Kumar Pal	Anisotropic hard magnetic nanoparticles and nanoflakes obtained by surfactant assisted ball milling, TU Dresden
Diana Pohl	Elektrochemische Fe-Ga-Legierungsabscheidung zur Herstellung von Nanostrukturen, TU Dresden
Tobias Ritschel	Electronic self-organization in layered transition metal dichalcogenides, TU Dresden
Martha Scheffler	Microscopic tunneling experiments on atomic impurities in graphene and on magnetic thin films, TU Dresden
Thomas Schied	Zum Sauerstofftransport in Li-O2-Zellen: Eine Computermodell-unterstützte Experimentalstudie, TU Dresden
Hamed Shakur Shahabi	Study of deformation – induced structures in Zr-based bulk metallic glass via high energy x-ray diffraction, TU Dresden
Wenping Si	Designing Electrochemical Energy Storage Micro-Devices: Li-Ion Batteries and Flexible Supercapacitors, TU Chemnitz

Frank Silze	Entwicklung und Untersuchung Ag-reduzierter Vakuumhartlote auf Cu-Basis, TU Dresden
Frank Steckel	Thermische und elektrische Transportuntersuchungen an niederdimensionalen korrelierten Elektronensystemen, TU Dresden
Robert Streubel	Imaging Spin Textures on Curved Magnetic Surfaces, TU Chemnitz
Juliane Thielsch	Wechselwirkungsdomänen in permanentmagnetischen Seltenerd-Übergangsmetall-Verbindungen, TU Dresden
Uwe Treske	Valence changes at interfaces and surfaces investigated by X-ray spectroscopy, TU Dresden
Daniel Wadewitz	Ternäre 3d Übergangsmetalloxide als Konversionselektroden in Lithiumionenbatterien, TU Dresden
Eugenio Zallo	Control of electronic and optical properties of single and double quantum dots via electroelastic fields, TU Chemnitz
Jiaxiang Zhang	Single- and entangled-photon emission from strain tunable quantum dot devices, TU Chemnitz

Diploma and Mater Theses

Wei Ding	Nonvolatile capacitance switching in BiFeO3 coated metal-insulator-semiconductor diodes, TU Chemnitz
Konstantin Firlus	Anpassung des selektiven Laserschmelzens auf die höchstfeste Eisenbasislegierung Fe85Cr4Mo1V1W8C1, TU Dresden
Martin Fritzsche	Untersuchung eines CNT-basierten schwammartigen Materials für die Anwendung in Lithium-Schwefel-Batterien, TU Dresden
Hagen Fuchs	Models and simulations of chiral magnetic systems, TU Dresden
Clemens Gütter	Streufeldverteilungen von aufgerollten ferromagnetischen Nanomembranen, TU Dresden
Carsten Habenicht	Electron Energy-Loss Spectroscopy on MoS2, TU Dresden
Robert Heider	Nanoskalige Sn-Co-Verbindungen durch Füllen von CNT, BTU Cottbus-Senftenberg
Michael Hering	Thermisch induzierte Segregationsprozesse in kohlenstoffreichen Übergangsmetall-Nanopartikeln, TU Dresden
Christian Kozalla	Realisierung ultradünner granularer Eisen-Platin-Schichten auf SrTiO3 zur Behandlung in einem Elektrolyten, TU Dresden
Bandari Vineeth Kumar	Fabrication of Organic Single Crystal Transistors, TU Chemnitz
Till Meißner	Konstruktion und Entwicklung eines Kryo-Magnetkraftmikroskops, HTW Dresden
Georg Mühsig	Umbau einer Gifford-McMahon-Kältemaschine für den Einsatz als kryotechnischer Praktikumsversuchsstand, HTW Dresden
Georg Rutkiewicz	Umbau einer Hochrate-Zerstäuber-Beschichtungsanlage mit drei Magnetrons für den Gleichstrom- bzw. Hochfrequenzbetrieb, Staatliche Studienakademie Riesa
Marco Schmidt	Strukturänderungen in Cu-Zr-Al-basierten metallischen Gläsern durch Rascherhitzung, TU Dresden
Sebastian Schneider	Zirkularer magnetischer Elektronenenergieverlustdichroismus an Eisen-Platin-Nanopartikeln, TU Dresden
Tobias Schorr	Kernspinresonanz-Spektroskopie an eisenbasierten Supraleitern, speziell $BaFe_2As_2$, unter uniaxialam Druck, TU Dresden
Franziska Seifert	Synthese von dotiertem polykristallinien Mn Si und Charakterisierung, TU Bergakademie Freiberg
Florian Senftleben	Einfluss der Abkühlbedingungen auf die Phasenbildung martensitischer Ti-Nb Legierungen, TU Dresden
Anne Vornberger	CuTi-Dünnschichtsystem für SAW-Bauelemente - Darstellung und Charakterisierung von Dünnschicht-systemen aus Cu-Ti-Mehrfachlagen für Elektrodenstrukturen von SAW-Bauelementen, TU Dresden
Clemens Wagner	Strukturelle und elektronische Eigenschaften von Titan (III) phosphat, TU Dresden

Calls and Awards

Professorships

Prof. Dr. Jens Freudenberger	Honorary Professor at Bergakademie TU Freiberg

Awards

Dr. Julia Hufenbach	DGM Nachwuchspreis 2015
Dr. Robert Streubel	Ernst-Eckhard-Koch-Prize 2015, for outstanding doctoral thesis in the field of research with synchrotron radiation
Prof. Dr. Ludwig Schultz	DGM-Honorary Membership 2015 IEEE Distinguished Lecturer 2015
Juan Balach	Poster Award of the 8th International Conference on Materials for Advanced Technologies (ICMAT2015) in Singapore
Bo Liu	Most Excellent Paper Award, 3rd International Conference on Renewable Energy and Environment
Dr. Guodong Li	Outstanding Poster Award, 34th International Conference on Thermoelectrics
Dmitriy Karnaushenko	Best Poster Prize, 581. Wilhelm und Else Heraeus-Seminar on Flexible, Stretchable and Printable High Performance Electronics

IFW Awards

Dr. Robert Niemann	IFW Junior Research Award 2015
Dr. Robert Streubel	Tschirnhaus-Medal of the IFW for excellent PhD theses
Dr. Michael Melzer	Tschirnhaus-Medal of the IFW for excellent PhD theses
Dr. Frank Steckel	Tschirnhaus-Medal of the IFW for excellent PhD theses
Dr. Tobias Ritschel	Tschirnhaus-Medal of the IFW for excellent PhD theses
Dr. Arne Helth	Tschirnhaus-Medal of the IFW for excellent PhD theses
Dr. Markus Klose	Tschirnhaus-Medal of the IFW for excellent PhD theses
Dr. Juliane Thielsch	Tschirnhaus-Medal of the IFW for excellent PhD theses
Dr. Robert Niemann	Tschirnhaus-Medal of the IFW for excellent PhD theses
Dr. Maria Krautz	Tschirnhaus-Medal of the IFW for excellent PhD theses
Dr. Veronika Hähnel	Tschirnhaus-Medal of the IFW for excellent PhD theses

Scientific conferences and IFW colloquia

Conferences

Jan. 12 – 14	581. Wilhelm und Else Heraeus-Seminar Flexible, Stretchable and Printable High Performance Electronics
July 3 – 4	3rd German-Korean Workshop on Thermoelectrics, Dresden
July 27 – 29	Condensed Matter Summer School 2015, Prague, Czech Republic
Aug. 3	Workshop „Zukunftsperspektiven supraleitender Anwendungen“, Dresden
Aug. 28 – Sept. 4	Summer School Spectroelectrochemistry
Aug. 31 – Sept. 3	Workshop on the two-dimensional chalcogenides: exotic electronic orders, superconductivity and magnetism
Sept. 4	Symposia „International Symposium on light scattering in superconductors“
Sept. 13 – 19	Quantum Magnets Workshop, in Kolymbari, Crete
Sept. 14 – 17	Workshop on Mechanical Properties of Vitrified Metals – VitriMetTech

Quantum Matter Colloquium

14.01.2015	Prof. Dr. Andreas Mayer, HS Offenburg - University of Applied Science, Acoustics wedge waves: Effects of anisotropy and nonlinearityc spacers
08.04.2015	Prof. Thomas T. M. Palstra, University of Groningen, Netherlands, Controling the electrical properties of perovskites by organi
22.04.2015	Prof. Dr. Philippe Mendels, University of South Paris in Orsay, Quantum Kagome Spin Liquids
13.05.2015	Prof. Dr. Patrick M. Woodward, Ohio-State University, Competing superexchange interactions in osmate double perovskites
20.05.2015	Prof. Dr. Eugene Mele, University of Pennsylvania and Loughborough University, The Winding Road to Topological Insulators
03.06.2015	Prof. Ilya Eremin, Ruhr-Universität Bochum, Spin excitations in layered magnetic superconductors: Cooper-pairing and itinerancy effects
10.06.2015	PD Dr. Arthur Ernst, Max-Planck-Institute of Microstrukture Physics, Halle, Magnetism from first-principles
17.06.2015	Prof. Dr. Rossitza Pentcheva, University of Duisburg-Essen, Designing electronic phases in (001) and (111) oriented perovskite superlattices
01.07.2015	Prof. Dr. Dipl.-Ing. Alois Loidl, Universität Augsburg, Ferroelectric skyrmion phase in multiferroic GaV4S8
22.07.2015	Prof. Dirk K. Morr, University of Illinois at Chicago, Magnetically Mediated Cooper Pairing in Heavy Fermion Superconductors
30.09.2015	Prof. Dr. Sebastian Eggert, University of Kaiserslautern, Quantum phase transitions in anisotropic and frustrated systems
02.10.2015	Prof. Dr. Igor Mazin, Center for Computational Material Science, Washington, Magnetic, structural and superconducting phase diagram in bulk Fe-chalcogenides: nematic fluctuations and biquadratic exchange
28.10.2015	Prof. Dr. Ute Kaiser, University of Ulm, Properties of quantum materials obtained by low-voltage aberration-corrected TEM
24.11.2015	Prof. Dr. Angel Rubio, Max Planck Institute for Structure and Dynamics of Matter, Hamburg, Group IV two-dimensional materials: Novel electronic and structural properties
02.12.2015	Prof. Dr. Thomas Pichler, University of Vienna, Unravelling advanced 1D and 2D carbon systems

Guests and Scholarships

Guest scientists (stay of 4 weeks and more)

Name	Home Institute	Home country
Dr. Bachmatiuk, Alicja	Wroclaw Research Centre ILT	Poland
Dr. Bollero, Alberto	Univ. Canto Blanco	Spain
Prof. Dr. Brenig, Wolfram	TU Braunschweig	Deutschland
Dr. Darinskiy, Alexander	Institute for Crystallography Moscow	Russia
Das, Sujit	MLU Halle Wittenberg	Germany
Dr. Garcia Javier	Univ. Hamburg	Spain
Prof. Dr. Garifullin, Ilgiz	Zavoisky Phys.-techn. Institute Kazan	Russia
Dr. Guix Noguera, Maria	Catalan Institute of Nanotechnology	Spain
Dr. Huang, Shao-Zhuan	Wuhan Univ. of Technology	China
Prof. Dr. Inoue, Akihisa Josai	Univ. Educational Corporation Tokyo	Japan
Dr. Jiang, Chongyun	Institute of Semiconductors Beijing	China
Dr. Jung, Hyoyun	Yonsei Univ.	Korea
Dr. Jung, Kyubong	Univ. of Tokyo	Korea
Dr. Kandpal, Hemchandra	Indian Institute of Technology Roorkee	India
Dr. Kataeva, Olga	A. E. Arbuzov Institute Kazan	Russia
Prof. Dr. Kikoin, Konstantin	Univ. Tel-Aviv	Israel
Dr. Krupskaya, Yulia	Univ.Genf	Russia
Dr. Kumar, Sanjeev	IISER Mohali, Faculty of Physics	India
Prof. Kusmartsev, Fedor	Univ.Loughborough	UK
Dr. Kuzian, Roman	Institute for Materials Science Kiev	Ukraine
Dr. Lebernegg, Stefan	MPI CPfS Dresden	Austria
Dr. Liu, Fupin	Univ. of Science and Technology Hefei	China
Dr. Liu, Xianghong	Renmin Univ. Beijhing	China
Dr. Machata, Peter	Slovak TU Bratislava	Slovakia
Dr. Mandarino, Angelo	Instituto C. Elio Vittorini, San Pietro Clarenza	Italy
Dr. Mikhailova, Daria	MPI CPfS Dresden	Russia
Dr. Morozov, Igor	Staatliche Univ. Moscow	Russia
Dr. Naidyuk, Yurii	Verkin Institute Kharkov	Ukraine
Assoc. Prof. Dr. Nicoara, Mircea	Politehnica Univ. Timisoara	Rumania
Dr. Nishimoto, Satoshi	TU Dresden	Japan
Dr. Otalora, Jorge	Univ. Tecnica Federico Santa Maria	Chile
Park, Kyoung-Tae	KITECH	Korea
Dr. Parzych, Grzegorz	TU Dresden	Poland
Prof. Patra, Ajit Kumar	Central Univ. of Rajasthan	India
Pessoa, Davi Felipe	TU Dresden	Brazil
Dr. Prando, Giacomo	TU Dresden	Italy
Dr. Rata, Diana	MLU Halle Wittenberg	Rumania
Dr. Ray, Rajyavardhan	TU Dresden	India
Dr. Reja, Sahinur	Univ. of Cambridge	India
Dr. Rezaev, Roman	Tomsk Polytechnic Univ.	Russia
Dr. Rienks, Emile	TU Dresden	Netherlands
Prof. Dr. Rossetti, George Andrew	Univ. of Connecticut	USA
Dr. Sakalas, Paulius	TU Dresden	Lithuania
Prof. Saporiti, Maria Fabiana Sonia	Univ.Buenos Aires	Argentina
Dr. Seo, Seok-Jun	KITECH	Korea
Dr. Setti, Thirupathaiah	Indian Institute of Science Bangalore	India

Prof. Dr. Sheka, Denys	Taras Shevchenko National Univ. of Kyiv	Ukraine
Dr. Smirnova, Elena	Ioffe Phys.-Techn. Institute St. Petersburg	Russia
Prof. Dr.Stremy, Maximilian	Slovak TU Bratislava	Slovakia
Dr. Sturza, Mihai-Ionut	Argonne National Lab.	Rumania
Dr. Sulka, Martin	Slovak TU Bratislava	Slovakia
Dr. Sulkova, Katarina	Slovak TU Bratislava	Slovakia
Dr. Vavilova, Evgeniia	Zavoisky Phys.-techn. Institute Kazan	Russia
Dr. Volegov, Alexey	Ural Federal Univ.	Russia
Dr. Yerin, Yuriy	Verkin Institute Kharkov	Ukraine
Dr. Zaripov, Ruslan	Zavoisky Phys.-techn. Institue Kazan	Russia
Prof. Dr. Zotos, Xenophon	Univ. of Crete	Greece

Scholarships

Name	Home country	Donor
Dr. Dassonneville, Bastien	France	Alexander von Humboldt Foundation
Dr. Ghimire, Madhav Prasad	Nepal	Alexander von Humboldt Foundation
Dr. Kim, Beom Seok	Korea	Alexander von Humboldt Foundation
Dr. Prando, Giacomo	Italy	Alexander von Humboldt Foundation
Dr. Zhang, Yang	China	Alexander von Humboldt Foundation
Dr. Kumar, Sarvesh	India	DAAD
Dr. Moravkova, Zuzana	Czech Rep.	DAAD
Dr. Thota, Subhash	India	DAAD
Pylypovskyi, Oleksandr	Ukraine	DAAD
Chakraborty, Abhra	India	DAAD
Chatterjee, Riddhi Pratim	India	DAAD
Harihara, Subramonia Anand	India	DAAD
Potnis, Gaurav	India	DAAD
Ghunaim, Rasha	Palestinian territories	DAAD
Madian,Mahmoud	Egypt	DAAD
Salazar, Enriquez C. D.	Columbia	DAAD
Shahid, Rub Nawaz	Pakistan	DAAD
Dr. Alfonsov, Alexey	Russia	DFG
Linnemann, Julia	Germany	Deutsche Bundesstifung Umwelt
Surrey, Alexander	Germany	Graduiertenakademie TU Dresden
Vieira, Rafael	Portugal	EU Erasmus
Metelkova, Radka	Czech Rep.	EU Erasmus
Miyakoshi, Shohei	Japan	SEEDS Foundation Chiba Univ.
Martins dos Santos, Jonadabe	Brazil	Capes Brazil
Dr. Du, Yun	China	China Scholarship Council
Zhang, Jing	China	China Scholarship Council
Deng, Liang	China	China Scholarship Council
Liu, Lixiang	China	China Scholarship Council
Lu, Xueyi	China	China Scholarship Council
Pang, Jinbo	China	China Scholarship Council
Sui, Yan Fei	China	China Scholarship Council
Sun, Xiaolei	China	China Scholarship Council
Wang, Pei	China	China Scholarship Council
Wang, Pei	China	China Scholarship Council
Xi, Lixia	China	China Scholarship Council

Xu, Haifeng	China	China Scholarship Council
Yin, Yin	China	China Scholarship Council
Yuan, Feifei	China	China Scholarship Council
Yuan, Xueyong	China	China Scholarship Council
Zhang, Long	China	China Scholarship Council
Chirkova, Alisa	Russia	International Graduate School
Güzeltürk, Burak	Turkey	International Graduate School
Liu, Bo	China	International Graduate School
Miyazaki, Taisuke	Japan	Graduate School Niigata Univ.
Iakovleva, Margarita	Russia	Foundation in home country
Zrodowski, Lukas	Poland	Foundation in home country
Günes, Taylan	Turkey	Foundation in home country
Dr. Krupskaya, Yulia	Russia	Foundation in home country
Lopatina, Elena	Russia	Foundation in home country

Guest stays of IFW members at other institutes

Christian Becker	07. - 17.10.2015, IMDEA Nanoscience Madrid/Spain, Measurements and research cooperation
Jeroen van den Brink	07. - 30.09.15, University of California, Santa Barbara/USA, Workshop „New Phases and Emergent Phenomena in Correlated Materials with Strong Spin-Orbit Coupling“
Bastien Dassoneville	16.07.2015 - 11.08.2015, Instutut Néel, Grenoble/France, research cooperation
Jörg Fink	13.07.2015 - 26.07.2015 and 28.09.2015 - 11.10.2015, BESSY HZB Berlin, ARPES Measurements and research cooperation
Vadim Grinenko	05.05.-06.06.2015, University Nagoya/Japan, Research cooperation
Erik Haubold	24.08.2015 - 06.09.2015 BESSY HZB Berlin, ARPES Measurements and research cooperation
Arne Helth	26.03.2015 - 17.06.2015, Korea Institute of Industrial Technology (KITECH), Seoul Rep. Korea, research cooperation
Julia-Kristin Hufenbach	26.03.2015 - 05.06.2015 Korea Institute of Industrial Technology (KITECH), Seoul Rep. Korea, research cooperation
Vladislav Kataev	17.04.2015 - 03.05.2015, Zavoisky Physical Technical Institute, Kazan, Russia, Measurements and research cooperation on magnetic resonance spectroscopy
Andriy Leonov	01.11. - 27.12.15, RIKEN, Hirosawa, Wako, Saitama / Japan, Research cooperation
Jinbo Pang	14.09.2015 - 14.10.2015 and 01.11.2015 - 23.12.2015, Center of Polymer and Carbon Materials of Polish Academy of Sciences, Zabrze, Poland, research cooperation
Johannes Schoop	18.05.2015 - 31.07.2015 Friedrich Alexander University Erlangen-Nürnberg, R&D cooperation on Electron beam lithography
Mihai Stoica	1.10.2015 - 15.10.2015 The Institute of Advanced Manufacturing Technology and Institute of Metallurgy and Materials Science, Polish Academy of Sciences, Krakow, Poland
	31.10.2015 - 22.11.2015, University of Balearic Islands, Palma de Mallorca, Spain, guest lecturer

Board of trustees

Jörg Geiger, Saxonian Ministry of Science and Art - Head -
Dr. Herbert Zeisel, Federal Ministry of Education and Research
Prof. Dr. Gerhard Rödel, TU Dresden
Prof. Dr. Konrad Samwer, Univ. Göttingen (up to 31.12.2015)
Prof. Dr. Sibylle Günter, MPI for Plasma Physics (from 01.01.2016 on)

Scientific Advisory Board

Prof. Dr. Maria-Roser Valenti, Univ. Frankfurt, Germany - Head -
Prof. Dr. Silke Christiansen, HZB Berlin, Germany (from 01.10.2015 on)
Prof. Dr. Andrey Chubukov, Univ. of Minnesota, USA (from 01.10.2015 on)
Prof. Dr. Philippe M. Fauchet, Vanderbilt Univ., USA
Prof. Dr. Matthias Göken, Univ. Erlangen-Nürnberg, Germany
Prof. Dr. Alan Lindsay Greer, Univ. of Cambridge, U.K.
Prof. Dr. Rudolf Gross, Walter Meißner Institute Garching, Germany (up to 30.09.2015)
Prof. Dr. Rolf Hellinger, Siemens AG Erlangen, Germany
Prof. Dr. Xavier Obradors Berenguer, Univ. Autònoma de Barcelona, Spain
Prof. Dr. Roberta Sessoli, Univ. di Firenze, Italy
Prof. Dr. Eberhardt Umbach, Karlsruhe Institute of Technology, Germany

Picture credits

Jürgen Lösel	Page 3, 9, 25, 39, 43, 56, 69,
Matthias Hultsch	Page 13, 29, 33, 60, 73, 77, 81, 85
Jürgen Jeibmann	Page 4 (right photo), page 5 (left photo), page 8 (right photo)
Jose Poblete on behalf of DGM	Page 5 (right photo), page 6 (right photo) page 8 (middle photo)
All others: IFW Dresden	

Research organization of IFW Dresden

Institute for Solid State Research (IFF)

Prof. Dr. Bernd Büchner - 808

Secr.: Kerstin Höllerer - 300
Katja Schmiedel - 805

Surface dynamics

Dr. Hagen Schmidt - 278

Transport and scanning probe microscopy

Dr. Christian Heß - 533

Chemistry of nanomaterials

Dr. Alexey Popov - 871

Magnetic properties

Dr. Vladislav Kataev - 328

Electronic and optical properties

Prof. Dr. Martin Knupfer - 544

Synchrotron methods

Dr. Sergey Borisenko - 566

Crystal growth and synthesis of inorganic materials

Dr. Sabine Wurmehl - 519

Institute for Metallic Materials (IMW)

Prof. Dr. Kornelius Nielsch - 104

Secr.: Svea Fleischer - 102

Chemical synthesis of materials

Dr. Heike Schlörb - 230

Functional oxide layers and superconductors

Dr. Ruben Hühne - 716

Magnetic materials

Dr. Thomas G. Woodcock - 221

Functional magnetic films

Dr. Sebastian Fähler - 328

Quantum materials and devices

PD Dr. Andy Thomas - 746

Thermoelectric materials and devices

Dr. Gabi Schierning - 1875

Metal physics

Prof. Dr. Jens Freudenberger - 550

Magnetic microstructures

Prof. Dr. Rudolf Schäfer - 223

Metastable and nanostructured materials

Dr. Bernd Rellinghaus - 754

Institute for Complex Materials (IKM)

Dr. Thomas Gemming (temp.) - 298

Secr.: Brit Präßler-Wüstling - 217
Janett Schuster - 198

Solidification processes and complex structures

Assoc. Prof. Dr. Mihai Stoica - 644

Magnetic composites and applications

Dr. Anja Waske - 846

Micro- and nanostructures

Dr. Thomas Gemming - 298

Chemistry of functional materials

Dr. Annett Gebert - 275

Electrochemical energy storage

Dr. Lars Giebeler - 652

Alloy design and processing

Dr. Uta Kühn - 402

Metallic glasses and composites

Dr. Simon Pauly - 451

Institute for Integrative Nanosciences (IIN)

Prof. Dr. Prof. h. c. Oliver G. Schmidt - 800

Secr.: Kristina Krummer - 810

Tubular Nanomembrane Materials and Devices

Prof. Dr. Oliver G. Schmidt - 800

Rolled-up photonics

Dr. Libo Ma - 1153

Integrated nanophotonics

Dr. Fei Ding - 752

Micro- and nanobiomedical engineering

Dr. Mariana Medina Sanchez - 489

Institute for Theoretical Solid State Physics (ITF)

Prof. Dr. Jeroen van den Brink - 400

Secr.: Grit Rötzer - 380

Theoretical Solid State Physics

Prof. Dr. Jeroen van den Brink - 400

Quantum Chemistry

Dr. Liviu Hozoi - 1829

Quantum theory of complex nanoarchitectures

Dr. Carmine Ortix - 352

Numerical solid state physics

Dr. Manuel Richter - 360

Date: January 2016

Leibniz Institute for Solid State and Materials Research Dresden

Board of Trustees
Head: MDgt Jörg Geiger

Executive Board

Scientific Director	Administrative Director
Prof. Dr. Manfred Hennecke	Dr. Doreen Kirmse
Ass.: Dr. Carola Langer -234	Ass.: Kristin Koßmann -376
Secr.: Katja Steinbrink -100	Secr.: Anja Hänig -200

Scientific Advisory Board
Head: Prof. Dr. Maria-Roser Valenti
J.-W. Goethe-Univ. Frankfurt

Public Relation, Media	Project Funding, EU-office	Knowledge and Technology Transfer
Safety Officer	Internal Auditor	Controlling

Member of the Leibniz Association

Institute for Solid State Research (IFF)	Institute for Metallic Materials (IMW)	Institute for Complex Materials (IKM)	Institute for Integrative Nanosciences (ITF)	Institute for Theoretical Solid State Physics (ITF)	Research Technology Division (BFT)	Administrative Division (BVW)
Prof. Dr. Bernd Büchner -808	Prof. Dr. Kornelius Nielsch -104	Dr. Thomas Gemming (temp.) -298	Prof. Dr. Prof. h. c. Oliver G. Schmidt -800	Prof. Dr. Jeroen van den Brink -400	Prof. Dr. Dirk Lindackers -580	Dipl.-Kffr. Friederike Jaeger -620
Secr.: Kerstin Höllerer -300 Katja Schmiedel -805	Secr.: Svea Fleischer -102	Secr.: Brit Präßler-Wüstling -217 Janett Schuster -198	Secr.: Kristina Krummer -810	Secr.: Grit Rötzer -380	Secr.: Nicole Büttner -505	Secr.: Ulrike Nitzold -621
Surface dynamics	Chemical synthesis of materials	Solidification processes and complex structures	Tubular Nanomembrane Materials and Devices	Theoretical Solid State Physics	Electrical Engineering and Electronics	Finance Deparment
Transport and scanning probe microscopy	Functional oxide layers and superconductors	Magnetic composites and applications	Rolled-up photonics	Quantum Chemistry	Mechanical Engineering	Human Resources
Chemistry of nanomaterials	Magnetic materials	Micro- and nanostructures	Integrated nanophotonics	Quantum theory of complex nanoarchitectures	Information Technologies	Purchase and Disposal
Magnetic properties	Functional magnetic films	Chemistry of functional materials	Micro- and nanobiomedical engineering	Numerical solid state physics		Library
Electronic and optical properties	Quantum materials and devices	Electrochemical energy storage				Facility Management
Synchrotron methods	Thermoelectric materials and devices	Alloy design and processing				
Crystal growth and synthesis of inorganic materials	Metal physics	Metallic glasses and composites				
	Magnetic microstructures					
	Metastable and nanostructured materials					

Labour Council	Representative Body for Disabled Employees	Data Security Officer
Equal Opportunity Commissioner	Confidential Representative (Ombudsperson)	Scientific-Technical Councill (WTR)

Standort Chemnitz
Smart Systems Campus
Technologie-Campus 1
D-09126 Chemnitz

Standort Niedersedlitz
InfoCenter SupraTrans
Straße des 17. Juni 25
D-01257 Dresden

Visitor's Address	Mailing Address	Phone	Internet
Helmholtzstrasse 20 D-01069 Dresden	PF 27 01 16 D-01171 Dresden	Tel.: +49 351 46 59-0 Fax: +49 351 46 59-540	www.ifw-dresden.de info@ifw-dresden.de

Date: January 2016

Organization chart of the IFW Dresden